UQAC
Université du Québec
à Chicoutimi

Evaluation of effects of geomechanical parameters and in-situ stress on rockburst occurrence in deep excavations

By: Behzad Dastjerdy

Supervisors: Prof. Ali Saeidi and Dr. Shahriyar Heidarzadeh

Thesis presented to the Université du Quebec à Chicoutimi in partial fulfillment of requirements for the degree of Doctor of Philosophy (PhD) in Civil engineering

BOARD OF EXAMINERS:

Dr. Alain Rouleau, Department of Applied Sciences at UQAC, President of the Board

Dr. Ferri Hassani, Professor, Department of Mining & Materials Engineering, McGill University, External Member of the Board

Dr. Li Li, Professor, Department of Mining Engineering, Polytechnique Montreal, External Member of the Board

Dr. Ali Saeidi, Professor, Department of Applied Sciences at UQAC, Internal Member of the Board

Dr. Shahriyar Heidarzadeh, Rock Mechanics Engineer, AECOM, Internal Member of the Board

Québec, Canada

RÉSUMÉ

La demande croissante en métaux et autres substances minérales a conduit l'exploitation minière souterraine à des profondeurs plus importantes, où les défis liés au maintien de la stabilité des excavations deviennent considérablement plus complexes. Parmi ces défis, les coups de terrain — définis comme des ruptures soudaines et violentes de la roche — représentent un danger majeur. Ces phénomènes sont provoqués par des conditions de contraintes élevées et sont fortement influencés par les paramètres géomécaniques et les contraintes in-situ, qui présentent tous deux une incertitude inhérente. Malgré des recherches approfondies, les mécanismes sous-jacents aux occurrences de coups de terrain demeurent partiellement compris. Cette thèse examine les effets des paramètres géomécaniques et des contraintes in-situ sur les occurrences de coups de terrain, en comblant des lacunes importantes dans les connaissances et en proposant des méthodologies avancées pour une évaluation améliorée des risques dans les excavations profondes. Pour traiter les incertitudes liées aux paramètres géomécaniques, une méthodologie robuste en trois étapes a été développée. Cette approche intègre des techniques de traitement statistique des données pour garantir une quantification fiable des paramètres, une analyse détaillée des effets de la schistosité sur le comportement de la roche, ainsi que des études pétrographiques pour saisir l'influence des compositions minéralogiques. Cette approche intégrée permet d'améliorer la compréhension de la variabilité inhérente aux propriétés géomécaniques et de ses implications pour la stabilité des excavations. Une attention particulière a été accordée à l'examen des méthodes de détection des valeurs aberrantes et à la sélection des techniques de traitement des données optimales pour développer des paramètres d'entrée fiables pour les modèles prédictifs. Cette recherche a également mené une caractérisation approfondie des contraintes in-situ, un facteur crucial pour l'analyse des excavations souterraines. En combinant des méthodes statistiques avec des connaissances géologiques, l'étude a affiné les relations existantes contrainte-profondeur pour le Bouclier canadien. Ce processus a impliqué une évaluation critique des approches traditionnelles et l'intégration de nouvelles données pour remédier aux limites des modèles précédents. Les relations contrainte-profondeur résultantes fournissent une base plus précise pour l'évaluation des risques de coups de terrain et constituent une contribution clé au domaine de la mécanique des roches souterraines. En utilisant les paramètres géomécaniques quantifiés et les relations contrainte-profondeur affinées, cette étude a systématiquement analysé l'applicabilité et les limites des critères existants de prédiction des coups de terrain. Des simulations numériques avancées ont révélé une variabilité significative de la précision prédictive entre les différents indices. Les critères intégrant la contrainte principale majeure, tels que les indices de Tao et Zhang, ont montré de meilleures performances pour identifier les zones à haut risque, en particulier près des zones de spandrel et des couronnes de tunnel. Les évaluations spécifiques aux frontières ont mis en évidence le rôle critique de la variabilité spatiale dans la susceptibilité aux coups de terrain, démontrant que les risques augmentent avec la distance par rapport à la paroi du tunnel et varient considérablement entre les unités rocheuses ayant des propriétés géomécaniques distinctes. Cette thèse comble les lacunes dans la compréhension des mécanismes de coups de terrain en intégrant des perspectives géologiques, statistiques et d'ingénierie. En abordant les incertitudes associées aux paramètres géomécaniques et aux contraintes in-situ, cette étude fournit un cadre complet pour prédire les occurrences de coups de terrain dans les projets souterrains profonds.

Mots-clés : *Prédiction des coups de terrain, Paramètres géomécaniques, Contraintes in-situ, Traitement statistique des données, Analyse des incertitudes, Excavations profondes, Bouclier canadien*

ABSTRACT

The increasing demand for natural minerals has driven underground mining to greater depths, where the challenges of maintaining excavation stability become significantly more complex. Among these challenges, rockbursts— defined as sudden and violent failures of rock—represent a critical hazard. These phenomena are driven by elevated stress conditions and strongly influenced by geomechanical parameters and in-situ stress, both of which exhibit inherent uncertainty. Despite extensive research, the mechanisms underlying rockburst occurrences remain partially understood. This thesis investigates the effects of geomechanical parameters and in-situ stress on rockburst occurrences, addressing key knowledge gaps and proposing advanced methodologies for enhanced risk evaluation in deep excavations. To address the uncertainties in geomechanical parameters, a robust three-step methodology was developed. This approach incorporates statistical data treatment techniques to ensure reliable parameter quantification, detailed analysis of schistosity effects on rock behavior, and petrographic studies to capture the influence of mineralogical compositions. This integrated approach can improve understanding of variability inherent in geomechanical properties and its implications for excavation stability. Particular emphasis was placed on reviewing outlier detection methods and selecting optimal data treatment techniques to develop reliable input parameters for predictive models. This research also conducted an in-depth characterization of in-situ stress, a crucial factor for underground excavation analysis. By combining statistical methods with geological insights, the research refined existing stress-depth relationships for the Canadian Shield. This process involved a critical evaluation of traditional approaches and the incorporation of new data to address the limitations of previous models. The resulting stress-depth relationships provide a more accurate basis for evaluating rockburst risks and form a key contribution to the field of underground rock mechanics. Employing the quantified geomechanical parameters and refined stress-depth relationships, this study systematically analyzed the applicability and limitations of existing rockburst prediction criteria. Advanced numerical simulations revealed significant variability in predictive accuracy across various indices. Criteria incorporating major principal stress, such as the Tao and Zhang indices, demonstrated better performance in identifying high-risk zones, particularly near spandrel areas and tunnel crowns. Boundary-specific assessments further highlighted the critical role of spatial variability in rockburst susceptibility, demonstrating that risks intensify with distance from the tunnel boundary and vary significantly between rock units with distinct geomechanical properties. This thesis bridges gaps in the understanding of rockburst mechanisms by integrating geological, statistical, and engineering perspectives. By addressing uncertainties associated with geomechanical parameters and in-situ stress, this study provides a comprehensive framework for predicting rockburst occurrences in deep underground projects.

Keywords: *Rockburst prediction, Geomechanical parameters, In-situ stress, Statistical data treatment, Uncertainty analysis, Deep excavations, Canadian Shield*

TABLE OF CONTENTS

LIST OF FIGURES

LIST OF TABLES

LIST OF SYMBOLS

Xm:	Mean	MC:	Medcouple
S:	Standard deviation	MAD:	Median absolute deviation
n:	Sample size	α_{nm}:	Probability
α:	Probability	Mi:	Modified Z-score
β:	Schistosity angle	σ_t:	Tensile strength
IQR:	Interquartile range	E:	Young's modulus
$SIQR_L$:	Semi-interquartile range for lower threshold	ν:	Poisson's ratio
$SIQR_U$:	Semi-interquartile range for upper threshold	σ_v:	Vertical Stress
f_L:	Upper fence	$\sigma_{have:}$	Mean horizontal stress
f_U:	Upper fence	σ_H:	Maximum horizontal stress
Q_1:	First quartile	σ_h:	Minimum horizontal stress
Q_2:	Second quartile or median	σ_1:	Major principal stress
Q_3:	Third quartile	σ_2:	Intermediate principal stress
PDF:	Probability distribution function	σ_3:	Minor principal stress
d_f:	Degree of freedom	K:	Stress ratio
t:	Student's t-distribution		

DEDICATION

To my beloved Father, Yaghoub, whose memory continues to inspire my path

To my devoted Mother, Monireh, whose support and love have guided me throughout the journey

And to the love of my life, Elaheh, my best companion in life, with whom every hardship becomes easier, every pain more bearable, and life itself as sweet as honey

ACKNOWLEDGMENTS

I would like to express my deepest gratitude to all those who have supported and guided me throughout this journey.

First and foremost, I would like to thank my supervisor, Prof. Ali Saeidi, for his continuous support, insightful feedback, and invaluable mentorship. His guidance has been crucial to the completion of this work, and I am deeply grateful for his dedication to my academic and professional growth.

I also wish to thank my co-supervisor, Dr. Shahriyar Heidarzadeh, for his contributions and valuable advice during my research.

I am thankful to my friends and colleagues at the Université du Québec à Chicoutimi (UQAC) for their support and collaboration.

I am also deeply grateful of my friends, family, and relatives in Iran, whose incredible love and support have kept me going, even from afar.

Last but not least, my utmost gratitude goes to my loving wife, Elaheh. Her support, patience, and understanding have been the main source of my strength and will. With her by my side, every challenge became easier, and every moment of joy more meaningful. I am infinitely grateful for her love and presence in my life.

CHAPTER 1

INTRODUCTION

1.1 General

In modern mining and geotechnical projects, there is a growing emphasis on deeper underground excavations to meet the ever-increasing demands for natural resources and infrastructure development. However, this depth increase brings various engineering challenges, among which rockbursts stand out as one of the most critical. These events, characterized by sudden and violent rock failures, become more common with deeper mining and the accompanying stresses (Kouame Arthur Joseph et al., 2017; Liu & Wang, 2018). Despite substantial advancements in understanding rockbursts, their unpredictable nature continues to pose significant risks in deep mining industry.

The phenomenon of rockbursts has been a subject of extensive investigation over decades, with researchers offering diverse perspectives on its defining characteristics. Some emphasize the dynamic and brittle failure mechanisms, while others focus on the seismic energy release or the ejection of rock fragments (Blake & Hedley, 2003; Solak, 2009; Li, 2014; Zhou et al., 2018). Although numerous methods have been utilized to predict and assess rockbursts, ranging from empirical to numerical techniques, achieving a comprehensive understanding of rockburst mechanisms remains a challenge (Wang et al., 2021). The literature highlights two principal factors contributing to rockburst occurrences: firstly, the geomechanical parameters of the intact rock, which impact a significant influence on the geomechanical characteristics of the rock mass; and secondly, the state of in-situ stress at different depth ranges (Zhou et al., 2018; Kaiser, 2019).

Globally, rockbursts have been reported in a wide range of geomechanical contexts, affecting deep mines in South Africa, Canada, and China, as well as underground construction projects in countries such as Norway, Chile, and Australia (Wang et al., 2021). This widespread rockburst occurrence underlines its status as a major concern in geotechnical engineering. Suorineni et al.

(2014) described rockburst as the "cancer" of contemporary deep mining, given its pervasive nature and the challenges it poses to engineering design and safety protocols.

1.2 Literature review

Rockbursts can be a serious challenge in deep underground excavations due to the complex interactions of geomechanical parameters, in-situ stress conditions, and site-specific geological factors. This thesis will be based on the review of the literature organized in three major sections: first, the examination of the uncertainties of the geomechanical parameters of rock and their relationships with the occurrence of rockburst; second, the review of characterization of in-situ stress-depth relationships in the Canadian Shield; and third, the role of numerical approaches in rockburst prediction is discussed to provide an insight into applications and limitations.

1.2.1 Uncertainties in geomechanical parameters and their implications for rockburst occurrence

The geomechanical properties of intact rock are fundamental to understand the mechanical behavior of rockmass and its response to complex stress conditions in various engineering challenges, in particular rockbursts (Connor Langford & Diederichs, 2015; Dastjerdy et al., 2024a; Heidarzadeh et al., 2021a). Key parameters including Uniaxial Compressive Strength (UCS), tensile strength, Young's Modulus, and Poisson's ratio provide valuable insights into the mechanical response of rocks when subjected to external loading conditions. These parameters are integral to the analysis of rockburst potential, as they influence the rock's capacity to withstand stress and deform elastically or plastically (Castro et al., 2012; Feng, 2017).

UCS is considered as a crucial parameter used to assess the strength of rock under uniaxial compression and serves as an important predictor of a rock's tendency to fail under stress. Higher UCS values generally correlate with increased rock brittleness, which in turn heightens the likelihood of sudden failure events, such as rockbursts (Ali et al., 2014; Bidgoli & Jing, 2014). Similarly, tensile strength, which is typically lower than compressive strength, is of significance in determining the vulnerability of rocks to failure, particularly in situations where redistributed stresses occur, as

commonly found in mining operations (Pepe et al., 2017). The interaction of tensile and compressive strengths becomes critical in understanding the failure mechanisms that can lead to rockburst events. Young's Modulus, which quantifies a rock's ability to deform elastically under stress, is another vital parameter in the analysis of rockbursts. A higher Young's Modulus implies a reduced capacity for energy dissipation via elastic deformation, thus increasing the likelihood of abrupt energy release, a key characteristic of rockbursts (Feng, 2017; Sainsbury, 2020). Moreover, Poisson's ratio, which reflects the ratio of lateral strain to axial strain under stress, influences the potential for shear failure, a crucial factor in confined rock masses subjected to high stress (Chen et al., 2021). Higher Poisson's ratio values typically could indicate a higher tendency for failure, contributing to the occurrence of rockbursts in underground excavations (Agliardi et al., 2016).

However, the inherent variability of geomechanical parameters in natural rock masses poses significant challenges in the accurate determination of these parameters. Laboratory experiments, commonly used to determine these parameters, often yield results with considerable scatter due to the heterogeneous nature of rocks even when proper testing protocols are followed (Cai et al., 2004; Pepe et al., 2017a; Sonmez et al., 2004). These variations necessitate careful data treatment to reduce uncertainties and improve the reliability of geomechanical analysis. The presence of extreme outliers—values that significantly deviate from the bulk of the data—further complicates the analysis, as they can distort the true mechanical behavior of the rockmass.

To address these uncertainties, researchers have developed various statistical methods to process geomechanical data and mitigate the impact of outliers in the rockmass characterization (Agliardi et al., 2016; Chen et al., 2021; Pereira, F. da Silva, et al., 2021). Thus, prior to determining intact rock parameters, an appropriate data treatment process for laboratory results must be undertaken to identify the most suitable methods for reducing uncertainties of geomechanical data. Techniques such as Chauvenet's criterion, Grubbs' test, and the Z-score method were commonly applied to identify and remove extreme values from datasets, ensuring that the results more accurately reflect the true characteristics of the rockmass (Dindarloo & Siami-Irdemoosa, 2015; Shao et al., 2019). The boxplot

method, often utilized in geomechanical studies, is another common approach for identifying outliers, though it may be less effective when dealing with heavily skewed datasets (Walker et al., 2018). While these statistical techniques provide valuable tools for refining the data, the selection of the most appropriate method remains a topic of debate, particularly when it comes to ensuring that the identified outliers are physically justifiable and do not misrepresent the rock's behavior.

Given the importance of these geomechanical parameters in predicting rockburst occurrences, addressing the uncertainties is crucial for improving the reliability of rockburst prediction models. Through the application of robust data treatment methods, researchers can better quantify the geomechanical properties of intact rock masses and enhance the predictive accuracy of rockburst models. This would allow for more informed decision-making in the design and management of underground excavations, contributing to safer and more effective mining operations.

1.2.2 In-situ stress-depth relationships in the Canadian Shield

The precise characterization of in-situ stress conditions plays a crucial role in understanding the geomechanical behavior of rock masses in underground excavations, particularly when evaluating the rockburst risk. Inaccurate or underestimated stress estimations can lead to a misjudgment of rock failure potential, resulting in poor excavation designs and insufficient support systems. Vertical stresses primarily arise from the weight of overlying rock layers, increasing with depth (Amadei & Stephansson, 1997; Maloney et al., 2006). In addition, horizontal stresses, affected by the complex tectonic and structural characteristics of a region, play a significant role. In certain areas, especially those with complex geological conditions, horizontal stresses may exceed vertical stresses due to tectonic plate interactions (Corkum et al., 2018; Langford, 2013; Zhao et al., 2013). When mining operations occur in such stress-sensitive zones, the redistribution of stresses can produce unpredictable consequences, leading to sudden energy releases, such as rockbursts (Martin et al., 2003; Ma et al., 2018). Therefore, characterization of in-situ stress state could be greatly important in

regions like the Canadian Shield, where the geological complexity and interplay of regional tectonic forces and local geological anomalies further complicate the stress field.

The estimation of in-situ stress has been advanced using various methods, each with its own strengths and limitations. The primary techniques include direct and indirect approaches. Direct measurement involves the use of tools such as hydraulic fracturing, overcoring, and the flat-jack methods to obtain stress values from within the rockmass (Zhao et al., 2013; Kaiser et al., 2016). These methods provide direct insight into the stress state but are often limited by accessibility, cost, and the ability to capture the three-dimensional nature of stress. The second approach is indirect (including borehole breakouts, core disking or strain relief methods), estimating stresses based on observed behavior of rock under existing conditions (Amadei & Stephansson, 1997; Zhao et al., 2013). In addition, back-analysis, which adjusts model parameters based on observed field data to align computational results with actual measurements, has been extensively utilized in numerous projects to refine in-situ stress estimates (Herget, 1973b; Dight & Hsieh, 2016). These measurements, however, are often subject to considerable uncertainties. These uncertainties stem from several factors, including the region's complex geological history, the heterogeneity of rock formations that can cause localized stress variations, the limitations of measurement techniques at great depths, ongoing tectonic activities that may subtly alter stress patterns, and external influences such as human-induced activities (Zhang et al., 2012; Kaiser et al., 2016; Corkum et al., 2018; Saeidi et al., 2021). Any significant errors or inaccuracies in interpreting the stress profile can lead to structural weaknesses, increased safety hazards, and potential environmental concerns. Therefore, a more thorough understanding of the in-situ stress state is critical to ensure the safety and effectiveness of mining operations.

The study of in-situ stress in the Canadian Shield has undergone significant progress since the 1970s. Early investigation in the region focused on the reliability of triaxial stress measuring tools, with the first practical application occurring at the G.W. Macleod Iron Mine in Wawa, Ontario (Herget, 1973b). Subsequently, the Canada Centre for Mineral and Energy Technology (CANMET)

initiated a comprehensive campaign to measure in-situ stresses across the Canadian Shield, leading to the development of a robust database on stress measurements (Herget & Arjang, 1990). Over time, researchers have proposed various methods for estimating stress components in the region, leading to the development of several stress-depth relationships that assisted capture the complexity of the Canadian Shield's geological conditions. One of the early contributions to understanding the stress-depth relationship in the Canadian Shield was Herget's (1982) proposal to divide the stress data into two depth zones: 0-900 m and 900-2200 m. This distinction was based on observed differences in horizontal and vertical stress magnitudes at these depths. Herget (1988) later refined these relationships, acknowledging the distinct behavior of the stress field at depths above and below 900 m. More recent research by Maloney et al. (2006) and Yong and Maloney (2015) further refined the stress-depth relationships, introducing three distinct stress zones: the stress-released zone (0-300 m), transition zone (300-600 m), and undisturbed stress zone (600-1500 m). These efforts aimed to capture the varying stress regimes at different depths, with the uppermost layer showing significant stress variations due to glacial and tectonic influences, while deeper layers are largely unaffected by these surface events.

Despite the progress made in understanding in-situ stress in the Canadian Shield, several challenges persist in accurately characterizing the stress state. One major issue is the use of linear models to represent stress variation with depth. Many existing stress-depth relationships assume a uniform change in stress with increasing depth, but this may not accurately capture the complexity of the geological environment, such as the effects of past tectonic movements, glaciation, and local structural features (Taherynia et al., 2016; Zhao et al., 2013). Additionally, while categorizing stress data into distinct depth zones has been useful, it does not fully account for the underlying geomechanical processes driving stress variations. This approach has the potential to oversimplify the stress state and may not be universally applicable across the entire Canadian Shield, particularly in regions where geological conditions differ significantly, which requires further evaluation. Although multiple methods exist to estimate in-situ stress, challenges persist in developing accurate

and site-specific models, particularly in complex geological areas like the Canadian Shield. The historical development of stress-depth relationships in the region underscores ongoing efforts to refine these models, but further research is essential to resolve uncertainties and enhance the reliability of stress predictions, especially in relation to rockburst risk.

1.2.3 Overview of numerical approaches in rockburst prediction

Numerous empirical criteria have been developed over the years to predict and categorize different types of rockbursts, providing valuable insights into the conditions and behaviors of rock in high-stress environments. This involves both qualitative and quantitative methods, which can be broadly divided into two primary areas: the rockburst potential of individual rock types and the potential within complex rock mass engineering (Zhou, 2015; Zhang et al., 2016). The first area evaluates the inherent susceptibility of specific rock materials to rockbursts, suggesting that if a rock does not possess intrinsic rockburst potential, it will not experience rockbursts during engineering activities. The second area examines the likelihood of rockbursts within a rock mass, considering factors such as in-situ stress, geological layering, and structural features based on site-specific fieldwork.

To assess rockburst potential, a variety of techniques are employed, including field observations, theoretical analyses, numerical simulations, and empirical methods. These approaches work together to provide a more comprehensive understanding of rockburst risk and to inform the development of tailored support systems and effective mitigation measures (Rojas Perez et al., 2024; Zhou et al., 2018). Additionally, integrating monitoring technologies and predictive approaches could lead to real-time assessments of rock behavior, ensuring safety and operational efficiency in deep mining activities (Kaiser & Cai, 2012; Mazaira & Konicek, 2015).

Numerical analysis has significantly advanced the study of rockbursts over the past decades, refining our understanding of the complex mechanisms and enhancing prediction accuracy. Early research, beginning with Salamon (1964), focused on the mechanisms behind rockbursts in

underground tunnels, emphasizing the role of stress concentrations and rock mass properties in triggering these events (Wang et al., 2021). In the 1970s, researchers employed methods like the finite difference method (FDM) to model elastic wave propagation under high-stress conditions, using tools such as the Split-Hopkinson pressure bar (Miranda, 1972). Blake (1972) introduced the finite element method (FEM) to predict areas prone to rockbursts, especially in high-stress pillars. In 1979, Brady employed the boundary element method (BEM) to analyze pillar failure, proposing a hybrid approach combining both continuum and discontinuous stress analyses. Board and Voegele (1981) applied BEM to evaluate elastic energy release rates and assess the rockburst potential of mining operations. By the 1980s, dynamic simulations of rockburst processes, especially in pillars and tunnels, became more advanced, with studies such as those by Zubelewicz & Mroz (1983). In the 2000s, Sun et al. (2007) utilized realistic failure process analysis (RFPA) and discontinuous deformation analysis (DDA) to simulate dynamic rockbursts in circular tunnels, emphasizing the role of rock heterogeneity and crack propagation. Cai et al. (2007) combined FLAC (Fast Lagrangian Analysis of Continua) and PFC (Particle Flow Code) to model excavation-induced acoustic emissions (AE), demonstrating the ability of these models to simulate AE in response to stress changes around underground excavations.

More recently, research has focused on refining rockburst indicators and improving the precision of numerical modeling. Sainoki and Mitri (2014a, 2014b) developed dynamic models to simulate fault-slip and stress changes resulting from production blasts. Naji et al. (2018) studied the impact of small-scale shear zones on rockbursts in deep hydropower tunnels using FLAC3D, revealing that principal stresses concentrate near shear zones, making them more susceptible to rockbursts. Manouchehrian and Cai (2018) also explored the influence of weak planes on rockburst occurrence and the resulting damage around underground openings. More recently, Wang et al. (2022) examined the behavior of yielding rock bolts under seismic loading using FLAC3D, while Fanjie et al. (2022) proposed an integrated approach to modeling rockburst evolution that considers crack propagation, stress criteria, and boundary effects.

These advancements in numerical modeling techniques contribute to an improved understanding of rockburst mechanisms and provide more reliable tools for assessing rockburst risk in deep underground mines. However, the complexity of geological conditions and stress redistribution in rock masses remains a significant challenge, making it crucial to continue refining these numerical approaches to better predict and mitigate the risk of rockbursts.

1.3 Problem statement

Accurate determination of geomechanical parameters and the in-situ stress state within rock formations is critical for ensuring stability of deep excavations, yet these factors pose significant challenges due to their inherent variability. The uncertainty surrounding geomechanical parameters and in-situ stress conditions plays a substantial role in the stability of underground structures, making their detailed analysis essential. Variability in rock properties can lead to inconsistent design decisions, underscoring the need for robust data treatment methods to accurately interpret and address these fluctuations.

Furthermore, understanding the variability of in-situ stress requires a comprehensive approach that integrates statistical analysis with geomechanical and geological reasoning. Stress conditions directly influence the design of underground structures, and oversimplifying these factors may compromise the accuracy of predictions. Thus, the main questions are listed as follows:

1. What data treatment method should be employed to determine and mitigate uncertainties in the geomechanical parameters of rocks?
2. What methodologies can be developed to address uncertainties associated with in-situ stress, which can trigger rockburst occurrences?
3. Among the various approaches for predicting rockburst occurrences in deep mining, including laboratory tests, stress-based criteria, and energy-based methods, which are the most applicable criteria? How do geomechanical parameters and in-situ stress influence the selection and accuracy of these criteria?

This research seeks to clarify these challenges and enhance predictive models, ultimately advancing safety and efficiency in deep underground excavations within the domains of mining and geotechnical engineering.

1.4 Research objectives

This study aims to address the limitations identified in previous research on evaluating rockburst phenomena in deep rock masses with variable geological settings. The primary objective of this thesis is to assess the applicability of rockburst prediction criteria and analyze the probability of rockbursts around deep excavations, considering uncertainties in rockmass geomechanical parameters and in in-situ prediction. To achieve these goals, four specific objectives have been outlined:

- Identifying optimal data treatment methods for geomechanical data
- Determining the uncertainties of geomechanical parameters of metamorphic rocks through incorporation of petrographic analyses
- Quantifying the uncertainties and developing new relationships for estimating the in-situ stress in the Canadian Shield
- Evaluating the effectiveness of rockburst prediction criteria by analyzing the influence of geomechanical parameters and in-situ stress on rockburst occurrence using numerical analysis

1.5 Research Methodology

The research methodology includes four main parts namely: (1) identification of the most applicable data treatment approaches, (2) determination of uncertainties associated with geomechanical parameters, (3) development of new relationships for estimating in-situ stress, and (4) assessment of rockburst prediction criteria and the probability of rockburst occurrences near tunnel boundaries through numerical analysis.

1.5.1 Identification of applicable outlier detection methods for geomechanical data

Determining applicable outlier detection methods for treating geomechanical data involves four main steps (Figure 1.1). Firstly, a complete review of outlier detection techniques is conducted to

establish a comprehensive understanding of their capabilities. Next, the outlier detection techniques are classified based on their suitability for geomechanical applications, considering factors such as data distribution, size, and complexity. Subsequently, each method is evaluated for its practical suitability, including robustness, ease of implementation, and ability to handle non-normal data distributions, extreme values, and skewness. Finally, the strengths and weaknesses of each method are discussed, highlighting their advantages and disadvantages to provide a framework for informed decision-making in geomechanical analysis (Figure 1.1).

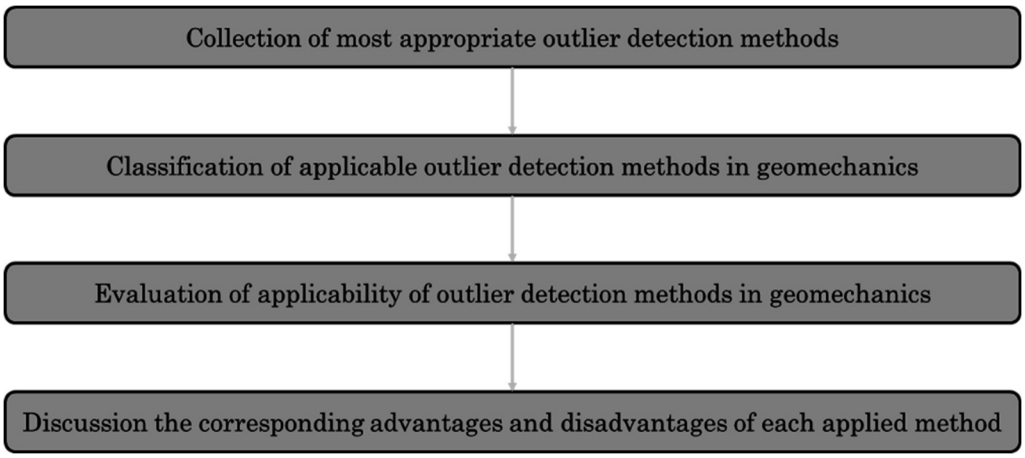

Figure 1.1 Proposed methodology for classification and assessment of outlier detection methods in geomechanics

1.5.2 Determination of uncertainties associated to geomechanical parameters of metamorphic rocks using petrographic analyses

To investigate uncertainties of geomechanical parameters of metamorphic rocks, five key steps are proposed (Figure 1.2), aiming at minimizing uncertainties and establishing meaningful links between influential factors. Firstly, an appropriate case study area, specifically the Westwood underground mine in Canada, known for its rockburst-prone nature, is selected for analysis. Step 2 involves a comprehensive statistical analysis of geomechanical parameters to characterize intact rock and identify outliers of geomechanical data using 17 statistical outlier detection methods. In Step 3, the most suitable data treatment methods are selected based on multiple decision-making criteria and

engineering judgment. Step 4 focuses on determining the best-fitted probability distribution function (PDF) for the treated dataset of geomechanical parameters, recognizing that normal distribution may not be the most accurate representation. Finally, the analysis investigates the influence of schistosity angle and mineralogy on rock strength uncertainties, aiming to establish links between mineral composition and geomechanical parameter variations (Figure 1.2). By integrating these steps, the methodology aims to minimize uncertainties associated with geomechanical parameters, providing insights into the variability and characteristics of metamorphic rocks.

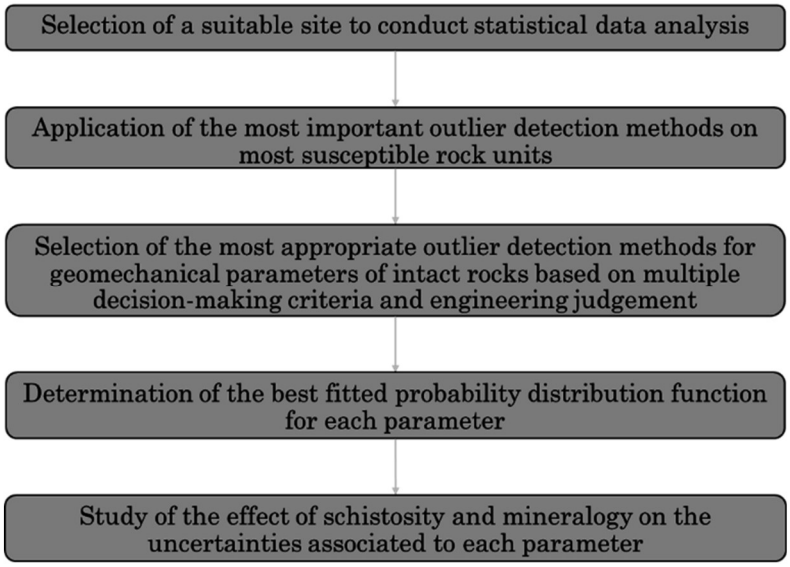

Figure 1.2 Methodology for determining uncertainties associated with the geomechanical parameters of intact rock

1.5.3 Development of new relationships for estimating the in-situ stress in the Canadian Shield

Once geomechanical data are characterized, the state of in-site stress and its related uncertainties are investigated. For this purpose, a proper approach is implemented to develop stress-depth relationships within the Canadian Shield (Figure 1.3). Initially, stress data from previous measurement campaigns within the Canadian Shield are collected and processed to ensure data accuracy. Then, stress orientation discrepancies are addressed by transforming collected stresses into the Cartesian system. This adjustment accounts for orientation uncertainties, enabling accurate

calculation of maximum and minimum horizontal stresses alongside corresponding vertical stress. Next, the limitations of relying solely on statistical methods for formulating stress-depth relationships will be critically evaluated, highlighting the necessity of integrating geological considerations. Moving to next step, the in-situ stress database is classified based on diverse geological regions of the Canadian Shield, considering specific structural and lithological similarities. Subsequently, the influence of major geotectonic events within each geological group is analyzed comprehensively, assessing their effects on stress patterns and redistributions. Finally, geological insights are integrated to establish reliable region-specific stress-depth relationships tailored to the Canadian Shield's unique geotectonic characteristics.

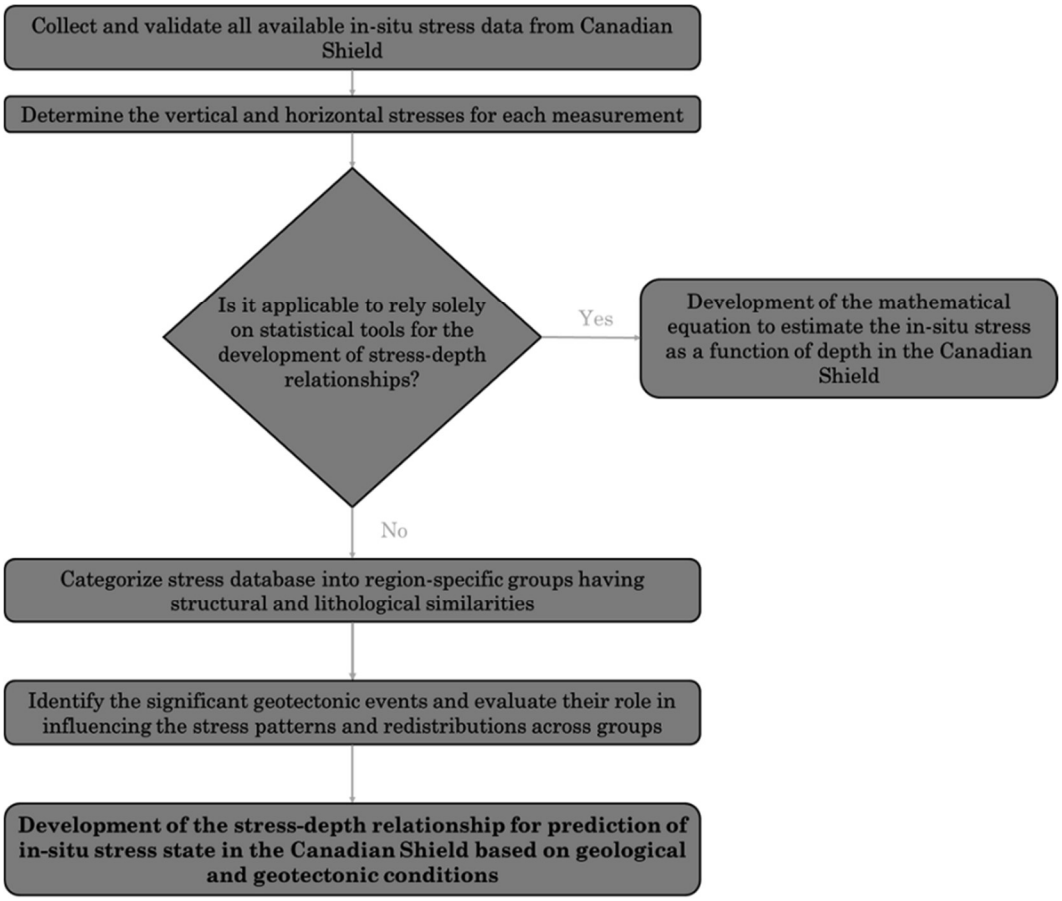

Figure 1.3 Suggested methodology to develop the in-situ stress-depth relationships

1.5.4 Assessment of rockburst prediction criteria and probability of rockburst around tunnel

This step aims to evaluate rockburst probability through numerical analysis, emphasizing the relevance of empirical prediction criteria while considering the effects of geomechanical parameters and in-situ stresses. As shown in Figure 1.4, the process begins by identifying rockburst-prone areas within the Westwood underground mine in Quebec (Canada), a site with a history of frequent rockburst occurrences. Next, geomechanical parameters of the rock mass are characterized using both deterministic and probabilistic approaches, along with an analysis of the in-situ stress conditions at the mine. Numerical modeling is then employed to assess the applicability of existing rockburst prediction criteria to the specific conditions of the Westwood Mine, identifying any limitations or opportunities for improvement. Lastly, a probabilistic evaluation is performed to estimate the

likelihood of rockburst events in the selected zones, with sensitivity analyses incorporated to examine the influence of various risk factors. This systematic approach aims to provide a comprehensive understanding of rockburst risks in underground environments.

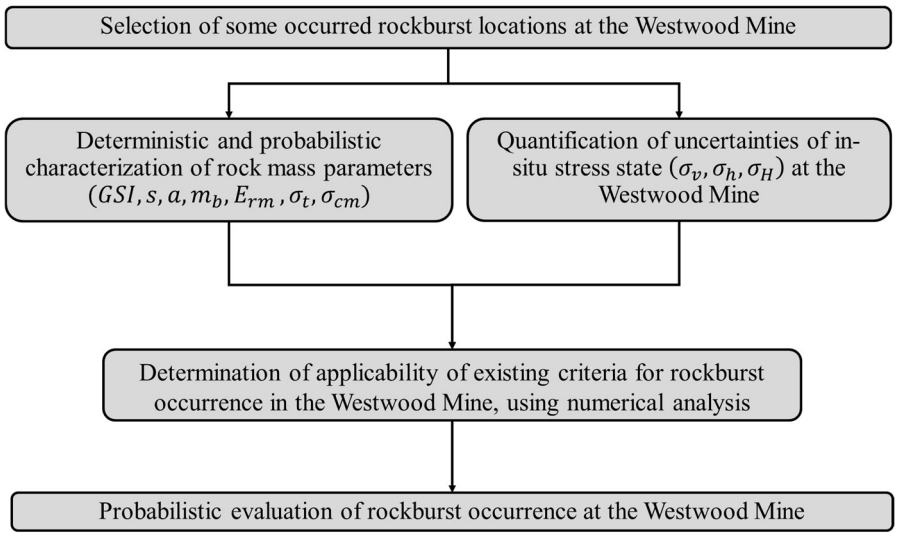

Figure 1.4 Novel approach to evaluate the effectiveness of rockburst prediction criteria and probability of rockburst occurrence using numerical analysis

1.6 Originality and contribution

This research introduces several innovative contributions:

- An extensive examination of outlier detection methods and their suitability for geomechanical studies stands as a crucial novelty. By evaluating these methods across various geotechnical contexts, the study aims to offer practical guidance on selecting the most effective technique for outlier detection in geomechanical analyses.

- A significant aspect of this study involves understanding the uncertainties surrounding geomechanical parameters specific to metamorphic rocks. Through a systematic three-phase methodology, the research seeks to clarify the influence of different data treatment techniques, variations in schistosity angle, and the presence of minerals on the variability of these parameters.

- By refining stress-depth relationships tailored to the geological and tectonic complexities of the Canadian Shield, this study aims to provide novel and region-specific insights into in-situ stress states

across diverse regions within the Canadian Shield. This effort integrates advanced modeling techniques with geological expertise to deliver refined models and practical insights.

- Another contribution of this study is the evaluation of the applicability of rockburst prediction criteria using advanced numerical analysis. By focusing on the Westwood Mine—known for frequent rockbursts—the research assesses the effectiveness of current prediction models. Sensitivity analyses and probabilistic assessments enhance the understanding of rockburst occurrences, identify the limitations of existing criteria, and provide insights for refining prediction and mitigation strategies in underground mining.

1.7 Thesis outline

This thesis is organized into six chapters, structured around four scientific journal articles (Chapters 2, 3, 4, and 5), each contributing to the overarching aim of advancing the understanding of data treatment, parameter uncertainty, stress-state estimation, and rockburst prediction in geomechanical studies. Each article-based chapter includes an abstract, introduction, detailed analysis, and conclusion. The thesis is designed to build systematically from foundational concepts to applied research findings, as outlined below:

- Chapter 1 provides a general introduction, outlining the research problem, objectives, and the innovative methodologies designed to tackle critical challenges in geomechanics. It highlights existing knowledge gaps in geomechanical data treatment, in-situ stress characterization, and rockburst prediction. The chapter emphasizes the novelty and importance of this research in advancing rock engineering practices and enhancing the stability of underground excavations.
- Chapter 2 presents a comprehensive literature review on the introducing applicable outlier detection methods and identifying optimal data treatment methods for geomechanical data. It provides a detailed examination of various outlier detection techniques and their suitability

for geomechanical studies, offering practical guidance on selecting the most effective methods for different geotechnical contexts.

- Chapter 3 develops a robust three-phase methodology to quantify uncertainties in geomechanical parameters specific to metamorphic rocks. It systematically investigates the impacts of data treatment techniques, schistosity angle variations, and mineralogical influences on parameter variability. The findings provide essential insights into the inherent uncertainties of rock properties, enabling more reliable inputs for numerical modeling and geotechnical design.
- Chapter 4 provides an appropriate methodology for quantifying uncertainties and developing new relationships for estimating in-situ stress in the Canadian Shield based on geological conditions. The chapter refines existing stress-depth relationships and integrates advanced modeling techniques with geological expertise to enhance the understanding of in-situ stress conditions in this region.
- Chapter 5 focuses on evaluating the effectiveness of rockburst prediction criteria. It employs numerical analysis to assess the applicability of existing prediction models, particularly in the context of the Westwood Mine, and explores the limitations of current models. Sensitivity analyses and probabilistic assessments are used to gain a deeper understanding of rockburst occurrences.

- Chapter 6 summarizes the key findings from Chapters 2 to 5 and highlights their significance for rock engineering practice. It explores the research's impact on improving rockburst prediction and geomechanical data reliability in deep underground excavations. The chapter concludes with recommendations for refining prediction models, reducing uncertainties in geomechanical analysis, and suggesting future research directions.

CHAPTER 2

Reliable prediction of rockbursts depends on the quality and reliability of geomechanical input data. Variability, inconsistencies, and the presence of outliers within datasets can significantly compromise the accuracy of numerical models and prediction criteria. This chapter addresses the challenge of identifying robust data treatment methods for handling uncertainties in geomechanical datasets. By systematically evaluating various approaches to outlier detection and data refinement, this chapter establishes a foundation for ensuring the consistency and reliability of critical geomechanical parameters. These parameters are vital for subsequent modeling efforts, directly affecting the accuracy of stress distribution analyses and the identification of rockburst-prone zones.

Article 1: Review of Applicable Outlier Detection Methods to Treat Geomechanical Data

Behzad Dastjerdy [1,*], Ali Saeidi [1] and Shahriyar Heidarzadeh [2]

[1] Department of Applied Sciences, University of Quebec at Chicoutimi, Saguenay, QC G7H 2B1, Canada

[2] Rock Mechanics Engineer at SNC-Lavalin, Montreal, QC H2Z 1Z3, Canada

Published, Geotechnics 2023, *3*(2), 375-396.

https://doi.org/10.3390/geotechnics3020022

2.1 Abstract

The reliability of geomechanical models and engineering designs depends heavily on high-quality data. In geomechanical projects, collecting and analyzing laboratory data is crucial in characterizing the mechanical properties of soils and rocks. However, insufficient lab data or underestimating data treatment can lead to unreliable data being used in the design stage, causing safety hazards, delays, or failures. Hence, detecting outliers or extreme values is significant for ensuring accurate geomechanical analysis. This study reviews and categorizes applicable outlier detection methods for geomechanical data into fence labeling methods and statistical tests. Using real geomechanical data, the applicability of these methods was examined based on four elements: data distribution, sensitivity to extreme values, sample size, and data skewness. The results indicated that statistical tests were less effective than fence labeling methods in detecting outliers in geomechanical data due to limitations in handling skewed data and small sample sizes. Thus, the best outlier detection method should consider this matter. Fence labeling methods, specifically, the medcouple boxplot and semi-interquartile range rule, were identified as the most accurate outlier detection methods for geomechanical data but may necessitate more advanced statistical techniques. Moreover, Tukey's boxplot was found unsuitable for geomechanical data due to negative confidence intervals that conflicted with geomechanical principles.

Keywords: Geomechanical uncertainties; Statistical data treatment; Outlier detection methods; Natural variability.

2.2 Introduction

The process of data analysis is a crucial step in experimental studies because the results significantly influence engineering decisions. In geotechnical engineering, natural materials such as soil or rock exhibit inherent variability, which can lead to significant uncertainties in data analysis. These natural uncertainties arise from the formation process and alterations over time, with the primary source varying depending on the type of geomechanical parameter being measured (Han et al., 2020; Mazraehli & Zare, 2020). For example, intact rock strength can be affected by variations in petrographic characteristics, such as mineral composition, texture, microstructures, and degree of chemical alteration. Meanwhile, deformability parameters such as Young's modulus can be affected by water content, degree of jointing, and blasting near mining areas (Connor Langford & Diederichs, 2015). The variation in laboratory data must also be statistically examined to exclude any possible abnormalities. As a result, even when the samples are properly prepared and the testing protocols strictly followed, their test findings are undoubtedly dispersed, and they should be taken as raw data with certain abnormal datapoints that distort the geomechanical analysis conclusions. Some laboratory measurements appear to be significantly outside of the expected range. These extreme values are known as outliers and can have a detrimental impact on data analysis (Barbato et al., 2011; Kannan et al., 2015; Saleem et al., 2021). An appropriate procedure must be applied to address the cause of this anomaly (Hadi et al., 2009). According to Peirce (1852), outliers are observations in a dataset that show patterns differing from the bulk of observations in the sample and can significantly violate the distribution assumptions, such as analysis of variance (ANOVA) and regression. Hence, before any decisions are made, the outliers should be detected and dealt with in the dataset, because doing so results in a better fit for parametric statistical models.

The methods of identifying outliers in engineering are mostly case specific and depend on the conditions and objectives of the analysis. In fact, the selection of the most appropriate methods for detecting outliers is crucial and requires the engineering judgment to be considered because the identified outliers should also be reasonable from the viewpoint of geomechanics. Some well-known approaches for outlier detection in the literature are frequently utilized. Peirce (1852) was the first to develop a criterion for identifying the outliers in a dataset, based on regression analysis, but this test is less well known than other methods (Peirce, 1852). The most widely used outlier method is boxplots, which has been applied in numerous fields of study. The boxplot has gained popularity in analyzing geomechanical data due to its simplicity and visual appeal. This technique has been utilized in a range of applications such as assessing the variability of rock strength and deformability parameters, as demonstrated by Bozorgzadeh et al. (2015); Heidarzadeh et al. (2021a); Shirani Faradonbeh et al. (2022); Tiryaki (2008), and also in several rockburst analyses conducted by Roy et al. (2023); Xue et al. (2020); Zhang et al. (2022). Additionally, some researchers utilized boxplots to find the outlier of machine learning analysis conducted to study slope stability (Lin et al., 2021; Manouchehrian et al., 2014; Zhou et al., 2019). Boxplots have some limitations, such as their inapplicability in greatly skewed data, which was later improved. Even though modifications have been made to address this limitation, no known geomechanical studies have utilized the modified boxplot to identify outliers. Another useful outlier detection method is Grubbs' test, which is commonly used in various engineering fields, particularly in quality control and industrial engineering (Tomaszewski et al., 2022). In civil engineering, Grubbs' test was used to identify outliers in geotechnical data, such as soil properties, rock mechanics, and foundation performance (Hunt, 2005; Pan et al., 2017). Several studies applied Grubbs' test to find the possible outliers in the shear strength data of rock at the 5% confidence level (Li et al., 2021; Shao et al., 2019). Grubbs' test assumes that the data are normally distributed, which is why it may not be appropriate for datasets that are not normally distributed. Apart from these methods, which were mostly applied on lab data, Chauvenet's test was used to find the irregular data of the Schmidt hammer test, which was confirmed

by the International Society of Rock Mechanics (Goktan & Ayday, 1993; Goktan & Gunes, 2005; Dindarloo & Siami-Irdemoosa, 2015a; Bolla & Paronuzzi, 2021). Dixon's test is another method that can be used to identify outliers and has been rarely utilized in geomechanics (Carmona et al., 2016). Overall, employing these methods helps engineers eliminate datapoints that are not representative of the underlying population and may skew the results of their analyses, thus improving the accuracy and reliability of the results.

The choice of an appropriate outlier detection method depends on the type and distribution of the data being analyzed and the objectives of the analysis. Some methods may be better suited for certain types of data, while others may be more appropriate for specific distributions. In general, a combination of methods should be used to detect outliers in geomechanical investigations because each method has its own strengths and limitations. Geomechanical data tend to be skewed because of a range of potential biases, including observer bias, instrument error, sampling bias, and inaccuracies in data interpretation. For this purpose, robust methods such as boxplots may be a proper choice because they are not sensitive to the shape of the data distribution and extreme values. However, some important tasks include the careful consideration of the assumptions and limitations of each method and the validation of the results by using multiple methods, especially when the dataset is small or when outliers have important implications.

The objective of this study is to improve the understanding of outlier detection methods in the geomechanical field by addressing two important goals. Firstly, we conduct a comprehensive overview of different outlier detection methods and evaluate their advantages and drawbacks in geomechanical domain; secondly, we determine the applicability of certain appropriate methods on real geomechanical data. For this purpose, an innovative methodology is developed to compare the applied methods. To further guide practitioners, some informative figures and flowcharts were created to provide a better understanding of the outlier detection process.

This study involved the collection and classification of all available outlier identification techniques in the literature. The methods were categorized based on their ability to analyze different

types of data and the statistical assumptions used in each method. It aimed to provide a clear explanation of the mathematical formulation of each method and then select the most appropriate outlier detection methods for the geomechanical data by assessing their suitability using specific statistical principles, which had not been applied in previous studies. This approach would help engineers select the best detection technique for their specific needs. Through a critical analysis of existing literature and a comparison of the performance of different methods, this paper will provide valuable insights into the context of outlier detection and foster the development of more effective strategies for detecting outliers in engineering applications.

2.3 Methodology

An appropriate methodology is developed to classify outlier detection methods such that their suitability in geomechanics is examined to help engineers obtain more accurate and reliable results. This methodology comprises four steps (Figure 2.1). First, a thorough review of various outlier detection techniques, including traditional statistical methods and more recent techniques, is conducted. Collecting and reviewing the different methods can establish a comprehensive understanding of various techniques and their capabilities. Second, the applicable outlier detection techniques for the field of geomechanics are classified. This step is crucial because geomechanical data can vary significantly in terms of its distribution, size, and complexity. Therefore, the choice of outlier detection technique should be based on factors such as the nature of the data and the computational requirements of each method. Third, the applicability of each method is evaluated based on its practical consideration (i.e., robustness and ease of implementation). The assessment procedure considers four elements: the capability of the methods to handle non-normal distributions of data, their responsiveness toward extreme values, their appropriateness for managing large datasets, and their recognition of skewness in the data. Finally, the strengths and weaknesses of each method are discussed by highlighting their pros and cons, thus providing a proper framework for informed decision-making in the field of geomechanics.

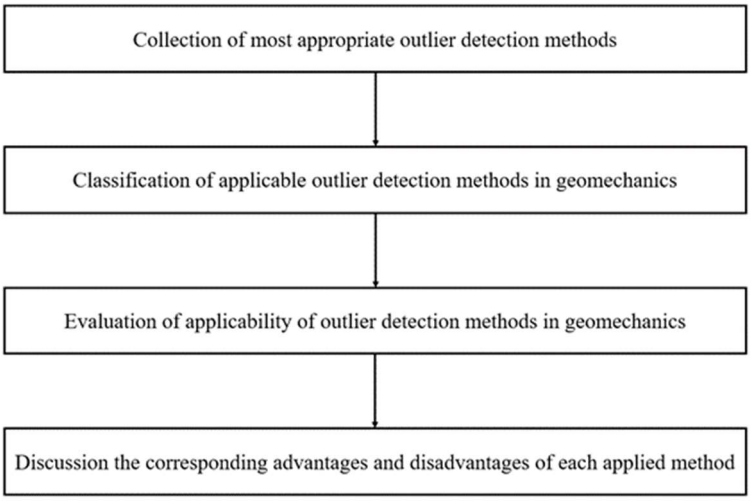

Figure 2.1 Proposed methodology for classification and assessment of outlier detection methods in geomechanics

2.4 Collection of existing outlier detection methods

We conducted a comprehensive literature review to gather information about existing methods proposed for identifying outliers. Each outlier test and its application domains were studied in detail, which includes understanding the mathematical formulation of the method, the assumptions made, and the types of data that each method is designed to work with, as well as the specific requirements of the problem that the method is designed to solve.

2.5 Classification of outlier detection methods in geomechanics

In statistics, outliers are typically detected using both univariate and multivariate methods. Univariate methods are designed to identify outliers in a single-variable dataset, while multivariate methods can detect outliers in multiple variables simultaneously, where outliers in one variable may impact other variables. Multivariate data often have a problem of swamping, which means that the presence of an outlier in one variable can swamp the presence of an outlier in another variable.

In geomechanical studies, the data can be taken as univariate because of their practicality and ease of implementation. In fact, these data include mechanical properties of rocks, such as rock strength or deformability values, in which the outliers are usually identified based on several

statistical measures such as mean, standard deviation, and percentiles. In this study, we classify the outlier methods in geomechanics into two groups: fence labeling methods and statistical tests (illustrated in Figure 2.2).

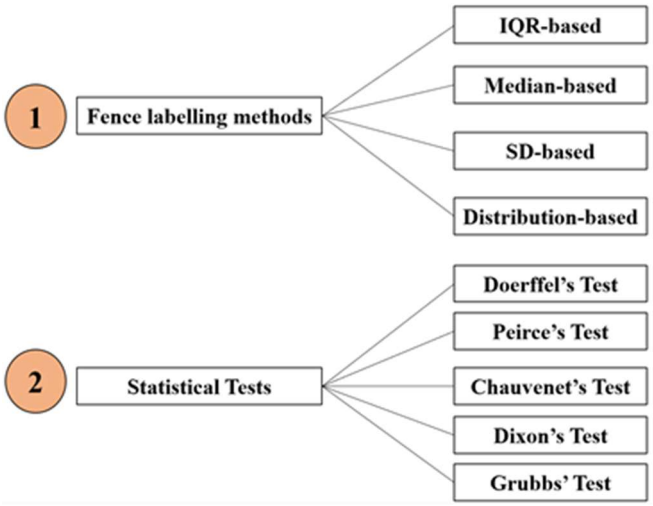

Figure 2.2 Classification of applicable outlier detection methods in geomechanics

2.5.1 Fence labeling methods

In the fence labeling approach, two fences should be created in the lower and upper thresholds of the dataset as a first step in identifying the possible outliers. Then, a range of observations is distinguished from the rest of the data such that the datapoints outside this range are considered outliers. This range can be specified through several approaches, classified in four groups: interquartile range (IQR)-, median-, SD-, and distribution-based methods (Barbato et al., 2011; Seo, 2006).

2.5.1.1 IQR-based methods

The box and whisker plot (often known as boxplot) introduced by Tukey (1977), is an outlier detection method based on IQR. The boxplot is popular among researchers in various engineering fields because of its relative efficacy, simplicity, and ease of interpretation (Almeida & Liu, 2018; Petrone et al., 2023; Sanou et al., 2022; Walker et al., 2018). It is a data visualization technique for quickly displaying data dispersion and identifying the outliers by means of two fences in the lower

and upper bounds. This method utilizes robust statistical tools such as the IQR and the first (Q1) and third (Q3) quartiles. These tools are designed to be less sensitive to extreme values in data. If data are sorted in ascending order, then Q1 represents the value below which 25% of the datapoints lie, while Q3 is the value below which 75% of the observations are situated, and IQR is the difference between Q1 and Q3 (see Figure 2.3). Outliers are detected by building the upper and lower fences using Eq. (1), beyond which the values are considered as outliers.

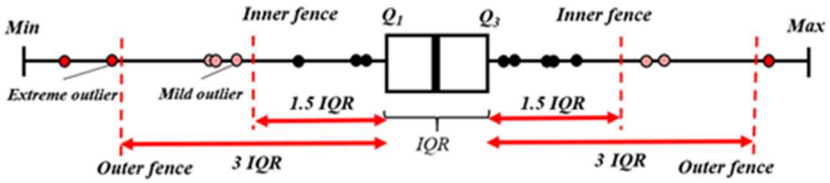

Figure 2.3 Tukey's Boxplot

Tukey proposed k = 1.5 to identify mild outliers between the inner and outer fences and k = 3.0 to label extreme outliers beyond the outer fences. Hoaglin and Iglewicz (1987) stated that using k = 1.5 may detect extra outliers (Dawson, 2011). G. Gignac (2019) suggested k = 2.2 for sample sizes between 20 and 300. Table 2.1 represents proposed formulas for IQR-based methods, such as Tukey's boxplot, and related techniques. Their timeline-based summary is briefly presented in Figure 2.4.

Table 2.1. Summary of most applicable IQR-based methods (f_L and f_U are fences in the lower and upper thresholds, respectively)

Author (year)	**Method**	**Formula**	**Equation**
Tukey (1977) (Tukey, 1977)	Traditional boxplot	$\begin{cases} f_L = Q_1 - k \times IQR \\ f_U = Q_3 + k \times IQR \end{cases}$	(1)
Barbato et al. (2011) (Barbato et al., 2011)	Log boxplot	$\begin{cases} f_L = Q_1 - 1.5 \times IQR[1 + 0.1 \log(n/10)] \\ f_U = Q_3 - 1.5 \times IQR[1 + 0.1 \log(n/10)] \end{cases}$	(2)
Schwertman and de Silva (2007) (Schwertman & de Silva, 2007)	Sequential fences	$\begin{cases} f_L = Q_2 - \frac{t_{df,\alpha_{nm}}}{k_n}(IQR) \\ f_U = Q_2 + \frac{t_{df,\alpha_{nm}}}{k_n}(IQR) \end{cases}$	(3)

		$d_f = 7.6809524 + 0.5294156n - 0.00237n^2$	(4)
Carling (2000) (Carling, 2000)	Median rule	$\begin{cases} f_L = Q_2 - 2.3\ (IQR) \\ f_U = Q_2 + 2.3\ (IQR) \end{cases}$	(5)
Kimber (1990) (Kimber, 1990)	SIQR rule	$\begin{cases} f_L = Q_1 - 1.5\ [2 \times SIQR_L] \\ f_U = Q_3 + 1.5\ [2 \times SIQR_U] \end{cases}$	(6)
		$\begin{cases} SIQR_L = (Q_2 - Q_1) \\ SIQR_U = (Q_3 - Q_2) \end{cases}$	(7)
Walker et al. (2018) (Walker et al., 2018)	Mix of SIQR and IQR	$\begin{cases} f_L = Q_1 - 1.5\ \left[IQR \times \dfrac{1 - B_c}{1 + B_c}\right] \\ f_U = Q_3 + 1.5\ \left[IQR \times \dfrac{1 + B_c}{1 - B_c}\right] \end{cases}$	(8)
		$B_c = \dfrac{SIQR_U - SIQR_L}{SIQR_U + SIQR_L}$	(9)
Hubert and Vandervieren (2008) (Hubert & Vandervieren, 2008)	MC boxplot	$if\ MC > 0 \rightarrow \begin{cases} f_L = Q_1 - 1.5e^{-4MC} IQR \\ f_U = Q_3 + 1.5e^{+3MC} IQR \end{cases}$	(10)
		$if\ MC < 0 \rightarrow \begin{cases} f_L = Q_1 - 1.5e^{-3MC} IQR \\ f_U = Q_3 + 1.5e^{+4MC} IQR \end{cases}$	(11)
		$\begin{cases} MC = \underset{x_i \le Q_2 \le x_j}{median} h\ (x_i, x_j) \\ h\ (x_i, x_j) = \dfrac{(x_j - Q_2) - (Q_2 - x_i)}{x_j - x_i} \end{cases}$	(12)

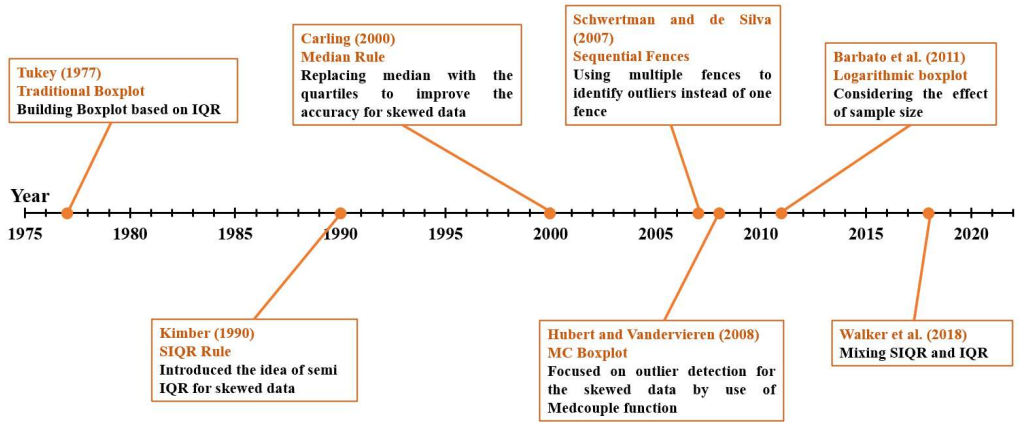

Figure 2.4 Summary of IQR-based methods

Tukey's boxplot did not consider the effect of sample size on fences, although it has a crucial effect, particularly in small sample sizes. Barbato et al. (2011) added the sample size (n) in a logarithmic relationship (Eq.2). In this modified boxplot, the data should follow a normal distribution.

Schwertman and de Silva (2007) proposed a more advanced approach called sequential fences, which divides the dataset into subgroups to consider the effect of sample size. Each subgroup has its own fences (Figure 2.5). The method creates a sequence of fences in the data, where the first fence (m = 1) is checked for minimum and maximum values, and if labeled as an outlier, then the second fence (m = 2) is focused on the second most extreme values. This process can proceed up to six fences (Schwertman & de Silva, 2007). However, the sequential fences are valid only for a sample size between 20 and 100. In this method, the second quartile (Q2) is utilized in creating fences, presented in Eqs. 3 and 4 (to calculate α_{nm} and k_n in Eq. 3; see Schwertman and de Silva (2007)). Even though it can identify outliers very accurately, the sequential fences method remains relatively obscure in the civil engineering literature.

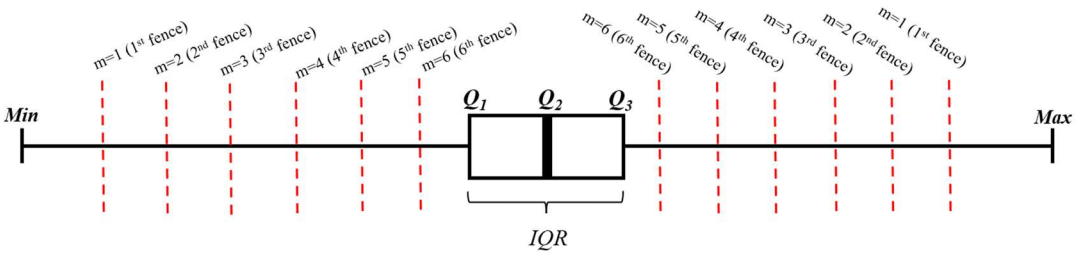

Figure 2.5 Sequential fences method

Carling (2000) modified Tukey's boxplot by replacing the median with quartiles to improve its accuracy for skewed data (see Eq. 5), but it has not gained as much popularity as the original boxplot. In skewed data, applying Tukey's boxplot may label some normal datapoints as outliers and violate the assumption of a symmetric or nearly symmetric distribution. Several studies have attempted to adjust the boxplot to be applicable for skewed datasets. The most significant methods are discussed below.

Kimber (1990) introduced the idea of semi-interquartile (SIQR) ranges (lower = $SIQR_L$ and upper = $SIQR_U$) to construct the fences for skewed data (see Eqs. 6 and 7). Figure 2.6 illustrates the SIQRs in left and right skewed data. If the samples are distributed symmetrically, then both SIQRs will become equal and similar to Tukey's fences.

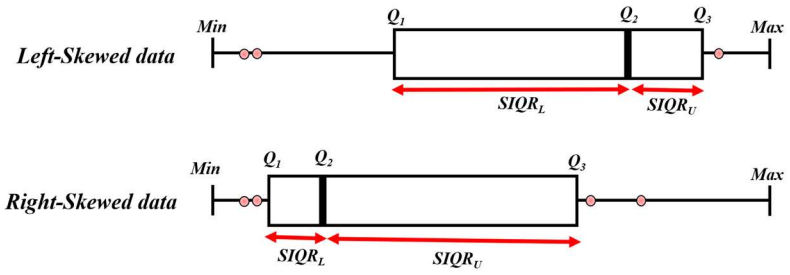

Figure 2.6 SIQR rule of Kimber for skewed data

However, some studies showed that Kimber's SIQR rule may not be widely used due to its slight effectiveness in detecting outliers in skewed data (Barnett & Cohen, 2000; Carling, 2000; Dovoedo & Chakraborti, 2015). Recently, Walker et al. (2018) combined Kimber's SIQR with Tukey's IQR such that the fences are constructed by means of a sample quartile-based measure of skewness (Bc), which uses quartiles to assess the degree of asymmetry in a dataset (see Eqs. 8 and 9). In the literature, no geomechanical study has applied the SIQR rule or Walker's boxplot.

Hubert and Vandervieren (2008) enhanced Tukey's method by incorporating the medcouple (MC) function to measure the skewness, resulting in a more robust statistical tool. The constructed fences depend on the MC value, ranging from −1 to +1 (right-skewed data $MC > 0$ and left-skewed data $MC < 0$). The relationships for MC boxplot are summarized in Eqs. 10–12. The MC boxplot technique applies to civil engineering research, particularly for analyzing data from rebound hammer and ultrasonic pulse velocity tests to conduct in situ strength assessments of concrete (Romão & Vasanelli, 2021). It is also a valuable tool for reducing errors and noise in surface displacement control data in remote sensing applications (M. Yang et al., 2022). Moreover, it detects uncertain data in digital shoreline analysis systems, contributing to the enhanced precision of results (Azad et al., 2022).

2.5.1.2 Median-based methods

Median-based methods are robust statistic techniques for locating potential outliers, and they utilize the fence labeling approach (Olewuezi, 2011). One commonly used tool is the median absolute

deviation (MAD), which serves as a reliable indicator of data dispersion that is less influenced by extreme values and non-normality (Eq. 13). Two methods, namely, 2MADe and 3MADe, classify values outside the fences as outliers. The lower and upper fences are defined in Eqs. 14–16 (Seo, 2006).

$$MAD = [median\ (|X_i - median|)] \quad (13)$$

$$2MAD_e\ method: \begin{cases} f_L = median - 2MADe \\ f_U = median + 2MADe \end{cases} \quad (14)$$

$$3MAD_e\ method: \begin{cases} f_L = median - 3MADe \\ f_U = median + 3MADe \end{cases} \quad (15)$$

$$MAD_e = 1.483\ \times MAD \quad (16)$$

Median-based outlier detection methods are utilized in various fields of civil engineering, such as correcting tunnel measurement data, improving hydrological data analysis, and correcting reference points in geodetic and surveying applications (Choi et al., 2022; Duchnowski, 2010; Hussain & Uddin, 2019).

2.5.1.3 SD-based methods

SD-based methods are basic, straightforward, and simple statistical approaches to detect outliers, and they are considered fence labeling methods. The outliers are screened by calculating the lower and upper cut-off values depending on the mean and standard deviation as defined in Eqs. 17 and 18 (Olewuezi, 2011; Seo, 2006)

$$2SD\ Method: \begin{cases} f_l = X_m - 2S \\ f_U = X_m + 2S \end{cases} \quad (17)$$

$$3SD\ Method: \begin{cases} f_l = X_m - 3S \\ f_U = X_m + 3S \end{cases} \quad (18)$$

Another SD-based method is the Z-score method, which shows how many standard deviations a suspicious extreme value is away from the mean value. However, unlike other methods, all datapoints

should have their Z-scores calculated first, and those with a Z-score of ±3 are labeled as outliers (Eq. 19)

$$Z_{score} = \frac{x_i - X_m}{S} \tag{19}$$

For it to be utilized in greatly dispersed datasets, the Z-score was modified such that the mean and standard deviation were replaced by the median and the MAD, which can now be considered a median-based method (Iglewicz & Hoaglin, 1993). In this method, the datapoints with modified Z-scores that exceed ±3.5 are outliers (Eq. 20)

$$Modified\ Z_{score} = \frac{0.6745\ (x_i - median)}{MAD} \tag{20}$$

While the SD-based methods can be sensitive to extremities, they have been employed across various disciplines, including civil and petroleum engineering, to accurately identify structural damages via the estimation of signal probability distribution and identification of anomalies (Azad et al., 2022; Wah et al., 2019). These techniques have also been utilized in geotechnical projects to precisely calculate soil parameter uncertainties and treat operational data of tunneling boring machines (Kor et al., 2021; Kottegoda & Rosso, 2008; H. Yang et al., 2022). In petroleum engineering, SD-based methods have successfully identified anomalies in experimental wax deposition values (Kamari et al., 2013). The modified Z-score method is extensively used in the oil industry to eliminate noise from field test data and reduce input data errors during directional drilling operations in offshore gas fields (Monteiro et al., 2020; Shaygan & Jamshidi, 2023).

2.5.1.4 Distribution-based approach

Gumbel (1958) devised a technique to detect outliers in heavily skewed data where extreme values are far from the majority of datapoints. In this method, the maximum values are assumed to follow the Gumbel distribution (Barnett & Lewis, 1994; Gumbel, 1958). To identify outliers, the cumulative distribution function (CDF) of the Gumbel distribution is calculated, and thresholds are specified for the upper and lower fences of the data. Any datapoint that falls outside these fences is

considered an outlier and may be investigated further or removed from the dataset (Figure 2.7). The thresholds are typically based on a desired level of significance or confidence level, such as a probability of 0.05. The approach was later extended to other extreme value distributions, such as the Fréchet, Weibull, and generalized extreme value distributions, by fitting the proper distribution to the data and calculating the related CDF. The method can be used for geomechanical datasets that follow extreme distributions. Choosing the appropriate distribution requires analyzing the data and conducting goodness-of-fit tests such as the Anderson-Darling test or the Kolmogorov–Smirnov test. Although implementing this method may be complex, it indirectly addresses the influence of data skewness by concentrating on the tails of the extreme value distributions.

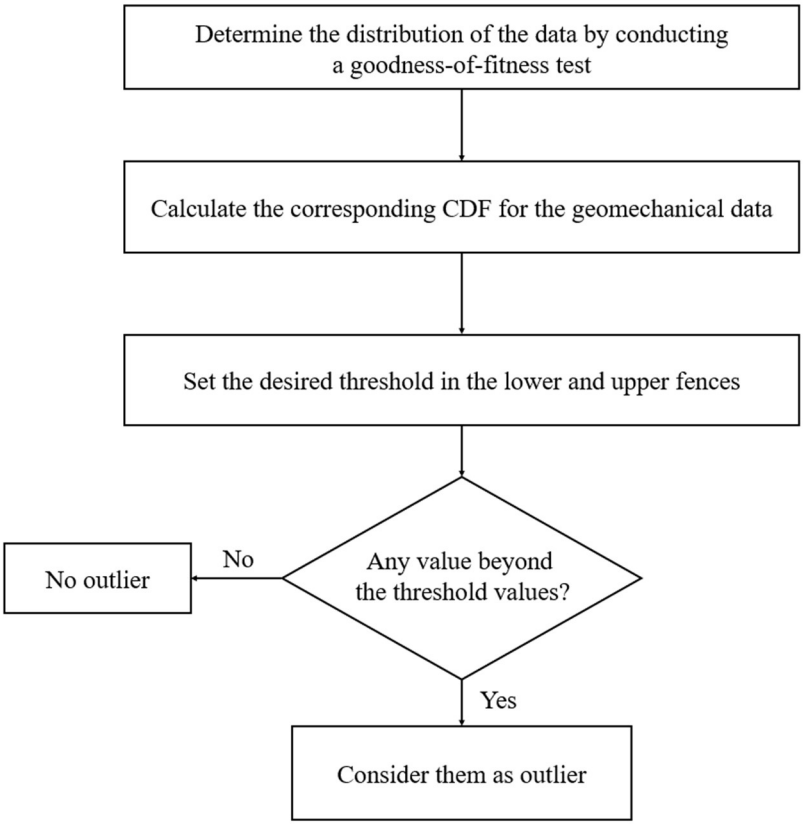

Figure 2.7 Distribution-based approach to detecting outliers

2.5.2 Statistical tests

These methods identify the outliers through statistical hypothesis tests, which are involved with null hypothesis and alternative hypothesis. In general, null hypothesis claims a statement about the data population while the alternative hypothesis rejects it (Barbato et al., 2011; Saleem et al., 2021; Seo, 2006). Examining whether an outlier is present in the dataset is possible by using this strategy. Test-based methods mostly rely on standard deviation and assume that the data follow a relatively normal distribution. In this paper, most applicable tests, including Doerffel, Peirce, Chauvenet, Dixon, and Grubbs, are reviewed, which can be applied on geomechanical data.

2.5.2.1 Doerffel's test

Doerffel's test was developed by Doerffel in 1967 to identify high extreme outliers. This test may be less applicable in geomechanical studies because it identifies high extreme outliers only

(Doerffel, 1967). The method starts by calculating the mean and standard deviation of the dataset regardless of the maximum value (Xn). Then, whether Xn is the outlier or not is checked by determining the threshold value (XA) (Figure 2.8). If Xn is identified as an outlier, then the test is re-run, focusing on the second highest value (Xn-1), to identify the next outlier, as illustrated in Figure 2.6. The "g" parameter of Doerffel's test can be calculated based on sample size, as shown in Figure 2.9.

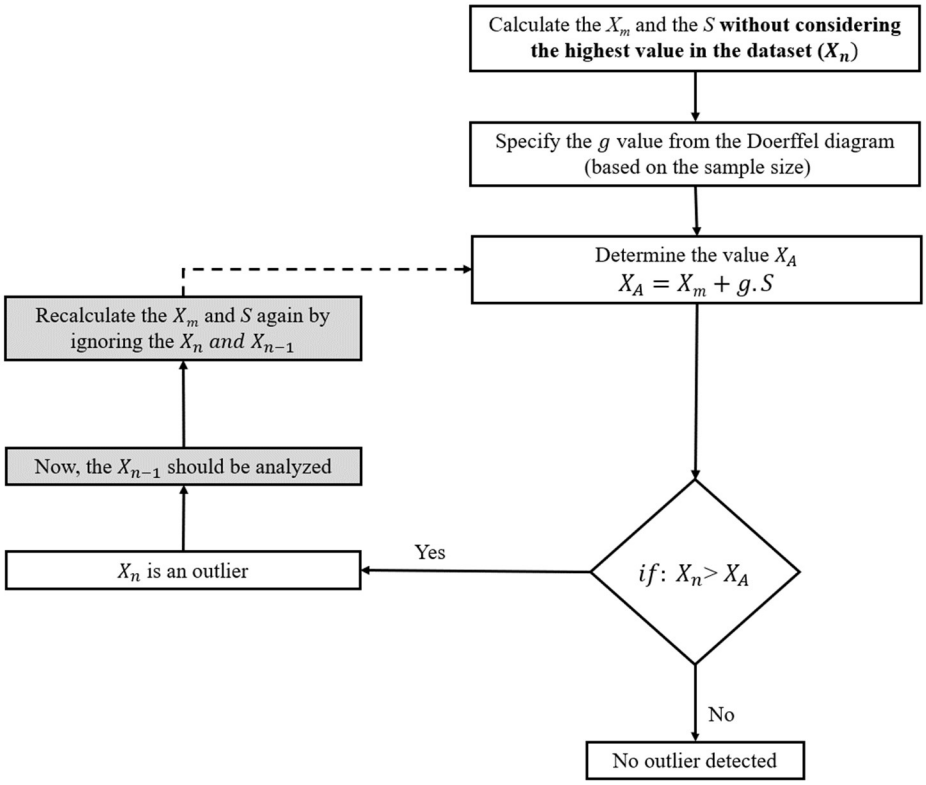

Figure 2.8 Procedure of Doerffel's test

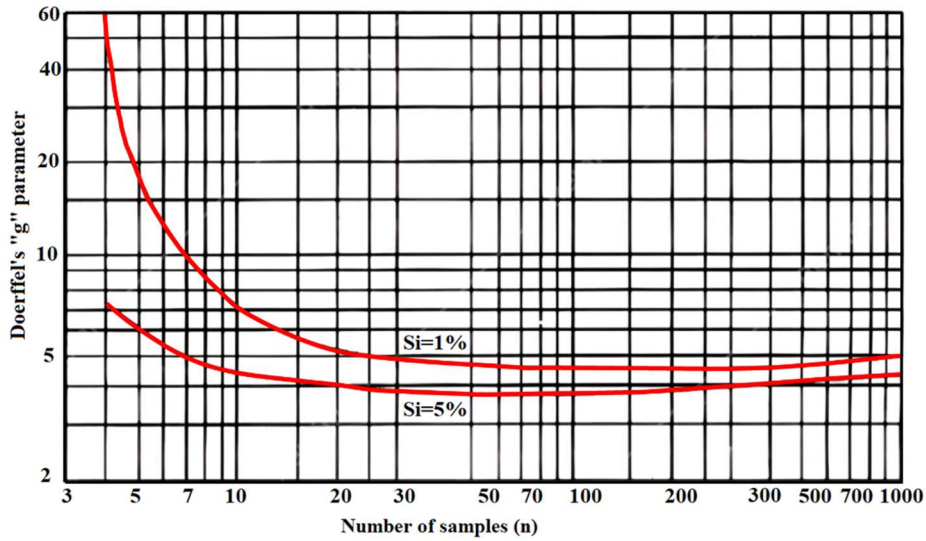

Figure 2.9 Doerffel's diagram for the "g" parameter in two confidence levels (5% and 1%) adopted from Doerffel (1967)

Doerffel's test is useful in civil and mining engineering across numerous applications. Afraei et al. (2018) utilized the technique to treat their rockburst database with confidence in two different

scenarios. Moreover, the test has provided a reliable method for determining uncertainty and correcting soil parameters (Sanou et al., 2022). In mining engineering, this method has also been instrumental in conducting geological data analysis to identify areas that have a high likelihood of containing valuable metal deposits, as evidenced in a study conducted in Iran's Kivi region (Adel et al., 2021).

2.5.2.2 Peirce's test

The Peirce criterion is widely acknowledged as the pioneering outlier detection method in the history of statistics for univariate data. It relies on the absolute difference between the extreme value (x_i) and the mean. If the absolute difference is greater than the $(R \times S)$, specified in Eq. 21, then x_i is an outlier (Peirce, 1852). This test is applicable up to 60 samples only, which was adopted in various fields of study (Rochim, 2021). The relevant equation is shown below:

$$if: |x_i - X_m| > R \times S \rightarrow x_i \; is \; an \; outlier \qquad (21)$$

where "R" is the ratio of the maximum allowable deviation of a datapoint from the mean to the standard deviation (S), which can be obtained from Peirce's table (Ross, 2003). Peirce's test is not commonly utilized in civil and mining engineering, and literature on the subject is scarce. However, Borosnyói (2014) examined the variability of in-situ rebound hardness testing of concrete by using Peirce's test. Also, Retamales et al. (2013) utilized Peirce's test to improve fragility curves in a seismic study of a building with cold-formed steel-framed gypsum partition walls.

2.5.2.3 Chauvenet's test

Similar to Peirce's test, this method uses mean and standard deviation. However, this test is applicable for up to 1,000 samples (Chauvenet, 1960). Chauvenet's test allows for only one run per dataset and involves calculating the standardized deviation from the mean (τ) for an extreme value and comparing it with the critical value (T) of Chauvenet's table, which is based on the sample size (see Gul et al. (2018)). If τ is greater than T, then this value is flagged as an outlier (Eq.22) (Limb et al., 2017).

$$if: \tau = \frac{|x_i - X_m|}{S} > T \rightarrow x_i \; is \; an \; outlier \qquad (22)$$

Chauvenet's test is widely used in geotechnical engineering to distinguish and eliminate faulty or inconsistent data, such as anomalies of rock strength measurements obtained using the Schmidt hammer test (Bolla & Paronuzzi, 2021; Goktan & Ayday, 1993; Goktan & Gunes, 2005) and reinforced concrete data in laboratory fatigue studies (Bawa & Singh, 2020; García et al., 2012; Mohammadi & Kaushik, 2005). The test is also employed in seismic studies to identify and remove outliers from a set of ground motion records (accelerograms) (Muscolino et al., 2022), thus making it critical to achieving accurate and reliable results in these applications.

2.5.2.4 Dixon's test

Dixon's outlier tests have been rarely applied due to the sample size limitation (up to 30) (Dixon, 1950). Verma et al. (2008b) enhanced these tests by extending the applicability for larger sample sizes up to 1,000. The tests are classified in two groups: the ratio of ranges and the truncated means (Verma et al., 2008b). Figure 2.10 shows the procedure of Dixon's tests based on the number of suspicious values. As shown in Table 2.2, the test statistics (TS) in each test is determined and compared with the associated critical values, as calculated by Verma et al. (2008a). Similar to other test-based methods, if the TS is greater than the critical value, then the suspicious value is an outlier.

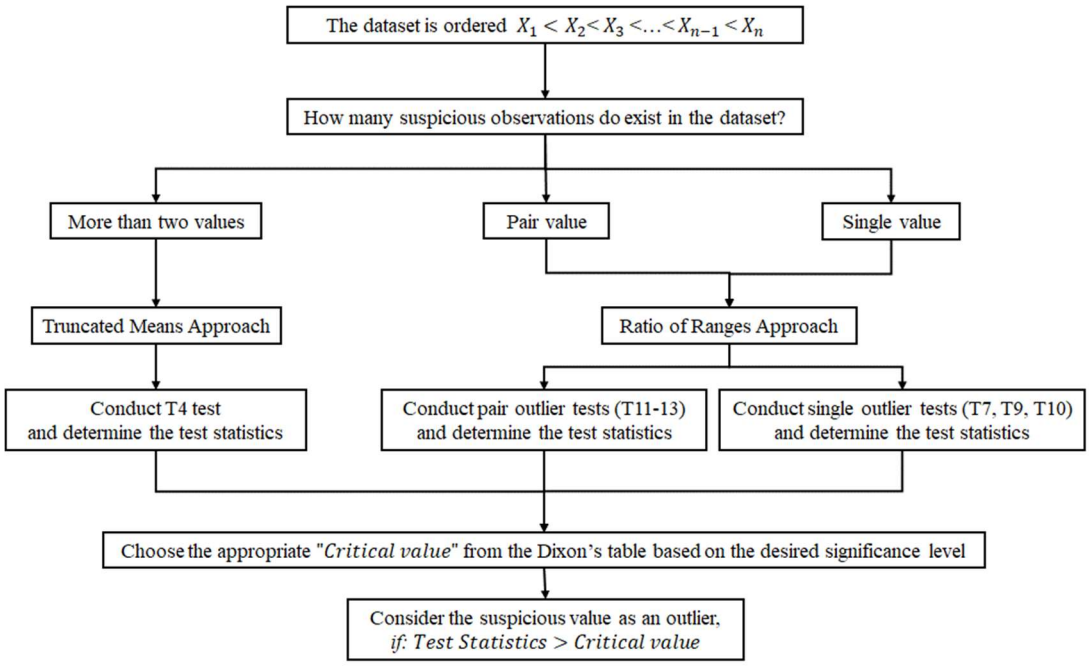

Figure 2.10 Flowchart of outlier detection by Dixon's test

Table 2.2. Dixon's tests: the ratio of ranges method (T7, T9-T12) and the truncated means method (T4)

(Verma et al., 2008b)

Test code	Upper-bound test statistic (TS)	Lower-bound test statistic (TS)	Tested values
T7	$TS7 = \frac{X_n - X_{(n-1)}}{X_n - X_1}$	*Not Applicable*	X_n
T9	$TS9_u = \frac{X_n - X_{(n-1)}}{X_n - X_2}$	$TS9_l = \frac{X_2 - X_1}{X_{(n-1)} - X_1}$	X_n, X_1
T10	$TS10_u = \frac{X_n - X_{(n-1)}}{X_n - X_3}$	$TS10_l = \frac{X_2 - X_1}{X_{n-2} - X_1}$	X_n, X_1
T11	$TS11_{up} = \frac{X_n - X_{(n-2)}}{X_n - X_1}$	$TS11_{lp} = \frac{X_3 - X_1}{X_n - X_1}$	X_1, X_2, X_n, X_{n-1}
T12	$TS12_{up} = \frac{X_n - X_{(n-2)}}{X_n - X_2}$	$TS12_{lp} = \frac{X_3 - X_1}{X_{(n-1)} - X_1}$	X_1, X_2, X_n, X_{n-1}
T13	$TS13_{up} = \frac{X_n - X_{(n-2)}}{X_n - X_3}$	$TS12_{lp} = \frac{X_3 - X_1}{X_{(n-2)} - X_1}$	X_1, X_2, X_n, X_{n-}

T4	*Lower bound*	$TS4_{1l} = \frac{S_1^2}{S^2}, S^2 = \sum_{i=1}^{n-1}(X_i - \bar{X})^2, S_1^2 = \sum_{i=2}^{n}\left(X_i - \overline{X}_1\right)^2, \left[\overline{X} = \frac{\sum_{i=1}^{n} X_i}{n}, \overline{X}_1 = \frac{\sum_{i=2}^{n} X_i}{n-1}\right]$	X_1
		$TS4_{2l} = \frac{S_{(1,2)}^2}{S^2}, S_{(1,2)}^2 = \sum_{i=3}^{n}\left(X_i - \overline{X}_{(1,\ 2)}\right)^2, \left[\overline{X}_{(1,2)} = \frac{\sum_{i=3}^{n} X_i}{n-2}\right]$	X_1, X_2
		$TS4_{3l} = \frac{S_{(1,2,3)}^2}{S^2}, S_{(1,2,3)}^2 = \sum_{i=4}^{n}\left(X_i - \overline{X}_{(1,\ 2,3)}\right)^2, \left[\overline{X}_{(1,\ 2,3)} = \frac{\sum_{i=4}^{n} X_i}{n-3}\right]$	X_1, X_2, X_3
		$TS4_{4l} = \frac{S_{(1,2,3,4)}^2}{S^2}, S_{(1,2,3,4)}^2 = \sum_{i=5}^{n}\left(X_i - \overline{X}_{(1,\ 2,3,4)}\right)^2, \left[\overline{X}_{(1,\ 2,3,4)} = \frac{\sum_{i=5}^{n} X_i}{n-4}\right]$	X_1, X_2, X_3, X_4
	Upper bound	$TS4_{1u} = \frac{S_n^2}{S^2}, S^2 = \sum_{i=1}^{n-1}(X_i - \bar{X})^2, S_n^2 = \sum_{i=1}^{n-1}\left(X_i - \overline{X}_n\right)^2, \left[\overline{X} = \frac{\sum_{i=1}^{n} X_i}{n}, \overline{X}_n = \frac{\sum_{i=1}^{n-1} X_i}{n-1}\right]$	X_n
		$TS4_{2u} = \frac{S_{(n,n-1)}^2}{S^2}, S_{(n,n-1)}^2 = \sum_{i=1}^{n-2}\left(X_i - \overline{X}_{(n,\ n-1)}\right)^2, \left[\overline{X}_{(n,n-1)} = \frac{\sum_{i=1}^{n-2} X_i}{n-2}\right]$	X_n, X_{n-1}
		$TS4_{3u} = \frac{S_{(n,n-1,n-2)}^2}{S^2}, S_{(n,n-1,n-2)}^2 = \sum_{i=1}^{n-3}(X_i - \overline{X}_{(n,\ n-1,n-2)})^2, \left[\overline{X}_{(n,n-1,n-2)} = \frac{\sum_{i=1}^{n-3} X_i}{n-3}\right]$	X_n, X_{n-1}, X_{n-2}

		$TS4_{4u} = \frac{S^2_{(n,\, n-1,n-2,n-3)}}{S^2}, S^2_{(n,\, n-1,\, n-2,n-3)} = \sum_{i=1}^{n-4}(X_i - \overline{X}_{(n,\ n-1,n-2,n-3)})^2 \ , \left[\overline{X}_{(n,\, n-1,n-2,n-3)} = \frac{\sum_{i=1}^{n-4} X_i}{n-4}\right]$	X_n, X_{n-1}, X_{n-2}, X_{n-3}
*The presented subscripts u, l, up, and lp are upper, lower, upper pair, and lower pair values, respectively			

Dixon's test is not commonly used in civil and mining engineering, but it can effectively identify and remove outliers in water engineering data, particularly in piezometric measurements (Lach, 2018). Kim et al. (2012) evaluated soil data accuracy by using this test, allowing for statistical adjustments that help improve engineering decisions.

2.5.2.5 Grubbs' test

Grubbs (1950) introduced a deviation-based approach that assumes a normality for the data, which is why it may be less appropriate for non-normal datasets. The outliers are detected by calculating the test statistics ($G_{statistics}$) for the lower and upper bounds by using mean and standard deviation. As shown in Eqs. 23 and 24, x1 and xn are minimum and maximum values in the dataset, respectively, which are called outliers if their $G_{statistics}$ are greater than the associated critical values. Grubbs' test does not have a sample size limitation for calculating the critical values ($G_{critical}$), and they can be determined for various confidence levels (α) so that the datasets can be analyzed by considering different probabilities (see Eq. 25) (Grubbs, 1950). In Eq. 25, "t" and n are the value of the Student's t-distribution and the sample size, respectively.

$$For\ lower\ bound\ \rightarrow G_{statistic} = \frac{X_m - x_1}{S} \tag{23}$$

$$For\ upper\ bound\ \rightarrow G_{statistic} = \frac{x_n - X_m}{S} \tag{24}$$

$$G_{Critical} = \frac{(n-1)}{\sqrt{n}} \sqrt{\frac{t^2_{(\alpha/n,n-2)}}{n-2+t^2_{(\alpha/n,n-2)}}} \quad (25)$$

Several geomechanical studies applied Grubbs' test (Bao et al., 2013). In the underground mining field, this test was conducted to treat the hang-up and secondary breaking vulnerability data collected for drawpoints in a mining operation, ensuring more accurate results (Garces et al., 2020). In addition, this method was successfully utilized to correct in-situ cone geotechnical tests and evaluate the shear strength parameters in triaxial testing (Lu et al., 2022; Wei, 2013).

2.6 Evaluation of applicability of outlier methods in geomechanics

In geomechanical data, the selection of the best outlier detection method should be accompanied by an engineering judgment considering the characteristics of the data and the desired outcome of the analysis. As illustrated in Figure 2.11, when the suitability of using outlier detection methods for analyzing geomechanical data is assessed, several key factors should be taken into consideration.

- An important factor to consider in the suitability of outlier detection methods is the shape of data distribution. Geomechanical data are generally assumed to be normally distributed. In reality, however, laboratory test results such as UCS values naturally show large variations, which leads them to be greatly skewed. Thus, the visual shape of the data frequencies should be primarily analyzed. Certain outlier detection methods, such as Doerffel, Chauvenet and Grubbs are suitable for symmetrically distributed data only (Chauvenet, 1960; Grubbs, 1950; Schwertman & de Silva, 2007). Many of the most applicable methods can be used for either symmetric or asymmetric distributions. Although most fence labeling methods do not explicitly consider the data distribution, they rely on several statistics that are related to the distribution. Therefore, methods with no distribution limitations may be better suited for geomechanical data.
- When outlier detection methods are evaluated, their sensitivity to extreme values is an important detail to consider. Deviation-based outlier methods, which incorporate standard

deviation in their formulas, are more sensitive to the presence of extreme values in the dataset (Barbato et al., 2011; G. Gignac, 2019). Thus, they may not be suitable for analyzing geomechanical data. However, some approaches such as IQR-based methods exhibit robustness against outliers. In addition, methods that use the median value instead of the mean value are generally less susceptible to violations of the dataset (Hoaglin & Iglewicz, 1987).

- The number of samples in a geomechanical dataset also affects the applicability of outlier detection methods. While geomechanical datasets may not have a large number of samples, certain statistical tests such as Peirce's test cannot be applied to sample sizes greater than 60 (Seo, 2006). For larger datasets, IQR- and median-based methods are more suitable because they can be applied to any sample size without being influenced by extreme datapoints (Dawson, 2011).
- Geomechanical data tend to be skewed because of their significant inherent variability, which is why a proper outlier method should address the effect of skewness. However, few methods such as MC boxplot, SIQR rule, and the mix of the SIQR and IQR methods consider the skewness by modifying the fences (Hubert & Vandervieren, 2008; Walker et al., 2018). Furthermore, the distribution-based approach indirectly takes the data skewness into account because it focuses on the distribution tails and can identify extreme outliers that are far away from the rest of the data. However, many outlier methods are still used for heavily skewed data.

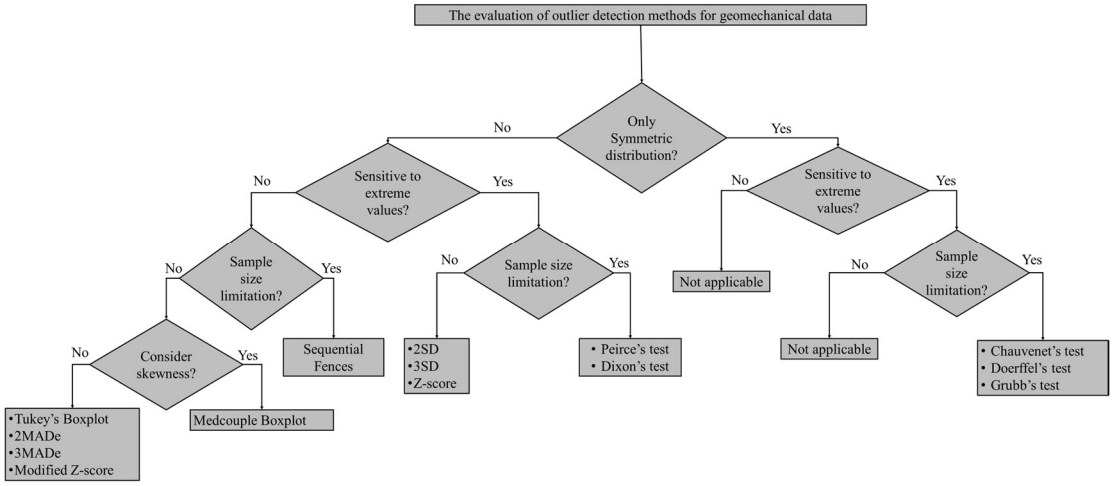

Figure 2.11 Flowchart of applicability of outlier detection methods for geomechanical data

To test the performance of the methods, we applied the reviewed outlier detection methods on actual data of uniaxial compressive strength (UCS) of rock samples extracted from Westwood Mine in Quebec, Canada. The dataset comprised 157 samples with a wide range of values, spanning from 32.10 MPa to 371.10 MPa. In the selection of an appropriate outlier detection method for UCS data, an important detail to consider is the expected mechanical behavior of the rock type in the dataset, which in this case consists of metamorphic rocks. Table 2.3 presents the results of all outlier detection methods applied on the UCS data. The confidence intervals for each method indicate a reliable range of UCS values, with any values falling outside this range being considered as outliers. Methods such as Peirce, Grubbs, and sequential fences were unsuitable for the UCS data because of the large sample size. However, in the selection of appropriate methods for the UCS data, the lower and upper threshold values should be aligned with rock mechanics principles because negative UCS values are meaningless. As illustrated in Figure 2.12, certain methods, such as Tukey's boxplot (using 3IQR and 2.2IQR), 3MADe, and 3SD, may not be able to detect outliers in the lower threshold due to their negative value. In addition, the suggested lower threshold for the modified boxplot (which is a mix of the SIQR and IQR methods) may not represent a reasonable UCS value. However, the MC boxplot, 2MADe, and 2SD methods provided reasonable UCS thresholds. We also applied distribution-based method on the UCS data. In this method, we first conducted the Anderson-Darling goodness-of-fit

test to determine the most fitted distributions for the dataset. The test showed that the data follow normal and logistic distributions. Then, we determined the associated CDF graphs, as illustrated in Figure 2.13. The threshold values of UCS (fences) should be computed based on the confidence level (0.05) to identify the outliers, and datapoints beyond this range were assumed as outliers, as presented in Table 2.3. In other statistical tests, we observed that Doerffel's test was not able to detect outliers in the lower threshold. Several methods, such as Dixon (ratio of ranges), Chauvenet, Z-score, and modified Z-score, were too conservative in labeling the outliers.

Table 2.3. Summary of outlier detection methods applied on the actual UCS dataset (Note: LB and UB are the lower and upper bounds of the dataset, respectively)

Outlier detection method	Confidence interval (MPa)	Number of outliers	
		LB	UB
Tukey's boxplot (1.5 IQR)	26.10 < UCS < 266.10	0	10
Tukey's boxplot (3.0 IQR)	−63.90 < UCS < 356.10	0	1
Tukey's boxplot (2.2 IQR)	−15.90 < UCS < 308.10	0	2
Log boxplot	15.34 < UCS < 276.86	0	5
Sequential fences	NA*	NA	NA
Median rule	11.80 < UCS < 287.80	0	4
MC boxplot	32.29 < UCS < 271.04	0	8
SIQR rule	15.00 < UCS < 255.00	0	11
Mix of SIQR and IQR	0.78 < UCS < 246.34	0	13
2MADe method	49.85 < UCS < 249.75	3	12
3MADe method	−0.13 < UCS < 349.71	0	1
2SD method	40.86 < UCS < 270.30	1	8
3SD method	−16.50 < UCS < 327.67	0	2
Z-score	−3.00 < Z-score < +3.00	0	2
Modified Z-score	−3.50 < modified Z-score < +3.50	0	2
Distribution-based approach	43.15 < UCS < 268.00	1	9

Doerffel's test	Statistical tests identify outliers based on statistical hypotheses	NA	1
Peirce's test		NA	NA
Chauvenet's test		0	1
Dixon's test (ratio of ranges)		0	0
Dixon's test (truncated means)		4	0
Grubbs' test		NA	NA

*Not applicable

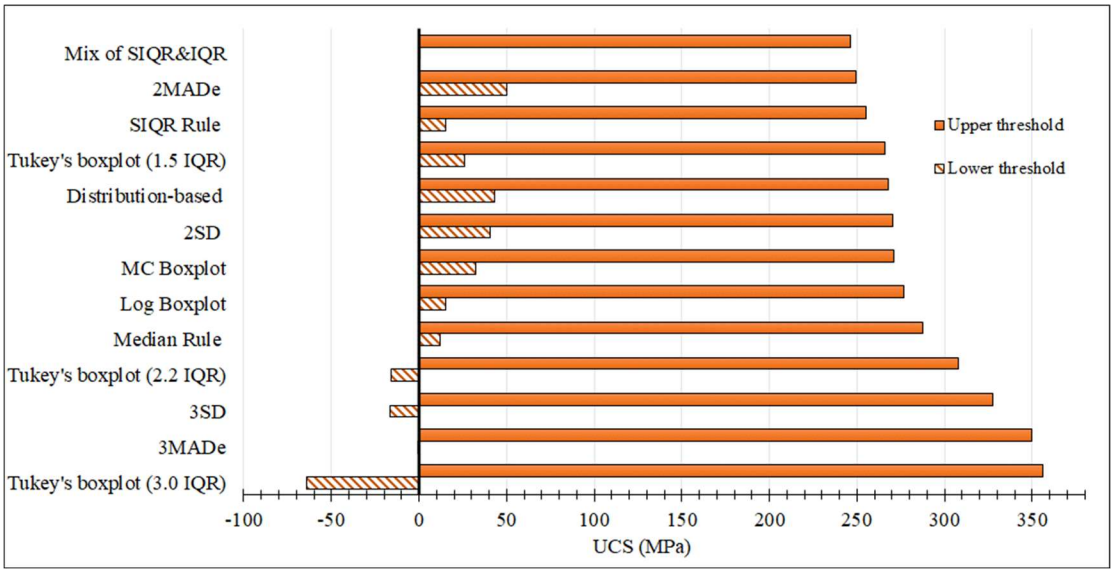

Figure 2.12 Estimated confidence range for the UCS data based on various outlier detection methods

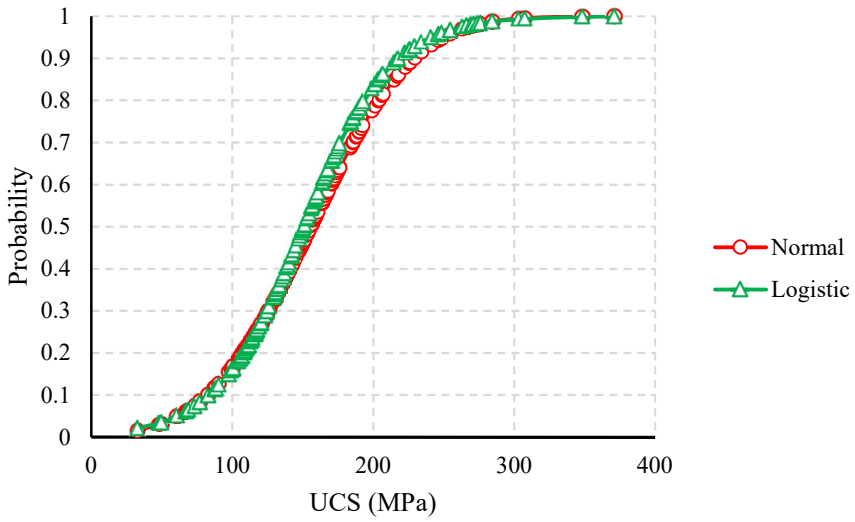

Figure 2.13 CDF of most fitted distributions on the UCS data

Notably, the selection of appropriate software for identifying outliers in geomechanical datasets depends on the practitioner's specific requirements and preferences, as well as the complexity of the data and the outlier detection method employed. Various computer programs offer built-in functions for outlier detection, such as boxplots, Z-scores, and modified Z-scores, which can facilitate the data treatment process and aid geomechanical practitioners in identifying outliers in their laboratory or field data. Popular software options in geomechanics include Microsoft Excel and its @Risk add-in

tool, Minitab, SPSS, and MATLAB (MATLAB R2022a, 2022; Minitab, 2021; @Risk, 2022; SPSS, 2022).

2.7 Discussion

Data treatment processes and outlier detection methods can sometimes be undervalued in geomechanical projects where there may not be a significant amount of lab data to analyze. However, inaccurate or unreliable data can lead to faulty design decisions that increase the risk of safety hazards, project delays, and catastrophic failure. Conducting tests on rock samples is costly, but making design decisions on inaccurate data can incur even higher costs. Therefore, an essential step for engineers and practitioners is to prioritize the data treatment process, including the selection of appropriate outlier detection methods in geomechanical projects. By using appropriate outlier detection methods, engineers can obtain a more accurate representation of the true range of variation in their data and make more informed design decisions. This approach can lead to more efficient designs and cost savings without compromising safety or reliability.

The selection of an appropriate outlier detection method in geomechanical projects depends on various factors such as data distribution, sample size, and other considerations. Each method has its own advantages and disadvantages. Statistical methods rely on a statistical model of the data and hypothesis testing to determine whether a data point is an outlier or not. One of the main advantages of statistical methods is their ability to provide a clear statistical basis for identifying outliers, which is particularly useful when dealing with large datasets. However, certain statistical tests such as Peirce and Grubbs are not suitable for large sample sizes, while Doerffel's test cannot detect outliers in the lower bound, which can be a significant drawback. In addition, statistical techniques have limitations with non-symmetrical or skewed data distribution, thus posing challenges to the selection of an appropriate statistical model, which may result in misidentifying outliers.

Conversely, fence labeling methods are often popular among geomechanical practitioners because they mostly provide graphical representations, such as boxplots or scatterplots, rather than

relying solely on statistical methods. These methods can also be robust to large data variations, especially the ones that use the median and MAD as tools to define the fences.

Geomechanical datasets can often exhibit significant uncertainties because of the complex nature of rock formation, making IQR- and median-based methods particularly suitable for identifying outliers. Accurate analysis and characterization of rock properties depend on the identification and treatment of outliers, making outlier detection methods an essential part of geomechanical data analysis. When dealing with normally distributed data, SD-based methods are simple and user-friendly options for detecting outliers in geomechanical data. However, if the data do not follow a normal distribution, then distribution-based methods may be more effective because they identify outliers on the basis of the behavior of extreme values and are thus a useful tool for datasets with skewed or heavy-tailed distributions.

The IQR-based methods are well known in geomechanics, with Tukey's boxplot being a popular tool because of its ability to provide a visual representation of the data distribution, which makes identifying outliers and understanding the overall pattern of the data easier. However, Tukey's boxplot has limitations because it relies on a single fence to identify outliers, which may not be suitable for certain geomechanical datasets. Modified boxplots such as the sequential fences method have been developed to address this issue.

The sequential fences method allows for the creation of multiple fences for the data, potentially providing more reliable identification of outliers. By utilizing a sequence of fences, the sequential fences method can better capture the distribution of the data and identify outliers that may be missed by other methods. However, the sequential fences method is limited to datasets with a sample size of less than 100.

Furthermore, the traditional boxplot has a limitation in heavily skewed data because it does not consider the skewness. Modified boxplots are designed to address the limitations of traditional boxplots by incorporating robust tools such as the SIQR or MC function, which allow the skewness and definition of fence limits to be computed. This approach is particularly beneficial in the case of

heavily skewed data because it can provide practitioners with more accurate results. Modified boxplots are more sensitive to outliers than traditional boxplots because they can identify outliers located far from the median or in the tails of the distribution. However, constructing and interpreting modified boxplots may require more advanced statistical techniques.

2.8 Conclusion

In this review paper, we thoroughly analyzed various outlier detection methods available in the literature and proposed a methodology for categorizing and assessing their suitability for geomechanical data. We classified the outlier detection methods into two main categories: fence labeling methods and statistical tests. Fence labeling methods identify outliers by defining upper and lower thresholds and by considering any data point outside this range as an outlier. Statistical tests utilize hypothesis testing by comparing the test statistics with the corresponding critical value to identify outliers.

An important detail to note is that the effectiveness of these methods largely depends on the nature of geomechanical data and requires engineering judgment to determine the most appropriate method. Therefore, a recommended approach when choosing an appropriate outlier detection method is to consider the specific characteristics of the data. We also developed a flowchart to guide geomechanical practitioners in selecting the appropriate outlier detection method based on their specific needs and the complexity of their data. This flowchart considers important considerations for geomechanical data and can be used as a helpful tool for practitioners in identifying outliers in their laboratory or field data.

The applicability of these methods in geomechanical data have been evaluated and we found that statistical tests are not as effective in detecting outliers because of their inability to handle skewed data and limited sample sizes. However, modified IQR-based methods, such as the MC boxplot and SIQR rule, appear to be the most accurate outlier detection methods in geomechanical data because they take into account the significant impact of skewness in outlier detection. This review paper provides valuable insights into the selection and application of outlier detection methods for

geomechanical data, thus possibly facilitating accurate data analysis and interpretation. Future research can further investigate and improve upon these findings to develop more robust and effective outlier detection methods for geomechanical data.

Author Contributions: Conceptualization, B.D. and A.S.; methodology, B.D. and A.S.; software, B.D.; validation, B.D., A.S. and S.H.; investigation, B.D.; writing—original draft preparation, B.D.; review and editing, B.D, S.H. and A.S.; supervision, A.S. and S.H. All authors have read and agreed to the agreed to the published version of the manuscript.

Funding: The authors would like to thank the Natural Sciences and Engineering Research Council of Canada (NSERC), IAMGOLD Corporation, and Westwood mine for supporting and funding this research (Grant number: RDCPJ 520428–17) and also NSERC discovery funding: RGPIN-2019-06693.

Data Availability Statement: Not applicable.

Conflicts of Interest: The authors declare no conflict of interest.

CHAPTER 3

The geomechanical behavior of metamorphic rocks exhibits significant variability, influenced by various factors such as mineral composition, schistosity angle, and localized geological conditions. This chapter examines these sources of uncertainty by combining petrographic analyses with extensive laboratory testing to quantify the effects of these variabilities on the mechanical properties of rocks, underscoring the challenges of identifying rockburst-prone zones. By addressing these variabilities systematically, the study enhances the accuracy and reliability of numerical models used in rockburst prediction. It serves as a bridge between raw data processing and advanced analyses, ensuring that geomechanical uncertainties are properly accounted for in the rockburst analysis.

Article 2: Determination of Uncertainties of Geomechanical Parameters of Metamorphic Rocks Using Petrographic Analyses

Behzad Dastjerdy [1, *], Ali Saeidi [1] and Shahriyar Heidarzadeh [2]

[1] Department of Applied Sciences, University of Quebec at Chicoutimi, Saguenay, QC G7H 2B1, Canada

[2] Rock Mechanics Engineer at SNC-Lavalin, Montreal, QC H2Z 1Z3, Canada

Published, Journal of Rock Mechanics and Geotechnical Engineering 2024, *16*(2), 345-364.

https://doi.org/10.1016/j.jrmge.2023.09.011

3.1 Abstract

Geomechanical parameters of intact metamorphic rocks determined from laboratory testing remain highly uncertain because of the great intrinsic variability associated to the degrees of metamorphism. The aim of this paper is to develop a proper methodology to analyze the uncertainties of geomechanical characteristics by focusing on three domains, namely, data treatment process, schistosity angle, and mineralogy. First, the variabilities of the geomechanical laboratory data of Westwood Mine (Quebec, Canada) were examined statistically by applying different data treatment techniques, through which the most suitable outlier methods were selected for each parameter using multiple decision-making criteria and engineering judgment. Results indicated that some methods exhibited better performance in identifying the possible outliers, although several others were unsuccessful because of their limitation in large sample size. The well-known Boxplot method might not be the best outlier method for most geomechanical parameters because its calculated confidence range was not acceptable according to engineering judgment. However, several approaches, including adjusted Boxplot, 2MADe, and 2SD, worked very well in the detection of true outliers. Also, the statistical tests indicate that the best-fitting probability distribution function for geomechanical intact parameters might not be the normal distribution, unlike what is assumed in most geomechanical

studies. Moreover, the negative effects of schistosity angle on the uniaxial compressive strength (UCS) variabilities were reduced by excluding the samples within a specific angle range where the UCS data present the highest variation. Finally, a petrographic analysis was conducted to assess the associated uncertainties such that a logical link was found between the dispersion and the variabilities of hard and soft minerals.

Keywords: Intact rock parameters, Natural variabilities, Outlier detection methods, Uncertainties, Westwood Mine, Mineralogy

3.2 Introduction

The strength and deformability parameters of rock masses are of great significance when dealing with site characterization in geomechanical projects. One major source of complication in rock mass characterization is the natural variability of intact rocks, which can generate considerable uncertainties in different types of rocks. Therefore, the geomechanical parameters of intact rocks must be carefully characterized because they can affect the analysis of the mechanical behavior of rock mass. In rock mechanics literature, several approaches can quantify the mechanical properties of intact rocks, which mostly rely on laboratory experiments (Cai et al., 2004; Pepe et al., 2017a; Sonmez et al., 2004). Considering that the intact rock samples are natural materials, they might show a great deal of inherent variabilities. Thus, the experimental results of intact rocks are scattered inevitably even when the rock samples are prepared well and the testing procedures are followed accurately (Pepe et al., 2017a). In fact, these dispersed results should be assumed as raw data, which must be treated accurately to reduce the existing uncertainties in geomechanical analysis (F Agliardi et al., 2016; Chen et al., 2021; Pereira, F da Silva, et al., 2021). From the statistical perspective, these extreme abnormal values are called outliers, which considerably diverge from the mainstream of the other values (Barbato et al., 2011; Kannan et al., 2015; Saleem et al., 2021).

Therefore, a key step to studying the uncertainties of geomechanical data is to focus on the treatment of very extreme values in a dataset, and prior to the determination of the intact rock

parameters, a suitable data treatment process for the laboratory results must be taken to reduce the uncertainties of geomechanical parameters. In underground rock mechanics, several statistical techniques were applied to treat the geomechanical laboratory data and even field data. With regard to the geomechanical field test, several researchers have treated the estimated values of UCS and Young's modulus via the Schmidt hammer test using a statistical approach known as Chauvenet's criterion, which is a treatment method based on mean and standard deviation (Bolla & Paronuzzi, 2021; Goktan & Ayday, 1993; Goktan & Gunes, 2005). Moreover, a very useful statistical technique called as Grubbs' test was applied by some scholars to treat data in various geomechanical investigations, ranging from determining the shear strength parameters of rocks and the uncertainties related to the statistical analysis of surface settlement in shallow tunnels (Dindarloo & Siami-Irdemoosa, 2015b; Shao et al., 2019). Chen, et al. (2021) also suggested an outlier detection algorithm based on the Z-score method to screen the rock mechanics parameters, such as Young's modulus and Poisson's ratio (Chen et al., 2021). However, the boxplot method, in which some important studies focusing on the treatment of laboratory intact data are mentioned herein, has been the most common outlier method used in geomechanical studies (Carter, 2021; Hassanpour et al., 2010; Heidarzadeh et al., 2021b; Manouchehrian et al., 2012; Tiryaki, 2008). In addition, this method was used to treat the rockburst index data to predict rockburst occurrences (Li et al., 2022; Liang et al., 2020; Xue et al., 2020; Zhou, Li, & Mitri, 2016); however, the boxplot method may not be the most suitable approach for greatly skewed data (Walker et al., 2018). Therefore, the fundamental methodology for applying a data treatment technique remains unclear, and although the application of an inappropriate outlier method can mislead the analysis of intact rock uncertainties, so far, no research has focused on providing a procedure to select the most appropriate treatment technique for geomechanical studies. In fact, the applied method should assure that the identified outliers are physically justifiable. As a result, a reasonable data treatment process should be considered to have a reliable and confident engineering judgment on the evaluation of the uncertainties of the tested rock specimens.

Furthermore, the huge impact of geomechanical intact parameters on the occurrence of rockburst should not be neglected because the research in rockburst detection heavily relies on quantifying the uncertainties of geomechanical intact characteristics; moreover, rockburst, as an abrupt and violent rock failure, is closely tied to intact rock parameters (Sainsbury, 2020). As a result, the accompanying uncertainties must be investigated thoroughly to minimize them reasonably so that the researchers can examine the rockburst events more confidently by having well-defined geomechanical parameters.

This paper investigates the significant uncertainties of geomechanical intact parameters by developing an appropriate methodology based on statistical and mineralogical analyses. In this methodology, the uncertainties are completely analyzed in three different parts. In the first part, the effects of various data treatment techniques on the characterization of geomechanical parameters are analyzed comprehensively, and the best outlier detection method for each intact parameter is determined statistically. Then, the significant impact of schistosity angle on the related uncertainties of rock strength is fully explored in the second part. Lastly, a petrographic study is carried out to establish a meaningful link between the uncertainties of minerals and intact rock parameters.

3.3 Methodology

The methodology used in this study aims to comprehensively investigate the uncertainties associated with geomechanical parameters of intact rock through an integrated framework of statistical data treatment techniques, analysis of schistosity effects, and thorough examination of mineralogy. The methodology consists of five main steps (Figure 3.1), designed to progressively minimize uncertainties and establish meaningful links between the influential factors.

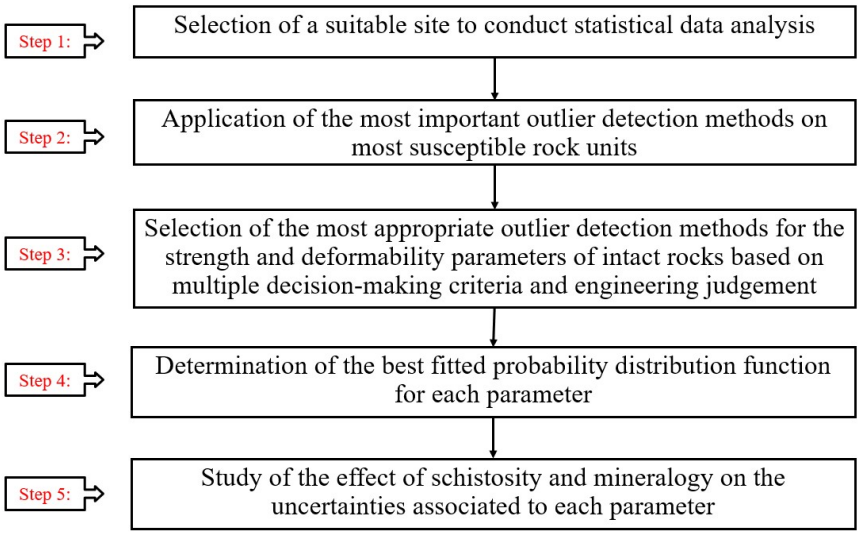

Figure 3.1 Methodology for determining uncertainties associated to the geomechanical parameters of intact rock

The first step concerns the selection of an appropriate mining site. This suggested methodology can be properly implemented to study the uncertainties of geomechanical intact parameters. For this purpose, Westwood underground mine, which is recognized as a rockburst-prone mine in Canada located in a regionally metamorphosed area, has been selected to conduct a statistical analysis in the variability of geomechanical parameters of intact rocks (Bouzeran et al., 2019; Kalenchuk et al., 2017; Tremblay, 2020). Moreover, given that the load-bearing capacity of intact rock is considered a major source of rockbursts, the characterization of the geomechanical intact parameters and their uncertainties is necessary and will be carried out in Step 2 through a comprehensive statistical analysis based on the data treatment techniques. In fact, to analyze uncertainties, 17 statistical data treatment methods are applied on every geomechanical parameter dataset in rockburst-prone rock units to identify possible outliers. By using the multiple decision-making criteria and the engineering judgement in Step 3, we have selected the most realistic methods to investigate the related uncertainties of geomechanical parameters of metamorphic rocks. Moving to Step 4, the best fitted probability distribution function is assigned to the treated dataset of the geomechanical parameters by applying goodness-of-fit tests. In contrast to the normality assumption used in many studies, our

analysis recognizes that the most precise probability distribution function (PDF) for the geomechanical parameters of intact rocks may not be the normal distribution, which will be fully analyzed in this paper. While the statistical data treatment techniques help reducing uncertainties, the remnants could be significantly influenced by the schistosity angle, which is the focus of Step 5. By analyzing the impact of schistosity angle on rock strength uncertainties, we identify a specific range of schistosity values within which the uniaxial compressive strength (UCS) exhibits the highest variations. By excluding the UCS values within this range, we could substantially mitigate the UCS uncertainty. Moreover, the analysis of mineralogy in Step 5 reveals a logical connection between the dispersion of hard and soft minerals and the variabilities of intact geomechanical parameters. By examining the mineral composition and its variation percentage, we aim to establish a meaningful link between the geomechanical parameter variations and the percentage distribution of different minerals. By meticulously integrating these three parts within the methodology, starting from statistical data treatment techniques, followed by the investigation of schistosity effects, and concluding with the examination of mineralogy, we strive to minimize the associated uncertainties of geomechanical intact parameters in a comprehensive manner. In overall, this integrated approach ensures that the uncertainties of geomechanical parameters are thoroughly analyzed, providing valuable insights into the variability and characteristics of metamorphic rocks.

3.4 Westwood Mine

Westwood Mine, which is situated in Abitibi greenstone belt, is one of the latest major deposit discoveries in Canada (Figure 3.2). This gold mine, which commercially begun its production in 2014, is located approximately 420 km northwest of Montreal in the province of Quebec (IAMGOLD, 2019a; Tremblay, 2020). The rock mass at the Westwood Mine is completely affected by regional metamorphism, which has impacted all lithological units changing from greenschist facies to the lower amphibolite facies. Also, Yergeau (2015a) recently developed a lithological classification system based on the mineral compositions and volcanic facies, in which six principal rock units (Unit 1 to 6) exist at the Westwood Mine, which are mainly in the east-west direction with steep to moderate

dips toward the south (Yergeau, 2015a). In the Westwood Mine, three lithological units (e.g., units 3, 4, and 5) are recognized as the most susceptible units to rockburst, in which the characterization of geomechanical intact parameters and the associated uncertainties would contribute to the probabilistic analysis of rockburst at this rockburst-prone mine (Tremblay, 2020).

Figure 3.2 Westwood Mine location in Quebec Province, Canada (IAMGOLD, 2019a)

In this study, we have used the geomechanical data of 47 drilled boreholes in rockburst-prone units of the Westwood Mine by conducting 465 geomechanical laboratory tests at the Université du Québec à Chicoutimi, Canada (UQAC) (Tremblay, 2020). All core samples were extracted from units 3, 4, and 5, where the recent rockburst occurrences caused the closure of the entire mine in previous years (Bouzeran et al., 2019; Kalenchuk et al., 2017; Tremblay, 2020). Table 3.1 presents the type and the number of laboratory tests that refer to each lithological unit, and a “meta” prefix was added to the name of the rock samples because the rock mass was partially metamorphosed. In addition, the sample parameters, such as the sample mean and variance, can be accepted as the population mean and variance because the number of samples in this research is higher than 30 (Gill et al., 2005; Spiegel, 1966).

The initial estimations of geomechanical parameters based on the sub-units and main units are presented in Figures 3.3–3.5. The mean value of all parameters and their associated uncertainties are assumed to be based on the main units because no considerable difference between the values of sub-units and main units are observed, as depicted in Figures 3.3-3.5.

Table 3.1. Type and number of laboratory tests conducted on the analyzed rock units (Units 3, 4, and 5) at the Westwood Mine

Location		Number of Tests					Rock type
		Total	UCS	Triaxial		Brazilian	
Unit	Sub-unit			(5MPa confinement)	(15MPa confinement)		
Unit 3	U3-3-0	97	47	12	11	27	Meta-Basalt, Meta-Andesite
	U3-3-1	26	14	4	0	8	
All Unit 3		123	61	16	11	35	
Unit 4	U4-2-0	80	45	8	7	20	Meta-Andesite, Meta-Dacite
	U4-3-0	81	43	12	10	16	Meta-Rhyodacite, Meta-Rhyolite
	U4-4-0	80	58	7	7	8	Meta-Basalt, Meta-Andesite
	U4-4-1	20	11	2	1	6	Meta-Gabbro
All Unit 4		261	157	29	25	50	
Unit 5	U5-1-2	25	22	1	2	0	Meta-Andesite, Meta-Dacite
	U5-1-3	15	13	1	1	0	Meta-Basalt, Meta-Andesite
	U5-1-4	10	10	0	0	0	Meta-Dacite
	U5-1-5	2	2	0	0	0	Meta-Dacite
	U5-2-1	10	8	1	1	0	Meta-Dacite, Meta-Rhyodacite
	U5-3-1	2	2	0	0	0	Meta-Rhyolite
	U5-3-2	2	2	0	0	0	Meta-Rhyolite
	U5-4-0	13	9	1	1	2	Meta-Basalt
	U5-5-3	2	2	0	0	0	Meta-Rhyodacite, Meta-Rhyolite
All Unit 5		81	70	4	5	2	

Total	465	288	49	41	87	
			90			

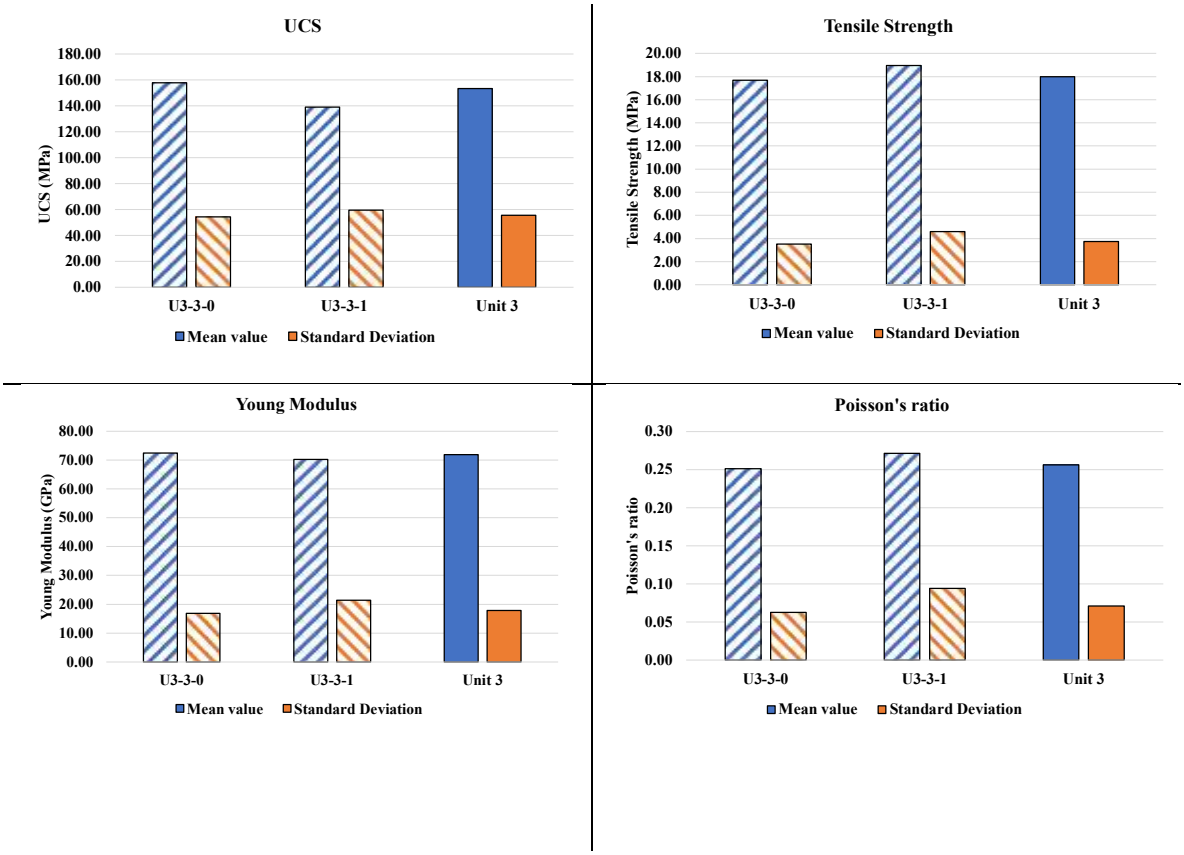

Figure 3.3 Comparison of mean and standard deviation values of the geomechanical intact parameters for Unit 3 and its sub-units

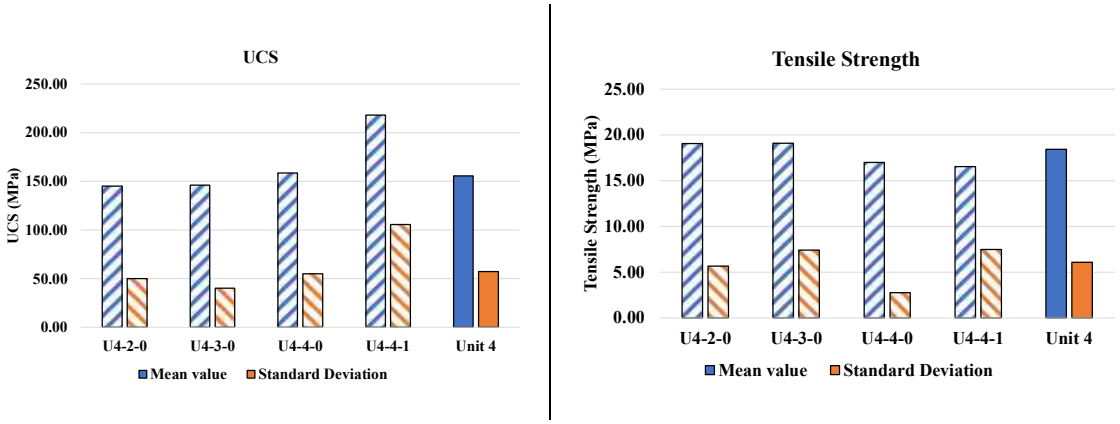

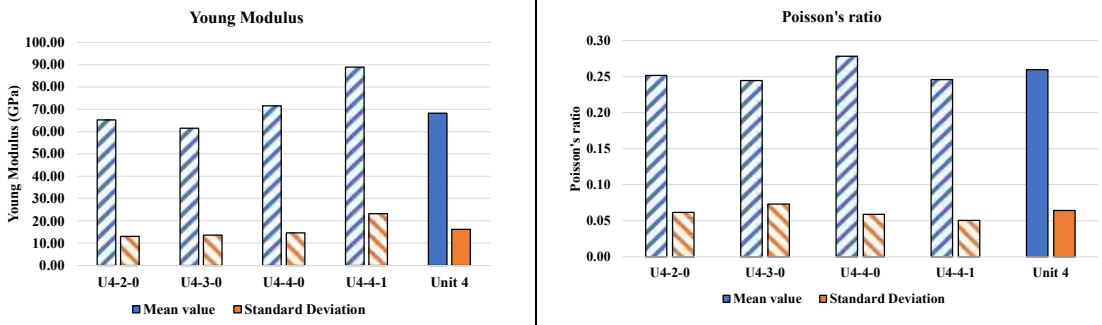

Figure 3.4 Comparison of mean and standard deviation values of the geomechanical intact parameters for Unit 4 and its sub-units

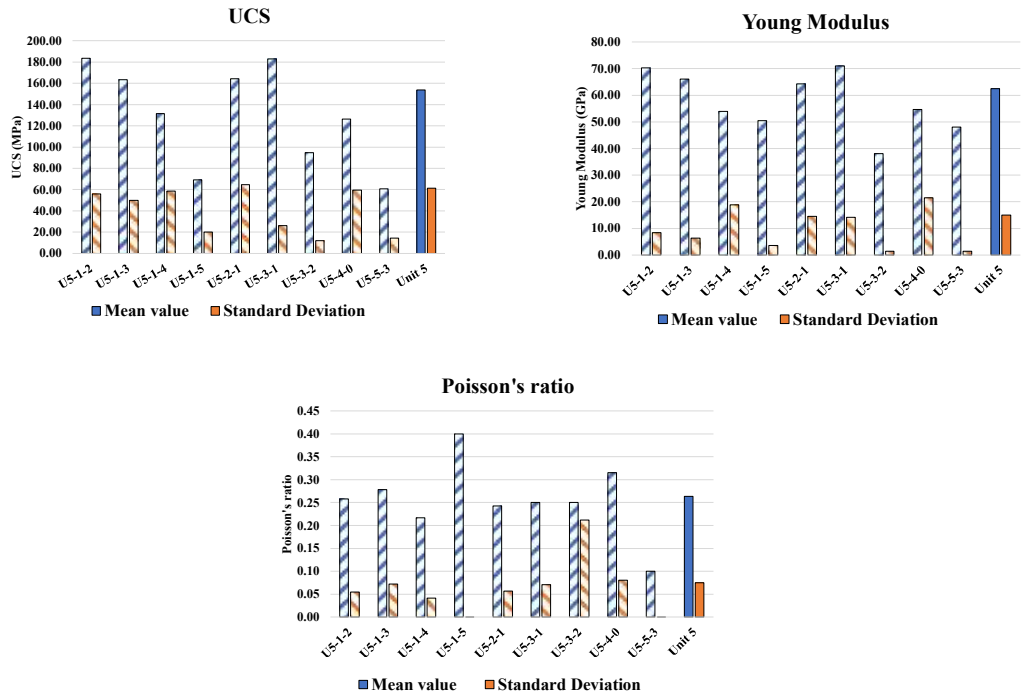

Figure 3.5 Comparison of mean and standard deviation values of the intact geomechanical parameters for Unit 5 and its sub-units

However, notable uncertainties remain unclear in each geomechanical parameter, which will be carefully investigated in this paper based on geomechanical and statistical concepts. From the rock mechanics perspective, certain uncertainties are associated with the intrinsic nature of the rock

materials. In fact, the rock formation process and its alterations over geological and mineralogical history can cause related uncertainties, and the major origin of uncertainties may vary in different geomechanical parameters (Connor Langford & Diederichs, 2015). Considering the intact rock strength, the variations in petrographic characteristics can create various microcrack patterns within each core sample, leading to some variabilities in the rock strength parameters. The petrographic parameters include mineral composition and texture, pores, and microstructures (e.g. grain boundaries and mineral cleavages) and the degree of chemical alteration, which has variations that can influence rock strength. Moreover, anisotropy, which is mostly seen in the foliation of foliated metamorphic rocks, can affect rock strength significantly. Likewise, the variations in Young's modulus and the Poisson's ratio are observed with the variability of several parameters as water content, degree of jointing, and the vibration effects of the blasting near the mining areas (Connor Langford & Diederichs, 2015; Heidarzadeh et al., 2021b). In terms of statistical analysis, the associated uncertainties of geomechanical parameters of intact rocks are mostly correlated with extreme values in every dataset. Hence, labelling any extreme value as an outlier without having a strong reason is highly likely incorrect, and the highest and lowest geomechanical parameters must be statistically checked to determine whether they are outliers or not.

3.5 Treatment of geomechanical laboratory data

In geomechanical datasets, the major associated uncertainties are analyzed statistically through a proper data treatment process that includes five main steps (Figure 3.6). The suggested data refinement flowchart in this study greatly contributes to the determination of the most suitable technique for detecting outliers, leading to the selection of the best treated data so that the uncertainties will be minimized, which has not been given focus in previous geomechanical studies. Also, the impact of various treatment techniques on the geomechanical data and related uncertainties is comprehensively assessed in this section. In the first step, a comprehensive statistical analysis is conducted on every geomechanical intact parameter in each rock unit by applying 17 different treatment approaches. The most reliable treatment methods are selected separately for every

parameter through a comparative evaluation according to engineering judgment. The outliers identified by the selected methods, which can substantially decrease the uncertainties, must be treated well because these extreme abnormal values are making huge variations in the data. Subsequently, to determine the best data treatment technique, we compare the selected methods by means of three goodness-of-fit tests, which are statistical procedures used to determine how well a sample data fits a certain distribution. Finally, the dataset with the best results among all the three fitting tests is selected as the dataset treated by the best treatment method.

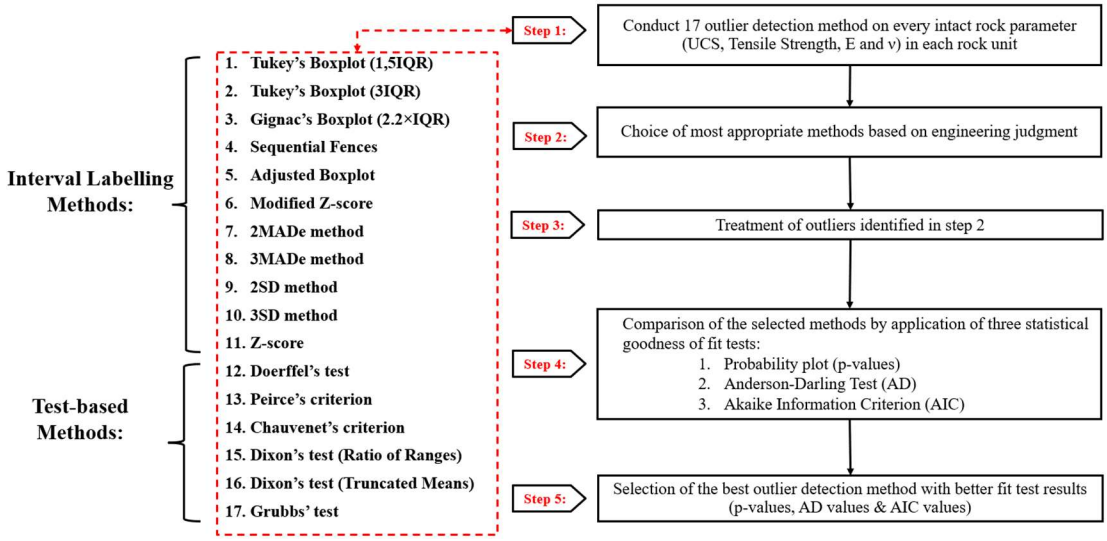

Figure 3.6 Data refinement flowchart to select the best data treatment technique

3.5.1 An overview of data treatment techniques

In this paper, we utilized a diverse set of 17 outlier detection methods, categorized into two main groups: interval labeling methods and test-based methods (as shown in Figure 3.6). The statistical principles governing outlier detection methods were thoroughly discussed by Dastjerdy et al. (2023) and summarized in the Appendix section of this paper. Interval labeling methods involve the establishment of lower and upper fences to identify outliers by defining a range within which observations falling outside are considered as outliers. These methods can be further classified into three groups based on the statistical tools employed to define the range. The first group includes methods utilizing the interquartile range (IQR), which is the difference between the first and third

quartiles. These methods are commonly employed in Tukey's Boxplots and its modified versions such as sequential fences and adjusted boxplot. Among IQR-based methods, the adjusted boxplot employs the medcouple function as a robust measurement tool of skewness, specifically useful in handling greatly skewed geomechanical data (see Eqs. 4-7). The second group consists of median-based methods that use the median as a measure of central tendency to identify outliers. Examples include the modified Z-score method, 2MADe, and 3MADe methods, where the median absolute deviation (MAD) is calculated as a robust measure of dispersion. The third group comprises standard deviation (SD) methods, which utilize the standard deviation as a measure of variability to detect outliers. Examples include 2SD, 3SD, and Z-score methods, where a specified number of standard deviations from the mean is used to define the outlier threshold. On the other hand, test-based methods identify outliers through statistical hypothesis tests, involving a null hypothesis and an alternative hypothesis. The null hypothesis puts forth a specific statement regarding the dataset, while the alternative hypothesis refutes this statement. By examining whether an outlier is present in the dataset, these methods can effectively identify outliers. Test-based methods predominantly rely on the assumption that the data follow a relatively normal distribution, which can be considered a limitation. The categorization of these methods provides a framework for understanding their fundamental principles and application in identifying outliers within geomechanical parameter datasets.

3.5.2 Selection of the most appropriate outlier detection methods for the geomechanical intact parameters and the outlier treatment

To determine the most appropriate outlier detection method, the statistical and geomechanical principles must be considered. First, the interval values estimated by different outlier methods must be physically meaningful. Second, the number of detected outliers ought to be statistically acceptable. After selecting the most suitable outlier method, the outliers must be treated. In general, two main approaches, namely, winsorizing method and trimming method, can be used to deal with the identified outliers. In the winsorizing approach, the nearest value in the dataset, a non-suspicious value, is usually replaced with the identified outliers, whereas the trimming method involves the removal of

the outliers from the remaining data (G. E. Gignac, 2019; Kwak & Kim, 2017). Some researchers suggest the replacement of the outliers in the lower and upper bounds with the 5th percentile and 95th percentile of the sample, respectively, which may produce some huge uncertainties (Ghosh & Vogt, 2012). In this study, the trimming method was preferred because its use may lead to the re-insertion of several identical values (either low or high) that could overshadow the actual probability distribution function by increasing the error in both distribution tails.

3.5.3 Effect of sample size on determining the best outlier detection method

The effect of sample size on identification of the best outlier detection method for each geomechanical parameter is an important aspect addressed in this study. In this regard, we carefully evaluated the performance of different outlier detection techniques across various dataset sizes. It is important to recognize that sample size often serves as a constraint during the outlier detection process. Generally, a larger sample size provides more robust statistical power, allowing for a more accurate assessment of data distribution and a more accurate identification of outliers. With a larger dataset, certain outlier detection methods such as median-based and SD-based techniques −which rely on statistical assumptions and require a sufficient number of observations, become more reliable (Barbato et al., 2011). These methods can effectively capture anomalies and distinguish them from the main dataset. However, it is crucial to consider the limitations that arise with smaller sample sizes. Limited data points can lead to increased uncertainty and potential biases, making it more challenging to accurately identify outliers (Dastjerdy et al., 2023). Some outlier detection methods may struggle to provide reliable outcomes or may fail to identify outliers accurately, when working with smaller datasets. This issue will be discussed in the subsequent sections.

3.6 Results

The results in all 17 outlier detection methods applied on each intact parameter are completely discussed herein. In order to determine the best outlier detection method for each geomechanical parameter, we followed a systematic approach that was consistent across all parameters in this study.

The criteria for selecting the best method involved considering the interval values provided by each method and the number of outliers detected for each parameter. It is worth emphasizing that our initial step was to assess the dataset and identify extreme values based on the specific characteristics and expected behavior of the rock type under study. We aimed to highlight extreme values that exceeded both the lower and upper thresholds. After identifying these extreme values, we systematically conducted a variety of outlier detection methods on each geomechanical dataset. The methods that presented ranges specifically tailored to each parameter, and demonstrated consistent and reliable performance, were determined as the most appropriate outlier detection methods for the respective parameter.

However, it is important to note that the interval values in the z-score and the modified z-score remain constant. With regard to the test-based methods, the only comparative criterion is the number of detected outliers, which may vary in different tests. The results indicated that these tests were not suitable methods for UCS data, as summarized in Table 3.2. Peirce and Grubbs tests are inapplicable for identifying the outliers in the UCS data because of their limitation in handling small sample size. Also, Doerffel's test could not detect low extreme outliers, which is a severe drawback that possibly leads to a significant increase in UCS uncertainties. Chauvenet's criterion and Dixon's test (ratio of ranges) had a conservative approach in labelling the outliers. However, Dixon's test (truncated means) detected the outliers excessively. Consequently, most interval labelling methods have created an incorrect value for the UCS data, thereby confirming their inapplicability in creating acceptable intervals for the UCS data because the negative bound values do not have any physical meaning. Therefore, these methods are rejected because they have almost ignored the low extreme values.

To assess whether a UCS value is extreme and qualifies as an outlier or not, it is beneficial to consider the typical range of UCS values associated with a specific rock type. It is crucial to note that rock strength can vary widely due to factors such as rock type, mineral composition, and geological conditions. However, as a general guideline for metamorphic rocks, the UCS range for meta-basalt typically falls between 70 MPa and 250 MPa, while meta-andesite can have a UCS range of 50 MPa

to 200 MPa which are presented in the unit 3 (Table 1) (Peng & Zhang, 2007; Zhang, 2016). These ranges could provide a reference guide for evaluating the strength values and identifying potential outliers in rock strength measurements. As a result, the intervals created by the adjusted boxplot and 2SD method are statistically and physically suitable for the UCS datasets.

Although each geomechanical parameter possesses unique characteristics and behaviors that require a customized approach, the analysis of UCS data and the application of various outlier detection methods offer valuable insights that can be extended to other geomechanical parameters. Our findings demonstrate that the sequential fences method, Grubbs' test, and Peirce's test are not well-suited for large geomechanical datasets due to their limitations in handling sample size. Therefore, it is reasonable to expect that these methods may encounter similar challenges when applied to other parameters with extensive datasets. Moreover, our investigation highlights that Doerffel’s test may not be an optimal technique for identifying outliers in geomechanical data, particularly those with low extreme values. This insight raises concerns about the reliability of this method for detecting outliers in datasets beyond the UCS parameter. In contrast, the adjusted boxplot method, which incorporates skewness, emerges as a promising approach for handling skewed geomechanical parameters. This method's ability to account for skewness enables more accurate outlier detection and robust analysis, making it a suitable candidate for other parameters exhibiting similar skewness characteristics. By leveraging these insights, we can confidently extend the outcomes derived from the UCS data analysis to enhance outlier detection and improve the robustness of data analysis for other parameters sharing similar characteristics. The results and implications of the analysis conducted on tensile strength, Young's modulus, and Poisson's ratio are discussed in the following.

Table 3.2. Summary of outlier detection methods applied on UCS data in the rock units (3, 4 and 5)

Outlier detection methods	Interval values (MPa)			Number of detected outliers		
	Unit 3	Unit 4	Unit 5	Unit 3	Unit 4	Unit 5

				LB	UB	LB	UB	LB	UB
Tukey's boxplot (1.5IQR)	-10.9 < UCS < 321.1	26.1 < UCS < 266.1	-47.2 < UCS < 356.1	0	0	0	10	0	0
Tukey's boxplot (3IQR)	-135.4 < UCS < 445.6	-63.9 < UCS < 356.1	-198.5 < UCS < 507.3	0	0	0	1	0	0
Gignac's boxplot (2.2IQR)	-69.0 < UCS < 379.2	-15.9 < UCS < 308.1	-117.8 < UCS < 426.6	0	0	0	2	0	0
Sequential fences	-56.5 < UCS < 360.3	62.4 < UCS < 237.1	-112.5 < UCS < 408.1	0	0	4	15	0	0
Adjusted boxplot	6.9 < UCS < 336.7	32.2 < UCS < 271.0	16.5 < UCS < 432.8	0	0	0	8	0	0
2MADe method	23.3 < UCS < 280.4	49.8 < UCS < 249.7	-10.8 < UCS < 306.4	0	0	3	12	0	0
3MADe method	-40.9 < UCS < 408.9	-0.1 < UCS < 349.7	-90.2 < UCS < 465.1	0	0	0	1	0	0
Modified Z-score	-3.5 < Mi < 3.5	-3.5 < Mi < 3.5	-3.5 < Mi < 3.5	0	0	0	2	0	0
Z-score test	-3 < Z-score < 3	-3 < Z-score < 3	-3 < Z-score < 3	0	0	0	2	0	0
2SD method	42.2 < UCS < 264.5	40.8 < UCS < 270.3	30.6 < UCS < 280.4	1	2	1	8	0	1
3SD method	-13.3 < UCS < 320.1	-16.5 < UCS < 326.6	-31.7 < UCS < 342.8	0	0	0	2	0	0
Doerffel's test	Test-based methods identify the outliers based on critical values			N/A	0	N/A	1	N/A	0
Peirce' test				N/A	N/A	N/A	N/A	N/A	N/A
Chauvenet's test				0	0	0	1	0	0
Dixon's test				0	0	0	0	0	0
Grubbs' test				0	0	N/A	N/A	0	0

Note: The LB and UB are the lower and upper bound, respectively. Mi is the Modified Z-score, and N/A means Not Applicable

When examining the tensile strength data of metamorphic rocks, it is crucial to pinpoint extreme values that deviate significantly from the expected range. Table 3.3 briefly compares the results of outlier methods applied on the tensile strength data to select the most appropriate outlier methods.

As reported in the literature, a typical range of tensile strength values for metamorphic rocks falls within the range of 8-30 MPa (Abdaqadir & Alshkane, 2018; Khanlari et al., 2014; Perras &

Diederichs, 2014). By carefully considering the rock types and their standard range of tensile strength values in Units 3 and 4 (metavolcanic rocks), we evaluated the interval values estimated by various methods, in which the outliers detected by Tukey's boxplot (1.5 IQR) (providing the intervals $10.1 < \sigma_t < 26.5$ for Unit 3 and $8.1 < \sigma_t < 30.8$ for Unit 4) and Gignac's boxplot (estimating the intervals $7.2 < \sigma_t < 29.3$ for Unit 3 and $4.1 < \sigma_t < 34.8$ for Unit 4) seem to be more suitable based on engineering judgement, aligning well with the expected behavior.

Conversely, we found that several other methods, including Tukey's boxplot (3IQR), modified z-score, z-score, 3SD method, and Grubbs' test, could not identify any outliers in the tensile strength data despite the presence of very extreme datapoints - especially in Unit 4. Furthermore, our analysis unveiled the potential of the adjusted boxplot method in successfully identifying outliers in the tensile strength data, since the intervals estimated by this method showed promise as a reliable option.

Table 3.3. Summary of outlier detection methods applied on the tensile strength data (σ_t) in two rock units (3 and 4)

Outlier detection methods	Interval values (MPa)		Number of detected outliers			
	Unit 3	Unit 4	Unit 3		Unit 4	
			LB	UB	LB	UB
Tukey's boxplot (1.5IQR)	**$10.1 < \sigma_t < 26.5$**	**$8.1 < \sigma_t < 30.8$**	1	0	5	1
Tukey's boxplot (3IQR)	$3.9 < \sigma_t < 32.6$	$-0.4 < \sigma_t < 39.4$	0	0	0	0
Gignac's boxplot (2.2IQR)	**$7.2 < \sigma_t < 29.3$**	**$4.1 < \sigma_t < 34.8$**	0	0	1	0
Sequential fences	$7.9 < \sigma_t < 27.6$	$4.6 < \sigma_t < 33.4$	1	0	6	0
Adjusted boxplot	$12.6 < \sigma_t < 29.6$	$8.1 < \sigma_t < 30.8$	1	0	5	1
2MADe method	$10.9 < \sigma_t < 24.7$	$9.6 < \sigma_t < 28.4$	1	1	6	2
3MADe method	$7.4 < \sigma_t < 31.6$	$4.9 < \sigma_t < 37.8$	0	0	1	0

Modified Z-score	$-3.5 < M_i < 3.5$	$-3.5 < M_i < 3.5$	0	0	0	0
Z-score test	-3 < Z-score < 3	-3 < Z-score < 3	0	0	0	0
2SD method	$10.4 < \sigma_t < 25.4$	$6.2 < \sigma_t < 30.6$	1	1	4	1
3SD method	$6.7 < \sigma_t < 29.2$	$0.1 < \sigma_t < 36.6$	0	0	0	0
Doerffel's test	Test-based methods identify the outliers based on critical values		N/A	0	N/A	0
Peirce's test			1	0	0	0
Chauvenet's test			1	0	0	0
Dixon's test			1	0	0	0
Grubbs' test			0	0	0	0

With regard to the deformability parameters of intact rock, a proper treatment approach should be sufficiently applicable in identifying the most unusual values as outlier, because the presence of outliers in the dataset can greatly influence the respective mean value and standard deviation, which is of great significance in the study of susceptible units to rockbursts. Therefore, extreme values (high or low) should be carefully examined for Young's modulus or Poisson's ratio data. Moreover, considering the rock types and their general deformability values in the present study, which are all partially metamorphosed (Table 3.1), the extreme values for Young's modulus and Poisson's ratio could be considered the contaminant datapoints, which were evaluated by using various outlier methods. For instance, in Rock Unit 3, four Young's modulus have values greater than 100 GPa (e.g. 101, 105, 106, and 107 GPa), which are considered unusual values based on the presented rock type in Table 3.1 and might be detected as outlier. Extreme values of Young's modulus in metamorphic rocks can be identified based on their stiffness and resistance to deformation. Young's modulus represents the ratio of axial stress to axial strain, and in the case of metamorphic rocks, their low displacement during compressive testing indicates high stiffness. In the context of the studied rock types, such as meta-basalt and meta-andesite, the typical range of Young's modulus falls within 10-

90 GPa for meta-basalt and 20-100 GPa for meta-andesite (Peng & Zhang, 2007). Comparing these typical ranges to the extreme values observed (e.g. 101, 105, 106, and 107 GPa), it becomes evident that these values exceed the upper limit of the expected range. Statistically, they are distant from the majority of the dataset and represent a significant deviation from the expected behavior. As summarized in Table 3.4, several methods, such as Tukey's boxplot (3IQR), Gignac's boxplot, 3MADe method, z-score, modified z-score, 3SD method, and almost all test-based methods, were unable to recognize any outliers in the Young's modulus data. Only the adjusted boxplot and 2MADe method identified those high extreme values in Unit 3, although the estimated interval value of the adjusted boxplot in the lower bound might sound incorrect – particularly in Unit 5. As a result, these two methods (e.g. adjusted boxplot and 2MADe) are selected as the best methods for Young's modulus data.

In the Poisson's ratio data, the normal range of the data can be quantified based on the rock type. Considering meta-basalt and meta-andesite as the two main rocks of Unit 3, some Poisson's ratio values, such as 0.4, 0.41, 0.43, 0.45, and 0.46, are recognized as unusual. Outliers in Poisson's ratio can signify irregularities in the material or measurement errors. In the case of metamorphic and metavolcanic rocks, which exhibit low plasticity and limited displacement during compressive testing, Poisson's ratio tends to be relatively small (Gercek, 2007; Peng & Zhang, 2007; Zhang, 2016). Deviations from this expected range, particularly high values exceeding 0.4, may indicate anomalies and potential issues in the measurement setup or instrumentation used during testing (Gercek, 2007; Peng & Zhang, 2007; Zhang, 2016). These irregularities could stem from inaccurate lateral displacement measurements, anisotropic properties beyond the norm, localized deformation zones, or variations in sample quality or heterogeneity. Therefore, extreme Poisson's ratio values serve as strong indicators of abnormalities and warrant further investigation into potential errors or unique geological features within the rock sample (Gercek, 2007). Meanwhile, despite the presence of these abnormal values, most of the applied methods could not label these values as outlier. In this study, the 2MADe method and Dixon's test statistically recognized these outliers, even though these

methods apply two different statistical approaches, which were reviewed earlier in this paper. According to the results, the 2MADe method and Dixon's test are selected as the two best data treatment methods for the Poisson's ratio data (Table 3.5). In all intact rock laboratory data, these two selected methods will be compared with each other to determine the best outlier detection method based on three goodness-of-fit tests, which will be discussed in detail.

Table 3.4. Summary of outlier detection methods applied on Young's Modulus (E) data in the three rock units (3, 4 and 5)

Outlier detection methods	Interval values (GPa)			Number of detected outliers					
	Unit 3	Unit 4	Unit 5	Unit 3		Unit 4		Unit 5	
				LB	UB	LB	UB	LB	UB
Tukey's boxplot (1.5IQR)	39.0 < E < 107.0	27.0 < E < 107.0	20.1 < E < 105.1	4	0	0	4	0	0
Tukey's boxplot (3IQR)	13.5 < E < 132.5	-3.0 < E < 137.0	-11.7 < E < 137.0	0	0	0	0	0	0
Gignac's boxplot (2.2 IQR)	27.1 < E < 118.9	13.0 < E < 121.0	5.2 < E < 120.0	1	0	0	0	0	0
Sequential fences	31.3 < E < 116.6	39.8 < E < 98.1	10.6 < E < 120.3	1	0	1	9	0	0
Adjusted boxplot	25.3 < E < 95.9	13.3 < E < 95.1	-12.8 < E < 85.7	1	4	0	12	0	1
2MADe method	47.3 < E < 100.6	39.3 < E < 98.6	35.8 < E < 95.1	7	4	1	9	4	0
3MADe method	33.9 < E < 127.3	24.5 < E < 128.3	21.0 < E < 124.8	3	0	0	0	0	0
Modified Z-score	-3.5 < Mi < 3.5	-3.5 < Mi < 3.5	-3.5 < Mi < 3.5	1	0	0	0	0	0
Z-score test	-3 < Z-score < 3	-3 < Z-score < 3	-3 < Z-score < 3	0	0	0	0	0	0
2SD method	36.1 < E < 107.7	36.0 < E < 100.5	32.5 < E < 92.2	3	0	0	8	2	0
3SD method	18.2 < E < 125.6	19.9 < E < 116.6	17.6 < E < 107.1	0	0	0	0	0	0

Doerffel's test	Test-based methods identify the outliers based on critical values	N/A	0	N/A	0	N/A	0
Peirce' test		1	0	N/A	N/A	N/A	N/A
Chauvenet's test		1	0	0	0	0	0
Dixon's test		0	0	0	0	0	0
Grubb's test		0	0	N/A	N/A	0	0

Table 3.5. Summary of outlier detection methods applied on Poisson's ratio (ν) datasets in the three rock units (3, 4 and 5)

Outlier detection methods	Interval values			Number of detected outliers					
	Unit 3	Unit 4	Unit 5	Unit 3		Unit 4		Unit 5	
				LB	UB	LB	UB	LB	UB
Tukey's boxplot (1.5IQR)	0.05 < ν < 0.44	0.07 < ν < 0.43	0.07 < ν < 0.43	0	1	0	1	0	0
Tukey's boxplot (3IQR)	-0.09 < ν < 0.59	-0.06 < ν < 0.57	-0.06 < ν < 0.57	0	0	0	0	0	0
Gignac's boxplot (2.2IQR)	-0.01 < ν < 0.51	0.01 < ν < 0.49	0.01 < ν < 0.49	0	0	0	0	0	0
Sequential fences	-0.00 < ν < 0.49	0.12 < ν < 0.39	0.01 < ν < 0.50	0	0	4	5	0	0
Adjusted boxplot	-0.15 < ν < 0.64	0.07 < ν < 0.43	0.07 < ν < 0.43	4	0	0	1	0	0
2MADe method	0.11 < ν < 0.37	0.14 < ν < 0.38	0.11 < ν < 0.41	1	3	5	6	2	1
3MADe method	0.04 < ν < 0.51	0.08 < ν < 0.50	0.04 < ν < 0.56	0	0	0	0	0	0
Modified Z-score	-3.5 < Mi < 3.5	-3.5 < Mi < 3.5	-3.5 < Mi < 3.5	0	0	0	0	0	0

Z-score test	-3 < Z-score < 3	-3 < Z-score < 3	-3 < Z-score < 3	0	0	0	1	0	0
2SD method	0.11 < ν < 0.40	0.13 < ν < 0.38	0.11 < ν < 0.41	1	1	4	6	2	1
3SD method	0.04 < ν < 0.47	0.07 < ν < 0.45	0.04 < ν < 0.49	0	0	0	1	0	0
Doerffel's test	Test-based methods identify the outliers based on critical values			N/A	0	N/A	0	N/A	0
Peirce' test				1	1	N/A	N/A	N/A	N/A
Chauvenet's test				1	1	1	0	0	0
Dixon's test				4	4	4	4	4	4
Grubb's test				0	0	N/A	N/A	0	0

3.7 Determination of the best outlier method using goodness-of-fit tests and assignment of the best fitted probability distribution function for each parameter

To determine the best outlier method, three goodness-of-fit tests, including the probability plot, Anderson-Darling (AD) test, and Akaike information criterion (AIC) test, are used. The goodness-of-fit tests are statistical tools used to characterize how well a sample datum follows a specific distribution. The selected outlier detection methods are compared with one another. Finally, the dataset that obtained the best results among all the three fitting tests will be introduced as the best outlier detection method. Two computer programs, i.e. SPSS v.28 and the JMP v.16, were used for conducing these statistical analyses (JMP-Pro, 2021; SPSS, 2022).

The probability plot method is a graphical tool that compares the p-values and the theoretical distributions (Chambers et al., 2018). In this method, the p-values must be compared with the significance level (usually equal to 0.05) to investigate whether or not the data come from a specific distribution. If the p-value is equal or less than the significance level, then the related dataset fails to follow the specific distribution. However, the larger the p-value, the better fit to the distributions (Chambers et al., 2018). Additionally, any dataset can be visually compared by two confidence

interval (CI) lines (Figure 3.7), as if the p-values are located inside the CI lines, thereby confirming that the data follows a particular distribution.

Considering the UCS data, the adjusted boxplot and 2SD methods are compared with each other in every rock unit. According to the probability plot method, the UCS dataset treated by the adjusted boxplot had greater p-values than the 2SD method (Table 3.6). The probability plots of the UCS data revealed that although both datasets are following a normal distribution, the dataset treated by the adjusted boxplot is more fit for this distribution (p-value = 0.68) than the 2SD method (p-value = 0.414) (Figure 3.7 a and b). Some other distributions, such as lognormal, exponential, and loglogistic, were invalid because their p-values were less than the significance level (< 0.05). The probability plot suggested that the adjusted boxplot is a better outlier detection method for UCS data rather than that of the 2SD method.

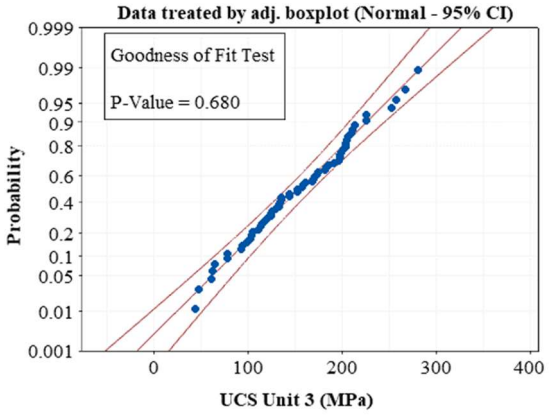

(a)

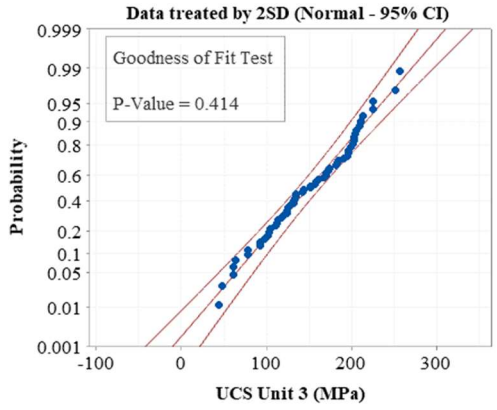

(b)

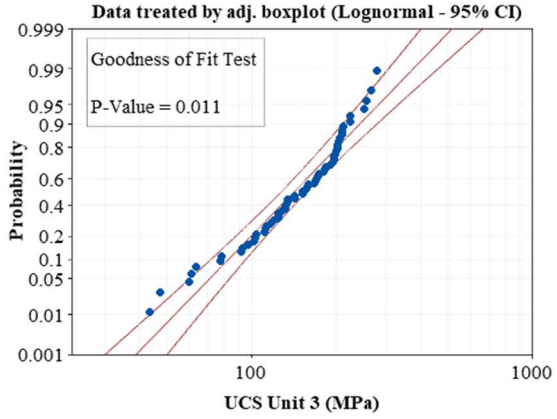

(c)

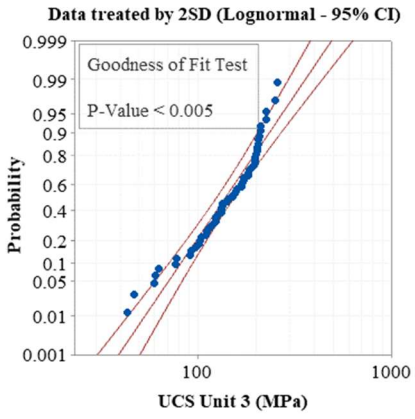

(d)

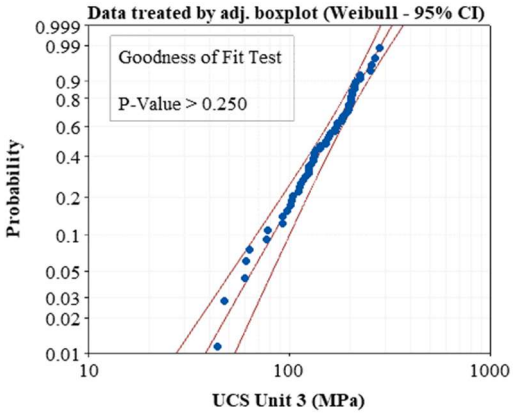
Data treated by adj. boxplot (Weibull - 95% CI)
Goodness of Fit Test
P-Value > 0.250
Probability
UCS Unit 3 (MPa)

(e)

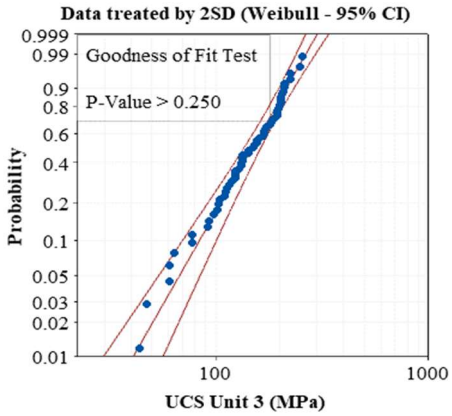
Data treated by 2SD (Weibull - 95% CI)
Goodness of Fit Test
P-Value > 0.250
Probability
UCS Unit 3 (MPa)

(f)

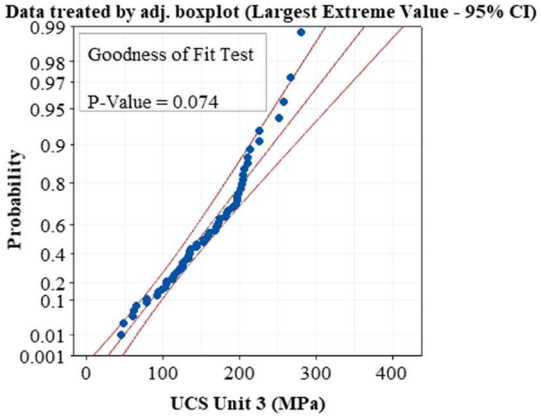
Data treated by adj. boxplot (Largest Extreme Value - 95% CI)
Goodness of Fit Test
P-Value = 0.074
Probability
UCS Unit 3 (MPa)

(g)

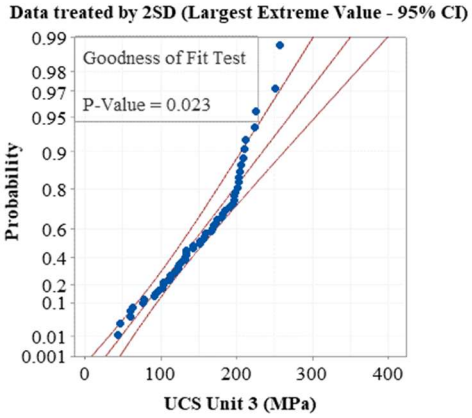
Data treated by 2SD (Largest Extreme Value - 95% CI)
Goodness of Fit Test
P-Value = 0.023
Probability
UCS Unit 3 (MPa)

(h)

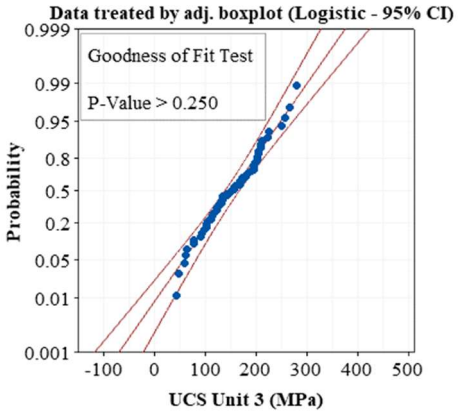
Data treated by adj. boxplot (Logistic - 95% CI)
Goodness of Fit Test
P-Value > 0.250
Probability
UCS Unit 3 (MPa)

(i)

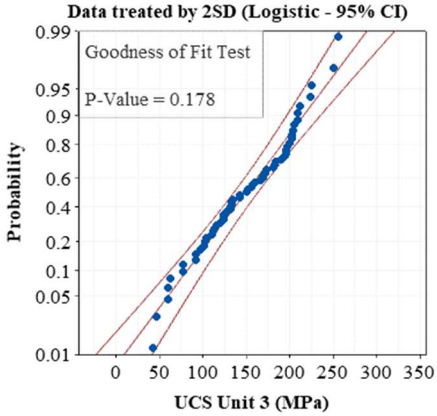
Data treated by 2SD (Logistic - 95% CI)
Goodness of Fit Test
P-Value = 0.178
Probability
UCS Unit 3 (MPa)

(j)

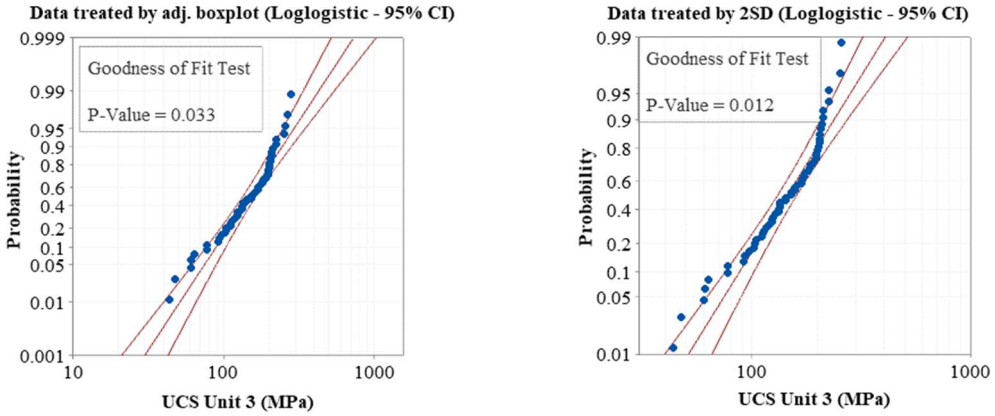

(k) (l)

Figure 3.7 Probability plots of UCS Unit 3 dataset treated by adjusted boxplot and 2SD method

The middle line is the expected percentile from the distribution and left and right curved lines are the lower and upper bounds of the CIs.

Table 3.6. Summary of probability plots (p-values) for UCS data treated by adjusted (adj.) boxplot and 2SD method in three rock units

Distribution	Unit 3		Unit 4		Unit 5	
	adj. boxplot	2SD	adj. boxplot	2SD	adj. boxplot	2SD
Normal	0.680	0.414	0.065	0.04	0.023	0.015
Lognormal	0.011	< 0.005	< 0.005	0.061	< 0.005	< 0.005
Exponential	< 0.003	< 0.003	< 0.003	< 0.003	< 0.003	< 0.003
Weibull	> 0.25	> 0.25	0.022	0.011	0.04	0.024
Largest extreme value	0.074	0.023	< 0.01	0.044	< 0.01	< 0.01
Logistic	> 0.25	0.178	0.202	0.113	< 0.005	< 0.005
Loglogistic	0.033	0.012	0.21	> 0.25	< 0.005	< 0.005

The AD and AIC tests are also conducted to select the best outlier method for the UCS data (Akaike, 1974; Anderson & Darling, 1952). In both tests, the lesser values of AD and AIC statistics

are considered a better fit to the distributions. Figure 3.8 presents the results of the AD and AIC tests conducted on the UCS Unit 3 data to analyze the adjusted boxplot and 2SD method. As summarized in Table 3.7, the AD values of the adjusted boxplot dataset are lesser than those of the 2SD method dataset, thereby confirming its better fit to the distributions, though the fit ranking may differ in the two datasets. In the adjusted boxplot dataset, the best fitted probability distribution function is Pert (AD value = 0.245), whereas this distribution was less fitting to the 2SD method dataset (AD value = 0.269), as presented in Figure 3.8 a and b. The AD test results for the UCS in all rock units are in good agreement with the probability plots (Table 3.7), which indicates that the adjusted boxplot dataset had better fit than the 2SD method, whereas the AIC test results for the same datasets cannot confirm this finding. Lehmann (2015) conducted a comparative statistical analysis on the geodesy and geophysics data through the use of Monte Carlo simulations, and it was proven that the AIC test obtained more accurate results than the AD test. Therefore, the AIC test results was preferred than the AD test in this study. According to the AIC test, the UCS data treated by the 2SD method are more fit to the distributions (Figure 3.8 c and d, Table 3.7). Consequently, the 2SD method is preferred to become the best outlier detection method for the UCS dataset in all three rock units.

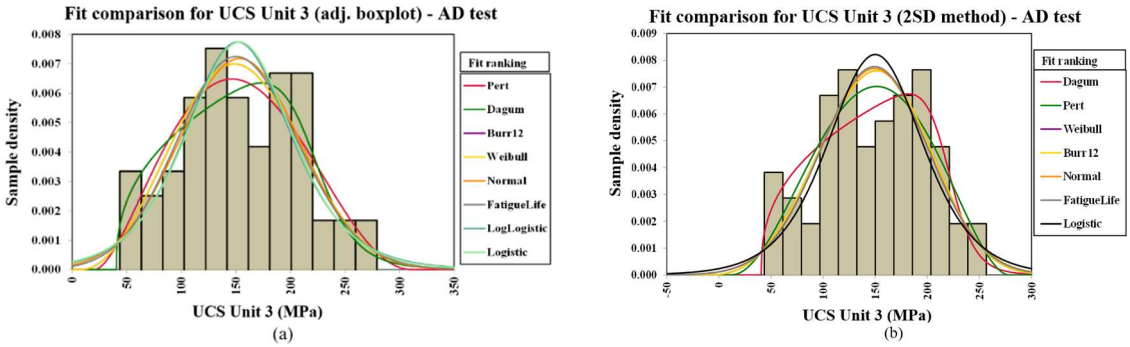

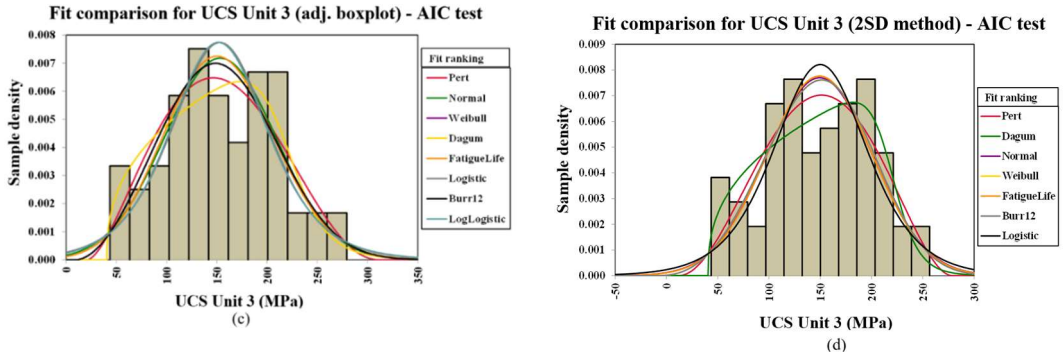

Figure 3.8 Graphical comparison of UCS datasets (Unit 3) treated by adjusted box plot and 2SD method: (a, b) AD test, and (c, d) AIC test

Table 3.7. Comparison of UCS datasets treated by adjusted boxplot and 2SD method based on the AD and the AIC tests in three rock units

Distribution	AD test						AIC test					
	Unit 3		Unit 4		Unit 5		Unit 3		Unit 4		Unit 5	
	Adj. boxplot	2SD	Adj. boxplot	2SD	Adj. boxplot	2SD	Adj. boxplot	2SD	Adj. boxplot	2SD	Adj. boxplot	2SD
Burr12	0.26	0.35	0.27	0.29	0.87	0.94	669.55	639.66	1570.02	1552.44	779.94	765.88
Dagum	0.25	0.25	0.22	0.26	N/A	N/A	667.84	635.98	1569.72	1553.59	N/A	N/A
Erlang	N/A	N/A	0.35	0.3	0.94	0.99	N/A	N/A	1567.83	1550.06	781.7	767.64
Fatigue Life	0.27	0.38	0.35	0.29	0.92	0.98	668.63	638.72	1567.79	1550.05	782.17	767.96
Gamma	N/A	N/A	0.35	0.3	0.94	0.99	N/A	N/A	1567.83	1550.06	781.7	767.64
Loglogistic	N/A	N/A	0.23	0.24	1.02	1.07	N/A	N/A	1568.37	1551.74	788.59	774.44
Logistic	0.37	0.48	0.46	0.54	1.02	1.08	669.47	640.06	1568.76	1553.4	786.78	772.46
Normal	0.26	0.37	0.7	0.79	0.88	0.95	666.51	636.51	1568.59	1552.72	780.6	766.1
Pert	0.24	0.26	1.65	1.22	0.79	0.89	666.27	635.5	1576.41	1555.39	774.25	759.91
Weibull	0.26	0.35	0.7	0.56	0.87	0.94	667.26	637.35	1570.39	1551.51	777.69	763.62

In the tensile strength data, Tukey's boxplot and Gignac's boxplot were compared. In this case, the probability plots cannot be utilized to determine the best treated data because the p-values of the datasets in Unit 4 were less than the significance level. However, the AD and AIC test results demonstrated that the dataset treated by Tukey's boxplot was more fitted to the distributions, though

the AD values related to the Unit 3 of Gignac's boxplot in some distributions, such as Burr12, Fatigue Life, and Normal, were a slightly better than that of Tukey's boxplot (Table 3.8). Consequently, the Tukey's boxplot is recognized as the most suitable outlier method for the tensile strength data.

Similar to the tensile strength dataset, the probability plots for the deformability parameters were not also applicable because of the very low p-values. With regard to the Young's modulus data, the 2MADe method was determined as the best method for Units 3 and 5 data owing to the fact that the AD and AIC statistical values have had better fit to the distributions, whereas the adjusted boxplot method treated the Unit 4 data better than the 2MADe method. Table 3.9 summarizes the AD and AIC test results conducted on the Young's modulus data. Concerning the Poisson's ratio data, the goodness-of-fit tests showed very close results for the 2MADe method and Dixon's test. However, the 2MADe method was determined as the best method for Units 3 and 4, and Dixon's test was selected because of its better fit to the distributions in Unit 5 (Table 3.10).

Table 3.8. Comparison of tensile strength datasets treated by Gignac's boxplot and Tukey's boxplot based on the AD and AIC tests

Distribution	AD test				AIC test			
	Unit 3		Unit 4		Unit 3		Unit 4	
	Gignac's boxplot	Tukey's boxplot	Gignac's boxplot	Tukey's boxplot	Gignac's boxplot	Tukey's boxplot	Gignac's boxplot	Tukey's boxplot
Burr12	0.21	0.31	0.44	0.27	197.87	184.52	314.44	257.33
Fatigue Life	0.24	0.25	0.98	0.45	197.61	183.1	315.37	256.51
Normal	0.25	0.29	0.98	0.45	195.23	181.72	313.11	254.22
Pert	0.59	0.35	1.29	0.67	199.89	181.35	317.39	257.54
Rayleigh	2.46	0.34	3.01	2.43	208.07	179.55	323.46	265.12
Weibull	0.31	0.31	0.63	0.31	197.8	181.94	313.29	255.07

Table 3.9. Comparison of Young's modulus datasets treated by adjusted boxplot and 2MADe method based on the AD and AIC tests

Distribution	AD test			AIC test		
	Unit 3	Unit 4	Unit 5	Unit 3	Unit 4	Unit 5

	Adj. boxplot	2MADe	Adj. boxplot	2MADe	Adj. boxplot	2MADe	Adj. boxplot	2MADe	Adj. boxplot	2MADe	Adj. boxplot	2MADe
Dagum	0.3	0.26	0.2	0.32	N/A	N/A	442.33	366.02	1114.99	1142.48	N/A	N/A
FatigueLife	1.39	0.35	0.86	0.62	1.61	1.12	450.71	364.6	1125.56	1152.51	553.33	519.02
HypSecant	0.93	0.3	1.25	0.96	1.53	1	446.27	363.73	1137.68	1162.39	558.20	520.29
Logistic	0.97	0.29	1.03	0.77	1.44	0.96	446.97	363.19	1131.99	1157.42	556.54	519.2
Normal	1.39	0.34	0.84	0.57	1.58	1.1	448.48	362.34	1123.48	1150.46	553.15	516.82
Pert	0.71	0.37	0.55	0.69	0.56	0.58	441.93	363.41	1117.16	1146.01	542.53	512.2
Rayleigh	4.6	2.21	2.44	1.71	3.05	2.74	467.89	373.08	1130.27	1150.91	561.2	524.92

Table 3.10. Comparison of Poisson's ratio datasets treated by 2MADe method and Dixon's test based on the AD and AIC tests

Distribution	AD test						AIC test					
	Unit 3		Unit 4		Unit 5		Unit 3		Unit 4		Unit 5	
	2MADe	Dixon	2MADe	Dixon	2MADe	Dixon	2MADe	Dixon	2MADe	Dixon	2MADe	Dixon
Beta General	N/A	N/A	0.76	0.78	N/A	N/A	N/A	N/A	-433.48	-420.49	N/A	N/A
Burr12	0.5	0.62	1.15	0.84	0.58	0.58	-148.09	-148.88	-428.75	-420.41	-165.23	-165.32
Dagum	0.49	0.5	0.85	0.81	N/A	N/A	-151.19	-151.91	-432.52	-421.11	N/A	N/A
HypSecant	0.72	0.91	1.83	1.56	1.29	1.18	-145.29	-145.19	-412.51	-408.05	-152.74	-153.23
Logistic	0.62	0.79	1.59	1.31	1.24	1.11	-147.86	-147.97	-419.69	-414.28	-155.05	-155.52
Normal	0.5	0.65	1.27	0.99	1.37	1.18	-151.29	-151.59	-429.19	-421.28	-157.09	-157.77
Pert	0.43	0.52	0.84	0.83	0.59	0.53	-152.55	-153.09	-435.14	-421.11	-168.19	-168.97
Weibull	0.5	0.62	1.15	0.84	0.58	0.58	N/A	N/A	-430.87	-422.53	-167.51	-167.62

After determining the most appropriate geomechanical intact parameters in each rock unit, the most fitted probability distribution function is assigned for every parameter in each rock unit. Figure 3.9 presents the best fit distribution plotted on the geomechanical parameters, in which the most reliable calculated mean and the standard deviation values were illustrated. Although the related uncertainties are still considerable, the mean values of UCS data in Units 3, 4, and 5 are 149.25 MPa, 148.37 MPa, and 152.47 MPa, respectively. The distribution fit ranking of the UCS data treated by 2SD method indicates that the Pert distribution is determined as the most suitable one for Units 3 and 5, whereas Fatigue Life distribution is the best fitted distribution for Unit 4, as illustrated in Figure

3.9 a–c. In the tensile strength data, the Rayleigh and normal distributions are selected as the most suitable fit models for Units 3 and 4 with mean values of 18.25 MPa and 19.56 MPa, respectively (Figure 3.9 d and e). Furthermore, the best fit models and the most suitable mean values are specified for the deformability parameters. With regard to the Young's modulus data treated by 2MADe and adjusted boxplot, the normal distribution in Unit 3 (mean value of 74.31 GPa), Dagum distribution in Unit 4 (mean value of 65.2 GPa), and Pert distribution in Unit 5 (mean value of 6.15 GPa) were determined, and the best assigned distributions for the Poisson's ratio data were Pert distribution (Units 3 and 5) and Beta General (Unit 4) distributions (Figure 3.9 f–k). Table 3.11 presents the calculated mean and standard deviation based on the most fitted probability distribution function for every parameter in each rock unit.

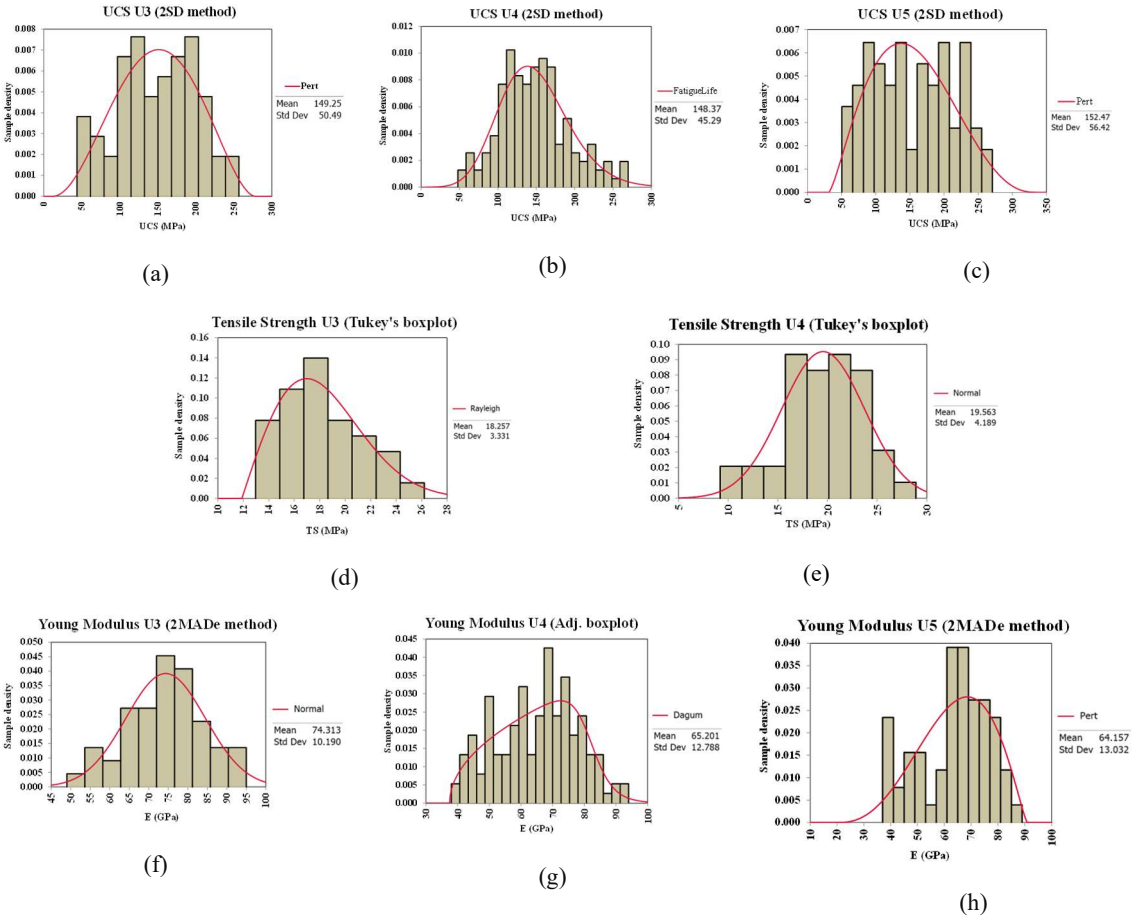

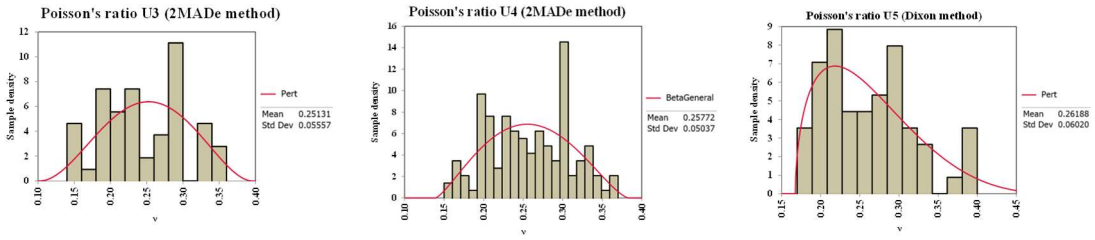

(i) (j) (k)

Figure 3.9 Best distribution assigned for the geomechanical parameters of intact rock

Table 3.11. Most appropriate mean (X_m), standard deviation (S), and probability distribution function (PDF) computed for every geomechanical intact parameter at the Westwood Mine

Parameter	Rock Unit								
	Unit 3			Unit 4			Unit 5		
	X_m	S	PDF	X_m	S	PDF	X_m	S	PDF
UCS (MPa)	149,25	50,49	Pert	148,37	45,29	Fatigue Life	152,47	56,42	Pert
Tensile Strength (MPa)	18,25	3,33	Rayleigh	19,56	4,18	Normal			
Young's Modulus (GPa)	74,31	10,19	Normal	65,2	12,78	Dagum	64,15	13,03	Pert
Poisson's ratio	0,251	0,55	Pert	0,258	0,05	Beta General	0,261	0,06	Pert

Based on all statistical analyses conducted on the geomechanical intact data, the following conclusive points can be drawn:

1. Considering that the intact rock properties significantly contribute to the occurrence of rockburst, analyzing the intrinsic uncertainties of geomechanical characteristics is a key step to predict rockburst in underground excavations, which was statistically analyzed in this paper.
2. The main objective of applying various data treatment methods was to demonstrate the significant impact of every outlier method on the characterization of geomechanical intact parameters and the related uncertainties. Therefore, by selecting the most suitable data

treatment technique for each parameter based on engineering judgements, the more fitted probability distribution function, which has not been focused in any geomechanical research, was assigned.

3. Given that extracted intact rock samples are the group of specimens taken from the whole population of a rock, a suitable treatment process can assist the experts to estimate the mean and standard deviation of the sample to be closer to its population.
4. Due to the various degrees of metamorphism, the geomechanical parameters of metamorphic intact rocks most likely show extreme variation, leading to the presence of several abnormal high or low values in the dataset, which need to be fully investigated to check whether these extreme values are statistical and physically acceptable or not. Therefore, the proposed statistical data treatment approach for each parameter considerably eliminated the uncertainties.
5. Having comprehensively examined the uncertainties of geomechanical parameters through a rigorous statistical analysis, including outlier detection and determination of best-fitting PDFs, further investigation is essential to address the remaining uncertainties. While the statistical data treatment techniques have provided valuable insights into the characterization of geomechanical parameters, additional factors, such as schistosity angle and mineralogy, can significantly influence the associated uncertainties. Therefore, in order to gain a more comprehensive understanding of these uncertainties, the following sections focus to explore the impact of schistosity angle and conduct a detailed analysis of mineralogy. By integrating these aspects into our methodology, we aim to establish a more complete framework that accounts for the intrinsic variability of metamorphic rocks and provides a logical link between the variation in geomechanical parameters and the pertinent geological features.

3.8 Effects of schistosity and mineralogy on the geomechanical uncertainties

Despite treating the geomechanical laboratory data using the most appropriate outlier detection methods and assigning the most fitted probability distribution function, all geomechanical parameters were still greatly dispersed in different lithological units (Figure 3.9). In this step, only the uncertainties referred to the datasets of Units 3 and 4 are comprehensively analyzed because these units were more prone to rockburst phenomena at the Westwood mine. To analyze the associated uncertainties, the considerable impacts of the schistosity and the mineralogy will be evaluated.

3.8.1 Impact of schistosity angle on the dispersion of UCS dataset

The schistosity angle (β), which has a dominant effect on rock strength, should be primarily considered for the analysis of the dispersion of the UCS dataset in the aforementioned rock units. The schistosity angle (β) represents the angle between the schistosity plane and the direction of external forces or loading (Figure 3.10 a). The significance of the schistosity angle lies in its impact on the structural characteristics, shear strength, and overall mechanical properties of rocks. A smaller angle causes a higher anisotropy, affecting the strength and deformability of the rock in relation to the orientation of applied stress, while a larger angle signifies stronger interlocking and enhanced resistance to deformation (Yin et al., 2021). Understanding the physical significance of schistosity angle is essential for assessing stability and designing structures in geotechnical engineering.

Several numerical and experimental studies have confirmed that the variation in rock strength is largely correlated to the angle between the schistosity plane and loading orientation, which needs to be considered in the analysis of the uncertainties (Ali et al., 2014; Cui, 2021; Saeidi et al., 2013; Z. Wang et al., 2022; Zhang et al., 2011). However, the variation in the schistosity angle may not have a huge impact on other geomechanical parameters, as much as it affects the UCS variation. In this study, the schistosity angle of all tested core samples of Units 3 and 4 has been measured by observational approach. Figure 3.11 displays the schistosity angle of samples in both rock units

against their respective UCS values. The schistosity values in both units fluctuate between 30° and 90°. According to the literature, the UCS values are not greatly influenced by the schistosity angle less than 30°or greater than 60°, whereas the highest dispersion can be expected for the rock strength, when the associated schistosity values are between 30° and 60° (Koca & Kıncal, 2022; SOUFI et al., 2018). This schistosity range which the UCS values shows the maximum dispersion can be called the variation range, as highlighted in Figure 3.10 b. In addition, the schistosity planes have a key role in the failure mechanism of rock, particularly, when the schistosity angle ranges from 30° to 60°, and the weakness planes might dominate the failure behavior, thereby resulting in rock strength that cannot be a suitable representation of that rock type.

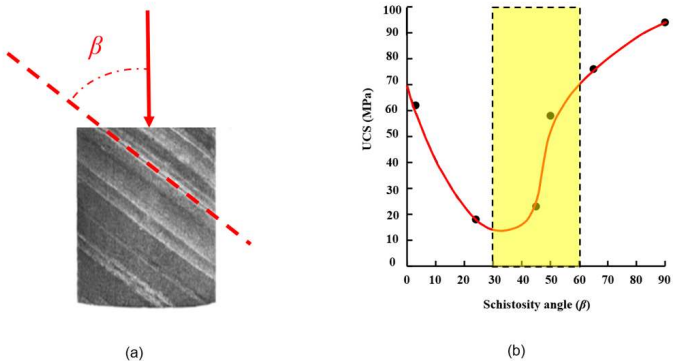

Figure 3.10 (a) The schematic illustration of schistosity angle, and (b) The schistosity range (highlighted) with the highest UCS variation (modified from Hoek (2007))

Consequently, by excluding the UCS values of the variation range ($30^{\circ} \leq \beta \leq 60^{\circ}$) from the remaining data, the related uncertainties can be greatly improved, and the negative impact of schistosity plane on the UCS variation is eliminated. Hence, to remove the effect of schistosity on the variation of UCS data of Units 3 and 4, the core samples within the variation range must be eliminated (Cui, 2021; Z. Wang et al., 2022; Zhang et al., 2011). Figure 3.12 shows that the schistosity angle of many rock samples in Unit 3 are found in this range ($30^{\circ} \leq \beta \leq 60^{\circ}$), whereas most samples of Unit 4 data have a schistosity angle higher than 70° (Figure 3.12 a and b). Afterwards, the UCS variability was changed in the two studied unit, so that the standard deviation of the UCS data in Unit 3 is

currently less than that of Unit 4 (Figure 3.13). Consequently, the associated uncertainties in the UCS dataset do not depend on the schistosity angle.

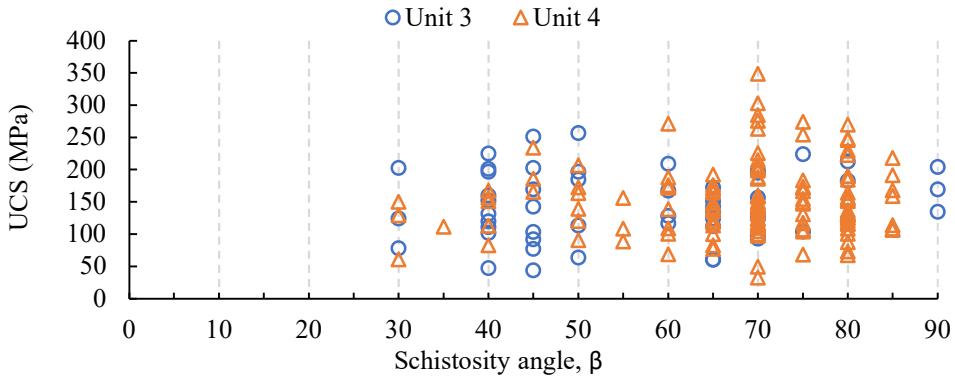

Figure 3.11 Schistosity angle of core specimens of Unit 3 and Unit 4 against UCS

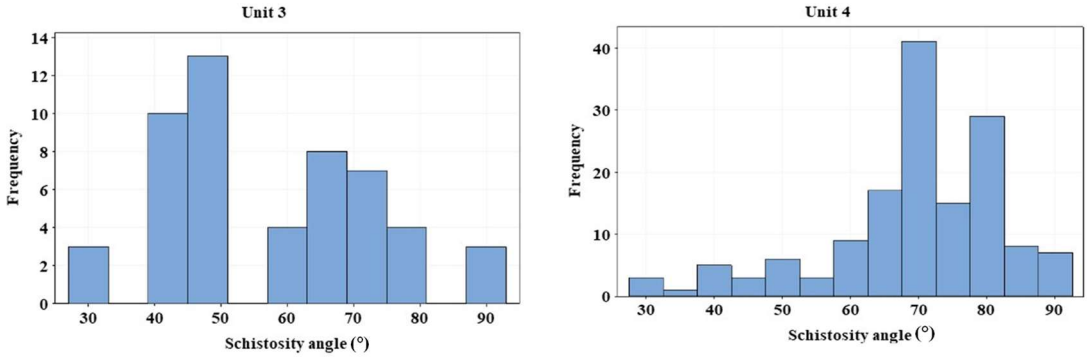

(a) (b)

Figure 3.12 Distribution of core samples in terms of schistosity angle: a) Unit 3, b) Unit 4

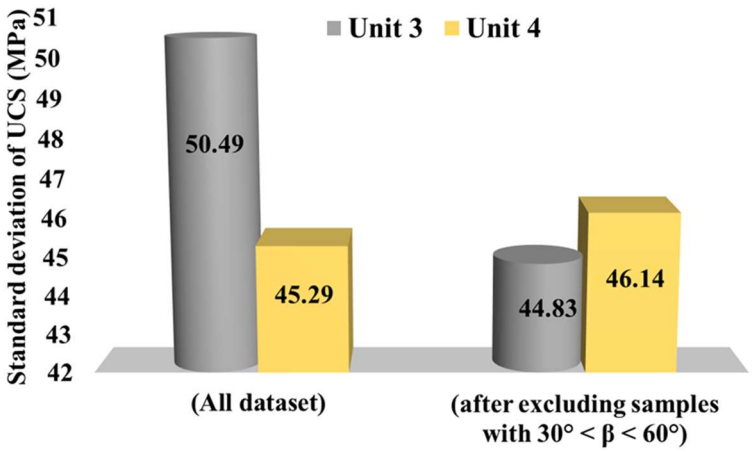

Figure 3.13 Variability of UCS dataset in Unit 3 and Unit 4 before and after the schistosity effect

3.8.2 Effect of mineralogy on the uncertainties of geomechanical parameters

A detailed laboratory investigation has besen conducted to assess how different minerals impact the geomechanical parameters of intact rocks. The study primarily involved processing field-collected core samples and conducting a range of petrographic analyses, including lithogeochemical and isotopic analyses. These analyses played a crucial role in gaining insights into the mineralogical composition, petrographic textures, and hydrothermal alteration of the rocks around the Bousquet fault at the Westwood Mine, considering that these factors could impact the strength and deformability of rocks through several mechanisms (Goulet et al., 2022).

Hydrothermal alterations, for instance, can weaken rocks either by replacing strong minerals with weaker ones or through the dissolution of minerals, resulting in reduction of shear strength. Conversely, alteration process can strengthen rocks by precipitating cementing minerals, increasing cohesion and resistance to deformation (Del Potro and Hürlimann, 2009; Julia et al., 2014). Furthermore, changes in mineral composition and structure during alteration process could also affect the mechanical properties of rock (Coutinho, 2020; Mordensky et al., 2022). Additionally, alterations

can create anisotropic conditions, causing directional variations in strength and deformability parameters of rock (Bidgoli and Jing, 2014).

To demonstrate the role of mineral composition in variation of geomechanical parameters, a petrographic analysis was performed on the selected thin sections of rocks by means of X-ray diffraction (XRD) method at the University of Quebec in Chicoutimi. This analysis also provided a comprehensive mineralogical and textural description of the rocks, showcasing the significant effect of mineral composition in the dispersion of geomechanical data. A representative example of the petrographic characterization for Unit 3, located more than 30 m from the Bousquet fault, is shown in Figure 3.14 (a and b). The rock exhibits a banded texture with bands containing a fine-grained matrix rich in quartz-feldspars-chlorite-sericite-epidote, along with hornblende porphyroblasts. The analyses indicated that as the distance from the fault increases, the abundance of hornblende porphyroblasts gradually intensifies, suggesting a potential connection to the mineral assemblage and its effects on the mechanical properties of the rock (Bidgoli and Jing, 2014). At a distance of 10-30 m from the fault, Unit 3 shows bands of cooler quartz-feldspar-sericite-chlorite-epidote, with some bands being richer in sericite and others in epidote which can have a considerable impact on the geomechanical parameters. The epidote content in these bands can reach up to 80% of the rock in certain places. In contrast, Unit 4, located at a distance of 40 m or more from the fault, does not show any signs of hydrothermal alteration (Figure 3.14 c and d). The samples consist of a very fine-grained matrix predominantly composed of quartz, feldspar, and chlorite, with minor amounts of biotite, epidote, and sericite.

After performing the XRD experiments, the predominant minerals are identified for each rock unit. As a result, a database that consists of 62 thin-section samples (25 samples in Unit 3 and 37 samples in Unit 4) was found. The XRD analysis results indicated that the main minerals in both lithological units (Units 3 and 4) were identical, but their proportion was considerably different. To investigate the influence of mineralogy on the intact rock strength and the deformability parameters

in this study, the minerals are divided into two main groups: hard minerals (e.g. quartz, epidote, amphibole, plagioclase, pyrite, and magnetite) and soft minerals (e.g. feldspar, chlorite, sericite, muscovite, carbonate and biotite). All geomechanical intact data were measured for each thin-section rock sample, which also needs to be treated well before interpreting the XRD results and their effects on the related uncertainties. The treatment process was based on the best outlier method determined for every parameter earlier in this paper. To this end, the chosen best outlier method is applied to treat the data. Consequently, by treating the geomechanical data referred to the thin-section database, we have created four different thin-section datasets for each rock unit, as presented in Table 3.12. For instance, the adjusted boxplot method and the 2SD method were used to treat the respective UCS data of the thin-section samples, in which only one outlier was detected in data of Unit 3, whereas four outliers were identified in the corresponding dataset of Young's modulus. Table 3.12 summarizes all the statistical analyses conducted on the hard and soft minerals along with the calculated mean and standard deviations for each unit, which can be utilized to evaluate the uncertainties of geomechanical parameters in terms of mineral variations. The mineralogy results demonstrated that the higher variation of the UCS data of Unit 4 compared with Unit 3 can be attributed to the dispersion of hard and soft mineral proportions because the standard deviation of Unit 4 (19.7) was greater than that of Unit 3 (18.4), which is in agreement with the resulted uncertainties of the UCS dataset. The dispersion of hard and soft minerals related to both units are represented in Figure 3.15. Nonetheless, no reasonable relationship could be anticipated between soft and hard minerals in both rock units because the UCS values vary (Figure 3.16).

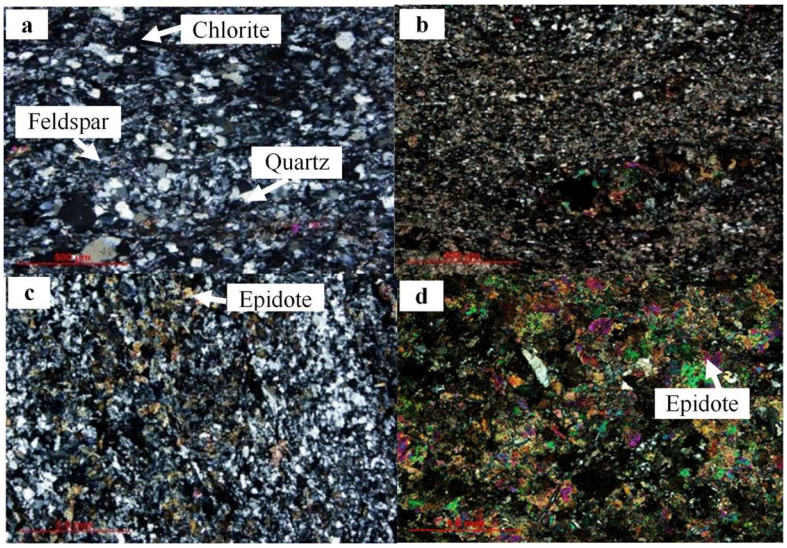

Figure 3.14 Sample of petrographic thin section images: (a, b) Unit 3, and (c, d) Unit 4

Table 3.12. Mean and standard deviation of hard and soft minerals' proportion referred to Units 3 and 4

Geomechanical parameter	Unit	Mineral type	Treated sample size	Number of detected outliers	St. Dev. (%)	Mean (%)	Min (%)	Max (%)
UCS dataset	U3	Hard	24	1	18.4	51.8	13	79
		Soft				48.2	21	87
	U4	Hard	37	0	19.7	47.9	15	91
		Soft				52.1	9	85
Tensile strength dataset	U3	Hard	11	1	16.8	55.4	20	74
		Soft				44.6	26	80
	U4	Hard	20	0	19.6	49.9	16	91
		Soft				50.2	9	84
Young's modulus dataset	U3	Hard	19	4	19	49.4	13	79
		Soft				50.6	21	87
	U4	Hard	27	1	20.8	48.4	15	91
		Soft				52.6	9	85
Poisson's ratio dataset	U3	Hard	19	4	16.3	54.1	20	79
		Soft				45.9	21	80
	U4	Hard	25	3	20.8	47	15	91
		Soft				53	9	85

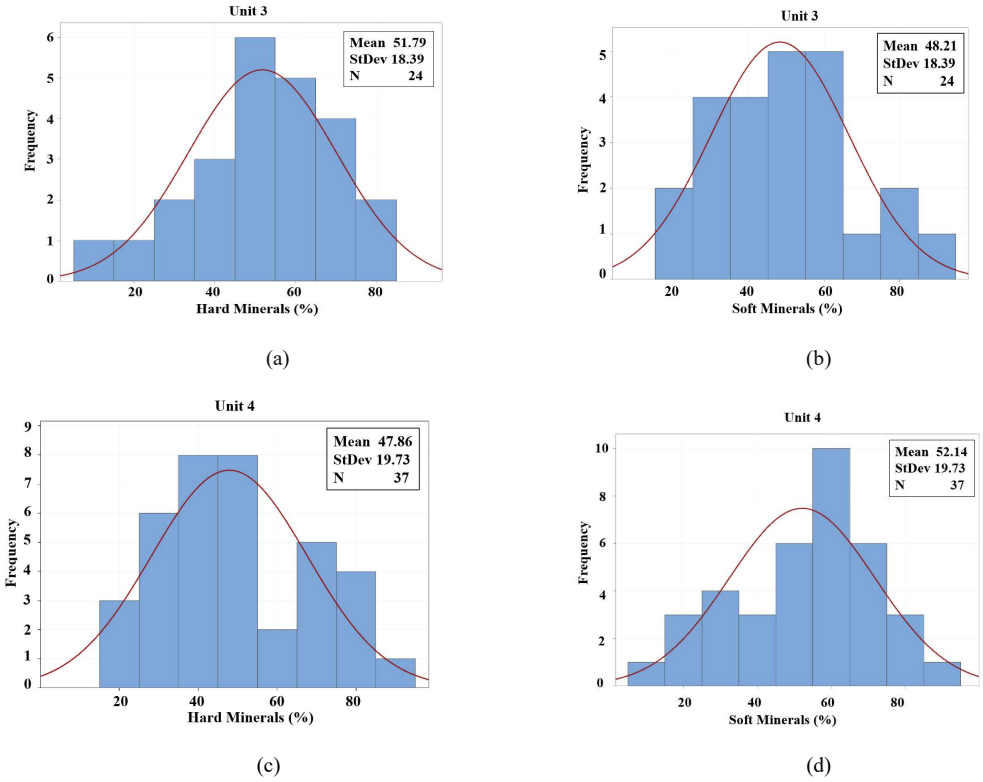

Figure 3.15 Dispersion of hard and soft minerals: (a, b) Unit 3, and (c, d) Unit 4 referred to samples with the UCS data.

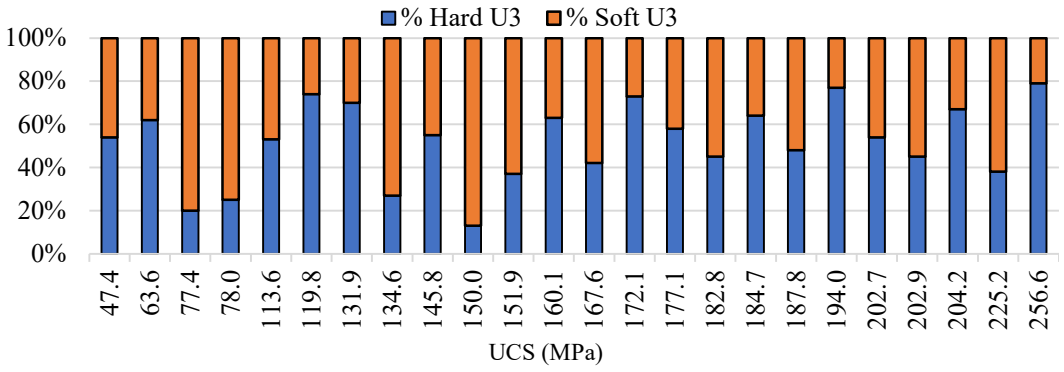

(a)

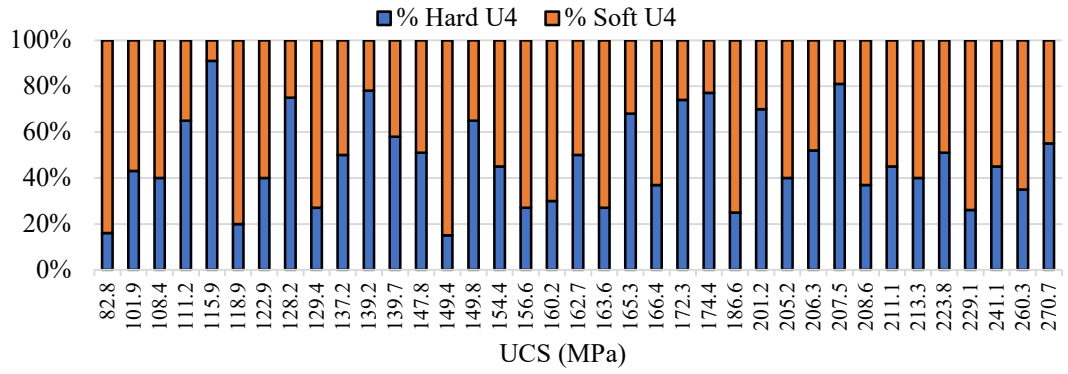

(b)

Figure 3.16 Proportion of hard and soft minerals based on the UCS value: a) Unit 3, b) Unit 4

With regard to the tensile strength dataset, the uncertainties of both rock units may be fairly explained using the mineralogy analysis (Table 3.11). To this end, by analyzing the mineral proportion of 31 rock samples and their tensile strength values, the variability of hard and soft minerals in Unit 4 (St. Dev. = 19.6%) was greater as compared with Unit 3 (St. Dev. = 16.8%), thereby verifying the more scattered data in Unit 4 (4.18) rather than that of Unit 3 (3.33), as illustrated in Figure 3.9 d and e. Moreover, the uncertainties of the Young's modulus data sound reasonable because the standard deviation of mineral proportions (either hard or soft) referred to in Unit 4 was greater than that of Unit 3 (Table 3.12). However, the scatteredness in the Poisson's ratio data might not be justified with the help of mineralogy analysis, although it should be mentioned that the uncertainties resulted in Units 3 and 4 being so close to each other. Also, no clear trend was observed between the percentage of hard and soft minerals when geomechanical parameters fluctuated.

3.9 Discussion

The characterization of geomechanical intact parameters would surely demand an appropriate methodology to analyze the uncertainties in three domains and eliminate any outliers from the raw laboratory data because of the huge natural variabilities of metamorphic rocks related to the degrees of metamorphism.

In the first part, the laboratory results of metamorphic rocks were thoroughly analyzed using 17 data treatment techniques, thereby leading to the selection of the best outlier method for every parameter based on engineering judgment. Among the applied methods, the commonly known treatment method, which is Tukey's 1.5IQR rule, detected some extra outliers, particularly in the UCS data of Unit 4. Meanwhile, the 3IQR rule was too conservative in the detection of outliers despite the extreme values within the datasets. Only Gignac's 2.2IQR should be mentioned as a reasonable outlier method rather than the Tukey's boxplot. Also, the sequential fence method could not be considered a strong method because it has limitations in large datasets (e.g. Unit 4). In general, the best outlier method should address the skewness of the data better because of a high possibility for the raw geomechanical data to be skewed. The only method that considers skewness was the adjusted boxplot method, which was selected as the best outlier method for the UCS and Young's modulus data. In terms of test-based methods, only Dixon's test (truncated means approach) was selected as a better method to detect the outliers in the Poisson's ratio dataset, although this outlier test still had too liberal approach compared with other data. Furthermore, Peirce, Doerffel, and Grubbs tests almost did not detect the outliers in datasets because of the ultra-conservative approach or inapplicability in large datasets. Also, Z-score and its modified method were unsuccessful in labeling any outliers in most datasets. However, the 2SD and the 2MADe methods are specified as the most suitable outlier techniques for the UCS and deformability parameters data, respectively. Subsequently, the statistical goodness-of-fit tests showed that the Pert distribution had the best fit with the UCS data (Units 3 and 5), Young's modulus data (Unit 5), and Poisson's ratio data (Units 3 and 5), whereas the normal distribution function was specified as the most appropriate fit model for tensile strength data (Unit 4) and Young's modulus data (Unit 3).

In the second part of the methodology, the remaining uncertainties were assessed by focusing on the schistosity angle of metamorphic rocks. When the angle between the schistosity plane and the loading direction was observed between 30° and 60°, the UCS dataset showed the highest variation,

and by excluding the related data from the UCS dataset, the effect of schistosity on the high uncertainties of the UCS data can be highly mitigated.

In the third part of the methodology, a complete petrographic investigation was performed on the chosen thin-section rock samples to highlight the function of minerals in the related variabilities of geomechanical intact parameters. To evaluate the impact of mineralogy on intact rock strength and deformability parameters, the minerals were grouped as hard and soft minerals. The petrographic analyses confirmed that the variation of hard and soft mineral proportions in Unit 4 was higher than that of Unit 3, thereby conforming to the uncertainties of the UCS, tensile strength, and Young's modulus in both units. However, the related uncertainties of the Poisson's ratio data could not be explained by mineralogy analysis, despite the similarities in the uncertainties in Units 3 and 4.

3.10 Conclusions

In this paper, a suitable methodology was developed to analyze the uncertainties of metamorphic intact rocks. Considering that the geomechanical intact parameters have a crucial role in the occurrences of rockburst, evaluating the inherent uncertainties of geomechanical parameters is a critical step in predicting rockburst in underground openings. Several important conclusions are summarized as follows:

1. The methodology presented the best data treatment technique for every geomechanical intact parameter in each rock unit.
2. Engineering judgment has a significant role in selecting the best data treatment method because this process must also follow the rock mechanics principles. Tukey's boxplot, as the most common data treatment method in many geomechanical studies, were unable to identify the true outliers in most data because the suggested interval values and the number of detected outliers were unacceptable in terms of engineering judgement. Meanwhile, the adjusted

boxplot method, as the only method that considers the skewness of the data, is recommended as the best alternative for traditional boxplots because they provide more precise CIs.

3. The test-based outlier methods almost failed to investigate the uncertainties of metamorphic rocks. Doerffel's test cannot be a proper method to treat the geomechanical laboratory data because this test cannot label the outliers in the lower threshold of the dataset.
4. In contrast to normality assumption for the geomechanical data in many studies, the results showed better fit models.
5. The dominant influence of schistosity planes in metamorphic rocks played a significant role in the uncertainties of UCS data, which greatly varied in specific schistosity ranges.
6. The mineralogy results showed that the variation of mineral proportions had a crucial effect on the uncertainties of intact laboratory data. However, as the geomechanical parameters change, no logical pattern between the variation of soft and hard minerals in both rock units could be expected.

CHAPTER 4

Understanding the in-situ stress environment is essential to rockburst analysis, as stress concentration is a primary trigger for these events. This chapter develop stress-depth relationships specific to the geological context of the Canadian Shield. By integrating extensive field measurements and geological surveys, this study aims to enhance the understanding of stress distribution patterns as a function of depth. The chapter not only refines existing models but also addresses critical uncertainties in traditional stress estimation approaches by incorporating region-specific geological complexities, such as various tectonic events, lithological variability, and anisotropic stress regimes. The findings directly contribute to the thesis's main objective by providing robust and reliable stress inputs, enabling more realistic predictions of rockburst occurrence.

Article 3: Development of New Relationships for Estimating the In-Situ Stress in the Canadian Shield based on Geological Conditions

Behzad Dastjerdy [1, *], Ali Saeidi [1] and Shahriyar Heidarzadeh [2]

[1] Department of Applied Sciences, University of Quebec at Chicoutimi, Saguenay, QC G7H 2B1, Canada

[2] Rock Mechanics Engineer at SNC-Lavalin, Montreal, QC H2Z 1Z3, Canada

Submitted to Canadian Geotechnical Journal 2024,

4.1 Abstract

The accurate assessment of in-situ stress is crucial for ensuring the stability of rock masses in deep underground projects, especially in the complex landscape of the Canadian Shield. Despite extensive prior research on characterizing the in-situ stress state in this region, uncertainties persist in stress-depth relationships, necessitating critical reassessment. Previous works often relied on categorizing stress data into depth domains, lacking robust geological justifications and potentially oversimplifying the complex geological conditions. This study introduces a novel region-specific methodology, dividing the stress database into six distinct groups within the Canadian Shield based on lithological and structural similarities. This innovative approach enhanced the accuracy of stress-depth relationships by capturing the exclusive complexities of each defined group, ensuring statistically sensible and geologically representative equations that account for the profound influence of tectonic activities. We critically evaluated the applicability of relying solely on statistical tools for establishing reliable stress-depth relationships, emphasizing the integration of geological conditions with statistical methods. The analysis of past equations revealed that designated depth-domains for stress data may not be universally applicable throughout the entire Canadian Shield. Moreover, we explored the influence of tectonic activities on stress redistribution by identifying key regional geotectonic events and their crucial impact on stress patterns in specified groups across diverse regions of the Canadian Shield. The customized stress-depth relationships within the six defined

groups considered regional tectonic events as influential factors. Detailed regression analyses for each group yield equations for key stress parameters, providing valuable perspectives for various geomechanical and engineering applications which could be utilized for the stability and design of underground structures.

Keywords: In-situ stress estimation; stress-depth relationship; regional tectonic influence, regression analysis, Canadian Shield

4.2 Introduction

During the design phase of underground structures, it is crucial to address two key considerations: the determination of geomechanical parameters of rocks and the characterization of in-situ stress in the ground. The uncertainties inherent in geomechanical parameters can introduce substantial deviations in design outcomes, necessitating a careful mitigation approach (Dastjerdy et al., 2024a). Meanwhile, within the earth's crust, the in-situ stress state represents the inherent and undisturbed stress conditions prior to any engineering activities. As a foundational element of project design and construction, an accurate assessment of in-situ stress is essential for solving engineering challenges. This is particularly evident in deep underground projects where in-situ stress emerges as a main external factor governing the stability of rock mass (Amadei & Stephansson, 1997).

The Canadian Shield, a vast expanse of ancient Precambrian rocks covering much of eastern and central Canada, is of high geological and economic significance. Carrying a complex array of geotectonic and metamorphic histories, the Canadian Shield has evolved over various geological eras by multiple tectonic activities. Its rich deposits of minerals such as gold, nickel, copper, and zinc have long attracted mining operations (Percival et al., 2012). However, the efficient and safe extraction of these resources, as well as the planning of infrastructure like tunnels and dams, necessitates a precise estimation of the in-situ stress state present within the various geological formations. However, significant uncertainties often associated with in-situ stress estimations / measurements. Key factors driving these uncertainties include the shield's diverse geological history, which has spanned billions

of years of various processes; the heterogeneity of rock formations, leading to localized stress discrepancies; limitations inherent to measurement methods in great depths; ongoing tectonic activities that might subtly influence stress patterns; and external influences like human-induced activities can also be sources of variability (Corkum et al., 2018; Kaiser et al., 2016; Saeidi et al., 2021; Zhang et al., 2012). Any significant misinterpretation or inaccuracy in depicting this stress profile can lead to structural vulnerabilities, elevated safety risks, and potential environmental challenges. Hence, a more comprehensive analysis of the Canadian Shield's in-situ stress state is essential, to ensure the safety and efficiency of mining operations within this geologically multifaceted domain.

Regarding the assessment of in-situ stresses, two primary approaches are often employed. The first approach includes direct methods, wherein stress is measured explicitly within the rock mass using techniques such as hydraulic fracturing, overcoring, or the flat-jack method. This approach yields precise measurements of the inherent stresses within the rock. The second approach is indirect (including borehole breakouts, core disking or strain relief methods), estimating stresses based on observed behavior of rock under existing conditions (Amadei & Stephansson, 1997; Zhao et al., 2013). In addition, back-analysis, which adjusts model parameters based on observed field data to align computational results with actual measurements, has been extensively utilized in numerous projects to refine in-situ stress estimates (Dight & Hsieh, 2016; Herget, 1973c).

The study of in-situ stress state within the Canadian Shield has undergone continuous refinement since 1970s. Early experiments focused on the reliability of triaxial rock stress measuring tools, with their first practical application at the G.W. Macleod Iron mine in Wawa, Ontario (Herget, 1973a, 1973c). Subsequently, the Canada Centre for Mineral and Energy Technology (CANMET) launched a comprehensive in-situ stress measurement campaign centered on the Canadian Shield. In collaboration with Herget and Arjang, CANMET established a robust database on in-situ stress

measurements (Herget & Arjang, 1990). Over time, researchers have attempted to propose estimating equations for in-situ stress components that would capture the complexities of the Canadian Shield.

While many experts have contributed to the determination of in-situ stress state in the Canadian Shield, certain relationships have gained prominent attention in the literature, distinguished by their grouping of stress data into distinct depth domains, which was briefly illustrated in Figure 4.1. Primarily, Herget (1982) split the stress-depth relationships into two specific depth ranges: 0-900 m and 900-2200m, with formulas for average horizontal stress (σ_{ha}), and vertical stress (σ_v) for each range. Later, Herget (1988) refined his equations, leading to slightly altered formulations and depth domains. Herget (1982 & 1988) noted that the stress data revealed a distinct behavior above 900m depth when compared to the values at greater depth. In more recent contributions, Maloney et al. (2006) and Yong and Maloney (2015) suggested dividing the depth into three distinct categories, namely the stress-released zone (0-300m), transition zone (300-600m), and undisturbed stress zone (600-1500m). According to Maloney et al. (2006), the uppermost layer-reaching up to 300m-exhibits stress variations resulting from periodic events such as glacial movements and tectonic shifts, in which the structural anomalies and changes in rock stiffness can cause localized or more widespread stress variations. While deeper below within the domain 3, rock mass appears predominantly undisturbed, and the positioned zone between these distinct layers is a transitional zone. Although the stress-depth relationships proposed for the Canadian Shield have been extensively studied, certain unclear points still persist which need to be examined in detail:

- Historically, most proposed stress-depth relationships have been linear, suggesting a uniform change in stresses from near-surface depths to greater depths (Arjang, 1989, 1998; Herget, 1973a, 1980, 1982; Herget & Arjang, 1990; Maloney et al., 2006; Yong & Maloney, 2015). This linear representation might not sufficiently account for the effects of past tectonic events or ongoing regional geological conditions that can alter the stress distribution. It is plausible that these linear stress-depth models might not fully capture the profound impacts of

geological factors and structural geology on stress determinations. A more realistic representation might involve nonlinear models that reflect the varied geological impacts on stress distributions. In this paper, we aim to delve deeply into this critical consideration and reassess the adequacy of linear stress-depth relationships.

- Moreover, the categorization of stress data from the Canadian Shield into different depth zones has raised some areas of uncertainty (Maloney et al., 2006; Yong & Maloney, 2015). In understanding the Canadian Shield's stress profiles, even though, it is evident that rock mass behavior can vary significantly across different depths, yet the establishment of specific domains based on depth presents its own set of challenges. While this categorization offers some insights into varying stress trends at different depths, the precise geological and geomechanical reasons behind these domains have not been clearly explained. These divisions appear to be driven more by statistical considerations rather than an understanding of rock behavior. Besides, introducing arbitrary boundaries between depth domains might present a skewed perspective of the stress profile in the Canadian Shield. Moreover, describing vast areas of the Canadian Shield's rock mass beyond 600m depth as "undisturbed", could oversimplify the complexities involved. Such depth-based models might be relevant in certain construction or mining sites, but their universal validity across the entire Canadian Shield could be subject to debate. The absence of defined equations for Maloney's Domain 2, due to data inconsistencies, further hints at the complexities in this methodology. This underscores a potential need to re-evaluate and understand these relationships with a more refined perspective.
- Most proposed stress-depth relationships have predominantly characterized stresses in their principal state, assuming σ_1 and σ_2 as horizontal stresses and σ_3 as the vertical stress. However, this approach might overlook crucial stress orientation components (trend and plunge), potentially leading to analytical uncertainties in the geomechanical interpretation. For instance, consistently considering σ_1 and σ_2 as horizontal stress components across a

large dataset of the Canadian Shield might be problematic, particularly when certain data points exhibit a plunge exceeding 75 degrees, indicative of a vertical or semi-vertical stress orientation. Similarly, assuming σ_3 as a consistent vertical stress can also lead to inaccuracy, especially for datapoints with a plunge under 30 degrees (see Figure 4.4). Furthermore, the pattern of these stresses needs a more detailed examination from perspective of structural geology. Regional tectonic events, for instance, can significantly influence and even shift this conventional stress pattern so that the σ_1 can be vertical under certain geologic conditions. Neglecting these crucial details has the potential to distort the representation of stress trends within the Canadian Shield. This emphasizes the importance of adopting a more comprehensive approach, one that ensures the integration of these specific aspects to provide a thorough understanding of the stress profiles.

Categorizing regions within the Canadian Shield according to their shared lithological and tectonic characteristics allows us to create distinct datasets that better represent the structural geology of each region. This approach ensures that the resulting stress-depth relationships are not just statistically sound but also closely aligned with the geological realities of each specific area. This region-specific methodology, combining statistical analysis with geological insights, has the potential to fill possible gaps in our current knowledge of the in-situ stress state within the Canadian Shield.

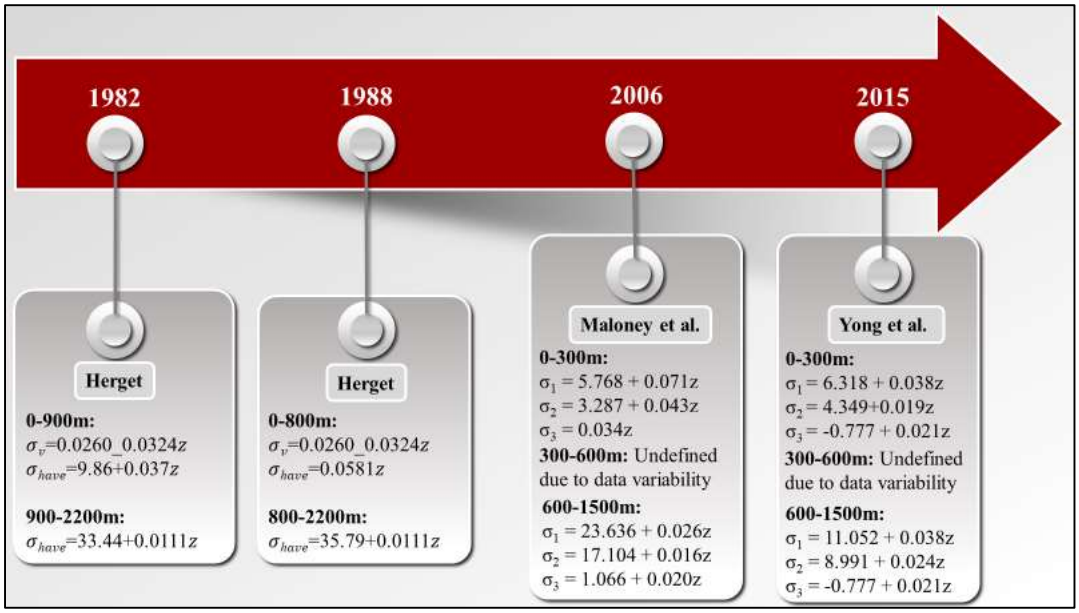

Figure 4.1 Past stress-depth relationships considering depth domains

The main objective of this study is to develop accurate and reliable stress-depth relationships for the Canadian Shield using a region-specific methodology. By addressing the possible ambiguities in previous models, this paper aims to clarify the overlooked aspects and contribute a more refined understanding to the field. Our suggested methodology takes into account the unique structural geology of the Canadian Shield. Rather than using a generalized approach, we segmented the Canadian Shield into specific groups based on regional lithological and structural similarities. This categorization allows for stress models that more properly reflect the complexities of each group. Additionally, we examine the applicability of various statistical tools in developing these relationships and delve into the profound influence of tectonic activities on stress redistribution across diverse areas of the Canadian Shield, ensuring that the models are both statistically sound and geologically representative.

4.3 Methodology

A robust methodology is adopted to develop stress-depth relationships within the Canadian Shield, as shown in Figure 4.2. Step 1 involves the collection of stress data from previous stress

measurement campaigns and other technical reports, while ensuring the accuracy of this collected information. In Step 2, we eliminate the misleading impact of stress orientation through transforming the collected stresses into the Cartesian system, effectively accounting for discrepancies and uncertainties of orientation. Subsequently, we calculate both the maximum and minimum horizontal stresses, in conjunction with their corresponding vertical stress. In the next step, we analyze the potential limitations of relying solely on statistical methods and tools, evaluating their adequacy in formulating the stress-depth relationships for the Canadian Shield. This critical analysis would reveal that depending only on statistics might not provide a reliable estimate of in-situ stress state at various depths, highlighting the necessity of integrating geological considerations for a more accurate determination. Step 4 focused on categorizing the in-situ stress database based on the diverse geological regions of the Canadian Shield, considering structural and lithological attributes specific to each region. In Step 5, we thoroughly analyze the influence of major geotectonic events within each geological group, providing a comprehensive assessment of their effects on stress patterns and redistributions in the Canadian Shield. Finally, Step 6 integrate these geological insights to establish reliable region-specific stress-depth relationships for each created group, tailored to the Canadian Shield's unique geotectonic characteristics.

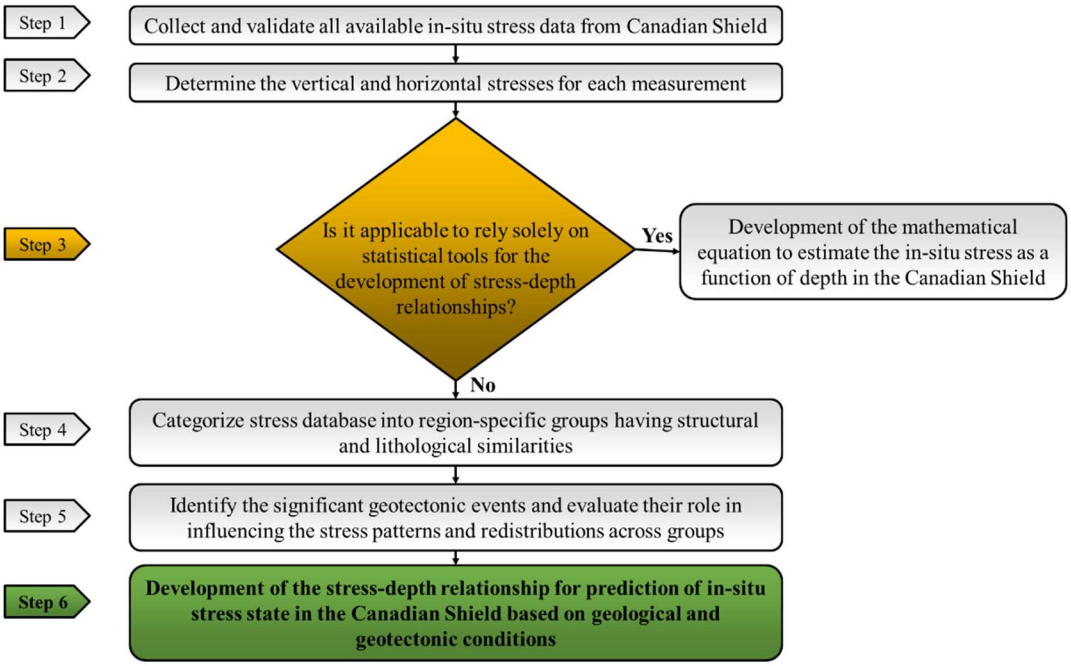

Figure 4.2 Suggested methodology to develop the in-situ stress-depth relationships in the Canadian Shield

4.4 In-situ stress data collection and interpretation

Our dataset consisting of 324 stress values with corresponding orientations stands out for its size compared to those employed in previous studies. It also covers a broader range of depths from 11 to 2550 meters, indicating a significant increase in both dataset size and depth coverage. This extensive dataset emphasizes the enhanced reliability of our analysis, carefully collected from various sources, integrating data from recent measurement campaigns and literature resources. Figure 4.3 shows a geographical map of the Canadian Shield pinpointing the locations where stress data were collected. The datapoints are sourced from three key geological provinces: Grenville (10 datapoints), Southern (59 datapoints), and Superior provinces (255 datapoints). In the Superior province, the data were collected from specific subprovinces—Abitibi, Wawa, Uchi, Berens River, Quetico, Wabigoon, and Pikwitonei—allowed us to conduct a region-specific analysis that considers the unique geological characteristics and stress patterns within each subdivision (Figure 4.3 b) (Card, 1990; Lucas & St-

Onge, 1998; Percival et al., 2012). The database also includes geological information specific to the Canadian Shield, such as the geological province, subprovince, rock type, and measurement methods.

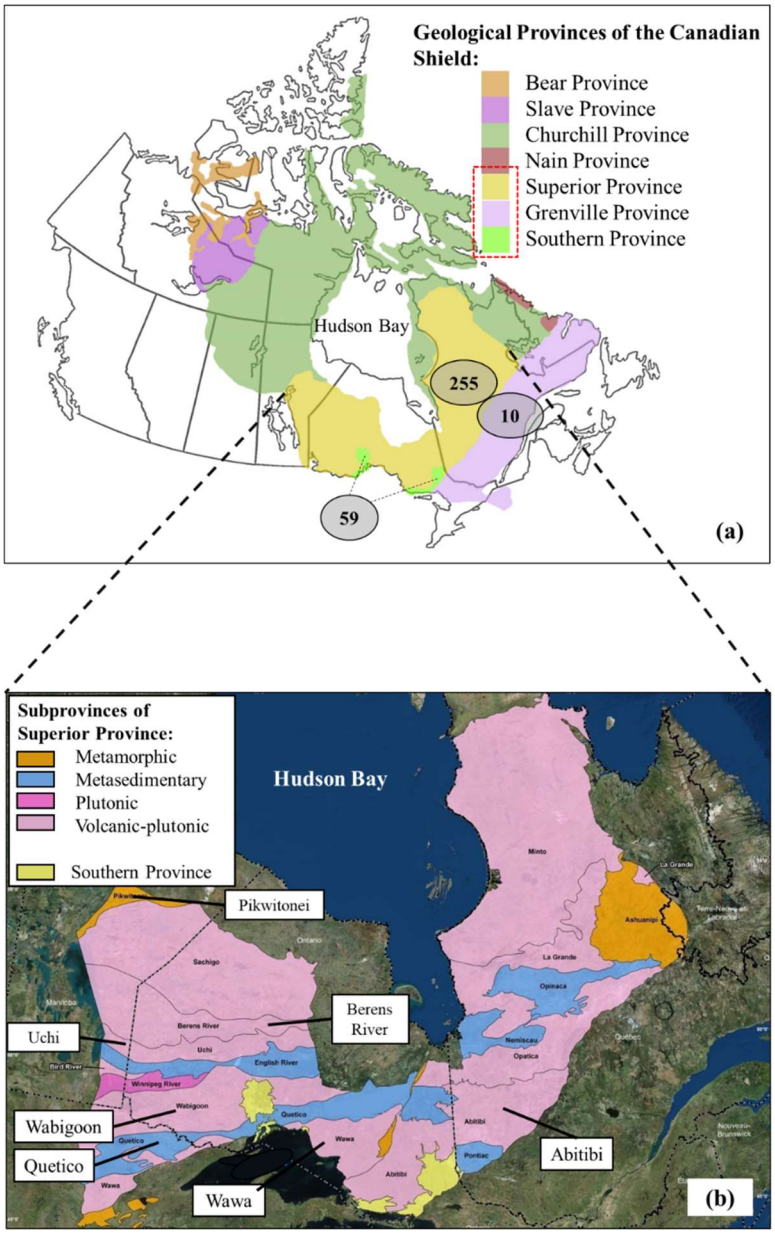

Figure 4.3 Geographical distribution of collected stress data - (a) Across the Canadian Shield, (b) Within subprovinces of the Superior Province (modified from Lucas and St-Onge (1998); Panabaker (2006))

Notable contributions to this dataset include the pioneering work of Herget (1973c) in the Wawa subprovince of the Superior province. Interpretations by Herget and Arjang (1990), mostly measured in Northern Ontario and Eastern Quebec, covered extensive geographic areas, including the Superior,

Grenville, and Southern provinces of the Canadian Shield. Furthermore, Martin (1990) compilation of 99 triaxial overcoring tests, carried out at the Atomic Energy of Canada Limited (AECL) underground research laboratory in the Wabigoon subprovince of the Superior province made a valuable contribution. More recent studies by researchers like Yong and Maloney (2015), primarily focused on the Superior and Southern provinces within the Canadian Shield. The dataset was further developed through the inclusion of other stress values from various mining sites located in West and Northwestern Quebec, carried out in studies by researchers such as Corthésy et al. (1997); Corthésy and Leite (2000, 2013); Corthésy et al. (1996), Golder (2012), Lalancette (2018), and Hammoum (2017). This well-established stress database serves as the cornerstone of our study on stress-depth relationships within the Canadian Shield.

4.5 Determination of in-situ stress tensor in the Canadian Shield

In this study, we address the critical tasks of determining the 3D stress tensor within the Canadian Shield and extracting both vertical and horizontal stresses from the initial stress state. The collected stress values were initially represented in the principal state (σ_1, σ_2 and σ_3) and accompanied by their respective orientations. Each datapoint entry featured nine components, comprising the three stress values, as well as the trend and plunge angles. The trend angle indicates the compass direction of the principal stress, and the plunge angle represents the inclination of the stress from the horizontal plane (Fossen, 2016). According to the literature, it is assumed that σ_3 represented the vertical stress component within the Canadian Shield (Herget, 1987; Maloney et al., 2006; Martin, 1990; C. D. Martin et al., 2003), which basically need to have a plunge angle of approximately 75 to 90 degrees. However, our analysis across the entire database revealed that merely 30% of plunge values of the σ_3 belong to this range (as highlighted in Figure 4.4). This discrepancy raises concerns about the applicability of this convention across the extensive region of the Canadian Shield. Recent stress measurements at Niobec Mine in Quebec, Canada, conducted with the modified doorstopper

technique, revealed that there is a noticeable change at depths exceeding 800m whereby the vertical stress component shifts from σ_3 to σ_1 (Saeidi et al., 2021).

To mitigate these uncertainties, we determined the 3D stress tensor by employing a rotation matrix, as depicted in Figure 4.5. This transformation facilitated the recalibration of stress components, enabling us to accurately recalculate maximum and minimum horizontal stresses Equations 2 & 3. Consequently, the vertical stress could be reliably estimated as Sigma (z) within the 3D stress tensor, ultimately providing a more precise representation of the in-situ stress state. This methodology would enhance the accuracy of stress estimation and engineering decision-making in the Canadian Shield.

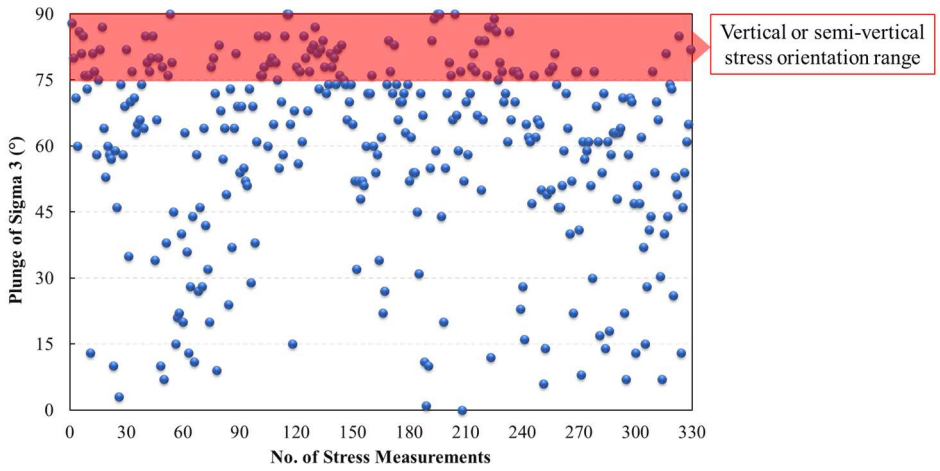

Figure 4.4 The plunge of Sigma 3 component of the stress data within the Canadian Shield

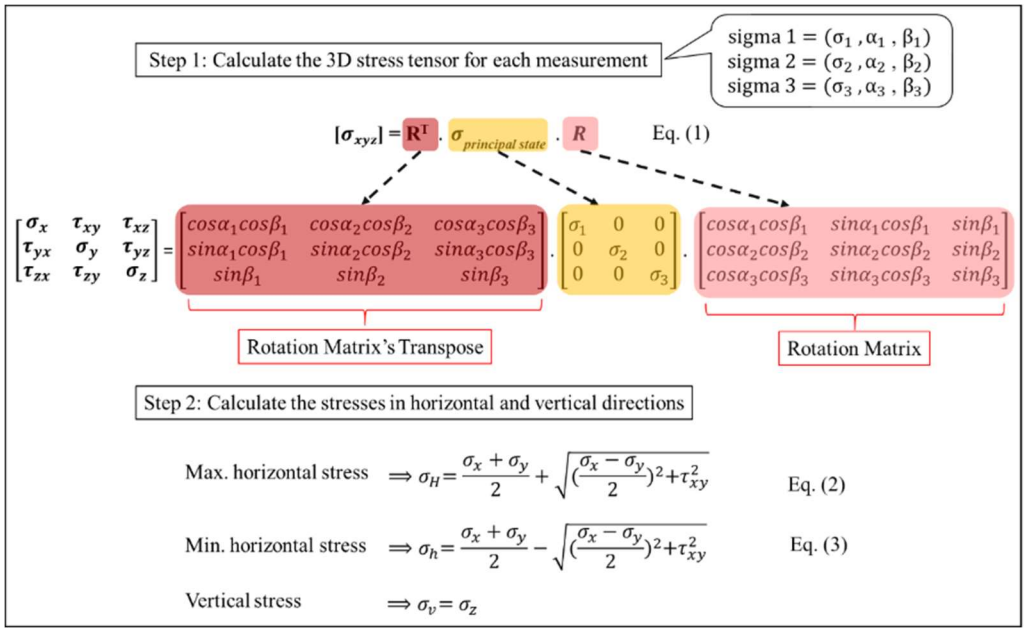

Figure 4.5 Transformation of in-situ stresses from principal state to the horizontal and vertical state (α and β indicate the trend and plunge for each measurement, respectively)

4.6 Evaluation of the applicability of pure statistical analyzing tools to develop stress-depth relationships in the Canadian Shield

In this step, we assess the adequacy of relying solely on statistical analysis to establish stress-depth relationships within the Canadian Shield, highlighting the need for an integrated approach that combines strong geological insights for interpretation. This analysis includes three key aspects:

- Statistical assessment of domain-based approaches
- Refining depth domains through cluster analysis

4.6.1 Statistical assessment of domain-based approaches

In evaluating stress-depth relationships within the Canadian Shield, we systematically apply depth domains to our dataset of 324 stress values, as proposed by Herget (1982) and Maloney et al. (2006). Unlike previous studies, our approach benefits from a significantly larger dataset, allowing for a more thorough and representative analysis of stress-depth equations for each depth domain across all stress components ($\sigma_H, \sigma_h, \sigma_v$), as illustrated in Figures 4.6 & 4.7. thus, enhancing the applicability of our findings. This broader dataset enhances the strength and relevance of our findings, making them more applicable to real-world scenarios. To assess the impact of depth categorization on these relationships, we compared the coefficient of determination (R^2) value within each depth domain with the R^2 derived from the overall dataset. Figures 4.6 and 4.7 illustrate a clear trend—R^2 values within each depth domain were consistently lower than those derived from the entire dataset. This trend underscores the limited predictive accuracy of stress-depth relationships when the Canadian Shield is grouped into distinct depth domains. Consequently, such categorization leads to less robust and more uncertain predictions for all three stress components. The results indicated that prior relationships may have been influenced by statistical inferences from the specific studies, and often overlooking the complex geology of the Canadian Shield. Additionally, classifying zones deeper than 500-600m as undisturbed zones might not be universally applicable across the Canadian Shield.

The subsequent section will delve into a comprehensive cluster analysis to define specific depth domains within the stress database.

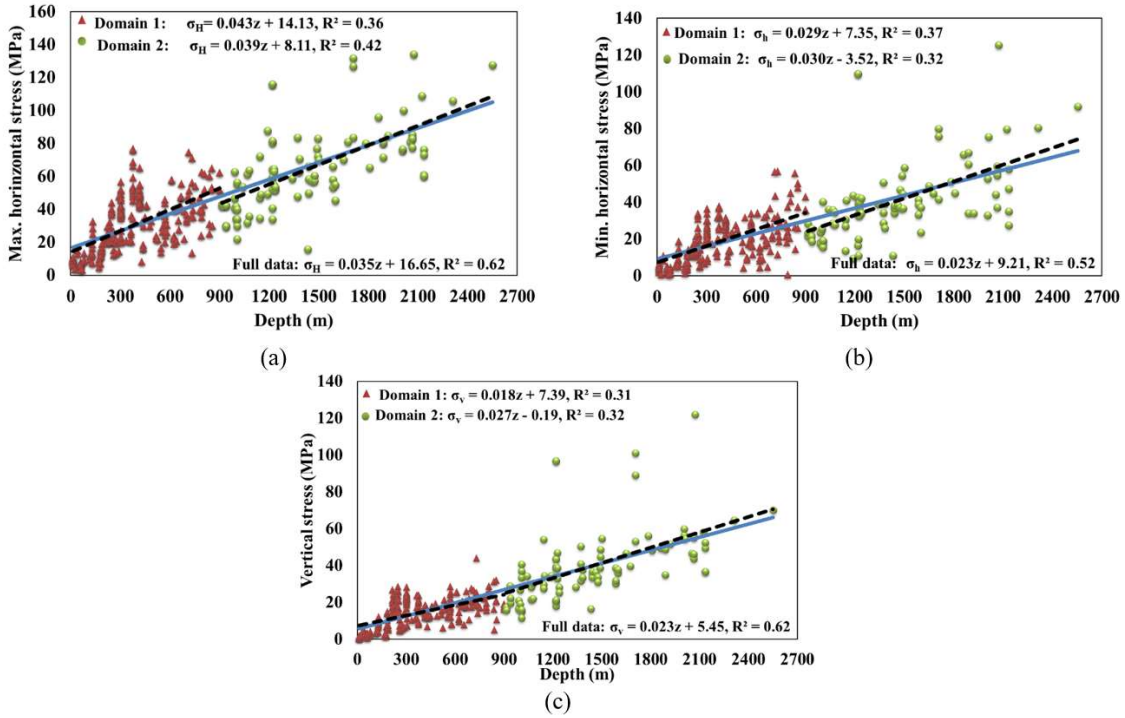

Figure 4.6 Stress-depth equations using the depth domains, proposed by Herget (1982)

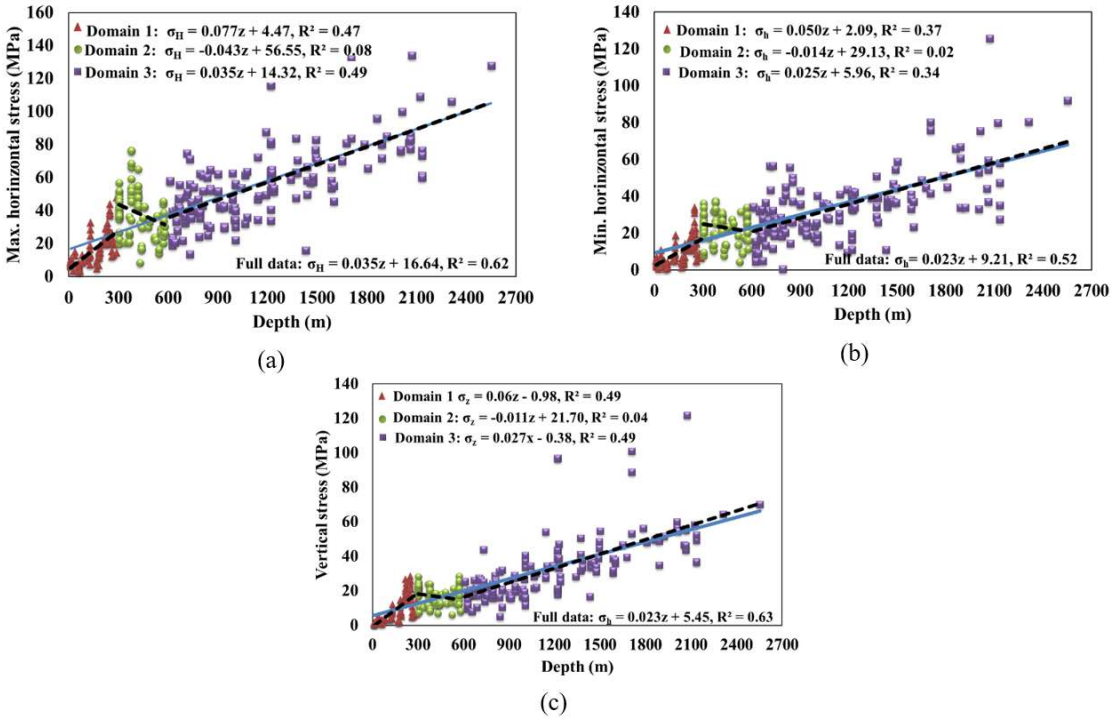

Figure 4.7 Stress-depth equations using the depth domains, suggested by Maloney et al. (2006)

4.6.2 Refining depth domains through statistical approaches

In this phase, we aim to establish meaningful depth ranges through statistical tools for effectively classifying the entire stress database into distinct groups. To initiate the process, a thorough data treatment analysis was conducted to inspect extreme stress values and determine whether they qualify as outliers—data points significantly deviating from the majority (Afraei et al., 2018; Dastjerdy et al., 2023). Focusing on the stress-depth data, where stress and depth serve as two key parameters, we employed the Mahalanobis method for multivariable outlier detection. This method assesses the multivariate distance of a data point from the distribution center, flagging points with significantly different Mahalanobis distances compared to the expected distances within the distribution (Yazdanpanah et al., 2022; Yu et al., 2023; Zheng et al., 2021). The outcome of the outlier detection analysis revealed 25 outliers by the Mahalanobis method, as visually depicted in Figure 4.8.

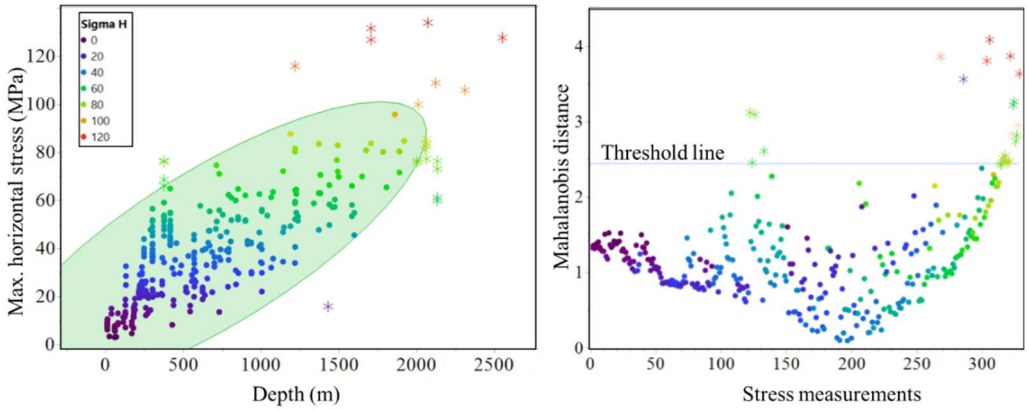

Figure 4.8 Treatment of stress-depth data of the Canadian Shield using Mahalanobis method

Following the treatment of stress database (detection and removal of outliers) , a detailed cluster analysis was conducted on the refined stress data in order to identify certain depth domains in the Canadian Shield. Initially, we utilized the Elbow method to determine the optimal number of clusters. This technique involves plotting the variance captured as a function of the number of clusters and identifying the “elbow point” where adding more clusters does not significantly improve the model's ability to capture patterns in the data (Yan et al., 2023; Yu & Xu, 2021). As shown in Figure 4.9 (a), four clusters were concluded to be optimal for our dataset. Subsequently, we employ K-means and

Hierarchical clustering methods to establish four meaningful depth domains (Kim et al., 2021; Shirani Faradonbeh et al., 2020). K-means clustering is a technique that partitions a dataset into K clusters, iteratively assigning data points to the nearest centroid and updating cluster centers based on the mean of the assigned points. On the other hand, hierarchical clustering forms a tree-like structure of clusters by merging or splitting them based on similarity (Kim et al., 2021; Misra et al., 2019; Nazareth & Lana, 2021). In this study, hierarchical approach showed more efficiency, yielding clusters with clearer distinctions compared to the relatively overlapped clusters of K-means, as visually presented in Figure 4.9 (b & c). Accordingly, the resulting depth domains are presented as follows: 0-750m, 751-1250m, 1251-1750m, and 1751-2500m (Figure 4.9 (d)). To rigorously assess the impact of these depth domains on stress determinations, the statistical robustness of the estimated equations for each domain was examined, which was shown in Table 4.1. Despite the structured statistical approach, the R^2 and the adjusted R^2 values for all domains remain considerably lower compared to the case where data are not categorized for the entire database. This implies that although clustering methods provide statistical structure to the depth domains, the regression analysis for these clusters did not yield satisfactory results in the developed models.

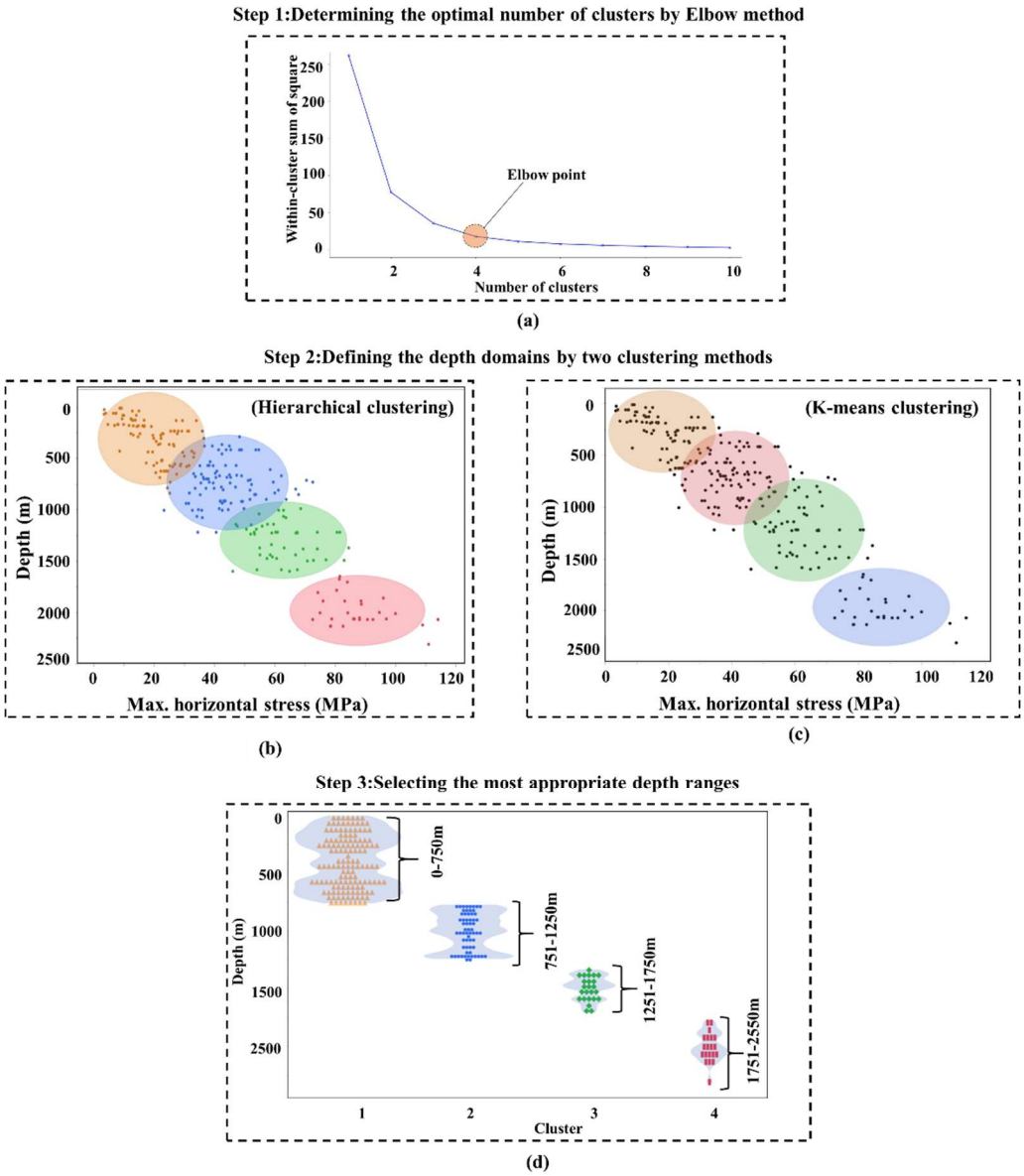

Figure 4.9 Categorization of Stress database of the Canadian Shield by application of clustering methods

Table 4.1. Statistical assessment of stress-depth relationships across clusters in the Canadian Shield

Dataset	Depth domains (m)	R2	Adjusted R2
Cluster 1	0-750	0.51	0.50
Cluster 2	751-1250	0.19	0.18
Cluster 3	1251-1750	0.05	0.01

Cluster 4	1751-2550	0.23	0.19
Entire database	0-2550	0.78	0.78

It should be noted that the extreme data points, identified and removed as outliers, might hold geological or tectonic significance. Rather than excluding them, a thorough geological analysis may be essential since these extreme stress values could be linked to unique geological or tectonic scenarios. This issue will be further discussed in the next section. In conclusion, the development of stress-depth relationships in the Canadian Shield, primarily based on statistical methods, highlights the potential for misleading interpretations when solely relying on these tools. While statistical methods provide valuable insights, their results may be inadequate, emphasizing the need for incorporation of geological and geotectonic considerations into stress determinations. This integration ensures a more accurate understanding of the geological factors influencing stress distributions within the Canadian Shield, contributing to the development of reliable predictive models.

4.7 Geological and geotectonic analysis of the Canadian Shield:

In this section, we conducted a thorough investigation on the geological and tectonic history of the Canadian Shield, with a specific focus on establishing a meaningful connection between the intricate geological characteristics and the characterization of in-situ stress. The Canadian Shield, shaped over two billion years of geological evolution, showcases a diverse array of rock types, encompassing granites, gneisses, and metamorphic rocks (Card, 1990; Lucas & St-Onge, 1998). Our study focuses on three main geological provinces—the Superior, Southern, and Grenville provinces—where stress data were collected. Notably, the Superior province emerges as pivotal in analyzing the in-situ stress state, given its extensive coverage within the Canadian Shield and its dominance in the stress dataset, constituting 78% of our dataset (Fig 4.3 b). The following section introduces a novel grouping approach for the Superior province, with the aim of enriching our geological understanding and estimating the in-situ stress state in the Canadian Shield.

4.7.1 Classification of the Superior province

Given the critical role of the Superior province in stress determination, an in-depth geological and tectonic understanding would significantly clarify the uncertainties related to regional in-situ stress trends for various assessments. We propose a novel geological classification for the Superior province based on three key factors: (i) structural characteristics and tectonic history, (ii) metamorphism and (iii) regional lithological composition, which are schematically presented in Figure 4.10. These parameters have a profound influence on the in-situ stress of rocks within the Canadian Shield. Structural characteristics and tectonic history provide insights into the present and past state of geological structures, affecting stress redistributions. Moreover, metamorphism and lithological composition have great impacts on the mechanical behavior of rocks. Following a detailed geologic study, the sub-provinces of the Superior province were categorized into four distinct groups: Abitibi & Wawa group, Uchi & Berens River group, Wabigoon & Quetico group, and Pikwitonei group. The groups are briefly described below.

4.7.1.1 The Abitibi & Wawa group:

- This group displays a shared tectonic feature with dominant east-west trending structures and significant dextral shear zones. The presence of major domal antiforms and synforms suggests multiple deformation phases, including isoclinal folds, recumbent folds, axial plane foliation in Vermilion greenstone belt of Wawa and Abitibi greenstone belt. Also, volcanic activities in this group such as Timiskaming-type volcanism in Wawa and sedimentation, proves a complex tectonic history (Lucas & St-Onge, 1998; Davis, 2002; Percival et al., 2012).

- The metamorphic history within this group is characterized by predominantly low-grade metamorphism in both subprovinces. The Abitibi subprovince displays instances of regional metamorphism and metasomatism, including events related to sea-floor activity and

hydrothermal metasomatism, however, the Wawa subprovince exhibits a varied metamorphic phases, ranging from greenschist to upper amphibolite facies in different zones (Percival et al., 2012).

- The lithological composition of this group reveals similarities in both subprovinces. Supracrustal rocks in the form of mafic to intermediate volcanic rocks dominate both the Abitibi and Wawa subprovinces. Additionally, felsic volcanic and sedimentary rocks are less common but present in both areas. The presence of plutonic rocks, including gabbro, diorite, tonalite, granodiorite, and granite, is consistent across both subprovinces. The Wawa subprovince, similar to Abitibi, features granitoid intrusions such as synvolcanic tonalite and granodiorite, as well as later intrusions of granites and pegmatites, contributing to a unified lithological understanding (Lucas & St-Onge, 1998; Roberts & Bally, 2012).

4.7.1.2 The Uchi & Berens River group:

- This group is defined by early isoclinal folding and transitioning from ductile to brittle conditions. Polyphase deformation, low-pressure regional deformation, and north-south shortening mark the Uchi & Berens River's tectonic history. Compared to other groups, it exhibits a less complicated tectonic history compared to other groups (Lucas & St-Onge, 1998).
- Both subprovinces exhibit distinct metamorphic patterns, with the Uchi subprovince undergoing low-pressure greenschist to amphibolite facies metamorphism during early ductile deformation in the Rice Lake greenstone belt in Ontario, and the Berens River subprovince experiencing metamorphism under intermediate pressure-temperature conditions associated with early isoclinal folding (Card & Ciesielski, 1986; Corfu & Stone, 1998).
- Lithological similarities emerge in the diversity of supracrustal rocks, with both subprovinces presenting various rock types, including metamorphic rocks. The Uchi subprovince,

however, showcases a broader range, encompassing basalt-andesite-rhyolite sequences, marble, ironstone, and conglomerate (Card, 1990; Percival et al., 2012).

4.7.1.3 The Wabigoon & Quetico group:

- Both subprovinces share a complex tectonic history involving various plate interactions and deformation styles, suggesting a combination of shear and compressional forces. This group is marked by significant north-south shortening, leading to the development of shear zones and late-stage faulting (Percival et al., 2004; Tóth et al., 2022).
- The Wabigoon and Quetico subprovinces experienced significant regional metamorphism. The metamorphic gradient within the group ranged from greenschist facies to amphibolite facies, indicating diverse thermal and pressure conditions during their geological history (Percival et al., 2004; Percival et al., 2006; Stone, 2010).
- In terms of lithological composition, both areas display low- to medium-grade rocks primarily of metasedimentary origin. The occurrence of mafic gneiss, metasedimentary rocks like wacke and siltstone, and the presence of oxide-facies iron-formation are common features, suggesting a parallel lithological evolution between the two subprovinces (Percival et al., 2006; Stone, 2010).

4.7.1.4 The Pikwitonei group:

- Positioned at the northwestern margin of the Superior Province, this subprovince stands out as a high-grade gneiss region in the Canadian Shield, exhibiting isoclinal folding associated with amphibolite facies metamorphism. Notably, it features granulite-grade metamorphism and the superimposition of northeast-trending structures over the original east-west trending structures. The Pikwitonei-Thompson belt contact, representing the eastern limit of Proterozoic influences, involves the transformation of Pikwitonei granulites and the transposition of Molson dikes (Lucas & St-Onge, 1998).

- The Pikwitonei Subprovince is in tectonic contact with the Paleoproterozoic Trans-Hudson Orogen. This region is characterized by high-grade gneiss, offering a cross-section through the middle and lower crust. The contact zone with the Thompson belt witnesses structural complexities, including the Setting Lake fault zone with dip-slip and sinistral strike-slip movements (Card, 1990; Couëslan, 2019).

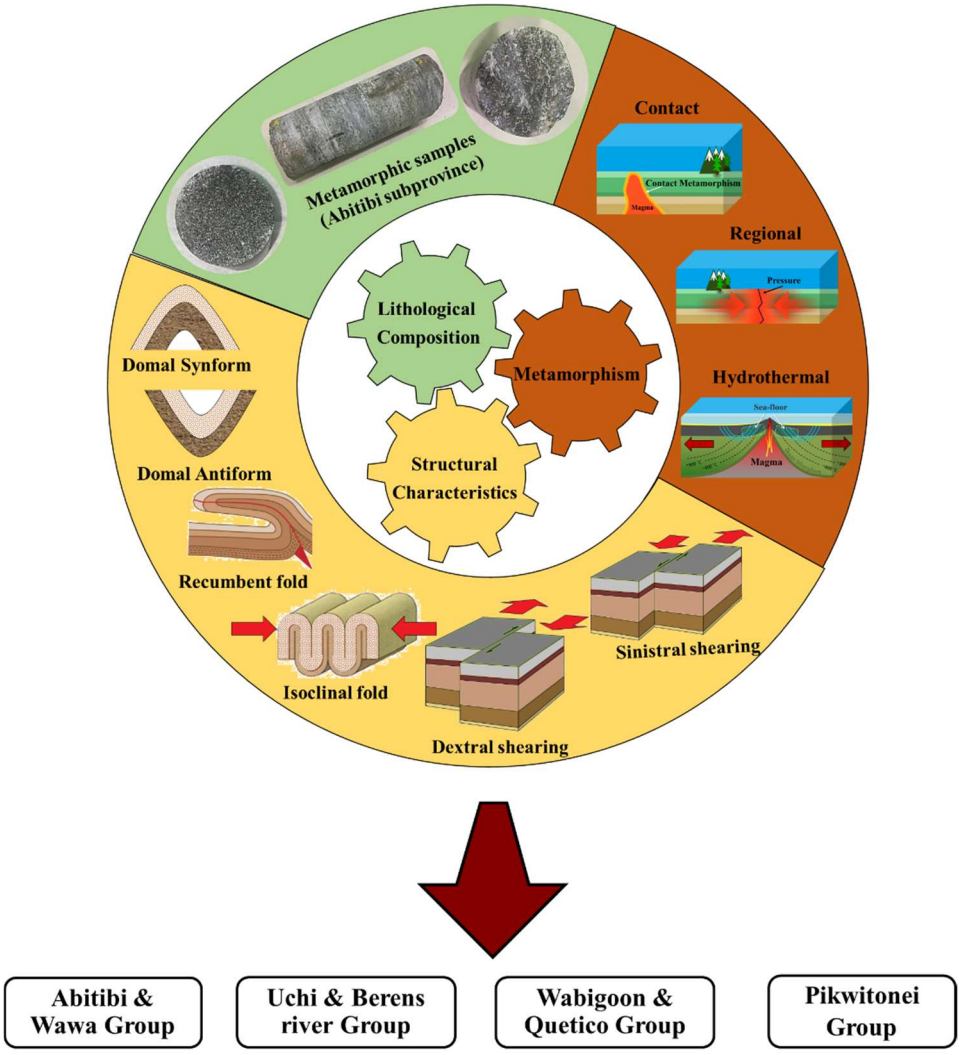

Figure 4.10 Classification of the Superior province based on three key factors

This classification can enhance our understanding of the geological occurrences, which impacted the in-situ stress state in the Canadian Shield. The following section will spotlight key regional

geotectonic occurrences within each group, emphasizing their pivotal role on establishing stress-depth relationships for precise regional assessments.

4.7.2 Identification of major regional geotectonic events in the Canadian Shield

In this section, we determine the major regional geotectonic events in each group, as understanding the key tectonic events is crucial to evaluate the in-situ stress state in the Canadian Shield.

In the vast area of the Abitibi & Wawa group, two major regional tectonic events are potentially dominant: synvolcanic extension in the Abitibi subprovince and transpressional tectonics in the Wawa subprovince (Lucas & St-Onge, 1998; Ludden et al., 1986). As shown in Figure 4.11 (a), synvolcanic extension involves the stretching and pulling apart of the Earth's crust during volcanic activity, resulting in extensional forces that give rise to major faulting (Chown et al., 1992). Within the Abitibi subprovince, this process can play a crucial role in the evolution of the Abitibi greenstone belt, contributing to the formation of domal antiforms and volcanic sequences (Percival et al., 2012). In the Wawa subprovince, transpressional tectonics, as seen on Figure 4.11 (b), entails simultaneous horizontal compression and displacement (sliding) event, creating a complex and variable stress environment (Fossen, 2016; Percival et al., 2012). Unlike simpler compression or extension-dominated environments, transpression introduces an additional component that may potentially reorient principal stresses. In Wawa, transpressional tectonics could induce structural changes, such as the reactivation of pre-existing faults or create new ones, the formation of complex fold patterns and stress variations with depth. These processes might lead to the redistribution of stresses locally and regionally. Together, these events can introduce complex stress fields that may result in changes in the state of in-situ stress.

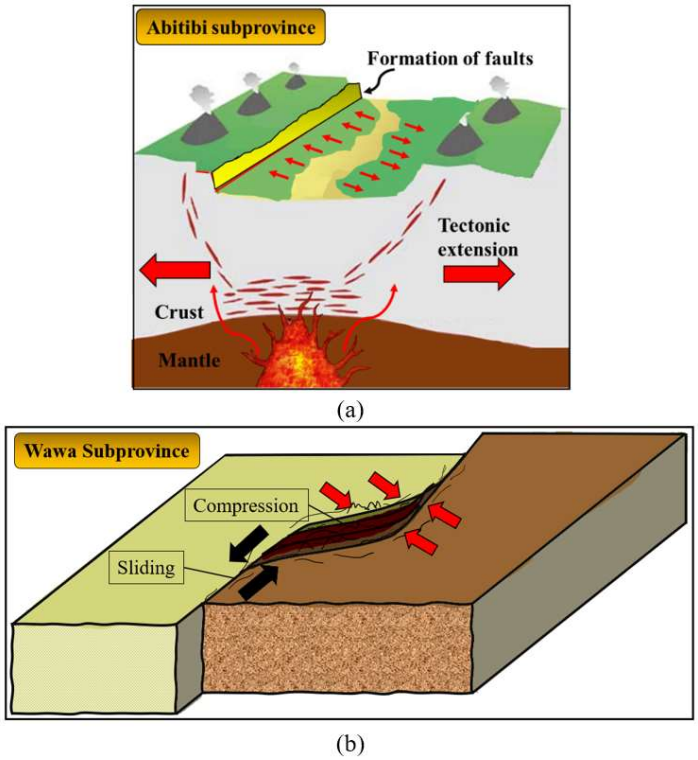

Figure 4.11 Significant regional tectonic event: a) synvolcanic extension in the Abitibi subprovince, b) transpressional tectonic in the Wawa subprovince (adapted from Fossen (2016))

In the Uchi & Berens River group, a notable regional structural phenomenon can be tectonic transport and thrust stacking (Corfu & Stone, 1998; Lucas & St-Onge, 1998). This geological process is characterized by the convergence of two tectonic plates, inducing compressional stress and the initiation of thrust faults. Figure 4.12 shows that this tectonic event involves the northward movement of rock masses, generating differential loading as one plate moves over the other. Also, the thrust stacking, characterized by early faulting and folding, further complicates the stress regime (van Gool et al., 1999). The rearrangement of rock units with different mechanical properties through thrust stacking would probably create irregular stress pathways. When lighter rock units are thrust over denser ones, the overall lithostatic pressure from the overlying rocks might be less than expected for that depth. This intricate scenario of tectonic forces during transport and thrust stacking combined with the inherent properties of the rocks, potentially leads to deviations in the expected vertical stresses within the Uchi & Berens River group.

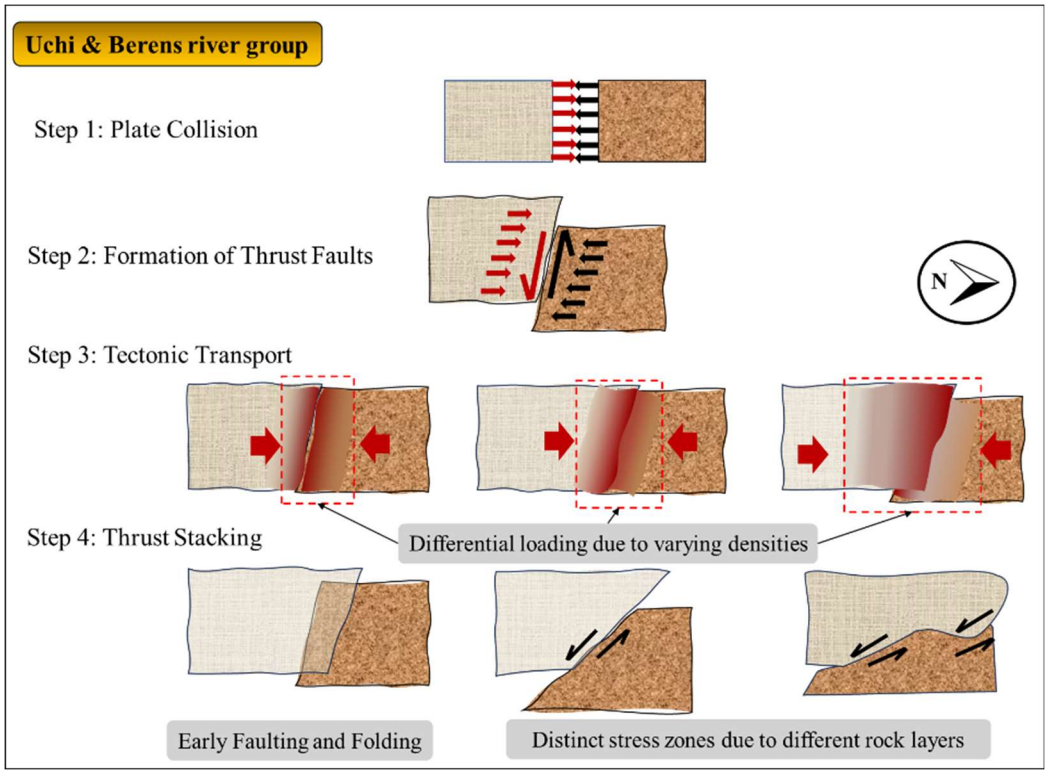

Figure 4.12 Schematic representation of tectonic transport and thrust stacking in the Uchi & Berens River group

Within the Wabigoon & Quetico group, the regional geology is significantly shaped by two distinct tectonic processes known as thin- and thick-skinned tectonism (Figure 4.13) (Card, 1990; Lucas & St-Onge, 1998). Thin-skinned tectonism predominantly involves deformation in the uppermost layers of the crust, primarily affecting sedimentary layers. This process typically begins with the formation of a décollement layer, facilitating horizontal movement along faults and folds. The overlying sedimentary layers can undergo compression, folding, or thrusting over adjacent regions, leading to localized stress variations (Madritsch et al., 2008; Pfiffner, 2017). These structural complexities induced by thin-skinned tectonism would introduce variations in stress concentrations, particularly in proximity to faults or folds. Conversely, thick-skinned tectonism operates at a deeper level, penetrating into both the sedimentary layers and the more rigid crystalline rocks in the middle and lower sections of the crust. This deeper involvement often occurs in regions subjected to intense compressional forces, leading to substantial stress variations across a broader expanse of the crust.

The regional compressional stresses associated with thick-skinned tectonism can result in reverse (thrust) faulting, and initiating deep-rooted deformation. This process may lead to the uplift of deeper crustal sections, introducing rocks to the surface that were once at greater depths. The retained tectonic overpressure in thick-skinned tectonism could contribute to vertical stresses that surpass lithostatic pressure (Pfiffner, 2017; Roberts & Bally, 2012).

The combination of these two tectonic mechanisms within the Wabigoon & Quetico group contributes to a complex geological setting, where stress variations are influenced by both shallow and deep-seated structural processes, possibly leading to diverse vertical stresses in areas affected by thick-skinned tectonism.

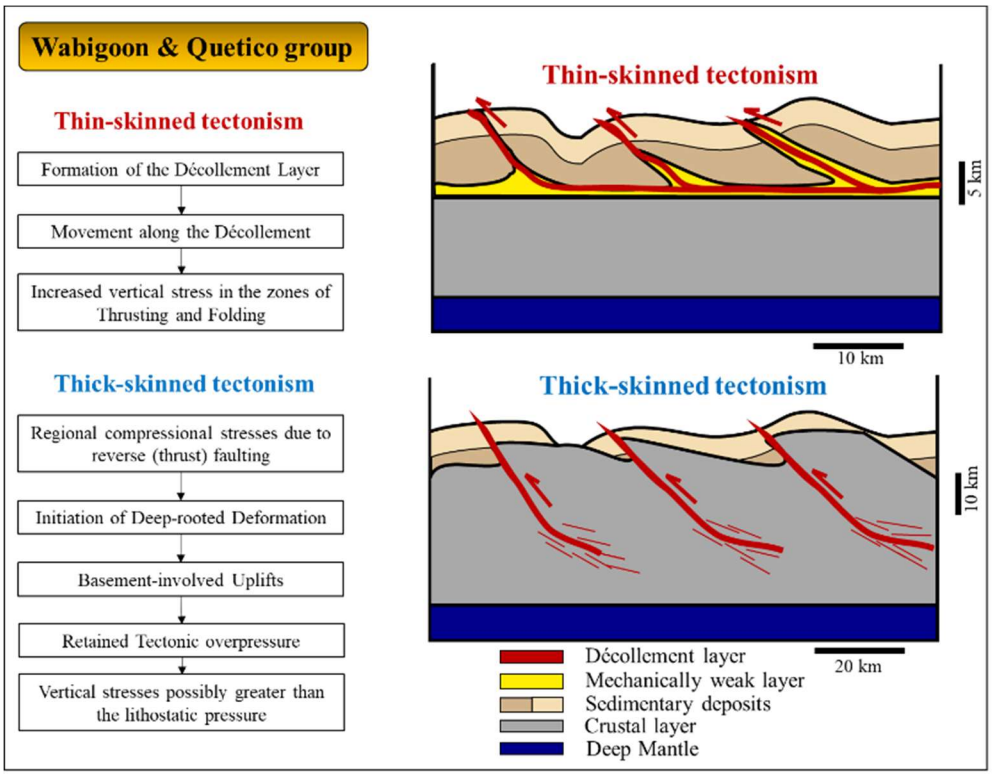

Figure 4.13 A simplified illustration of thin- and thick-skinned tectonism in the Wabigoon & Quetico group (adapted from Pfiffner (2017))

The Pikwitonei group is characterized by a significant tectonic overprinting phenomenon, in which older geological structures experience deformation and are subsequently overlaid by later

tectonic forces (Percival et al., 2012). Positioned at the boundary between the Superior Province's Archean craton and the younger Trans-Hudson Orogen, this region has witnessed historical tectonic collisions. The Pikwitonei Subprovince's contact with the Thompson belt shows evidence of tectonic and metamorphic occurrences during Paleoproterozoic orogenic events, subjected to multiple episodes of deformation and stress resetting, as shown in Figure 4.14 (Couëslan, 2019; Lucas & St-Onge, 1998). This transition zone has experienced the overprinting of newer structures over older ones through compressional, extensional, or shearing forces, resulting in varied stress regimes. This geological complexity is further highlighted by the uplift of deeper crustal levels of a granite-greenstone terrane, leading to early minor folds and advanced faulting. Figure 4.14 depicts these intricate geological processes, as they may have significant role in shaping the in-situ stress state and contributed to the intricate stress distribution within the Pikwitonei group.

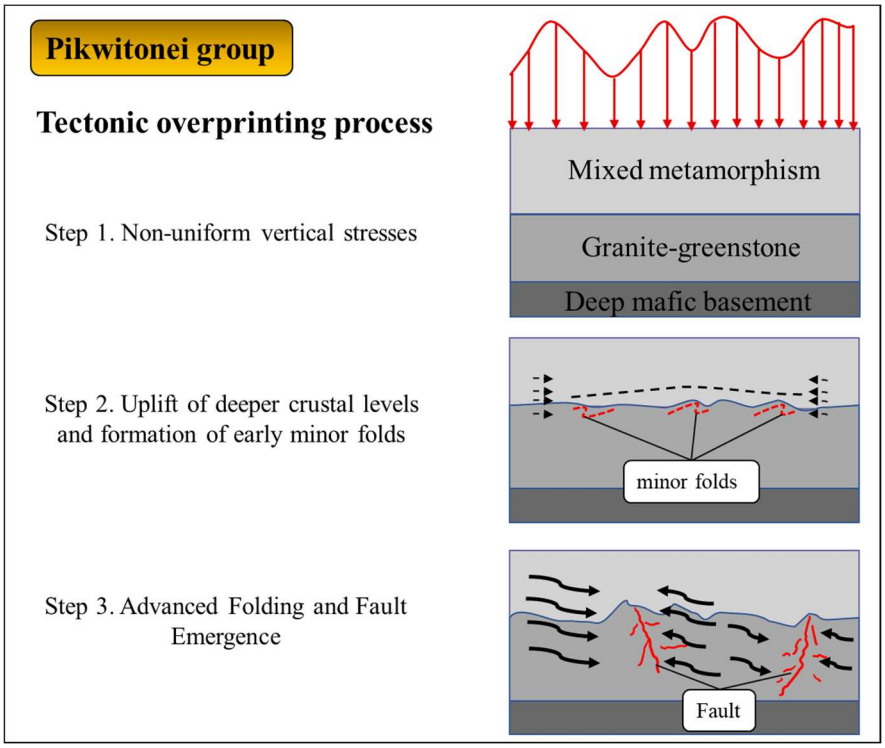

Figure 4.14 Schematic illustration of the tectonic overprinting in the Pikwitonei subprovince

In addition to the Superior province, the geotectonic condition of two other provinces within the Canadian Shield needs to be considered in this study. In the Grenville province, a prominent regional

tectonic event might be thrust imbrication (Labat et al., 2020; Lucas & St-Onge, 1998; Mitchell, 2007). This geological phenomenon, driven by compressional tectonic forces, results in the deformation and stacking of rock layers along thrust faults. Unlike thrust stacking, discussed in the Uchi & Berens river group, thrust imbrication is associated with convergent tectonics, where tectonic plates move towards each other, inducing horizontal compression and deformation of the Earth's crust (Hopgood, 1987). As illustrated in Figure 4.15, the collision of plates generates intense compressional forces, leading to the formation of thrust faults. These inclined fractures cause rocks not only to be displaced but also folded and stacked, forming imbricate slices. The compressional forces associated with thrust imbrication would potentially disturb the regional regime of horizontal and vertical stresses. The geometry of thrust faults and resulting imbricate slices might play a crucial role in determining the orientation and magnitude of these stresses.

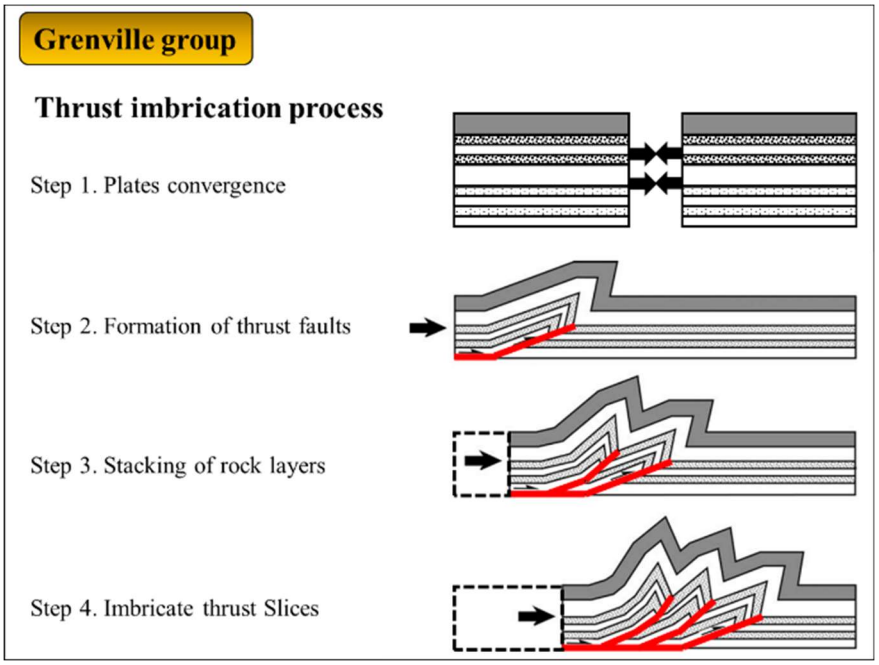

Figure 4.15 The process of thrust imbrication in the Grenville group (adapted from Poblet and Lisle (2011))

The geology of the Southern Province, notably in the Sudbury area, is shaped by the Late Precambrian Penokean Orogeny, a continental-continental collision (Percival & Easton, 2007; Rousell & Brown, 2009). This intense tectonic event, characterized by thrust faulting, folding, and

various deformations, played a key role in the geological evolution of the region. This regional tectonic event could cause variation in stress patterns through the crust. Notably, Kink bands, narrow zones of intense folding, formed during the Penokean Orogeny, serve as key indicators of this tectonic activity (Zolnai et al., 1984). The Kink bands induce the rotation of internal foliation within rocks, potentially altering mineral orientations. This process can influence the mechanical behavior of rocks and deviating stresses from their expected trends. Figure 4.16 provides a simplified illustration of the Penokean Orogeny and the associated Kink bands, offering a visual representation of the intricate geological processes in the Southern province.

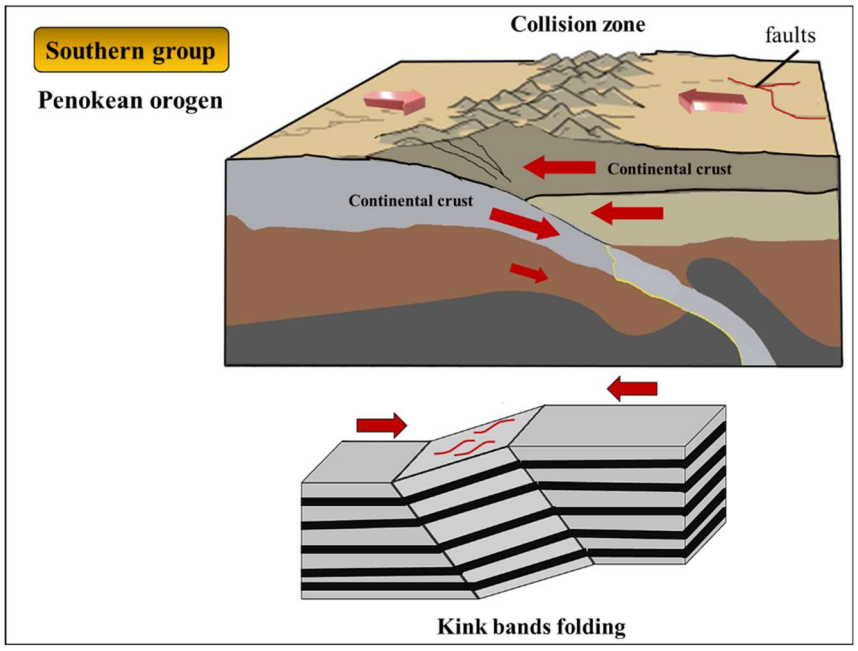

Figure 4.16 A simplified illustration of Penokean Orogeny and the Kink bands in the southern province

After identifying the key regional tectonic events in each geological group and examining the unique structural geology of the Canadian Shield, the next step involves the development of robust stress-depth equations where the statistical analyses are integrated with geological considerations. This approach would provide a comprehensive and reliable representation of the in-situ stress state within the Canadian shield.

4.8 Development of stress-depth relationships

In this section, we conducted a regression analysis to thoroughly examine the in-situ stress state as a function of depth in all designated geological groups within the Canadian Shield. The main objective is to develop reliable stress-depth equations for crucial parameters, including vertical stress (σ_v), maximum and minimum horizontal stresses (σ_H,σ_h) and stress ratios (K) (average, maximum and minimum). This approach potentially enhances our understanding of how these key stress parameters change with depth and how they impact the design phase of underground structures in different regions within the Canadian Shield.

In the Wabigoon & Quetico group, vertical stresses exhibit a unique behavior (Figure 4.17a), deviating notably from overburden or lithostatic pressure line (the expected vertical stress), which can be calculated by $P = \gamma h$ (γ and h are rock density and depth, respectively). Most datapoints also fall beyond a confidence interval of two standard deviations ($\pm 2SD$), proving significant variability. The regression analysis proposed a nonlinear model for vertical stress in this group ($R^2 = 0.51, \sigma_z = 1.08z^{0.49}$), potentially capturing this behavior and implying the influence of additional tectonic forces on vertical stress beyond the weight of overburden rock layers. It is also crucial to note that while the estimated model may not demonstrate a high level of predictability robustness, this can be accepted due to the high variability in existing scattered data, largely influenced by regional tectonic events. These include thin- and thick-skinned tectonism, likely contributing to the huge variability in stress environments within this geological group.

The horizontal stresses, as indicated in Figure 4.17b, seem to align with a trend similar to vertical stress, with a higher R2 values for both horizontal stresses. This alignment might suggest an influence from regional tectonism. However, these justifications should be essentially followed with caution, given the inherent uncertainties associated with the statistical estimations.

After determining the vertical and horizontal stress components, we utilized the Anderson faulting approach to identify the prevailing stress regime in the Wabigoon & Quetico group (Anderson, 1951a). According to this theory, the dominant stress regime in this region is thrust or Revere Faulting (RF), where σ_H represents the maximum principal stress, σ_v is the minimum principal stress, and σ_h acts as the intermediate stress. The overall tectonic regime aligns with the Canadian Shield. Figure 4.17c illustrates trends through a line graph. While RF predominantly governs the stress regime, an interesting shift to the Strike-Slip (SS) regime occurs in certain depth ranges, particularly around 180m to 250m. This observation suggests that, despite the predominant compressional force, there might be layers or zones experiencing shear stress, as highlighted in Figure 4.17c.

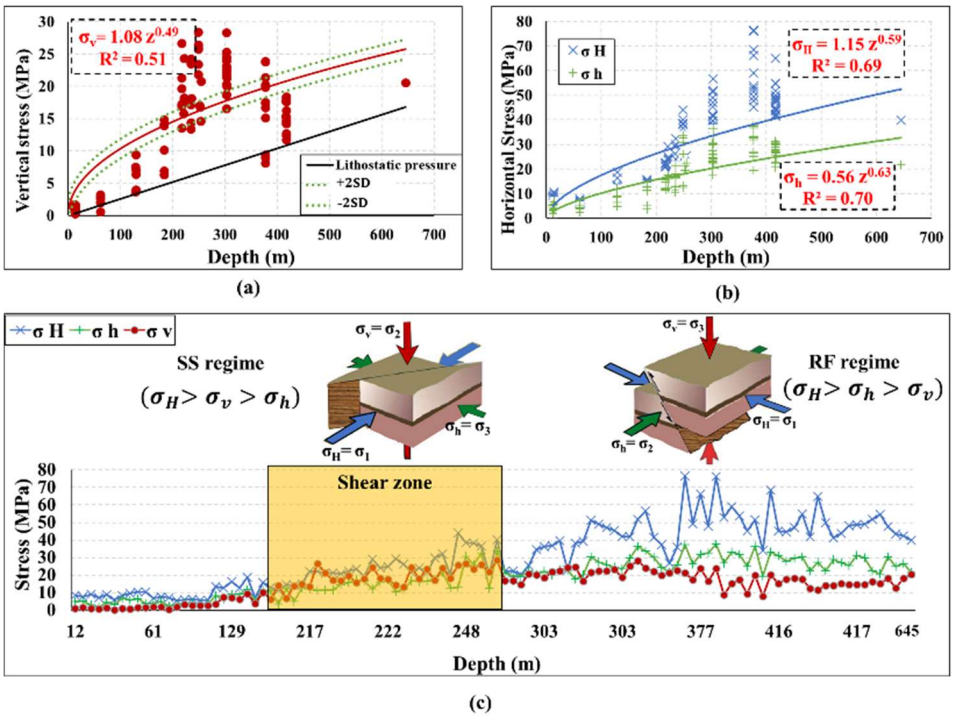

Figure 4.17 The proposed in-situ stress-depth relationships in the Wabigoon & Quetico group: a) Vertical stress, b) Horizontal stress, c) Analysis of stress regime (SS regime: Strike-Slip, and RF regime: Reverse Faulting)

Furthermore, the horizontal-to-vertical stress ratio plays a key role in the stability design of underground structures, in which significantly influences the selection of support systems and

excavation methods (Brown & Hoek, 1978; Taherynia et al., 2016). Therefore, establishing a reliable relationship in stress ratios could minimize risk and optimize construction processes, allowing engineers to anticipate and address challenges related to ground behavior.

In the Wabigoon & Quetico group, we developed relationships for three stress ratios— $K_{max}, K_{min}, K_{ave}$, representing maximum, minimum and average values, respectively. A comprehensive comparison was conducted with well-known past models, including Brown & Hoek (1978), Herget (1987), Arjang & Herget (1997), and Yong & Maloney (2015). As illustrated in Figure 4.18a&b, our equations exhibit a hyperbolic trend similar to Herget (1987), potentially representing a globally accepted trendline, supported by Brown & Hoek's global study. This trend suggests that our proposed models align well with existing relationships at moderate depths, particularly beyond 500m (Figure 4.18a&b). Moreover, high K values in shallow zones may align reasonably with geotectonic and rock mechanics principles. In contrast, relationships presented by Yong & Maloney (2015) show a constant linear function with a low gradient (-0.0006 for K_{max} and -0.0003 for K_{min}), indicating a less reliable relationship. Despite the coefficient of determination (R2) around 0.50, reflecting substantial data variation, our correlation values stand as the highest among the comparisons. It is worth mentioning that the equations proposed by Herget (1987) and Yong & Maloney (2015) did not provide the associated R2 values, which pose a limitation to their assessment. Table 4.2 presents the comparison of previous relationships within the Canadian Shield and proposed equations for the Wabigoon&Quetico group.

Furthermore, we calculated the average stress ratio (K_{ave}) for this region, defined as the ratio of average horizontal stresses to the vertical stress ($K_{ave} = ((\sigma_H + \sigma_h)/2)/\sigma_v$). The resulting regression line ($K_{ave} = 71.51/z + 1.51$) was compared with the suggested global range by Brown & Hoek (1978) ($100/z + 0.3 \leq K_{ave} \leq 1500/z + 1.5$) and the equation by Herget (1987), proposed for the entire Canadian Shield. As depicted in Figure 4.18c, our regression line not only falls within the Brown & Hoek range but also closely aligns with Herget's line. While correlation values were not

provided for the other models, our proposed line demonstrated a R2 value of 0.49, indicating a robust alignment with the expected trends and supporting the reliability of our estimations in the Wabigoon & Quetico group.

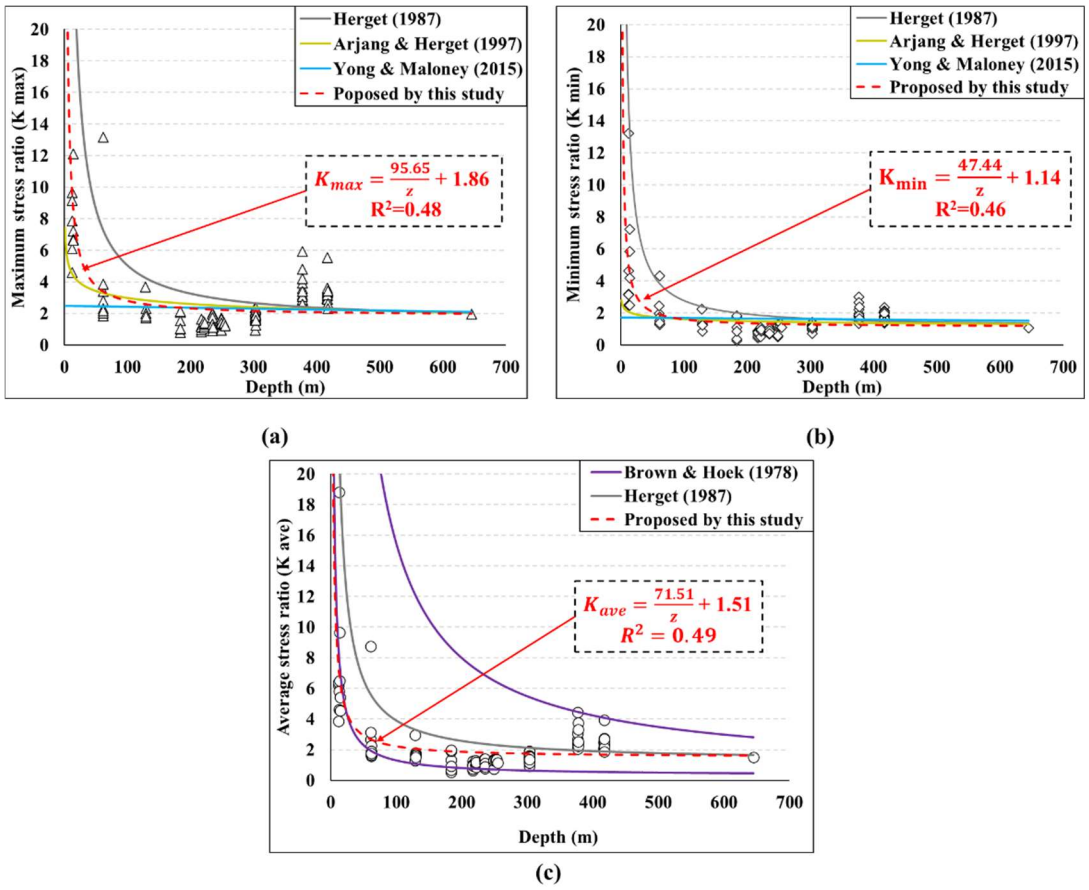

Figure 4.18 Comparison of developed stress ratio relationships for the Wabigoon&Quetico group with previous models: a) Maximum stress ratio, b) Minimum stress ratio, and c) Average stress ratio

Table 4.2. Comparison of past relationships with the proposed equations for the stress ratios within the Canadian Shield

Proposed relationships for stress ratios in the Canadian Shield		Maximum stress ratio ($K_{max} = \frac{\sigma_H}{\sigma_v}$)	Minimum stress ratio ($K_{min} = \frac{\sigma_h}{\sigma_v}$)
Herget (1987)	$Eq.$	$357/z + 1.46$	$167/z + 1.10$
	R^2	*Not provided*	

Arjang & Herget (1997)	$Eq.$	$7.44\ z^{-0.198}$	$2.81\ z^{-0.120}$
	R^2	0.36	0.16
Yong & Maloney (2015) (only for Superior province)	$Eq.$	$-0.0006z + 2.489$	$-0.0003z + 1.705$
	R^2	*Not provided*	
Proposed for Wabigoon&Quetico group	$Eq.$	$95.65/z + 1.86$	$47.44/z + 1.14$
	R^2	0.48	0.46

The regression results for various stress parameters across the defined groups—Wabigoon & Quetico, Uchi & Berens River, Pikwitonei, Abitibi & Wawa, Grenville, and Southern—are summarized in Table 4.3. The presented equations and their corresponding R2 values highlight the variability and distinct trends within each group. Our main objective was to develop equations that are statistically robust and in accordance with the principles of rock mechanics. It is important to note that while correlation values (R2) in certain groups, particularly the stress ratios of the Southern group, may appear relatively low, these values could still be considered reasonable due to the substantial variations present in the data for this particular group.

Table 4.3. Summary of regression results for in-situ stress relationships in the Canadian Shield as a function of depth (z)

Defined groups in the Canadian Shield		In-situ stress parameters					
		σ_v	σ_H	σ_h	K_{max}	K_{min}	K_{ave}
Wabigoon & Quetico group	*Eq.*	$1.08\ z^{0.49}$	$1.15\ z^{0.59}$	$0.56\ z^{0.63}$	$95.6/z + 1.8$	$47.4/z + 1.1$	$71.5/z + 1.5$
	R^2	0.51	0.69	0.70	0.48	0.46	0.49
Uchi &Berens River group	*Eq.*	$0.026z$	$0.045z$	$0.025z$	$1055.3/z + 0.9$	$435.2/z + 0.6$	$745.2/z + 0.8$
	R^2	0.79	0.51	0.70	0.38	0.29	0.41

Pikwitonei group	*Eq.*	$0.0002\ z^{1.84}$	$0.082\ z^{1.02}$	$0.0009\ z^{1.64}$	$894.6/z + 0.5$	$137.2/z + 1.04$	$515.9/z + 0.8$
	R^2	0.99	0.99	0.99	0.89	0.74	0.88
Abitibi& Wawa group	*Eq.*	$0.027z$	$0.47\ z^{0.68}$	$0.47\ z^{0.61}$	$7.3\ z^{-0.19}$	$3.4\ z^{-0.15}$	$5.3\ z^{-0.17}$
	R^2	0.65	0.66	0.49	0.29	0.18	0.30
Grenville group	*Eq.*	$0.030z$	$5.7\ z^{0.21}$	$1.8\ z^{0.28}$	$16.4\ z^{-0.34}$	$11.5\ z^{-0.42}$	$13.6\ z^{-0.36}$
	R^2	0.83	0.17	0.20	0.27	0.51	0.38
Southern group	*Eq.*	$0.028z$	0.042z+7.12	0.03z+0.65	$292.5/z + 1.5$	$242.9/z + 0.96$	$269.3/z + 1.2$
	R^2	0.59	0.66	0.54	0.11	0.19	0.17

In analyzing the vertical stress equations across the groups, defined in the Canadian Shield, distinctive trends can be identified. The Pikwitonei group, similar to the Wabigoon & Quetico, displays a non-linear trend, possibly attributed to the regional tectonic overprinting and high metamorphism, leading to substantial deviations from lithostatic pressure. In contrast, the Uchi & Berens River and Abitibi & Wawa groups show relatively predictable trends, closely aligning with lithostatic pressure, with equations ranging from 0.026z to 0.027z. However, the equations for the Grenville and the Southern groups were slightly elevated from the latter groups. The calculated coefficient of determination (R^2) for these groups falls within the range of 0.59 to 0.83, reflecting consistent and reliable vertical stress-depth relationships, as illustrated in Figure 4.19a.

Regarding the horizontal stresses, the regression lines for the Uchi & Berens River and the Southern groups demonstrate closely similar trends, especially noticeable in the maximum horizontal stress (Figure 4.19b&c). This similarity is expected to persist with increasing depth. Despite considerable data variation in the Southern group, both horizontal stresses maintain reasonable R^2 values (0.59 and 0.66). As shown in Figure 4.19b&c, the developed equations for the Abitibi & Wawa and Grenville groups share a similar non-linear trend, yet the Grenville group exhibits a notably greater scale factor ($\sigma_H = 5.7z\text{^}0.21$ and $\sigma_h = 1.8z\text{^}0.28$), especially in shallow depths which could

be linked to regional thrust imbrication. This tectonic activity could induce deviations in the magnitude of horizontal stresses. Conversely, the Abitibi & Wawa group maintains a slight difference between the max and min horizontal stresses. Both equations ($\sigma_H = 0.47z\text{^}0.68$ and $\sigma_h = 0.47z\text{^}0.61$) indicate a relatively consistent stress regime, possibly influenced by significant regional tectonic events, such as synvolcanic extension in the Abitibi subprovince and transpressional tectonics in the Wawa subprovince. Moreover, the established equations for the Pikwitonei group indicate an almost linear relationship in the case of maximum horizontal stress, whereas the minimum horizontal stress displays a non-linear pattern.

Following the characterization of relationships for vertical and horizontal stress in the Canadian Shield groups, the predominant stress regimes could be determined. The analysis revealed that the dominant stress regime might be Reverse Faulting (RF) regime, except for the Uchi &Berens River group, which exhibits stress relationships aligned with a Strike-Slip (SS) regime, as the equation for vertical stress (0.026z) exceeded the minimum horizontal stress (0.025z). This potentially suggests the presence of possible shearing zones within this group.

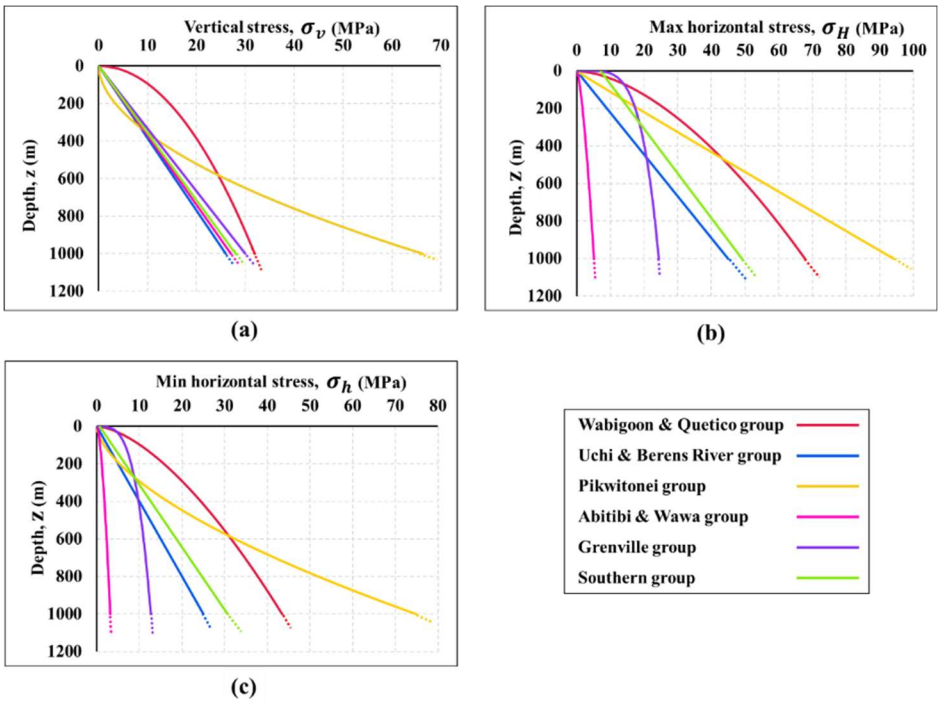

Figure 4.19 Comparative analysis of regression lines in the Canadian Shield groups, a) Vertical stress, b) Maximum horizontal stress and c) Minimum horizontal stress

In addition, Figure 4.20 illustrates the comparison of stress ratios across various groups. The developed equations, as summarized in Table 4.3, exhibit consistency with the global trend of Brown & Hoek (1978) and align with the findings of Herget (1987) for the entire Canadian Shield, except for the Abitibi & Wawa and the Grenville groups. As represented in Figure 4.20, with increasing depth, the stress ratios in each group tend to stabilize, conforming with the principles of geo-stresses. Nonetheless, differences emerge among the groups in the developed equations. Notably, the Wabigoon & Quetico group depict the highest stress ratios, while the Grenville group displays the lowest minimum and average stress ratios.

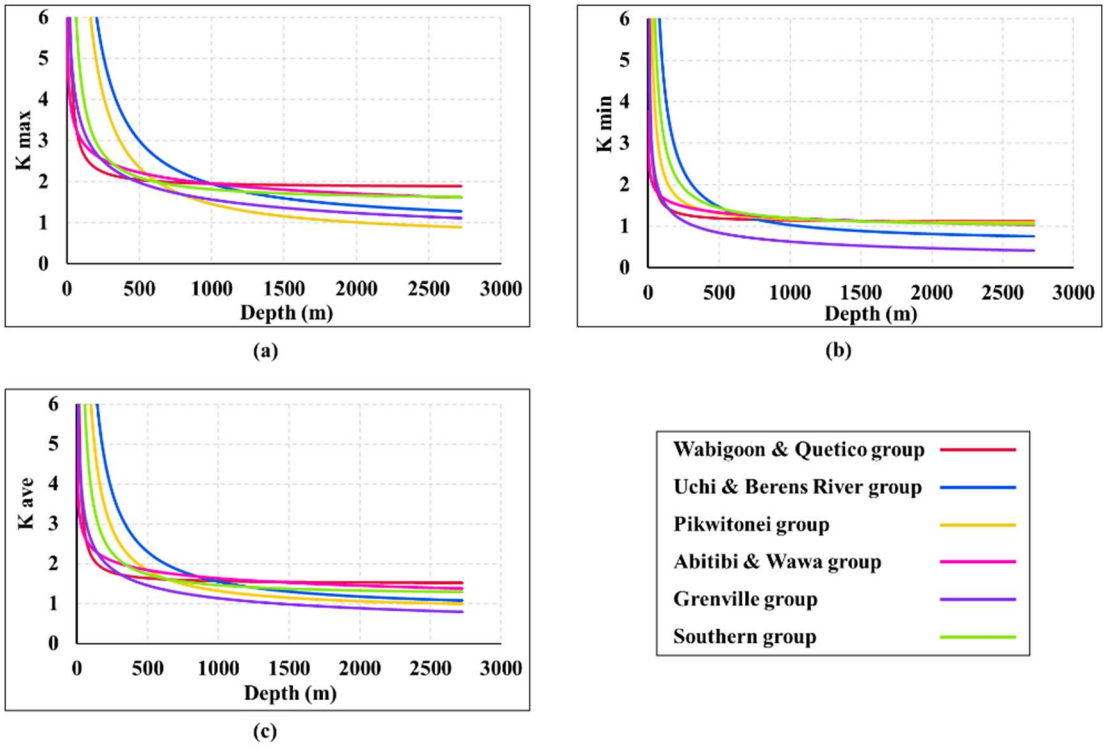

Figure 4.20 Comparative analysis of stress ratios across Canadian Shield groups: a) Maximum stress ratio (K_{max}), b) Minimum stress ratio (K_{min}), c) Average stress ratio (K_{ave})

4.9 Summary and discussion

This research aimed to develop reliable stress-depth relationships in the Canadian Shield by addressing major limitations in previous studies. In this study, we conducted a thorough analysis on the stress-depth equations, critically evaluating the applicability of past approaches that involve categorizing stress data into several depth domains. The findings indicated that the previous relationships were significantly influenced by statistical inferences. By highlighting the need for a more geologically justified classification for the in-situ stress data, we argued that arbitrary depth boundaries for stress-depth relationships could oversimplify the complex geological conditions in the Canadian Shield, lacking a strong reason aligned with rock engineering principles. It is emphasized that depth-based models, while relevant in specific sites, should not universally apply across the entire Canadian Shield, because these depth domains might provide a biased perspective in the analysis of

in-situ stress state. Also, previous relationships were mostly linear, considering a uniform change in stresses from near-surface depths to greater depths which might not sufficiently account for the effects of past tectonic events or current geological conditions impacting stress distributions. By examining nonlinear models, the results demonstrated that nonlinear equations could better represent the vertical and horizontal stresses in the Wabigoon&Quetico and the Pikwitonei groups. Moreover, the horizontal stresses in most regions would not follow linear trend, as presented in Table 4.3. In addition, past relationships were predominantly presented in their principal state, assuming σ1 and σ2 as horizontal stresses and σ3 as vertical stress throughout the Canadian Shield. Presentation in this form, might overlook stress orientation components, leading to analytical uncertainties in stress estimation. For instance, considering σ1 and σ2 consistently as horizontal across a large dataset of the Canadian Shield might be problematic for the data points having a plunge more than 75 degrees, as shown in Figure 4.4. In this article, to avoid these misleading assumptions, the 3D stress tensor was recalculated for each stress measurement, providing a more precise horizontal and vertical stress components.

In this study, we investigated the adequacy of statistical tools in developing stress-depth relationships, by applying previous equations to our extensive dataset. The results revealed that despite employing a structured approach, both R^2 and adjusted R^2 values for all domains remained notably lower compared to cases where data were not categorized across the entire database. Also, we employed clustering techniques to determine the optimal number of refined depth-domains; however, the outcomes were less than satisfactory. This indicates that while clustering methods provide statistical insights into depth domains, the lack of geological rationale behind these clusters could weaken predictive accuracy in model development. Therefore, our analysis highlights the need for integrating geological insights to achieve a more comprehensive understanding of stress-depth relationships and to develop realistic equations that account for the geological complexities of the Canadian Shield.

To address these complexities, we introduced a novel methodology that establishes a reasonable link between the in-situ stress state and the geology of the Canadian Shield. This approach integrated three main elements—lithological composition, metamorphism, and structural characteristics—to define six distinct geological groups that share similar lithology and structure. Thus, we identified key regional tectonic events within each group, providing possible justifications for the deviations of stress parameters from expected ranges. In the Wabigoon&Quetico group, deviations and unique trend of vertical stress ($\sigma_v = 1.08\, z^{0.49}$) is possibly attributed to thin- and thick-skinned tectonism. Also, the presence of regional thrust imbrication in the Grenville group would possibly induce deviations and huge variations in the horizontal stresses, resulting in lower R^2 values ($\sigma_H = 5.7\, z^{0.21}, R^2 = 0.17$ and $\sigma_H = 1.8\, z^{0.28}, R^2 = 0.20$), while its vertical component experienced a slight deviation from the lithostatic pressure ($\sigma_H = 0.030\, z, R^2 = 0.83$). Therefore, this approach could offer a more refined understanding of stress-depth relationships by integrating geological considerations with in-situ stress analysis.

The findings of this research have significant implications for engineering geology, particularly in design, by offering practical tools for engineers in selecting support systems and excavation techniques. Since in-situ stress is crucial for all underground constructions, predicting a reliable stress model could enhance construction efficiency and mitigate potential risks related to ground behavior. However, it is essential to recognize certain limitations. Lower R^2 values observed for the stress ratios in specific regions such as the Southern group (ranging between 0.11 and 0.19), may be attributed to the limited number of datapoints and potential human-induced errors during stress measurements. Furthermore, the predictability of the suggested stress ratio equations in the Abitibi&Wawa group is notably low (varying from 0.18 to 0.30), primarily owing to the substantial variability in the data. This self-critique highlights the need for caution when interpreting specific results, as the predictability of stress trends in several groups may be compromised. For very strategic construction

projects, we recommend extensive stress measurements across multiple depth zones to enhance the reliability of stress predictions.

4.10 Conclusion

This study aimed to expand our understanding of the in-situ stress state in the Canadian Shield, establishing a crucial link between geological conditions and stress-depth relationships. Several important conclusive remarks are summarized as follows:

1. The proposed novel methodology categorized the Canadian Shield into six distinct groups based on regional lithological and structural similarities. This innovative approach would enhance the accuracy of stress-depth relationships by capturing the complexities unique to each defined group.
2. This research assessed the limitations of relying only on statistical tools for establishing reliable stress-depth relationships and highlighted the importance of integrating geological insights with statistical methods. This integration ensures that the developed equations are not only statistically sound but also geologically representative, considering the profound influence of tectonic activities.
3. The analysis revealed the potential uncertainties resulting from characterizing stresses in their principal state. This study addresses such uncertainties by determining the 3D stress tensor for each measurement, offering a more precise understanding of stress orientations.
4. Analysis of past equations indicated that the designated depth-domains for the stress data may not be universally applicable throughout the entire Canadian Shield.
5. This research successfully identified key regional tectonic events in each geological group, providing potential justifications for deviations in vertical and horizontal stresses. The unique stress-depth relationships within the six defined groups consider regional tectonic events as possible influential factors.

6. Detailed regression analyses for each geological group provide equations for crucial stress parameters such as vertical stress, maximum and minimum horizontal stresses, and stress ratios, offering valuable perspectives for various geotechnical and engineering applications. Comparison of developed stress ratio relationships with previous models indicates the better robustness of the proposed equations in most groups, where the correlation values stand out among the comparisons.

CHAPTER 5

This chapter represents the final stage of this thesis, where the findings from the preceding chapters were applied to conduct a comprehensive rockburst analysis. By integrating the most suitable data treatment techniques, refined geomechanical parameters, stress-depth relationships, and uncertainty assessments, this chapter establishes a robust basis for evaluating the applicability and reliability of rockburst prediction criteria. Focusing on numerical analysis, this chapter utilizes the Westwood underground Mine in Quebec as a case study to assess the performance of these criteria under specific geological and geomechanical conditions. The outcomes of this chapter would significantly enhance rockburst prediction methodologies by providing practical insights into localized risk assessments, identifying rockburst-prone zones through probabilistic approaches, which are crucial for ensuring the safety of deep underground excavations.

Article 4: Evaluation of the Applicability of Rockburst Prediction Criteria through Numerical Modeling: A Case Study of the Westwood Mine, Quebec (Canada)

Behzad Dastjerdy [1,*], Ali Saeidi [1] and Shahriyar Heidarzadeh [2]

[1] Department of Applied Sciences, University of Quebec at Chicoutimi, Saguenay, QC, Canada

[2] Rock Mechanics Engineer at AECOM, Montreal, Canada

To be Submitted to Journal of Rock Mechanics and Geotechnical Engineering, 2025

5.1 Abstract

Rockbursts pose a persistent challenge in underground mining operations, necessitating accurate prediction methods to ensure safety and operational efficiency. This study evaluates the effectiveness of various rockburst prediction criteria through detailed numerical modeling, focusing on the Westwood Mine, Quebec, Canada. By analyzing the performance of rockburst criteria, this research highlights the role of major principal stress and displacement profiles in prediction accuracy and investigates the spatial distribution of rockburst risk around the tunnel, using three boundary distances—on-boundary, 0.5m, and 1m—emphasizing the importance of proximity in rockburst risk assessment. The analyses revealed noticeable variability in rockburst susceptibility between geological units, with Unit 4 exhibiting higher risk due to greater geomechanical heterogeneity. Criteria incorporating major principal stress, such as the Tao and Zhang indices, provided more reliable predictions, whereas vertical stress-based indices like the Stress Index (Si) consistently overestimated risk, particularly under complex stress conditions. Localized risk assessments demonstrated increased rockburst likelihood near the 1m boundary, especially in high-stress zones like spandrels. These findings underscore the importance of a multi-criteria approach, integrating spatial variability and geomechanical parameters, to improve prediction accuracy and guide the development of effective mitigation strategies, offering a more robust framework for enhancing underground safety protocols.

Keywords: *Rockburst Prediction, Numerical Modelling, Tunnel Safety, Westwood Mine, Risk Assessment, Geomechanical Parameters*

5.2 Introduction

With the increasing demand for mineral resources and the continuous depletion of shallow deposits, mining operations are progressively shifting to greater depths, exposing workers to more complex geotechnical challenges. This trend extends to various underground projects, such as tunnels and deep excavations, which are often constructed in high-stress environments with complicated geological conditions. In such settings, the ultimate in situ stress and intricate geological features can lead to significant hazards, including rockbursts, rock mass caving, large deformations of excavations, and elevated ground temperatures (Mazaira & Konicek, 2015; Feng, 2017). Rockbursts are dynamic and violent failures characterized by the rapid ejection of rock blocks and a sudden release of accumulated elastic energy within the surrounding rock mass. These events are particularly prevalent in high-stress environments, such as deep mines and tunnels, where geological conditions and excavation activities exert significant pressure on the rock mass. Due to their unpredictable nature and intense impact, rockbursts pose serious safety risks, often resulting in injuries, fatalities, and substantial financial losses (Wang et al., 2021). According to the literature, rockbursts are classified into three types: strain bursts, pillar bursts, and fault-slip bursts (Hedley, 1992; Kaiser & Cai, 2012). Strain bursts, the most common type, occur due to the concentration of excavation-induced tangential stress in relatively "soft" rock masses around fractured zones. Pillar bursts happen when accumulated elastic strain energy exceeds a critical threshold, leading to sudden pillar failure and significant rock release. Fault-slip bursts result from the slip along pre-existing faults or shear ruptures, releasing seismic energy and potentially triggering additional rockburst events (Cai, 2013).

Historical record reveals that over 4300 rockburst events have been documented across numerous mining regions worldwide since 1930, underscoring the pervasive threat they pose to the

mining industry and deep underground projects, as depicted in Figure 5.1 (Bennett & Marshall, 2001). This highlights the importance of understanding the mechanisms that trigger rockbursts and the factors influencing their occurrence, which is crucial for developing effective prediction and mitigation strategies in underground operations.

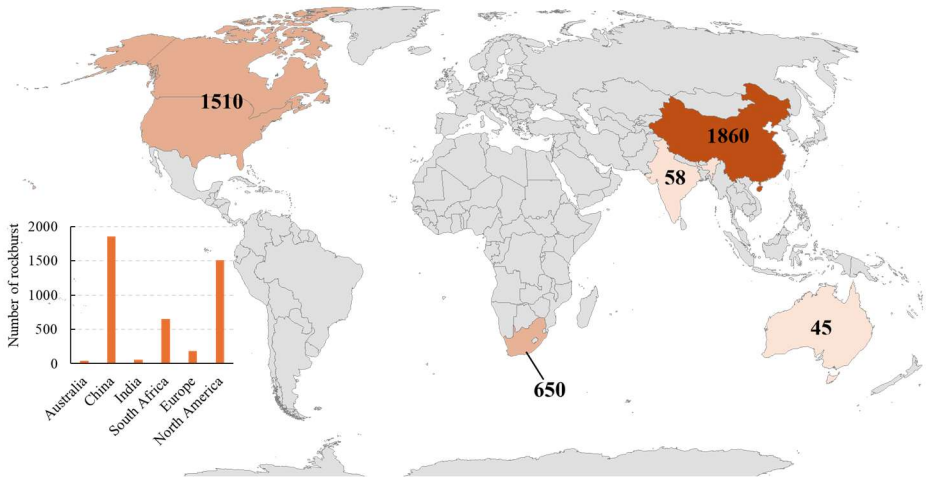

Figure 5.1 Geographical map of rockburst events in the world for 1931-2019 (modified from J. Wang et al. (2022))

In rock engineering, the analysis of rockburst is approached from two main perspectives: classifying rockburst types and predicting rockburst potential (Zhou, Li, & Mitri Hani, 2016; Zhou et al., 2018). Over decades, a variety of studies have explored the causes and damage mechanisms associated with rockbursts, utilizing various theoretical frameworks, including energy theory, strength theory, instability theory, and more advanced approaches like chaos and catastrophe theories (Afraei et al., 2018; Cai, 2016; Wang et al., 2021). Numerous empirical criteria have been developed to categorize different types of rockbursts, each contributing insights into the conditions and behaviors of rock under high-stress environments. Understanding rockburst potential is crucial for predicting these events, and ensuring the design and stability of underground excavations. This involves both qualitative and quantitative approaches, and can be divided into two main areas: the rockburst potential of individual rock types and the potential within complex rock mass engineering (Zhou,

2015; Zhang et al., 2016). The first area assesses the inherent proneness of specific rock materials to rockbursts, suggesting that if a rock lacks intrinsic rockburst potential, rockbursts will not occur in that material during engineering activities. The second area evaluates the probability of rockbursts within rock mass combined with its geological conditions, considering factors such as in-situ stress, geological layering, and structural features, according to the site field work. To guide these assessments, various techniques—including field observations, theoretical analyses, numerical simulations, and empirical methods—are employed, all aimed at predicting rockburst potential and informing risk mitigation strategies in deep excavation projects. These efforts might lead to the development of tailored support systems and effective mitigation measures. Furthermore, integrating monitoring technologies and predictive algorithms allows for real-time assessments of rock behavior, enabling proactive strategies that enhance safety, resilience, and efficiency in resource extraction.

The numerical analysis of rockburst has evolved significantly over the past decades, with various approaches advancing the understanding of rockburst mechanisms and enhancing prediction accuracy. Early studies, starting with Salamon (1964), focused on the mechanisms driving these events in underground tunnels, highlighting the critical roles of stress concentrations and rock mass properties in rockburst occurrence (Wang et al., 2021). In the 1970s, researchers employed techniques such as the finite difference method (FDM) to model elastic wave propagation under high-stress conditions, using tools like the Split-Hopkinson pressure bar (Miranda, 1972). Blake (1972) introduced the finite element method (FEM) for predicting rockburst-prone areas, particularly in high-stress pillars. Brady (1979) used the boundary element method (BEM) to analyze pillar failure, proposing a hybrid approach that combined continuum and discontinuous stress analysis. Board and Voegele (1981) applied BEM to evaluate elastic energy release rates and assess rockburst potential in mining operations. In the 1980s, dynamic simulations of rockburst processes, especially in pillars and tunnels, were advanced by studies like those by (Zubelewicz & Mroz, 1983). In the 2000s, Sun et al. (2007) utilized realistic failure process analysis (RFPA) and discontinuous deformation analysis

(DDA) to simulate dynamic rockbursts in circular tunnels, emphasizing the significance of rock heterogeneity and crack propagation. Cai et al. (2007) coupled FLAC (Fast Lagrangian Analysis of Continua) and PFC (Particle Flow Code) to model excavation-induced acoustic emissions (AE), demonstrating the method's ability to simulate AE in response to stress changes around underground excavations. Recent research has focused on refining rockburst indicators and enhancing modeling precision. Sainoki and Mitri (2014a, 2014b) developed dynamic models to simulate fault-slip and stress changes resulting from production blasts. Naji et al. (2018) studied the impact of small-scale shear zones on rockbursts in deep hydropower tunnels using FLAC3D, indicating that principal stresses concentrate near shear zones, making them more susceptible to rockburst. Manouchehrian and Cai (2018) also investigated the influence of weak planes on rockburst occurrence and damage around underground openings. J. Wang et al. (2022) examined the behavior of yielding rock bolts under seismic loading using FLAC3D. Fanjie et al. (2022) proposed a comprehensive approach to modeling rockburst evolution, integrating crack propagation, stress criteria, and boundary effects.

Despite significant advancements in rockburst prediction, prior numerical studies have not adequately evaluated the applicability of existing prediction criteria. Also, impacts of geomechanical parameters and the in-situ stress conditions on the rockburst prediction analysis have received limited attention in the literature. A comprehensive assessment of these factors is essential for improving rockburst analysis and enhancing prediction accuracy, which can provide engineers with more reliable tools for anticipating and mitigating rockbursts in underground operations. The objective of this study is to evaluate the applicability of rockburst prediction criteria through numerical simulations, with a particular focus on the influence of geomechanical parameters and in-situ stress. This research specifically investigates rockburst occurrence at the Westwood underground mine in Quebec, Canada, aiming to determine the probability of rockbursts near the tunnel boundary and in critical locations. Ultimately, the study seeks to identify the most appropriate rockburst prediction criteria for this case.

5.3 Methodology

Figure 5.2 outlines the proposed methodology for evaluating rockburst probability through numerical analysis, focusing on the applicability of empirical prediction criteria and accounting for the influence of geomechanical parameters and in-situ stresses. Initially, rockburst-prone zones are identified within the Westwood underground mine in Quebec (Canada), a site known for frequent rockburst incidents. Subsequently, we characterize the geomechanical parameters of the rock mass through both deterministic and probabilistic estimations, along with an analysis of in-situ stress state at this mine. We then apply numerical modeling to evaluate the suitability of existing rockburst prediction criteria for the Westwood Mine's conditions, identifying any limitations or potential areas for improvement. Finally, a probabilistic assessment is conducted to determine the likelihood of rockburst events in the selected zones, incorporating sensitivity analyses to highlight the impact of various risk factors. This structured approach could provide a detailed understanding of rockburst risks in underground settings.

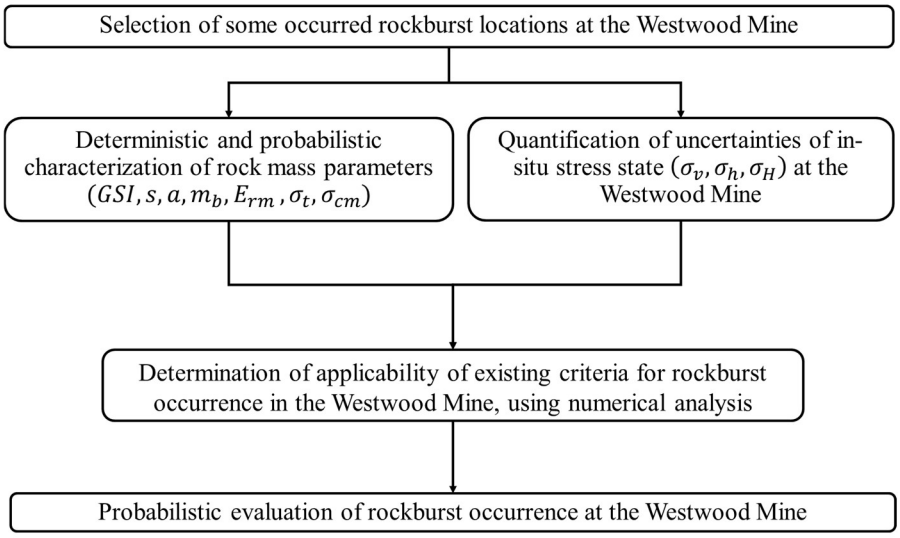

Figure 5.2 Proposed methodology to investigate rockburst predictions using numerical analysis

5.4 Westwood Mine

The Westwood Mine, located within the Abitibi greenstone belt in Quebec, approximately 420 km northwest of Montreal, is a significant gold deposit discovered in recent Canadian mining history (Figure 5.3). Since its commercial operations began in 2014, it has become a crucial asset for Canada's gold production (IAMGOLD, 2019b). The rock mass at the Westwood Mine has been significantly affected by regional metamorphism, which has altered the lithological units, transitioning them from greenschist to lower amphibolite facies. This metamorphic process has had a profound impact on the stability and behavior of the rock mass (Askaripour et al., 2022). Yergeau (2015a) developed a lithological classification system based on mineral compositions and volcanic facies, identifying six principal rock units (Units 1–6) at the mine. These units predominantly trend in the east-west direction with steep to moderate dips toward the south, reflecting the region's complex geological evolution. Among these, Units 3, 4 are recognized as the most susceptible to rockburst events. The characterization of their geomechanical intact rock parameters, along with the associated uncertainties, plays a crucial role in the probabilistic analysis of rockburst occurrence at

this rockburst-prone site (Askaripour et al., 2022; Bouzeran et al., 2019; Dastjerdy et al., 2024a, 2024c).

Figure 5.3 Westwood Mine location in Quebec Province, Canada (IAMGOLD, 2019b)

Recent studies have identified certain rock units within the Westwood Mine, particularly rock units 3 and 4, as being more susceptible to instability under elevated stress conditions, which increases the likelihood of rockbursts (Bouzeran et al., 2019; Kalenchuk et al., 2017). This highlights the need for thorough geomechanical characterization and risk assessment to ensure the safety and stability of underground operations. As shown in Table 5.1, several rockburst events recorded in recent years emphasize the importance of risk analysis. In Mining Block 104, located at a depth of 1040 meters along the Main Ramp, three large seismic events caused significant damage across multiple sublevels. The stability of the gallery was severely compromised, leading to large-scale ground displacement (Bouzeran et al., 2019; Kalenchuk et al., 2017). Fortunately, no injuries occurred, and all levels in the 104 horizons were immediately closed. In Mining Block 132, at a depth of 1275 meters along the Haulage Drifts, a rockburst at the working face caused severe convergence but no injuries. Another event in Mining Block 156, at a depth of 1560 meters in the Exploration Drift, was triggered by local seismicity and a secondary fault near the Bousquet Fault. This event affected both rock units 3 and 4, causing significant structural impacts but no injuries. In Mining Block 180, at a depth of 1800 meters

in the Exploration Drift, a rockburst induced by local seismicity impacted rock unit 3 (Tremblay, 2020).

Table 5.1. Summary of recent rockburst incidents at the Westwood Mine, QC (Canada) (Kalenchuk et al., 2017; Tremblay, 2020)

Mining level	Damage intensity	Location	Depth (m)
104-02/03&06-10	Unconsolidated ground composed mainly of mud, stability of the gallery compromised	Main Ramp	1040
132-02-07&10-11	Severe convergence at the working face	Haulage drifts	1275
156-00	Moderate local seismicity resulting in minor spalling and fracturing	Exploration drift	1560
180-00	Severe local seismicity accompanied by spalling, fracturing, and localized ejection of rock fragments near the tunnel boundary, concentrated at the crown and spandrels	Exploration drift	1800

Identification of major rockburst incidents in these high-risk areas allows for a realistic back-analysis to assess the effectiveness of empirical criteria in predicting rockbursts through numerical simulations. This approach will be useful to refine predictive models, improving risk assessments, and enhancing the safety and stability of future underground mining operations.

5.5 Characterizing Geomechanical Parameters of Rockmass and In-Situ Stress

5.5.1 Deterministic and Probabilistic Estimation of Rockmass Parameters

The strength and deformability parameters of rock masses are crucial for an accurate evaluation in geomechanical projects. One of the primary challenges in rock mass characterization lies in the inherent variability of intact rocks, which can introduce considerable uncertainty across different rock types (Dastjerdy et al., 2024a). As a result, carefully characterizing the geomechanical parameters of intact rock is essential, as these properties directly influence analyses of rock mass behavior.

At the Westwood Mine, extensive mapping and drilling campaigns have allowed systematic laboratory tests on core samples from various rock units to evaluate their physical and mechanical properties. These efforts have produced valuable data on the distinct characteristics of each lithological unit, enhancing the understanding of the Mine's geomechanical environment. Dastjerdy

et al. (2024a) compiled the laboratory results from these campaigns into a comprehensive database, encompassing 465 tests on samples from 47 boreholes drilled within rockburst-prone areas. This database supports detailed analysis and interpretation of intact rock properties, providing insights into the uncertainties of geomechanical parameters across the sampled zones at the Westwood Mine. After determining the most suitable geomechanical parameters for each rock unit, the best-fitting probability distribution functions were applied for parameters such as UCS, tensile strength, Young's modulus, and Poisson's ratio (Dastjerdy et al., 2024a). Table 5.2 presents the calculated mean and standard deviation for each parameter within each rock unit, as derived from these fitted probability distributions.

Table 5.2. Most appropriate mean (Xm), standard deviation (S), and probability distribution function (PDF) computed for all geomechanical intact parameters in each rock unit at the Westwood Mine (Dastjerdy et al., 2024a)

Parameter	Unit 3			Unit 4		
	X_m	*S*	*PDF*	X_m	*S*	*PDF*
UCS (MPa)	149.25	50.49	Pert	148.37	45.29	Fatigue Life
Tensile strength (MPa)	18.25	3.33	Rayleigh	19.56	4.18	Normal
Young's modulus (GPa)	74.31	10.19	Normal	65.2	12.78	Dagum
Poisson's ratio	0.251	0.05	Pert	0.258	0.05	Beta General

Following the characterization of geomechanical properties for the intact rock, the next step involved determining the Hoek–Brown (HB) failure criterion parameters for each lithological unit. For the HB criterion, it is essential to specify both the Geological Strength Index (GSI) and the material constant mi. The GSI values were obtained through detailed field observations, assessing the structural quality and surface condition of rock masses across different units, with values assigned based on observed fracturing, jointing, and weathering (Hoek & Brown, 2019). The mi parameter, which reflects intrinsic rock properties, was derived from uniaxial and triaxial compression tests conducted in prior campaigns. This parameter is influenced by factors such as mineral composition, grain size, foliation, and particle interlocking, which contribute to its variability (Hoek & Brown,

2019). In this study, we calculated both the mean and standard deviation for mi and GSI specifically in rock units 3 and 4, which are most susceptible to rockburst events. A goodness-of-fit test using the Akaike Information Criterion (AIC) was applied to select the most appropriate probability distribution function (PDF) for each lithological unit. According to the AIC test, the lower the AIC value, the better the fit for the corresponding distribution, ensuring a reliable probabilistic framework for the HB parameters across different units (Dastjerdy et al., 2024a). Figures 5.4 and 5.5 display the AIC test results and the selected PDFs for mi and GSI values in units 3 and 4. The results indicate that the Lognormal and Normal distributions are the most appropriate statistical distributions for the mi and GSI values, respectively.

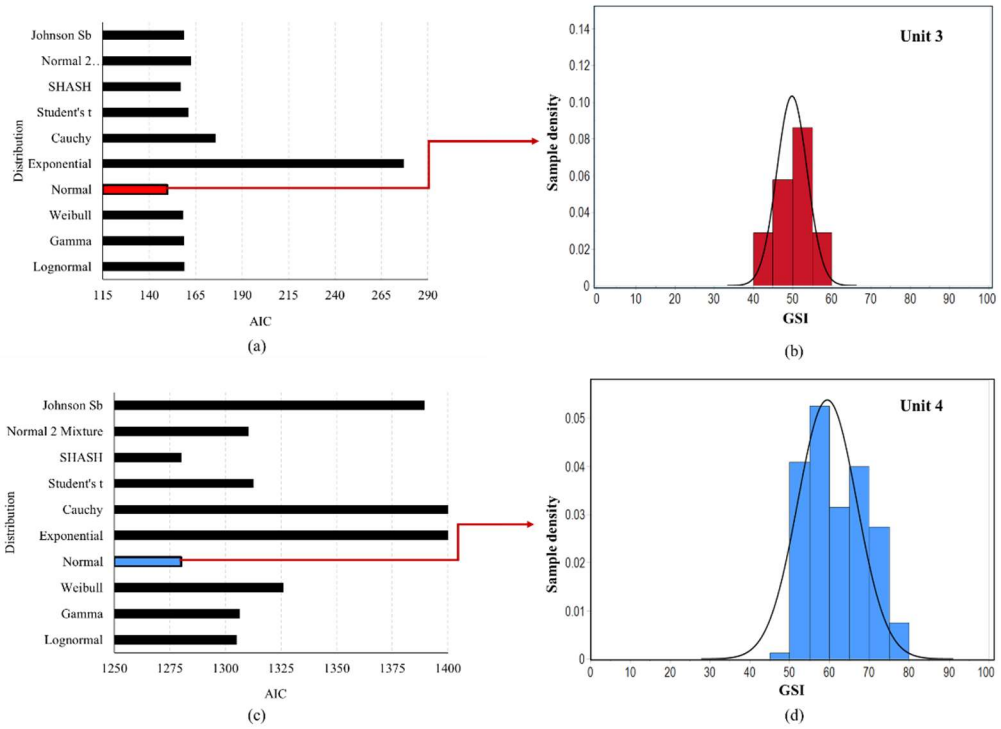

Figure 5.4 AIC test results for GSI distribution in Units 3 and 4: (a) and (c) show AIC values for each unit, and (b) & (d) display the best-fit PDFs

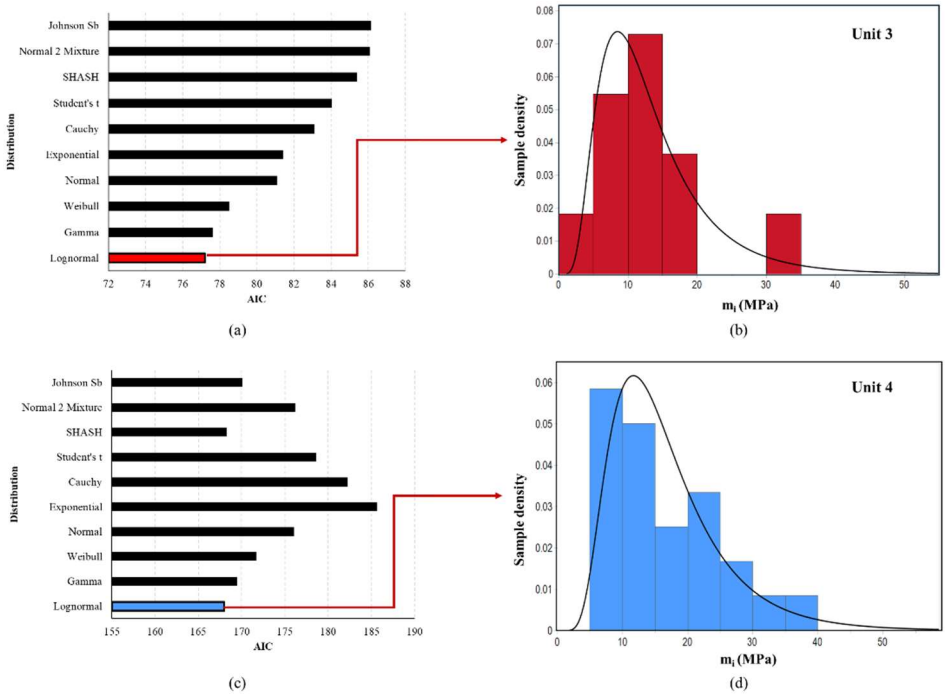

Figure 5.5 AIC test results for mi distribution in Units 3 and 4: (a) and (c) show AIC values for each unit, and (b) & (d) display the best-fit PDFs

Subsequently, the rockmass parameters for the HB failure criterion were calculated, along with their probabilistic estimates. The Monte Carlo simulation method was employed to provide a stochastic estimation of the HB rockmass geomechanical parameters by incorporating the associated variabilities of intact parameters (see Eqs. 1–6). This approach enabled the determination of the standard deviation and best-fit distribution function for each parameter, thereby enhancing the reliability of HB-based failure assessments across different rock units at the Westwood Mine.

$$m_b = m_i e^{\left(\frac{GSI-100}{28-14D}\right)} \tag{1}$$

$$s = e^{\left(\frac{GSI-100}{9-3D}\right)} \tag{2}$$

$$a = \frac{1}{2} + \frac{1}{6}\left(e^{\frac{-GSI}{15}} - e^{\frac{-20}{3}}\right) \tag{3}$$

$$\sigma_{cm} = \sigma_{ci} s^a \tag{4}$$

$$\sigma_t = \frac{s\sigma_{ci}}{m_b} \tag{5}$$

$$E_{rm} = E_i \left(0.02 + \frac{1 - \frac{D}{2}}{1 + e^{\left(\frac{60+15D-GSI}{11}\right)}}\right) \tag{6}$$

Where the parameters including m_b, s and a are the rockmass strength constants, which depend on factors such as the intact rock material properties, lithology, and the degree of fracturing or jointing within the rock mass (Hoek & Brown, 2019). The σ_{cm} and σ_t are compressive and tensile strengths of rock mass, respectively. E_{rm} represents the deformation modulus of rockmass. The parameter "D" represents the degree of disturbance of the rock mass (ranging from 0 to 1 for undisturbed in-situ rock masses to highly disturbed rock masses). Since the rockmass is assumed to be undisturbed by controlled blasting, the parameter "D" is considered equal to 0 for this study (Hoek & Brown, 2019). After the Monte-Carlo simulation, the best fitting distributions for each parameter were determined. Figures 5.6 and 5.7 display the histograms and associated distributions for the HB parameters in Units

3 and 4, respectively. The resulting mean, standard deviation, and best-fitting PDFs for the strength and deformability parameters of rock masses in both Units are presented in Table 5.3.

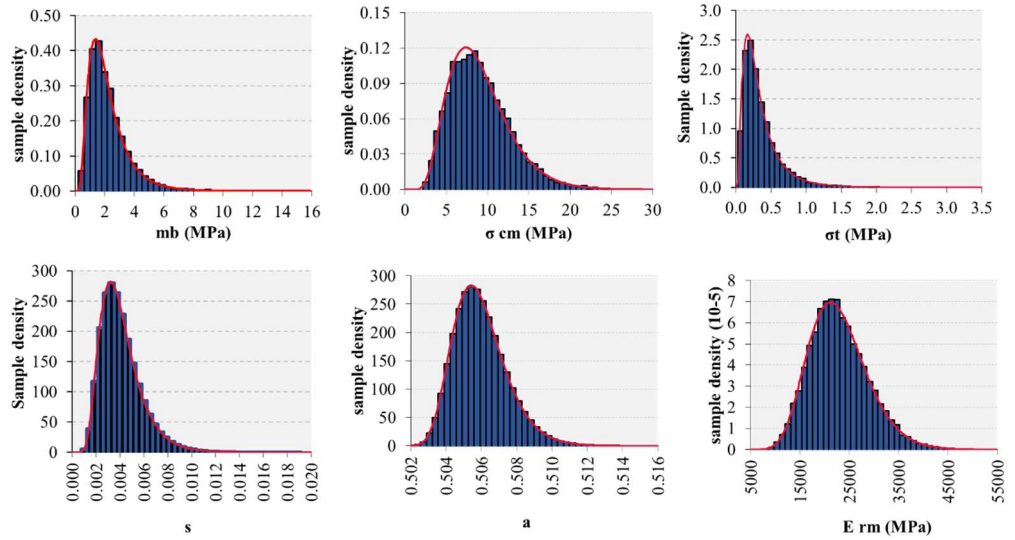

Figure 5.6 Histograms and best-fit probability distribution functions (PDFs) for the Hoek-Brown parameters of the Unit 3 rock mass

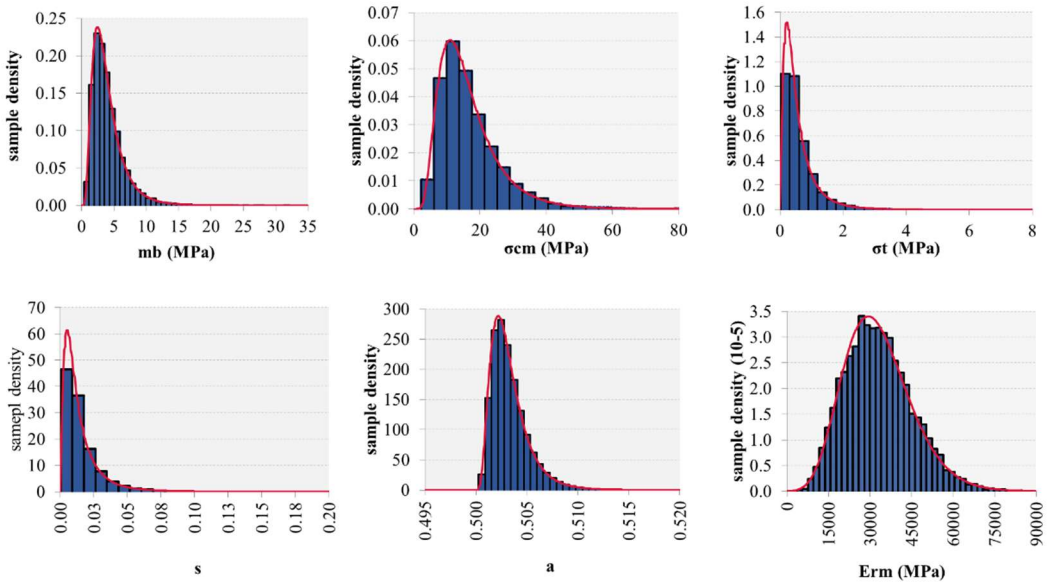

Figure 5.7 Histograms and best-fit probability distribution functions (PDFs) for the Hoek-Brown parameters of the Unit 4 rock mass

Table 5.3. Mean, standard deviation, and best-fitting probability distribution functions (PDFs) for the Hoek–Brown parameters of rock masses in units 3 and 4.

Parameter	Unit 3			Unit 4		
	Mean	Std. dev	PDF	Mean	Std. dev	PDF
UCS	149.25	50.49	Pert	148.37	45.29	Fatigue Life
ν	0.25	0.55	Pert	0.26	0.05	Beta General
E_i	7.43E+04	1.02E+04	Normal	6.52E+04	1.30E+04	Dagum
m_i	13.32	7.87	Lognormal	16.82	8.79	Lognormal
GSI	49.86	3.63	Normal	59.48	7.41	Cauchy
m_b	2.24	1.36	Lognormal	4.10	2.50	Lognormal
s	4.10E-03	1.00E-03	Lognormal	1.55E-02	1.53E-02	Lognormal
a	5.06E-01	1.00E-03	Lognormal	5.03E-01	2.00E-03	Lognormal
σ_t	0.36	0.28	Lognormal	0.62	0.58	Lognormal
σ_{cm}	9.11	3.65	Gamma	16.78	9.22	Lognormal
E_{rm}	2.30E+04	5.94E+03	Gamma	3.32E+04	1.22E+04	Gamma

In this study, both deterministic and probabilistic approaches were employed to characterize geomechanical parameters. However, the numerical simulations were conducted using deterministic values to maintain consistency and simplicity in evaluating rockburst risk. Deterministic values provide a stable foundation for the models, ensuring consistent results necessary for assessing worst-case scenarios, which are crucial for safety in underground mining operations. While the probabilistic analysis offers insights into the variability and uncertainty of rockmass parameters, its incorporation into the simulations would have added significant complexity and computational demands. Given the primary focus of this study on evaluating rockburst prediction criteria, the use of deterministic values could be more appropriate, providing clearer and more interpretable results. While the probabilistic data was not directly applied in the simulations, it still enhances the understanding of parameter variability and supports the development of effective mitigation strategies.

5.5.2 Estimation of in-situ stress at the Westwood Mine

In-situ stress plays a critical role in assessing the rockburst potential of underground excavations, as it significantly affects the stability and behavior of the surrounding rock mass. Reliable estimation of principal stresses—major (σ_1), minor (σ_3), and vertical (σ_v)—is essential for accurate prediction and mitigation of such sudden failure events. This study employed stress-depth relationships proposed

by Dastjerdy et al. (2024b), which were developed using a region-specific methodology that accounts for geological conditions of the Canadian Shield. Using this methodology, the Canadian Shield was systematically categorized into distinct geological groups based on three key factors: variations in lithological composition, the influence of metamorphic processes on rock properties, and structural characteristics such as faults, folds, and regional tectonic features that may affect stress distributions. For each geological group, stress-depth relationships were established to provide a localized and reliable representation of in-situ stress conditions.

At the Westwood Mine, located in the Abitibi region of Quebec, Canada, these stress-depth relationships were specifically applied. The equations used were refined to reflect the unique geological setting of the Abitibi region, ensuring more exact estimations of in-situ stress conditions for this study. The depth-dependent stress equations (7–9) derived by Dastjerdy et al. (2024b) are as follows:

$$\sigma_1 = 0.47z^{0.68} \quad (7)$$

$$\sigma_3 = 0.47z^{0.61} \quad (8)$$

$$\sigma_v = 0.027z \quad (9)$$

Where z represents the depth in meters. These equations facilitate a robust framework for incorporating stress conditions into the analysis, ensuring that the geomechanical modeling aligns with the regional geological characteristics.

5.6 Evaluation of existing rockburst prediction criteria

Rockburst prediction remains a significant challenge in underground engineering, where it plays a vital role in mitigating sudden and hazardous failures in rock masses. Accurate rockburst prediction not only improves safety but also enhances operational efficiency in mining and tunneling projects. Since the 1960s, various approaches have been developed and refined the rockburst prediction methods, based on experimental testing, numerical modeling, and machine learning techniques. Broadly, these approaches fall into two categories: Stress-based and Energy-based approaches. Stress-

based methods evaluate the magnitude of induced stresses relative to the geomechanical properties of the rock mass, which are particularly effective for identifying over-stressed zones, providing a direct link between stress distribution and the likelihood of rockburst occurrence. However, energy-based methods focus on the stored elastic energy within the rock mass prior to failure. By estimating the energy released during fracturing, they provide a detailed understanding of the dynamic nature of rockburst events. Both methods usually classify rockburst severity into four intensity levels: (1) no rockburst, where conditions are stable with no failure signs; (2) light rockburst, characterized by minor deformations, cracking, or rib spalling without significant material ejection; (3) medium rockburst, involving noticeable deformation, localized fracturing, and rock chip ejection; and (4) severe rockburst, marked by explosive failure with violent ejection, roaring sounds, air disturbance, and extensive damage to surrounding rock.

5.6.1 Selection of the most suitable criteria for the Westwood Mine

In this study, various empirical criteria were reviewed to identify the most suitable ones for predicting rockbursts at the Westwood Mine. The applicability of the selected criteria will be carefully evaluated through numerical analysis, considering the site-specific geological and stress conditions. Each criterion will be briefly explained, with a detailed assessment of its practical advantages and limitations in predicting rockbursts in underground excavations.

- **Tao index:** also known as the Tao Discriminant Index, is based on the stress reduction factor in the Q-system (Barton's classification). It is defined as the ratio of the uniaxial compressive strength (UCS) of the rock to the maximum principal in-situ stress (σ_1), as described by Tao (1988) (Eq. 10). This index is particularly useful for preliminary risk assessments in excavations where stress concentration dominates rock behavior (M. He et al., 2023; Zhou, Li, & Mitri, 2016; Zhou et al., 2012).

$$\text{Tao} : \frac{\sigma_c}{\sigma_1} \qquad (10)$$

- **Brittle Shear Ratio (BSR):** This differential stress criterion evaluates the stability of brittle rock masses in deep underground excavations. It is particularly effective for assessing rockburst potential, as it compares the differential stress (σ1−σ3) induced by mining to the unconfined compressive strength (UCS) of the intact rock (Eq. 11). BSR is widely used to assess rockburst potential in environments with significant stress redistribution (Castro et al., 2012; S. He et al., 2023; Rojas Perez et al., 2024; Shnorhokian et al., 2015).

$$BSR: \frac{\sigma_1 - \sigma_3}{\sigma_c} \quad (11)$$

- **Zhang index:** This method evaluates rockburst potential by examining the ratio of major principal stress (σ_1) to UCS (Eq. 12) (Zhang, 2008). It provides a straightforward approach to determining risk levels associated with high-stress environments (S. He et al., 2023; Meng et al., 2021; Rojas Perez et al., 2024; Shnorhokian et al., 2015).

$$Zhang: \frac{\sigma_1}{\sigma_c} \quad (12)$$

- **Russenes criterion:** This criterion assesses rockburst risk by examining the tangential stress (σ_θ) around excavation boundaries relative to the UCS of the rock (Eq. 13) (Russenes, 1974). Commonly used in tunneling and mining, it is effective in identifying stress concentration zones (Gong et al., 2023; M. He et al., 2023; Ma et al., 2018; Wang et al., 2021; Zhou et al., 2018).

$$\text{Russenes: } \frac{\sigma_\theta}{\sigma_c} \quad (13)$$

- **Stress index (S_i):** This index is defined as the ratio of UCS to the vertical in-situ stress (Eq. 14) (Askaripour et al., 2022; Owusu-Ansah et al., 2023). This criterion emphasizes the influence of vertical stress in inducing rockburst, and could offer a practical approach for environments dominated by high vertical stress (Dai et al., 2024; Zhou et al., 2018).

$$S_i = \frac{\sigma_c}{\sigma_v} \quad (14)$$

- **Rockmass Strength index (RS_i):** Introduced by Hawkes (1966), the strength index assesses rockburst potential by comparing three times the major principal stress to the UCS (Eq. 15). Its simplicity and intuitive nature make it a valuable tool for initial assessments (Afraei et al., 2018; Hunt, 2005; Liang et al., 2019; Saeidi et al., 2012).

$$\mathrm{RS}_i: \frac{3\sigma_1}{\sigma_c} \qquad (15)$$

- **Linear elastic energy (W_{et}),** developed by Wang and Park (2001), this energy-based criterion quantifies the elastic energy stored in rock before failure (Gong et al., 2023; M. He et al., 2023; S. He et al., 2023; Manouchehrian & Cai, 2018; Zhou, Li, & Mitri, 2016). It is calculated as the product of the major principal stress (σ_1) and the corresponding strain (ε_1), divided by 2 (Eq. 16).

$$\mathrm{W}_{et} = \frac{\sigma_1 . \varepsilon_1}{2} \qquad (16)$$

Each of these criteria provides unique insights into rockburst prediction, and their combined evaluation will contribute to a comprehensive understanding of the risk factors specific to the Westwood Mine. Table 5.4 summarizes the rockburst risk levels associated with these criteria.

Table 5.4. List of the selected rockburst prediction criteria and their classifications based on rockburst risk

Criterion	Rockburst risk level			
	No	Low	Medium	High
Tao: $\frac{\sigma_c}{\sigma_1}$	> 14.5	5.5~14.5	2.5~5.5	< 2.5
BSR: $\frac{\sigma_1 - \sigma_3}{\sigma_c}$	< 0.45	0.45~0.60	0.60~0.70	> 0.70
$Zhang$: $\frac{\sigma_1}{\sigma_c}$	< 0.15	0.15~0.20	0.20~0.40	> 0.40
$Russenese$: $\frac{\sigma_\theta}{\sigma_c}$	< 0.20	0.20~0.30	0.30~0.55	≥ 0.55
$Stress\ index$: $\frac{\sigma_c}{\sigma_v}$	NA	NA	< 2.5	2.5~5.0

RSi: $\frac{3\sigma_1}{\sigma_c}$	< 0.20	0.20~0.40	0.40~0.80	> 0.80
$W_{et} = \frac{\sigma_1 \times \varepsilon_1}{2}$	< 50	50~100	100~200	≥ 200
*NA refers as Not Applicable.				

5.6.2 Numerical modeling

Numerical modeling in this study was performed using RS2, a finite element analysis software from the Rocscience suite, to evaluate the potential for rockbursts at the Westwood Mine (Rocscience, 2022). The modeled tunnel section, with dimensions of 4 m x 5.2 m, operates as a self-supporting excavation, as illustrated in Figure 5.11, and therefore no support systems were included in the simulation.

The initial model was developed with a conservative boundary distance of 65 m from the tunnel perimeter to ensure that far-field stress conditions were fully captured. To evaluate the influence of boundary extent on stress distribution, a sensitivity analysis was conducted by progressively reducing the boundary distance to 45 m, 35 m, 25 m, and finally 15 m from the tunnel wall (Figure 5.8). Across all model sizes, the distribution of major principal stress (σ_1) shows that beyond approximately 10 meters from the tunnel boundary, the stress values tend to stabilize and closely approach the initial in-situ stress state. This indicates that the influence of the excavation on the surrounding stress field becomes negligible beyond this distance. As shown in Figure 5.9, even with more than a fourfold increase in model size, the variation in stress is minimal—highlighting that the essential stress conditions are reasonably captured in the 15 m model. Additionally, the total displacement at the 15 m boundary diminished to zero, indicating that the model domain was sufficiently extended to eliminate boundary-induced effects on the mechanical response of the excavation (Figure 5.10). As illustrated in Figure 5.10a, the displacement profiles derived from various modeling scenarios exhibit a clear convergence beyond the 15 m mark, where all curves flatten and overlap closely. This consistent behavior across models confirms that the mechanical equilibrium was achieved, and that the

displacement field is unaffected by artificial boundary constraints, thereby validating the adequacy of the selected domain extent.

Therefore, the 15m boundary was adopted as the final model configuration, offering a robust and computationally efficient solution. This adjustment ensured a more practical and accurate analysis of the stress environment surrounding the tunnel. A graded mesh composed of 3-noded triangular elements was used for the analysis to achieve higher resolution in critical areas. The mesh density was deliberately increased near the tunnel boundary to enhance precision in capturing excavation behavior, stress concentrations, and zones of potential instability. This approach would provide a reliable assessment of the mechanical response of the rock mass.

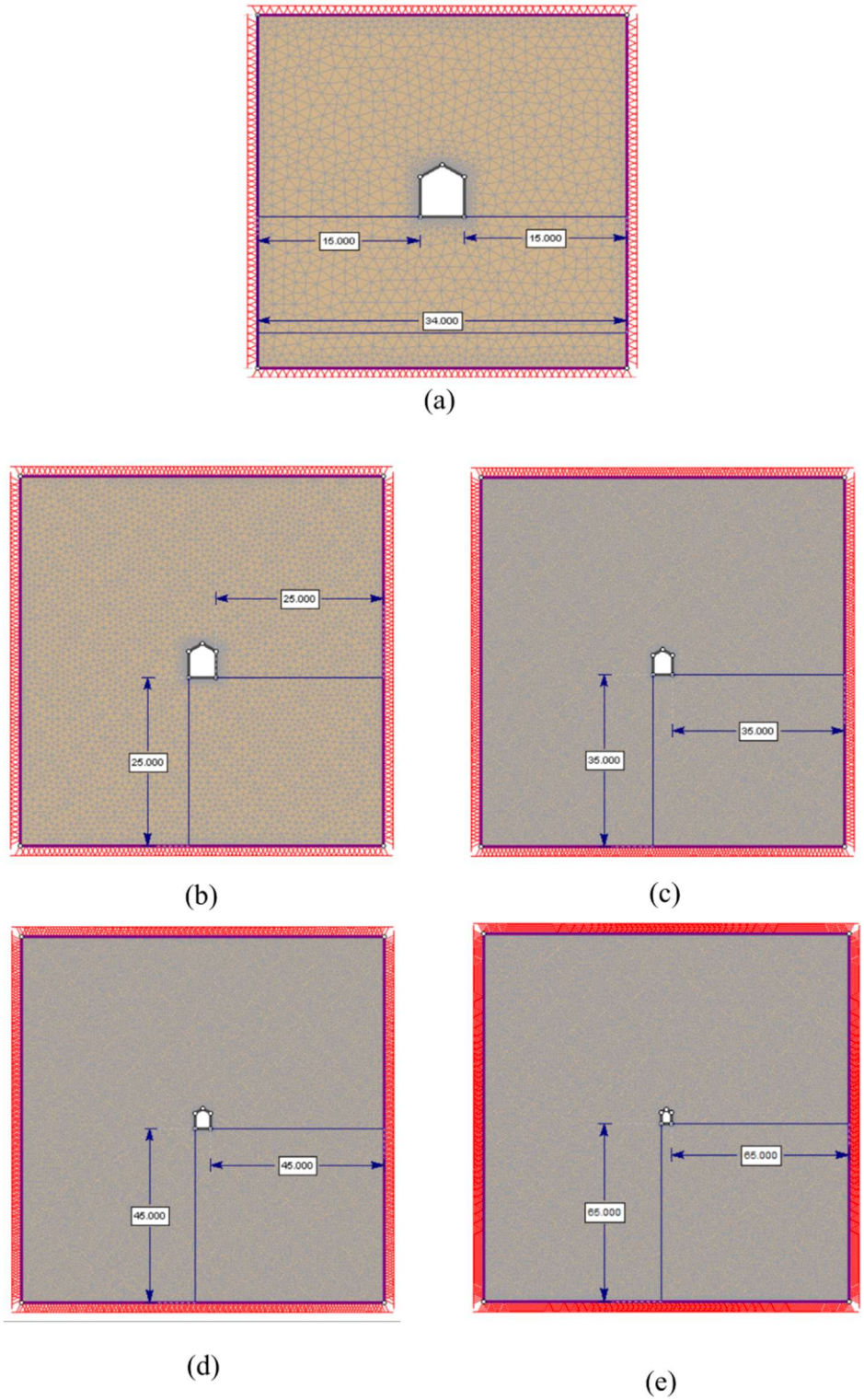

Figure 5.8. Numerical models used for boundary sensitivity analysis, showing different domain sizes with boundaries located at 15 m (a), 25 m (b), 35 m (c), 45 m (d), and 65 m (e) from the tunnel wall

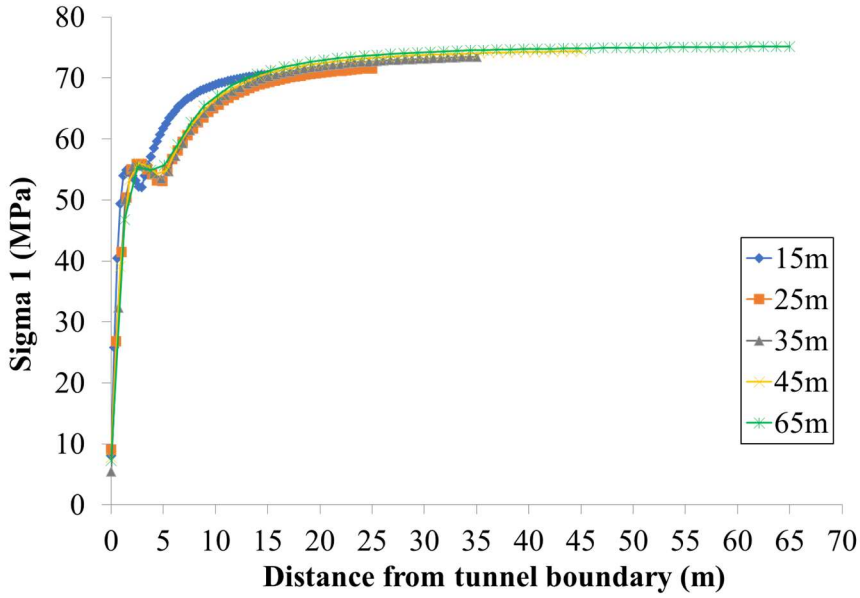

Figure 5.9. Distribution of major principal stress (σ_1) versus distance from the tunnel boundary for five different model sizes

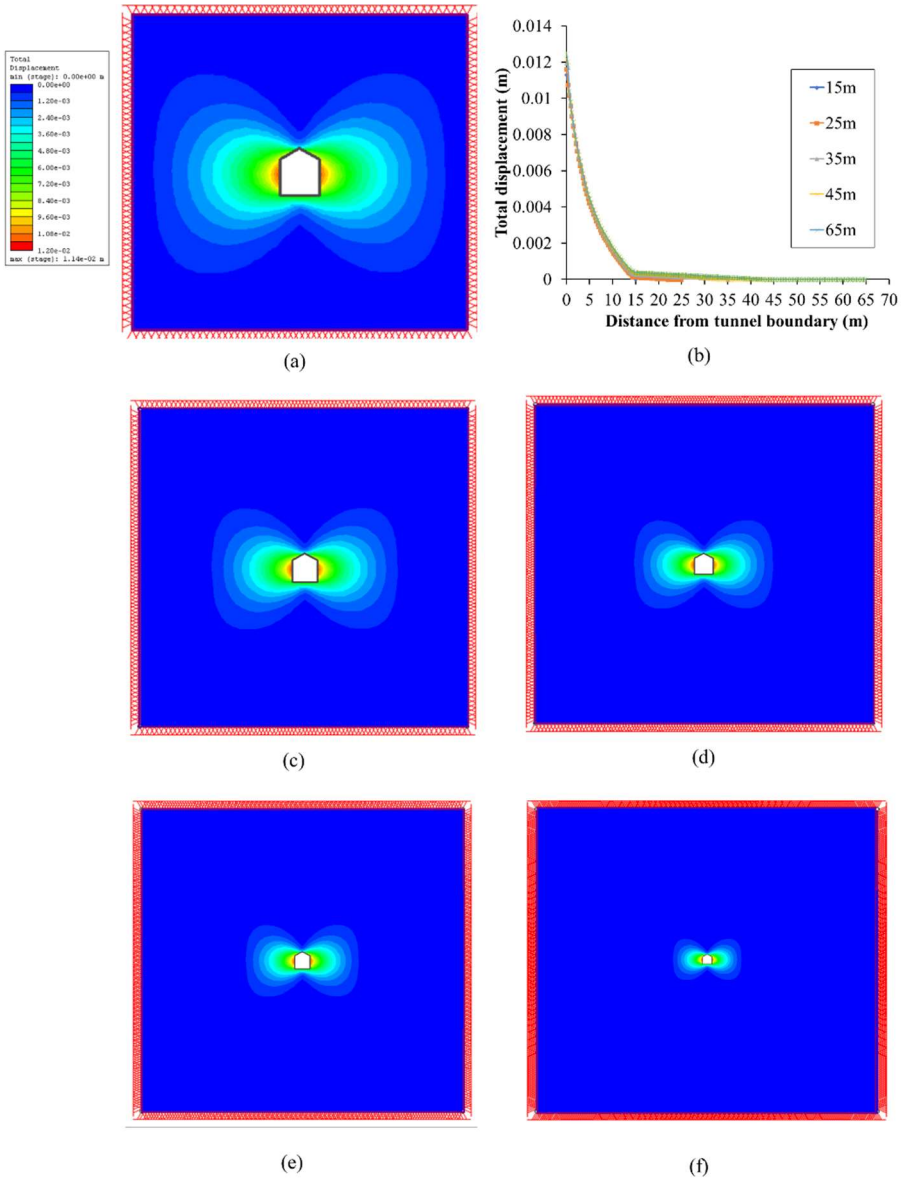

Figure 5.10. Comparison of the total displacement plots for models with varying boundary distances

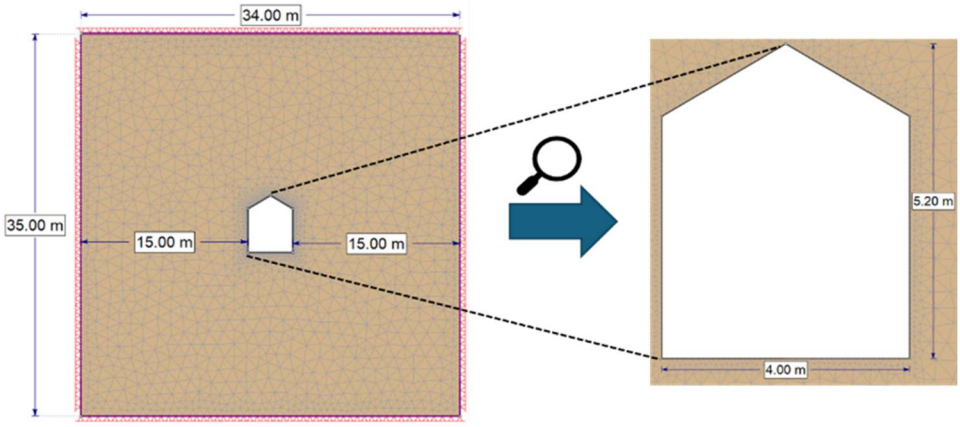

Figure 5.11 (a) Numerical model geometry, (b) Close-up view of the tunnel profile

Considering that rockbursts typically occur in extremely deep zones, all model boundaries were fixed to restrict both horizontal and vertical displacements. This boundary condition replicates the constrained behavior of the surrounding rock mass, ensuring that the in-situ stress state is accurately represented in the numerical analysis. The field stress values are determined for four distinct rockburst depth zones, as described earlier in this study. These values were derived using depth-dependent relationships proposed by Dastjerdy et al. (2024b), potentially offering a realistic approximation of the geological conditions at the Westwood Mine. A summary of the estimated field stress values for each depth range is presented in Table 5.5.

Table 5.5. Estimated in-situ stresses at the Westwood Mine in the four different depth zones

Proposed equations by Dastjerdy et al. (2024b)	Estimated In-situ stresses in multiple Depths of rockburst (m)			
	1040m	1275m	1560m	1800m
Sigma 1 ($\sigma_H = 0.47\ z^{0.68}$)	52.93	60.79	69.73	76.86
Sigma 3 ($\sigma_h = 0.47\ z^{0.61}$)	32.55	36.85	41.68	45.48

Sigma z ($\sigma_z = 0.27\ z$)	28.08	34.43	42.12	48.60

5.6.3 Applicability of rockburst prediction criteria to the context of the Westwood Mine

This section presents a comprehensive analysis of the numerical modeling results aimed at assessing tunnel stability and evaluating the applicability of rockburst prediction criteria within the geological setting of the Westwood Mine. The simulations were conducted for two lithological units (Unit 3 and Unit 4) across four depth zones (1040, 1275, 1560, and 1800 m), representing increasing levels of rockburst potential. The findings are structured systematically to ensure clarity and facilitate a logical interpretation of the results.

5.6.3.1 The effect of displacements in identifying susceptible zones

The initial stage of the analysis focused on total displacement patterns around the tunnel perimeter in Unit 3. Displacements were assessed at five locations: the right wall, right spandrel, crown, left spandrel, and left wall, using 5 m query lines extending outward from each point (Figure 5.12). This approach allowed for an evaluation of displacement variations as a function of distance from the tunnel boundary. As shown in Figure 5.13a, results at the depth of 1800m indicated a symmetrical behavior between the left and right sides of the tunnel, justifying the selection of three representative locations for further analysis: the right wall, right spandrel, and crown. The displacement values were compared across the four depth zones, with trends illustrated in Figure 5.13. Key observations revealed that displacements were minimal at a depth of 1040 m, with values increasing progressively at greater depths. Maximum displacement values were observed along the tunnel walls. At 1800 m, displacements were significantly higher, signaling a noticeable instability risk. These results underscore the increasing challenges associated with tunnel stability at greater depths and emphasize the critical role of depth in governing rockburst potential.

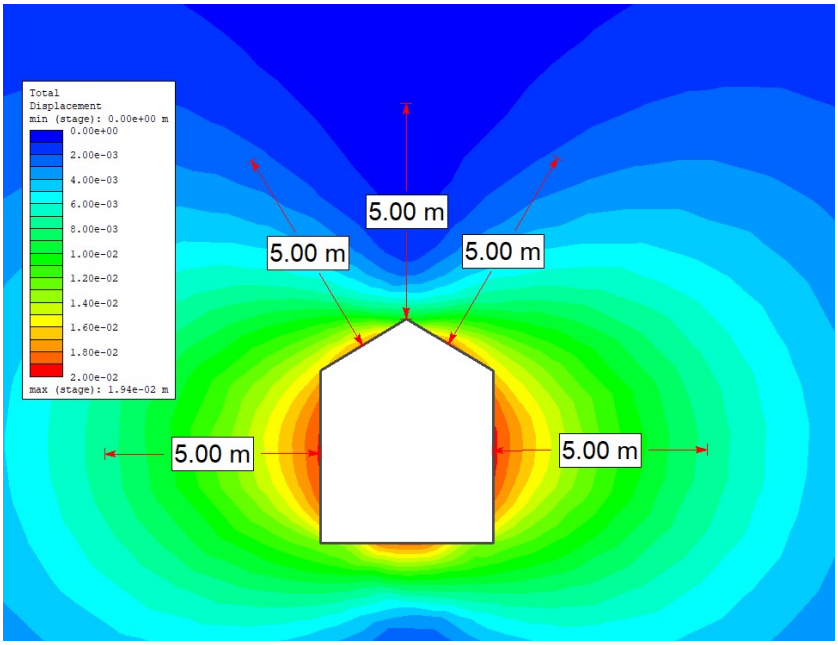

Figure 5.12 Contour plot of total displacement with 5 m query lines extending from critical locations around the tunnel boundary

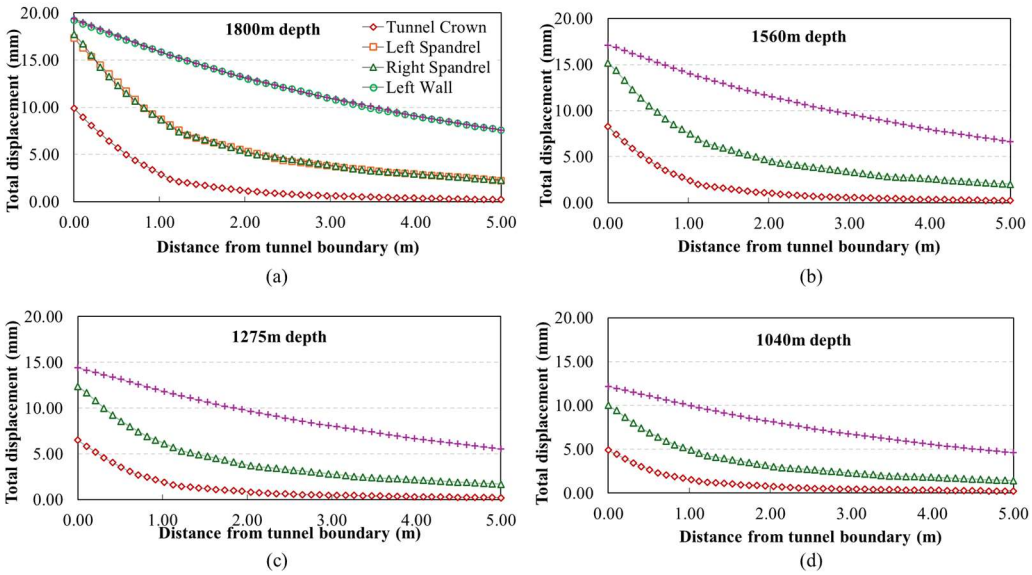

Figure 5.13 Total Displacement graphs at critical locations against distance from the tunnel boundary (up to 5 m) for varying depths: (a) 1800 m, (b) 1560 m, (c) 1275 m, and (d) 1040 m

We also analyzed displacement variations between the two lithological Units to investigate the impact of lithological properties on tunnel deformation. Displacement contours along the tunnel

boundary were assessed to identify potential zones of vulnerability. Comparative analyses between Unit 3 and Unit 4 revealed distinct differences in deformation behavior under similar stress conditions. As illustrated in Figure 5.14, displacement values were consistently higher in Unit 3 compared to Unit 4. This indicates a greater susceptibility of Unit 3 to deformation, likely due to differences in its geomechanical properties. These results may underscore the significant influence of lithological variability on tunnel stability and highlight the importance of incorporating unit-specific considerations into the tunnel design.

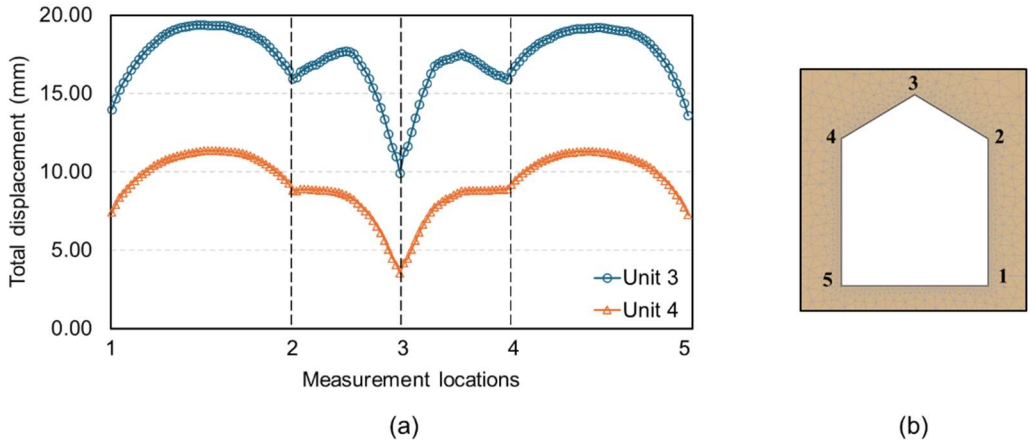

Figure 5.9 (a) Comparison of displacement profiles along the tunnel boundary for lithological Units 3 and 4; (b) Close-up view of measurement locations

5.6.3.2 The role of major principal stress in the assessment of rockburst prediction criteria

The applicability of rockburst prediction criteria was critically assessed by analyzing the variation of major principal stress (σ_1), a critical parameter governing tunnel stability and an integral factor in most rockburst prediction criteria. To achieve this, the variation of σ_1 was examined from the tunnel boundary to the model boundary at three critical locations: the right wall, right spandrel, and crown (as shown in Figure 5.15). This figure provides a contour plot of major principal stress around the excavation, highlighting the query lines used for the analysis. The σ_1 profiles for both lithological Units were plotted to capture spatial variations in this key stability parameter.

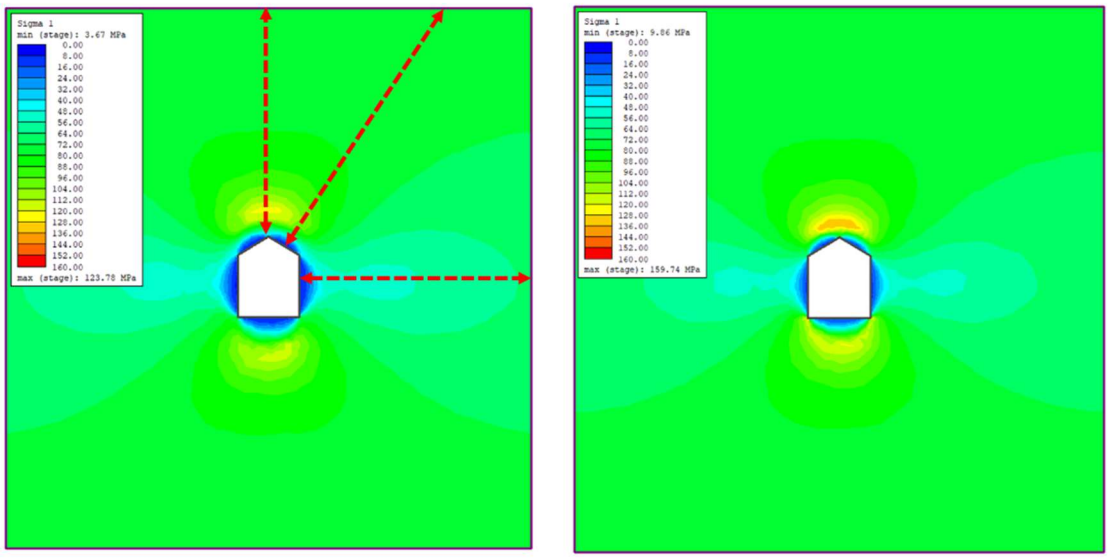

Figure 5.10 Contour plots of major principal stress (σ_1) around the excavation: (a) Unit 3 and (b) Unit 4

To evaluate the suitability of the selected criteria presented in Table 5.4, the σ_1 profiles were compared to the thresholds defined by these criteria for each unit, as shown in Figures 5.16 and 5.17. The σ_1 curves for the wall, spandrel, and crown were overlaid with the threshold lines corresponding to each rockburst prediction criterion. A color-coded risk scale—green (No Risk), yellow (Low Risk), orange (Medium Risk), and red (High Risk)—was used to visually represent rockburst risk levels, allowing for clear interpretation of the potential for rockburst across different criteria and locations. The σ_1 distribution pattern revealed that stress values were minimal at the tunnel boundary, peaked at approximately 2 m from the boundary, and then gradually decreased to their initial values at the model boundary. Among the three critical locations, the crown consistently exhibited the highest σ_1 values, followed by the spandrel, while the wall displayed the lowest values.

Figure 5.16 illustrates the comparative results of the rockburst prediction criteria alongside the σ_1 variation for Unit 3 at a depth of 1800 m. The findings showed that the Tao index predicted a high level of rockburst risk at the crown within 1 m of the tunnel boundary and a moderate risk at the spandrel (Figure 5.16a). In contrast, the BSR criterion anticipated no significant risk in the same locations (Figure 5.16c). The Zhang index identified a high level of risk for the crown and spandrel

near the tunnel boundary, with a moderate level of risk for the wall (Figure 5.16b). The Russenes index, which focuses on tangential stress, was evaluated for the crown and wall only, predicting a high rockburst risk at the crown and a negligible risk at the wall (Figure 5.16d). Similarly, the linear elastic energy criterion indicated a moderate to high rockburst risk at the crown, slight to moderate risk at the spandrel, and no risk at the wall (Figure 5.16g). Conversely, the Rockmass Strength index (RSi) and Stress Index (Si) exhibited an over-predictive trend. Particularly, the Stress index, which is based on vertical stress, forecasted high rockburst risk at all three locations near the tunnel boundary (Figures 5.16e and 5.16f). Comparative analyses across the lithological units revealed that Unit 4 exhibited higher susceptibility to rockburst than Unit 3, as represented in Figure 5.17. In Unit 4, stress conditions more frequently exceeded the thresholds defined by the prediction criteria, signaling a greater likelihood of rockburst occurrence. These findings highlight the significance of lithological variability in influencing rockburst risk and emphasize the necessity of tailored mitigation strategies for different geological units.

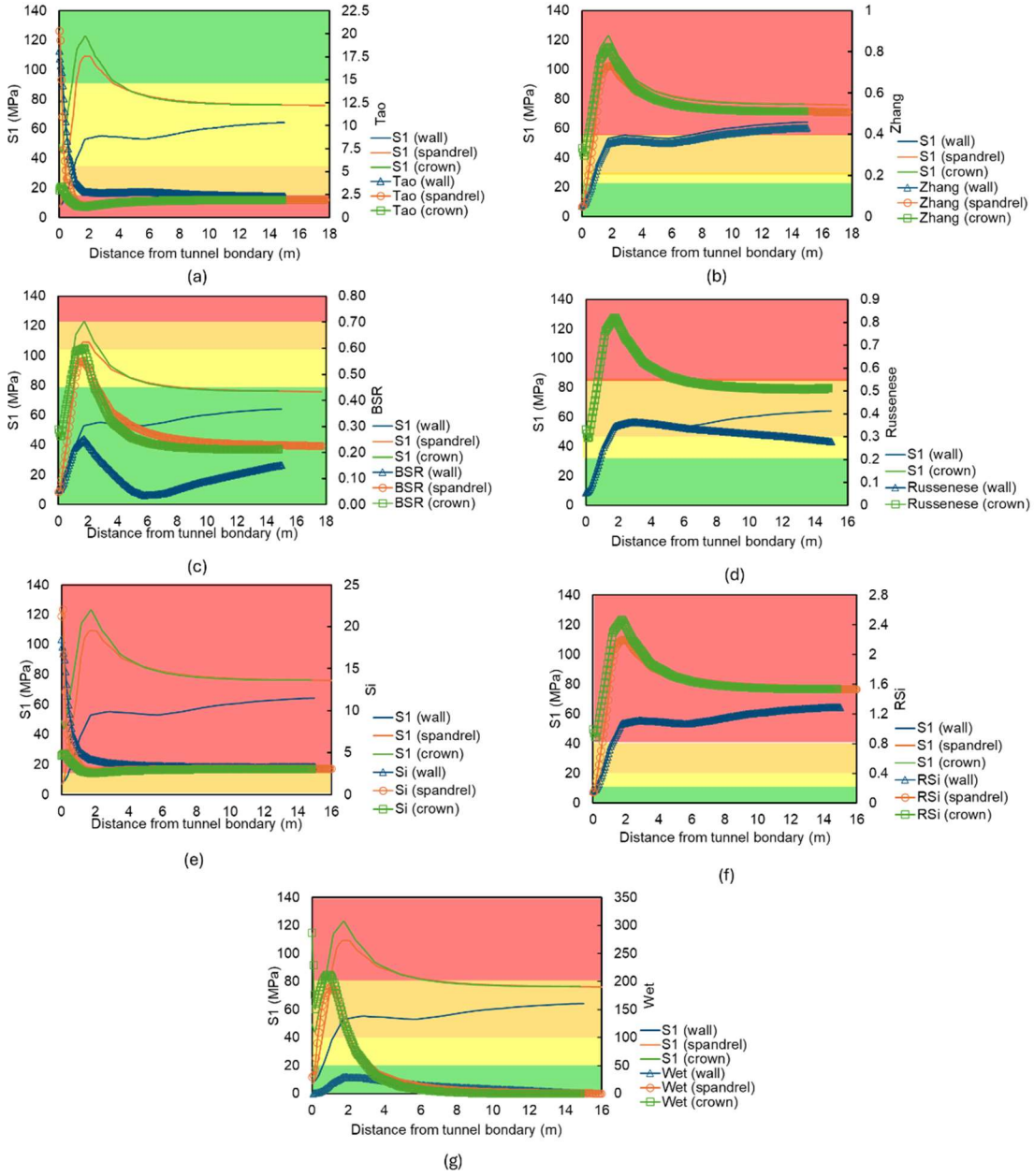

Figure 5.11 Comparative analysis of major principal stress (σ_1) variations and rockburst prediction criteria at three critical locations in Unit 3 at a depth of 1800 m: (a) Tao index, (b) Zhang index, (c) BSR criterion, (d) Russenes index, (e) Stress Index (Si) , (f) Rockmass Strength index (RSi), and (g) Linear elastic energy

criterion. Rockburst risk levels are color-coded: green (No risk), yellow (Low risk), orange (Medium risk), and red (High risk)

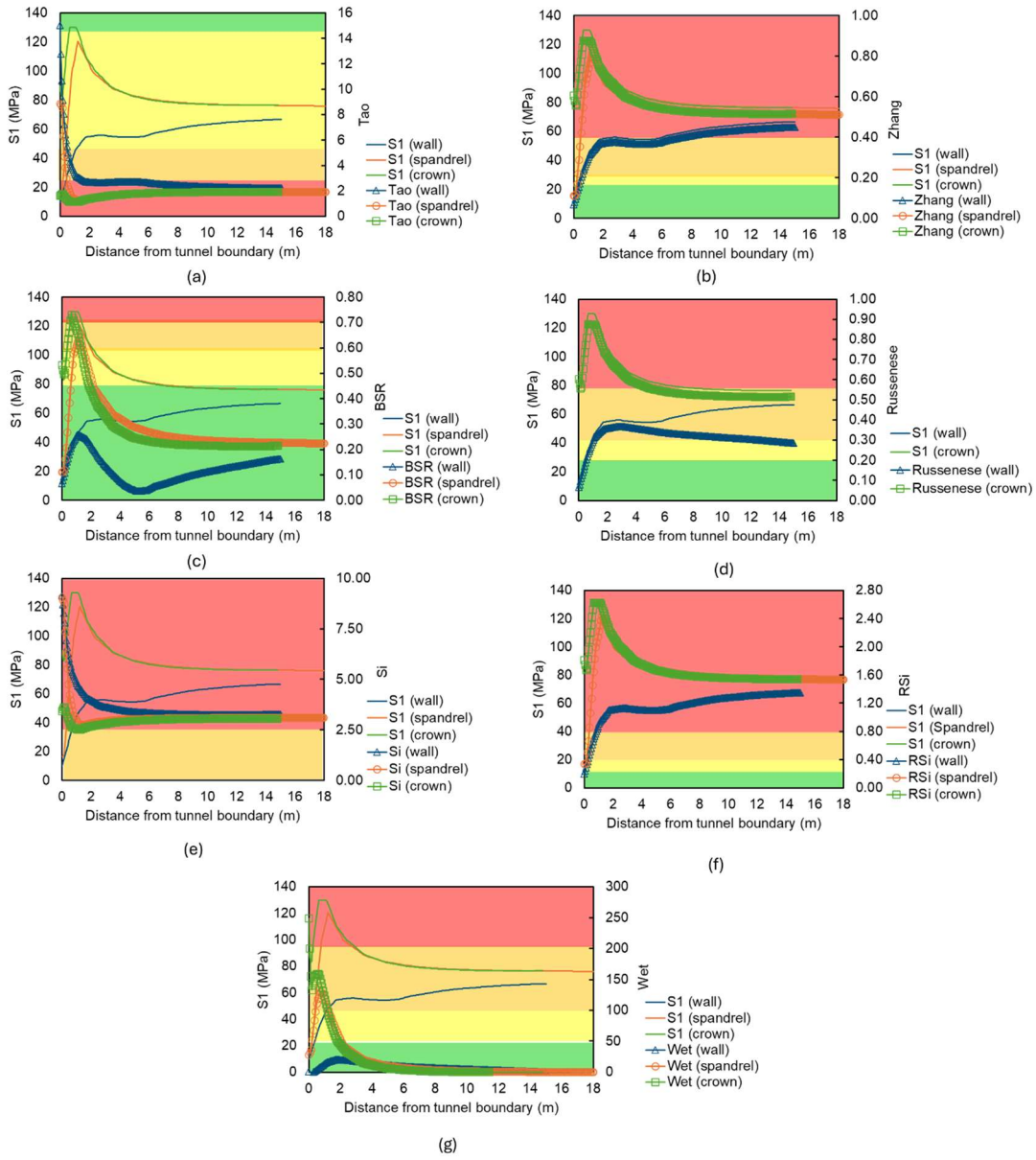

Figure 5.12 Comparative analysis of major principal stress (σ_1) variations and rockburst prediction criteria at three critical locations in Unit 4 at a depth of 1800 m: (a) Tao index, (b) Zhang index, (c) BSR criterion, (d) Russenes index, (e) Stress Index (Si) , (f) Rockmass Strength index (RSi), and (g) Linear elastic energy

criterion. Rockburst risk levels are color-coded: green (No risk), yellow (Low risk), orange (Medium risk), and red (High risk)

5.6.3.3 Evaluation of rockburst prediction criteria around tunnel boundaries

Following a detailed analysis of σ_1 variations and a comparative analysis of selected rockburst prediction criteria, this section further focused on evaluating the applicability of these criteria near the tunnel boundary at the critical depth of 1800 m. The analysis incorporated three key boundary lines: the on-boundary line (located exactly on the tunnel perimeter), the 0.5m boundary (0.5 m from the perimeter), and the 1m boundary (1 m from the perimeter), as schematically illustrated in Figure 5.18. This methodology provided insights into the predictive accuracy of each criterion in identifying rockburst potential at specific tunnel locations, including the right wall, right spandrel, left spandrel, and left wall, as depicted in Figures 5.19 and 5.20 for Units 3 and 4, respectively.

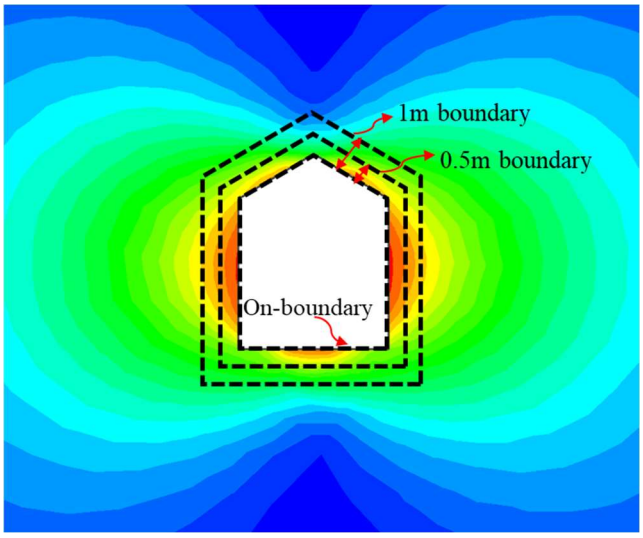

Figure 5.13 Schematic representation of boundary lines for rockburst analysis, including the on-boundary line (tunnel perimeter), 0.5 m boundary, and 1 m boundary

The analysis indicated that most criteria identified a significant rockburst risk at the 1 m boundary in both Units, aligning with the recorded incidents at the Westwood Mine at this depth. For example, the Tao index revealed high rockburst risk in the spandrels and medium risk in the walls at the 1 m boundary for Unit 3. At the 0.5 m boundary, the spandrels showed medium risk, while the

walls exhibited low-to-medium risk (Figure 5.19a). Along the tunnel perimeter, the risk was generally minimal. In contrast, the Tao index predicted more severe rockburst incidents in Unit 4, with heightened risks across all boundary lines, emphasizing the greater vulnerability of this unit (Figure 5.20a).

Similarly, the Zhang criterion predicted significant rockburst risk in the spandrels at the 1 m boundary while showing negligible risk along the tunnel perimeter for both Units (Figures 5.19b and 5.20b). The BSR index, however, did not predict any rockburst risk in Unit 3 at any boundary (Figure 5.19c), but it indicated medium-to-high risk in the spandrels of Unit 4, highlighting the role of lithological and geomechanical variations in rockburst susceptibility (Figure 5.20c).

The Stress Index (Si) consistently overpredicted rockburst risk, suggesting severe incidents even along the tunnel perimeter for both Units (Figures 5.19d and 5.20d). This overestimation points to its limited applicability for tunnel environments, likely due to its reliance on vertical stress, which may not fully capture the complexities of tunnel-induced stress conditions. The Rockmass Strength Index (RSi) presented a progressive increase in predicted rockburst severity from the tunnel perimeter to the 1 m boundary, suggesting a sensitivity to distance from the excavation surface (Figures 5.19e and 5.20e). Meanwhile, the Linear Elastic Energy Criterion offered a different perspective, identifying significant rockburst risk predominantly in the roof sections (spandrels) across all boundary lines, while predicting negligible risk in the walls (Figures 5.19f and 5.20f). This distinct pattern underscores the importance of considering elastic strain energy in rockburst assessments.

The Russenes criterion, defined as the ratio of tangential stress to uniaxial compressive strength (UCS), could not be effectively applied in this approach due to the complex nature of tangential stress around the tunnel perimeter. Tangential stress varies significantly in magnitude and direction, aligning with different stress components depending on the location—for example, σ_{xx} at the crown and $\sigma_{\gamma\gamma}$ at the mid-wall—while continuously rotating between these points. This spatial variability complicates consistent evaluation, as the criterion depends on a parameter that changes dynamically along the boundary. These challenges, combined with the computational demands of accurately resolving

tangential stress, made the Russenes criterion unsuitable for localized boundary analyses in this context.

These findings highlight the necessity of boundary-specific analyses for accurate predictions. They also emphasize the variability in predictive accuracy among the criteria, as well as the significant differences in rockburst susceptibility between Units 3 and 4. Unit 4 consistently demonstrated a higher likelihood of rockburst occurrence, reinforcing the importance of considering lithological and geomechanical factors in developing mitigation strategies. Furthermore, the discrepancies in predictions among the criteria underline the need for an integrated approach to rockburst assessment, ensuring a comprehensive understanding of potential risks in underground excavations.

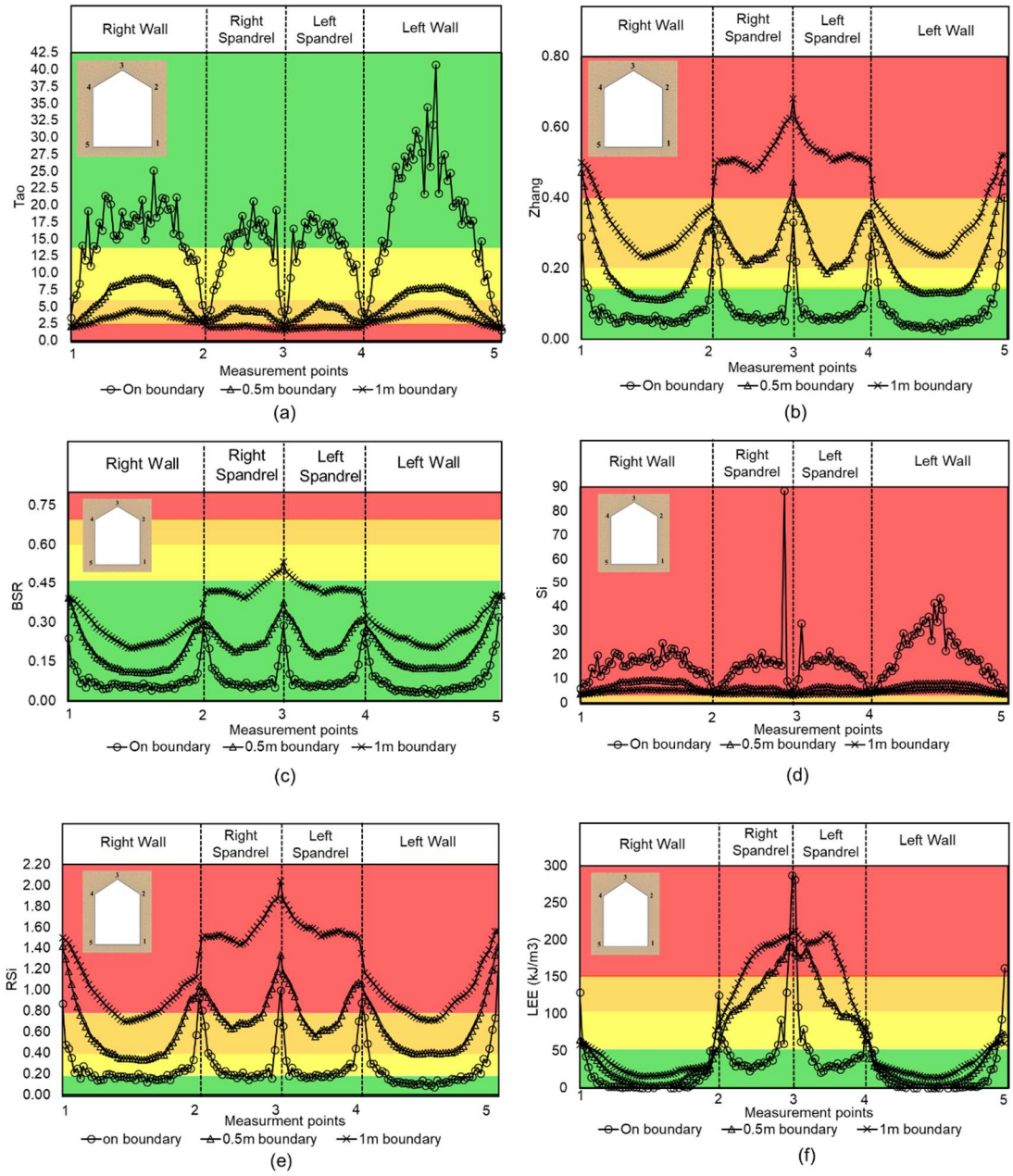

Figure 5.14 Comparison of rockburst prediction criteria at the tunnel boundary and surrounding regions (on-boundary, 0.5 m boundary, and 1 m boundary) for Unit 3 at a depth of 1800 m. Rockburst risk levels are color-coded: green (No risk), yellow (Low risk), orange (Medium risk), and red (High risk)

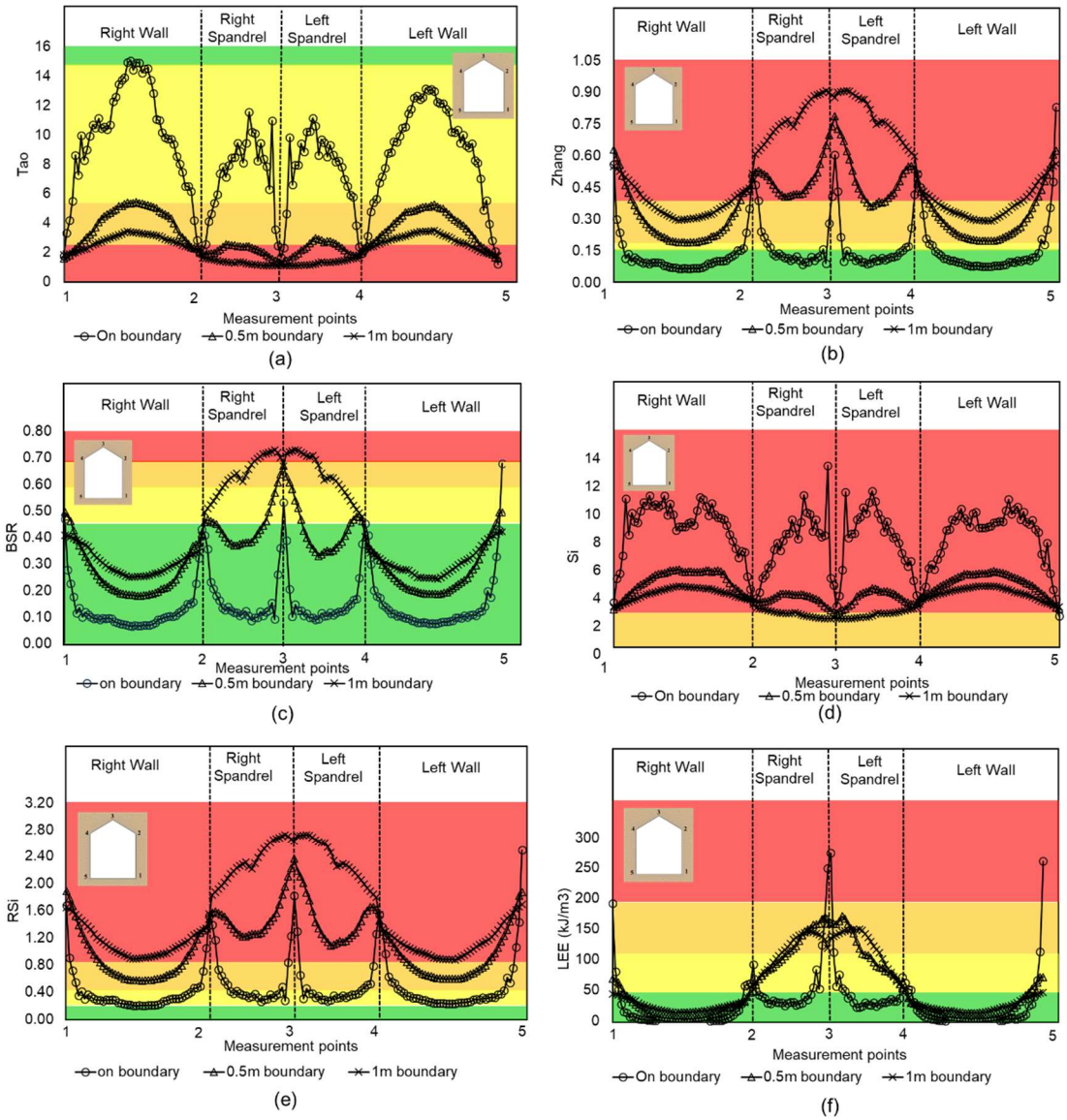

Figure 5.20. Comparison of rockburst prediction criteria at the tunnel boundary and surrounding regions (on-boundary, 0.5 m boundary, and 1 m boundary) for Unit 4 at a depth of 1800 m. Rockburst risk levels are color-coded: green (No risk), yellow (Low risk), orange (Medium risk), and red (High risk)

5.7 Probabilistic evaluation of rockburst occurrence at tunnel boundaries

This section presents the probabilistic assessment of rockburst occurrences around the boundary lines: on-boundary, 0.5 m boundary, and 1 m boundary. The probability of rockburst was determined using the thresholds defined by each criterion, enabling a comprehensive evaluation of risk across

tunnel boundaries. This approach not only facilitates localized risk assessment but also provides insights into the intensity of rockbursts, visualized through color-coded probability ranges corresponding to each prediction index. The results for Units 3 and 4 are shown in Figures 5.21 and 5.22.

For Unit 3, the Tao and Zhang indices largely predicted stable conditions along the tunnel perimeter (on-boundary), estimating approximately 60% and 90% probabilities of no risk, respectively (Figures 5.21a and 5.21d). Similarly, the RSi criterion suggested a 60% probability of no risk in the walls but identified a notable 50% likelihood of slight-to-moderate rockburst events occurring in the spandrels (Figure 5.21m). The LEE index largely predicted no risk around the tunnel perimeter but showed a 40% chance of low-to-moderate rockburst intensity in the right spandrel (Figure 5.21p). These findings point to potential limitations in the predictive capabilities of the examined criteria for accurately identifying rockbursts directly at the on-boundary line. This observation could reflect the low probability of rockbursts initiating at the exact tunnel boundary or the inherent insensitivity of these indices to the stress distribution characteristics at this location. However, given the inherent uncertainties and variabilities associated with boundary-specific evaluations, such interpretations must be approached with caution.

At 0.5 m from the tunnel perimeter, the probability of rockburst occurrence increased, indicating that damage associated with rockbursts may initiate beyond the immediate boundary. The Tao index indicated a clear risk of moderate intensity rockbursts in the spandrels, with a 40% likelihood of similar events in the walls (Figure 5.21b). Similarly, the Zhang index highlighted an elevated risk in the spandrels, while predicting more stable conditions in the walls (Figure 5.21e). Both the RSi and LEE indices identified approximately a 40% probability of strong rockbursts in the spandrels (Figures 5.21n and 5.21q). While RSi also indicated a moderate risk in the walls, the LEE index estimated no risk for these areas, emphasizing its distinct energy-based approach which incorporates both stress and strain in rockburst prediction.

As illustrated in Figures 5.21 and 5.22, the probability of rockburst occurrence escalates noticeably at the 1 m boundary, correlating with the elevated stress magnitudes, particularly the major principal stress (σ_1), observed at this distance. A majority of the criteria, including Tao, Zhang, RSi, and LEE, consistently identified high rockburst risks in the spandrels, with moderate-to-high risk levels predicted for the walls. An exception is the LEE index, which estimated a 90% probability of no risk in the walls. This outcome may reflect the unique energy-based formulation of the LEE index, which integrates both strain and stress parameters, potentially providing a more comprehensive interpretation of rockburst mechanisms in these regions.

The Stress Index (Si) consistently predicted a 100% likelihood of high-risk rockburst events across all boundary lines and tunnel locations in both Units (Figures 5.21 and 5.22). This overestimation may not only reflect an overly conservative approach but also highlight an inherent limitation of the index, primarily its dependency on vertical stress. As a result, this criterion fails to account for the complex stress states present in tunnel environments, leading to an overestimation of rockburst risk. The BSR index predicted no risk across all tunnel locations at the on-boundary line for both Units. However, at the 1 m boundary in Unit 4, it indicated moderate-to-high rockburst risk in the spandrels (Figure 5.21i). This might indicate limited applicability of the BSR index in accurately capturing localized stress variations, as it relies on differential stresses that might not adequately represent the intricate conditions around the tunnel boundary.

Furthermore, the analysis revealed a higher likelihood of more severe rockburst events in Unit 4 across all three boundary lines, compared to Unit 3. This increased risk can likely be attributed to greater geomechanical heterogeneity within Unit 4. The higher stress levels, coupled with the unit's specific lithological and geomechanical characteristics, contribute to its heightened susceptibility to rockbursts.

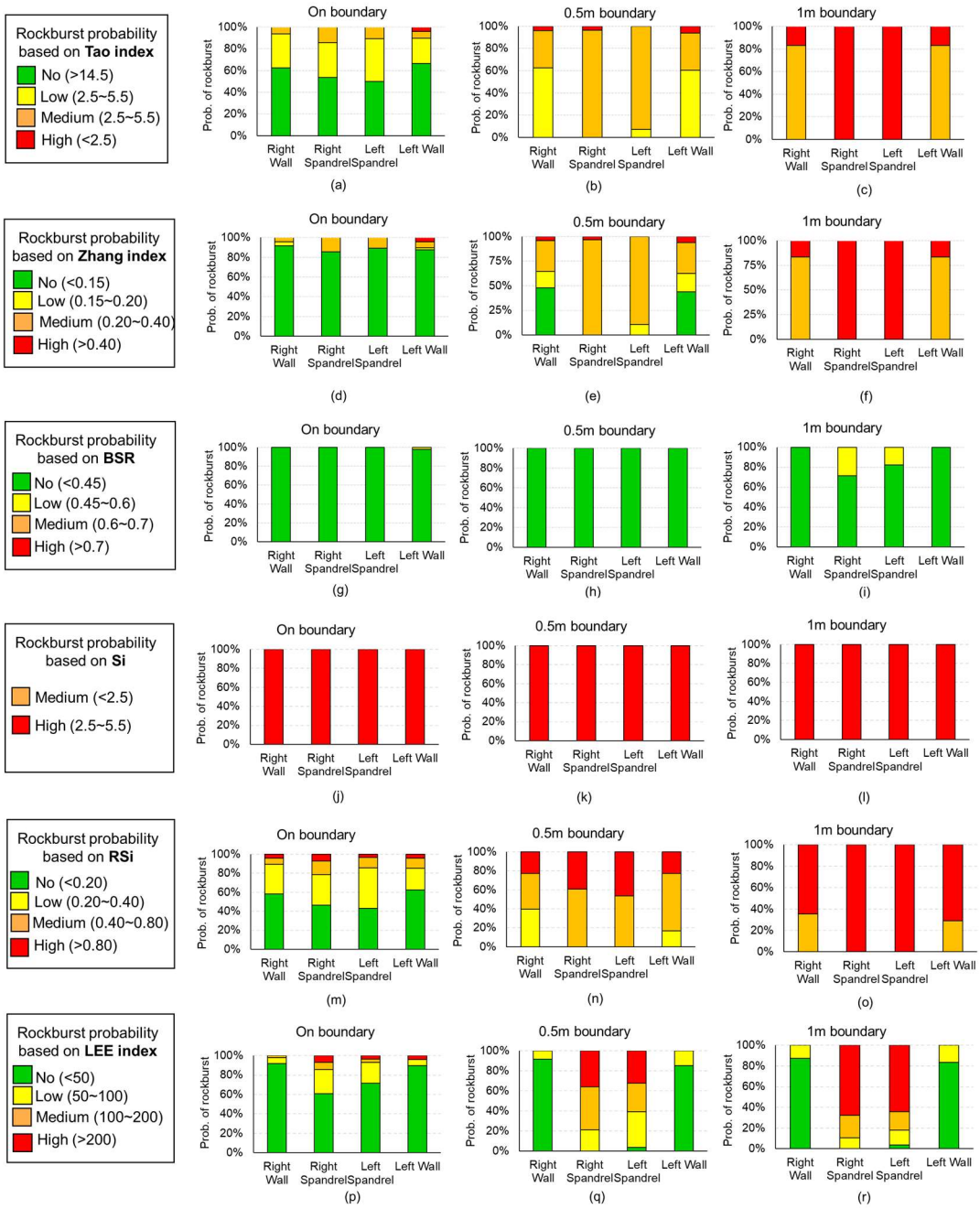

Figure 5.21 Probability assessment of rockburst risk for Unit 3 based on selected prediction criteria across three boundary lines (on-boundary, 0.5m boundary, and 1m boundary)

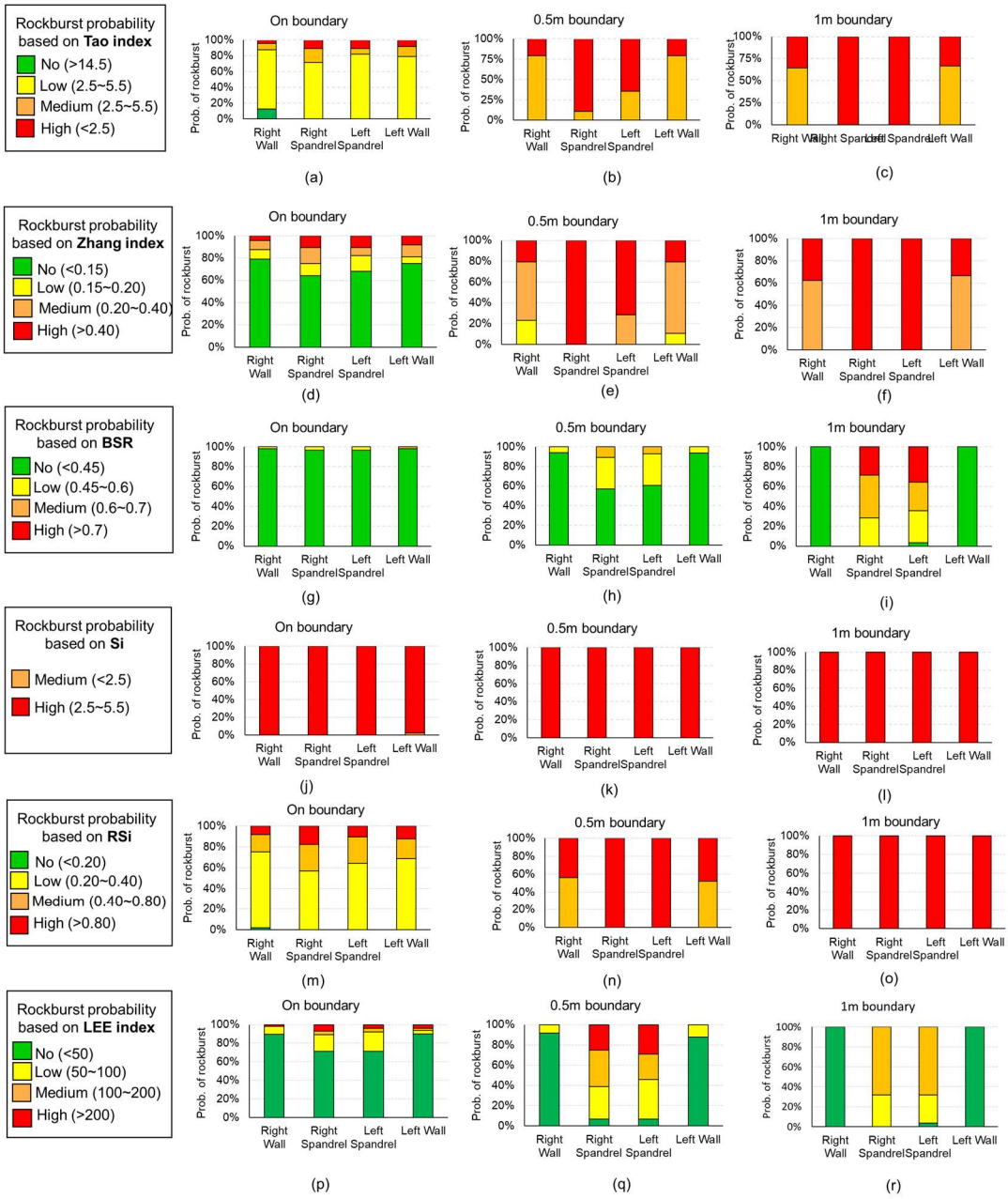

Figure 5.22 Probability assessment of rockburst risk for Unit 4 based on selected prediction criteria across three boundary lines (on-boundary, 0.5m boundary, and 1m boundary)

The probabilistic evaluation conducted in this study highlighted the critical importance of boundary-specific analyses in assessing rockburst risks, providing valuable insights into the performance of various predictive criteria. While most indices demonstrated an increasing probability of rockburst incidents with greater distance from the tunnel perimeter, their reliability varied

significantly. Indices like Tao and Zhang exhibited notable consistency in capturing stress-induced risks, making them valuable tools for boundary-sensitive analyses. In contrast, the Stress Index (Si) consistently overpredicted risks, highlighting its inherent limitations due to its dependence on vertical stress and its inability to address the complex stress state in underground excavations. The Linear Elastic Energy (LEE) index, with its energy-based framework, showed distinct advantages in identifying rockburst potential under energy-dominated conditions, demonstrating its suitability for specific geomechanical scenarios.

The observed differences between Units 3 and 4 underscore the significant impact of geomechanical variability on rockburst risk, particularly in Unit 4, where the potential for severe rockbursts is more noticeable. This may call for a reassessment of the tunnel profile and consideration of additional support measures to mitigate the risk of strong rockbursts. The findings highlight the importance of adopting a multi-criteria approach to rockburst prediction, one that utilizes the strengths of reliable indices while addressing their inherent limitations. This not only improves the accuracy of risk assessments but also ensures that mitigation strategies are tailored to the specific geomechanical conditions of each excavation. By implementing this comprehensive methodology, geotechnical engineers can enhance safety, optimize tunnel stability, and increase the predictive reliability of rockburst evaluations. This approach could contribute to the advancement of geotechnical engineering practices, fostering greater resilience and adaptability in the face of complex subsurface conditions.

5.8 Conclusions

The primary objective of this study was to evaluate the effectiveness of various rockburst prediction criteria in assessing the probabilistic risk of rockbursts in underground tunnels, with a specific focus on the Westwood Mine case study. The aim was to understand how different criteria perform in predicting rockburst occurrence at various boundary lines and tunnel locations, and to identify the most suitable criteria for practical rockburst risk assessment. The following conclusions were drawn from the analyses:

- The numerical analysis revealed significant variability in rockburst risk across the two studied units, with Unit 4 exhibiting a notably higher likelihood of severe rockbursts compared to Unit 3. This higher risk in Unit 4 can be attributed to the greater geomechanical heterogeneity and rockmass quality of this unit.
- Among the various rockburst prediction criteria evaluated, those incorporating major principal stress, such as the Tao and Zhang indices could provide more realistic and consistent outcomes. These indices predicted low-risk conditions near the tunnel perimeter, while the Stress Index (Si) consistently overestimated the likelihood of high-risk rockburst events across all boundary lines, particularly in Unit 4. The application of the Russenes criterion was found to be limited in its effectiveness due to the complexity of tangential stress variations around the tunnel perimeter.
- A general trend was observed where rockburst risk increased with proximity to the 1m boundary, especially in regions with higher stress concentrations, such as the spandrel zones. This significant spatial variability highlights the importance of localized risk assessments for more accurate predictions and tailored mitigation strategies.
- The multi-criteria approach used in this study, incorporating various rockburst prediction indices and probabilistic assessments across different boundary lines, provided a robust framework for evaluating rockburst risk. This methodology allowed for a detailed examination of how different prediction criteria performed across multiple tunnel locations and boundary distances. However, certain criteria, such as the Stress Index (Si), demonstrated significant limitations in practical application due to its over-reliance on vertical stress. This led to an overestimation of rockburst risk, particularly in areas with more complex, multi-directional stress states, suggesting the need for refinement in the stress-based criteria.
- Based on the findings, it is recommended to adopt a combined approach using multiple rockburst prediction criteria to obtain a more comprehensive risk assessment. While the Tao

and Zhang indexes proved valuable, additional parameters, such as lithological variation and more detailed stress state modeling, should be incorporated to enhance prediction accuracy.

- The variability in rockburst risk observed across different tunnel locations underscores the importance of conducting boundary-based risk assessments. Acknowledging the differences in rockburst risk between tunnel locations helps to better understand the unique geomechanical and stress conditions at each site, which is crucial for formulating effective mitigation strategies.
- The higher rockburst risk identified in Unit 4 emphasizes the necessity for targeted support and reinforcement strategies, particularly in areas with higher stress levels and geomechanical variability. Comprehensive monitoring systems should be implemented to track real-time stress changes and adjust support measures accordingly. The practical implications of this study are significant for mine safety and management, as it provides valuable insights into the importance of using a multi-criteria approach for rockburst risk assessment. By improving the accuracy of rockburst predictions, mining operations can enhance safety protocols and optimize design and support systems to minimize the risk of catastrophic events.

CHAPTER 6

CONCLUSIONS AND RECOMMENDATIONS

6.1 Conclusions

This research advances the understanding of rockburst prediction by exploring the complex relationship between geomechanical parameters, in-situ stress states, and their influence on rockburst occurrences in deep excavations, with a particular focus on underground settings such as the Westwood Mine. By integrating advanced statistical data treatment techniques, probabilistic analyses, and numerical simulations, this study provides valuable insights into assessing and predicting rockbursts in deep mining in rock masses. The key findings and contributions of this research are summarized below:

6.1.1 Advances in Data Treatment for Geomechanical Parameters:

- This research conducted a comprehensive review and categorization of outlier detection methods for geomechanical data, dividing them into two main groups: fence labeling methods and statistical tests. While statistical tests were found to be less effective due to their limitations in handling skewed data and small sample sizes, modified IQR-based methods, such as the MC boxplot and SIQR rule, emerged as the most reliable for detecting outliers, particularly by accounting for data skewness. The strengths and limitations of these methods were critically analyzed, resulting in a tailored categorization methodology that provides engineers with valuable insights to enhance data analysis and interpretation. Additionally, a practical flowchart was developed to guide practitioners in selecting the most appropriate outlier detection method based on specific data characteristics. These findings not only offer suitable tools for accurate geomechanical data analysis but also highlight avenues for future research to further refine outlier detection techniques.

6.1.2 Quantification of Geomechanical Uncertainties:

- A comprehensive methodology was established to analyze and mitigate uncertainties in geomechanical parameters, facilitating more reliable decision-making in rockburst analysis. Variabilities in geomechanical properties were found to be significantly influenced by schistosity planes and mineralogical compositions, underscoring their important roles in laboratory test outcomes. The study revealed the absence of consistent patterns in the variations of hard and soft minerals across the analyzed rock units, demonstrating the complexity of rock behavior under stress conditions.
- Mitigating these uncertainties may require a multistep approach: (1) employing reliable outlier detection methods, guided by engineering judgment; (2) addressing the impacts of schistosity angles and other factors contributing to data variability; and (3) understanding and accounting for the influence of mineralogical compositions on geomechanical properties. Also, engineering judgment remains crucial in selecting the most suitable data treatment methods and aligning them with rock mechanics principles.
- The statistical evaluation of geomechanical laboratory data from the Westwood Mine (Quebec, Canada) revealed significant variabilities, which were analyzed using various data treatment techniques. Through a rigorous selection process based on multiple decision-making criteria and engineering judgment, the most appropriate outlier detection methods were identified for each parameter. The analysis showed that some methods performed well in identifying outliers, while others failed, particularly those unsuitable for large datasets. The widely used boxplot method often fell short due to its inability to provide confidence ranges consistent with engineering judgment. In contrast, alternative approaches such as the adjusted boxplot, 2MADe, and 2SD demonstrated superior accuracy in identifying true outliers.

- The study at the Westwood Mine revealed that geomechanical intact parameters frequently deviate from the normal distribution, challenging widely accepted assumptions in geomechanical research. This deviation suggests that traditional modeling approaches may inadequately represent the true variability of rock properties. To address the variability in uniaxial compressive strength (UCS) data, samples with specific schistosity angles—where UCS exhibited the greatest variation—were strategically excluded, effectively mitigating the adverse effects of schistosity on data reliability. Additionally, petrographic analyses provided critical insights into the relationship between the dispersion of geomechanical properties and the proportions of hard and soft minerals. While this analysis established a logical link between mineral distribution and parameter variabilities, no consistent pattern emerged across different rock units, highlighting the complex and site-specific nature of mineralogical influences.

6.1.3 Development of In-Situ Stress Relationships:

- A novel approach was developed to categorize regions within the Canadian Shield based on geological and structural characteristics. This approach improved the accuracy of stress-depth relationships by integrating statistical principles with geological reasoning, addressing the limitations of previous models.
- A key advancement was the incorporation of three-dimensional stress tensors, which adjusted the adverse effects of stress orientation, particularly in geologically heterogeneous regions. The classification divided the Canadian Shield into six lithological and structural groups, capturing regional variability. Regression analyses specific to each group provided refined equations for vertical stress, maximum and minimum horizontal stresses, and stress ratios. For instance, in the Grenville group, vertical stress correlated closely with lithostatic pressure ($\sigma v = 0.030z$, $R^2 = 0.83$), offering significantly improved reliability over prior models.

- Unique nonlinear stress-depth relationships were identified, such as the vertical stress in the Wabigoon & Quetico group, modeled as σ_v=1.08$z^{0.49}$, potentially reflecting the influence of thin- and thick-skinned tectonism. In the Grenville group, significant horizontal stress deviations (σ_H=5.7$z^{0.21}$, R^2=0.17, σ_h=1.8$z^{0.28}$, R^2=0.20) might be attributed to regional thrust imbrication. Such findings underscore the importance of incorporating tectonic history into predictive models.
- Comparative analyses demonstrated that the proposed relationships outperform prior models, such as Herget (1982) and Maloney et al. (2006), which relied heavily on linear trends and lacked sensitivity to regional geological variability. For instance, the proposed stress ratio relationships exhibited higher correlation values, better reflecting the influence of structural and lithological heterogeneities.
- The study emphasizes the importance of combining geological insights with statistical tools to develop reliable stress-depth relationships. This integration ensures that resulting equations are both statistically robust and geologically representative, accounting for significant influence of tectonic activities on stress trends in deep excavations.

6.1.4 Applicability of Rockburst Prediction Criteria:

- The evaluation of various rockburst prediction indices revealed that the Tao and Zhang indices, incorporating major principal stress, provided better predictive accuracy. In contrast, the Stress Index (Si) overestimated risk, predicting a 100% probability of high-risk rockbursts at all boundary lines and tunnel locations in both Units, due to its reliance on vertical stress.
- Numerical simulations demonstrated that displacement values increased with depth, with maximum displacements observed at 1800 m, demonstrating higher instability risks at greater depths. Unit 3 showed consistently higher displacement values compared to Unit 4, indicating its greater susceptibility to deformation due to less favorable geomechanical properties.

- Boundary-specific assessments showed significant differences in risk predictions at varying distances from the tunnel perimeter. For instance, at the on-boundary line, the Tao and Zhang indices predicted 60% and 90% probabilities of no rockburst risk, respectively, while the RSi criterion suggested a 60% probability of no risk in the walls and a 50% chance of slight-to-moderate risk in the spandrels. At 0.5 m from the tunnel perimeter, the Tao index indicated a 40% probability of moderate intensity rockbursts in both the spandrels and walls. The Zhang index showed elevated risk in the spandrels while predicting more stable conditions in the walls. Both RSi and LEE indices identified a 40% probability of strong rockbursts in the spandrels. At the 1 m boundary, most indices predicted higher risks, with Tao, Zhang, RSi, and LEE indicating high risks in the spandrels and moderate-to-high risks in the walls. The LEE index predicted a 90% probability of no risk in the walls, reflecting its energy-based approach.
- The BSR index predicted no risk at the on-boundary line but indicated moderate-to-high risk in the spandrels at the 1 m boundary in Unit 4, suggesting limitations in capturing localized stress variations near the tunnel boundary.

6.2 Recommendations and future work

This research contributes to advancing the fields of rock mechanics and geotechnical engineering by addressing critical gaps in data treatment, stress modeling, and rockburst prediction. The methodologies and insights developed herein hold practical significance for enhancing the safety and efficiency of deep underground excavations in mining and civil engineering applications. Future work should focus on:

- **Evaluating the Impact of Mineralogy and Schistosity on Rockburst Occurrence:** Future research should focus on conducting both laboratory experiments and field studies to investigate how variations in these geomechanical properties affect rock mass response to

stress. This could lead to more localized and precise predictions of rockburst susceptibility, especially in heterogeneous rock masses.

- **Enhancing Stress-Depth Relationships with Additional Measurement Data:** To achieve more accurate stress-depth models, it is essential in future studies to incorporate a broader range of in-situ stress measurements. This is particularly important in regions like the Grenville Geological Province, where available data is limited. Also comparing the stress measurements from other regions, such as western Canada, can help understand the stress regime models in the Canadian Shield.
- **Integrating Rock Mass Discontinuities into Numerical Models for Better Rockburst Prediction:**

  Future research should incorporate Rock mass discontinuities, such as major faults and joints into numerical simulations using the Discrete Element Method (DEM), particularly software like 3DEC. Additionally, dynamic analysis of rockburst scenarios could provide insights into how prediction criteria perform when rockbursts actually occur, enhancing the predictive accuracy of existing models and contributing to more robust risk assessments.

By bridging theoretical models with practical applications, this research lays a crucial foundation for the enhancement of rockburst risk prediction accuracy. These developments will ultimately contribute to more reliable and sustainable underground excavation practices, reinforcing safety measures and optimizing engineering designs for complex geological environments.

REFERENCES

Abdaqadir, Z. K., & Alshkane, Y. M. (2018). Physical and mechanical properties of metamorphic rocks. Journal of Garmian University, 5(2), 160-173.

Adel, S., Mansour, Z., & Ardeshir, H. (2021). Geochemical behavior investigation based on k-means and artificial neural network prediction for titanium and zinc, Kivi region, Iran. Известия Томского политехнического университета. Инжиниринг георесурсов, 332(3), 113-125.

Afraei, S., Shahriar, K., & Madani, S. H. (2017). Statistical analysis of rock-burst events in underground mines and excavations to present reasonable data-driven predictors. Journal of Statistical Computation and Simulation, 87(17), 3336-3376.

Afraei, S., Shahriar, K., & Madani, S. H. (2018). Statistical analysis of rock-burst events in underground mines and excavations to present reasonable data-driven predictors. Journal of Statistical Computation and Simulation, 87(17), 3336-3376.

Agliardi, F., Sapigni, M., & Crosta, G. (2016). Rock mass characterization by high-resolution sonic and GSI borehole logging. Rock Mechanics and Rock Engineering, 49(11), 4303-4318.

Agliardi, F., Sapigni, M., & Crosta, G. B. (2016). Rock Mass Characterization by High-Resolution Sonic and GSI Borehole Logging. Rock Mechanics and Rock Engineering, 49(11), 4303-4318. https://doi.org/10.1007/s00603-016-1025-x

Akaike, H. (1974). A new look at the statistical model identification. IEEE transactions on automatic control, 19(6), 716-723.

Ali, E., Guang, W., zhiming, Z., & Weixue, J. (2014). Assessments of Strength Anisotropy and Deformation Behavior of Banded Amphibolite Rocks. Geotechnical and Geological Engineering, 32(2), 429-438. https://doi.org/10.1007/s10706-013-9724-5

Almeida, A. P., & Liu, J. (2018). Statistical evaluation of design methods for micropiles in Ontario soils. DFI Journal-The Journal of the Deep Foundations Institute, 12(3), 133-146.

Amadei, B., & Stephansson, O. (1997). Rock stress and its measurement. Springer Science & Business Media.

Anderson, E. M. (1951). The dynamics of faulting and dike formation with applications to Britain. Oliver and Boyd, Edinburgh, [1951].

Anderson, T. W., & Darling, D. A. (1952). Asymptotic theory of certain" goodness of fit" criteria based on stochastic processes. The annals of mathematical statistics, 193-212.

Arjang, B. (1989). Pre-mining stresses at some hard rock mines in the Canadian Shield. The 30th US Symposium on Rock Mechanics (USRMS),

Arjang, B. (1998). Canadian crustal stresses and their application in mine design. Mine Planning and Equipment Selection 1998,

Askaripour, M., Saeidi, A., Mercier-Langevin, P., & Rouleau, A. (2022). A Review of Relationship between Texture Characteristic and Mechanical Properties of Rock. Geotechnics, 2(1), 262-296.

Azad, S. T., Moghaddassi, N., & Sayehbani, M. (2022). Digital Shoreline Analysis System improvement for uncertain data detection in measurements. Environmental Monitoring and Assessment, 194(9), 646.

Bao, Y., Song, C., Wang, W., Ye, T., Wang, L., & Yu, L. (2013). Damage Detection of Bridge Structure Based on SVM. Mathematical Problems in Engineering, 2013, 490372. https://doi.org/10.1155/2013/490372

Barbato, G., Barini, E., Genta, G., & Levi, R. (2011). Features and performance of some outlier detection methods. Journal of Applied Statistics, 38(10), 2133-2149.

Barnett, O., & Cohen, A. (2000). The histogram and boxplot for the display of lifetime data. Journal of Computational and Graphical Statistics, 9(4), 759-778.

Barnett, V., & Lewis, T. (1994). Outliers in statistical data (Vol. 3). Wiley New York.

Bawa, S., & Singh, S. P. (2020). Analysis of fatigue life of hybrid fibre reinforced self-compacting concrete. Proceedings of the Institution of Civil Engineers-Construction Materials, 173(5), 251-260.

Bennett, T. J., & Marshall, M. E. (2001). Identification of rockbursts and other mining events using regional signals at international monitoring system stations. Science Applications International Corp Mclean VA.

Bidgoli, M. N., & Jing, L. (2014). Anisotropy of strength and deformability of fractured rocks. Journal of Rock Mechanics and Geotechnical Engineering, 6(2), 156-164.

Blake, W. (1972). Rock burst mechanics. 1970-1979-Mines Theses & Dissertations.

Blake, W., & Hedley, D. G. (2003). Rockbursts: case studies from North American hard-rock mines. SME.

Board, M., & Voegele, M. (1981). EXAMINATION AND DEMONSTRATION OF UNDERCUT AND FILL STOPPING FOR GROUND CONTROL IN DEEP VEIN MINING.

Bolla, A., & Paronuzzi, P. (2021). UCS field estimation of intact rock using the Schmidt hammer: A new empirical approach IOP Conference Series: Earth and Environmental Science,

Borosnyói, A. (2014). Variability case study based on in-situ rebound hardness testing of concrete: Part 1. Statistical analysis of inherent variability parameters. Építöanyag (Online)(3), 85.

Bouzeran, L., Pierce, M., Andrieux, P., & Williams, E. (2019, 24-25 June 2019). Accounting for rock mass heterogeneity and buckling mechanisms in the study of excavation performance in foliated ground at Westwood mine Deep Mining 2019: Proceedings of the Ninth International Conference on Deep and High Stress Mining, Muldersdrift. https://papers.acg.uwa.edu.au/p/1952_03_Bouzeran/

Bozorgzadeh, N., Dolowy-Busch, M., & Harrison, J. P. (2015). Obtaining Robust Estimates of Rock Strength for Rock Engineering Design 13th ISRM International Congress of Rock Mechanics,

Brady, B. H. G. (1979). Boundary element methods for mine design University of London].

Brown, E., & Hoek, E. (1978). Technical note trends in relationships between measured in-situ stress and depth. Int. J. Rock Mech. Min. Sci. and Geomech. Abstr, 15(4), 211-215.

Cai, M. (2013). Principles of rock support in burst-prone ground. Tunnelling and Underground Space Technology, 36, 46-56. https://doi.org/https://doi.org/10.1016/j.tust.2013.02.003

Cai, M. (2016). Prediction and prevention of rockburst in metal mines – A case study of Sanshandao gold mine. Journal of Rock Mechanics and Geotechnical Engineering, 8(2), 204-211. https://doi.org/https://doi.org/10.1016/j.jrmge.2015.11.002

Cai, M., Kaiser, P. K., Morioka, H., Minami, M., Maejima, T., Tasaka, Y., & Kurose, H. (2007). FLAC/PFC coupled numerical simulation of AE in large-scale underground excavations. International Journal of Rock Mechanics and Mining Sciences, 44(4), 550-564. https://doi.org/https://doi.org/10.1016/j.ijrmms.2006.09.013

Cai, M., Kaiser, P. K., Uno, H., Tasaka, Y., & Minami, M. (2004). Estimation of rock mass deformation modulus and strength of jointed hard rock masses using the GSI system. International Journal of Rock Mechanics and Mining Sciences, 41(1), 3-19. https://doi.org/https://doi.org/10.1016/S1365-1609(03)00025-X

Card, K. (1990). A review of the Superior Province of the Canadian Shield, a product of Archean accretion. Precambrian research, 48(1-2), 99-156.

Card, K., & Ciesielski, A. (1986). Subdivisions of the Superior Province of the Canadian shield. Geoscience Canada.

Carling, K. (2000). Resistant outlier rules and the non-Gaussian case. Computational statistics & data analysis, 33(3), 249-258. https://doi.org/https://doi.org/10.1016/S0167-9473(99)00057-2

Carmona, S., Molins, C., Aguado, A., & Mora, F. (2016). Distribution of fibers in SFRC segments for tunnel linings. Tunnelling and Underground Space Technology, 51, 238-249.

Carter, T. (2021). Towards improved definition of numerical modelling the Hoek-Brown constant m i for. The Evolution of Geotech-25 Years of Innovation, 93.

Castro, L., Bewick, R., & Carter, T. (2012). An overview of numerical modelling applied to deep mining. Innovative numerical modelling in geomechanics, 393-414.

Chambers, J. M., Cleveland, W. S., Kleiner, B., & Tukey, P. A. (2018). Graphical methods for data analysis. Chapman and Hall/CRC.

Chauvenet, W. (1960). A manual of spherical and practical astronomy, (Spherical astronomy) (5th ed., Vol. 1). Dover Publication.

Chen, X., Cao, W., Gan, C., Ohyama, Y., She, J., & Wu, M. (2021). Semi-supervised support vector regression based on data similarity and its application to rock-mechanics parameters

estimation. Engineering Applications of Artificial Intelligence, 104, 104317. https://doi.org/https://doi.org/10.1016/j.engappai.2021.104317

Choi, S.-I., Shim, S., Kong, S.-M., Kim, Y. B., & Lee, S.-W. (2022). Efficiency Analysis of Filter-Based Calibration Technique to Improve Tunnel Measurement Reliability. KSCE Journal of Civil Engineering, 26(6), 2926-2938.

Chown, E., Daigneault, R., Mueller, W., & Mortensen, J. (1992). Tectonic evolution of the northern volcanic zone, Abitibi belt, Quebec. Canadian Journal of Earth Sciences, 29(10), 2211-2225.

Connor Langford, J., & Diederichs, M. S. (2015). Quantifying uncertainty in Hoek–Brown intact strength envelopes. International Journal of Rock Mechanics and Mining Sciences, 74, 91-102. https://doi.org/https://doi.org/10.1016/j.ijrmms.2014.12.008

Corfu, F., & Stone, D. (1998). Age structure and orogenic significance of the Berens River composite batholiths, western Superior Province. Canadian Journal of Earth Sciences, 35(10), 1089-1109.

Corkum, A., Damjanac, B., & Lam, T. (2018). Variation of horizontal in situ stress with depth for long-term performance evaluation of the Deep Geological Repository project access shaft. International Journal of Rock Mechanics and Mining Sciences, 107, 75-85.

Corthésy, R., Gill, D. E., & Leite, M. H. (1997). Élaboration d'un modèle de prédiction des contraintes in-situ dans le nord-ouest Québécois.

Corthésy, R., & Leite, M. (2000). Mesure de contraintes in situ, Mine Niobec (In French) (Centre de développement technologique de l'École Polytechnique, Issue 1).

Corthésy, R., & Leite, M. (2013). Mesure de contraintes in situ, Mine Niobec - Niveau 2400 (In French).

Corthésy, R., Leite, M. H., & Gill, D. E. (1996). Mesures des contraintes in-situ à la mine Kiena: projet IRSST.

Couëslan, C. (2019). Field Trip Guidebook: Stratigraphy and ore deposits in the Thompson nickel belt, Manitoba. M. G. Survey.

Cui, Z. S. Q. L. Q. Z. G. I. t. A. o. M. P. o. S. R. w. P. N. M. (2021). Sustainability, 13(2).

Dai, J., Gong, F., & Xu, L. (2024). Rockburst criterion and evaluation method for potential rockburst pit depth considering excavation damage effect. Journal of Rock Mechanics and Geotechnical Engineering, 16(5), 1649-1666.

Dastjerdy, B., Saeidi, A., & Heidarzadeh, S. (2023). Review of Applicable Outlier Detection Methods to Treat Geomechanical Data. Geotechnics, 3(2), 375-396. https://www.mdpi.com/2673-7094/3/2/22

Dastjerdy, B., Saeidi, A., & Heidarzadeh, S. (2024a). Determination of uncertainties of geomechanical parameters of metamorphic rocks using petrographic analyses. Journal of Rock Mechanics and Geotechnical Engineering, 16(2), 345-364. https://doi.org/https://doi.org/10.1016/j.jrmge.2023.09.011

Dastjerdy, B., Saeidi, A., & Heidarzadeh, S. (2024b). A novel region-specific methodology to characterize in-situ stress-depth relationships in the Canadian Shield GeoMontreal 2024, Montreal.

Dastjerdy, B., Saeidi, A., & Heidarzadeh, S. (2024c). A Proper Methodology to Characterize the Associated Variability of UCS Data for the Metamorphic Rocks Based on Outlier Detection Methods Geo-Congress 2024, https://ascelibrary.org/doi/abs/10.1061/9780784485309.002

Davis, D. W. (2002). U–Pb geochronology of Archean metasedimentary rocks in the Pontiac and Abitibi subprovinces, Quebec, constraints on timing, provenance and regional tectonics. Precambrian research, 115(1), 97-117. https://doi.org/https://doi.org/10.1016/S0301-9268(02)00007-4

Dawson, R. (2011). How significant is a boxplot outlier? Journal of Statistics Education, 19(2).

Dight, P., & Hsieh, A. (2016). The study of stress determination and back calculation in the canadian shield. ISRM International Symposium on In-Situ Rock Stress,

Dindarloo, S. R., & Siami-Irdemoosa, E. (2015a). Maximum surface settlement based classification of shallow tunnels in soft ground. Tunn. Undergr. Space Technol., 49, 320-327.

Dindarloo, S. R., & Siami-Irdemoosa, E. (2015b). Maximum surface settlement based classification of shallow tunnels in soft ground. Tunnelling Underground Space Technology, 49, 320-327.

Dixon, W. J. (1950). Analysis of extreme values. The Annals of Mathematical Statistics, 21(4), 488-506.

Doerffel, K. (1967). Die statistische Auswertung von Analysenergebnissen (Vol. 2). Springer.

Dovoedo, Y., & Chakraborti, S. (2015). Boxplot-based outlier detection for the location-scale family. Communications in statistics-simulation and computation, 44(6), 1492-1513.

Duchnowski, R. (2010). Median-based estimates and their application in controlling reference mark stability. Journal of surveying engineering, 136(2), 47-52.

Fanjie, Y., Hui, Z., Haibin, X., Azhar, M. U., Yong, Z., & Fudong, C. (2022). Numerical simulation method for the process of rockburst. Engineering Geology, 306, 106760.

Feng, X.-T. (2017). Rockburst: mechanisms, monitoring, warning, and mitigation. Butterworth-Heinemann.

Fossen, H. (2016). Structural geology. Cambridge university press.

Garces, D., Rebolledo, H., & Miranda, P. (2020). Incorporating vulnerability of hang-ups and secondary breaking to drawpoints availability for short-term cave plans, El Teniente mine. MassMin 2020: Proceedings of the Eighth International Conference & Exhibition on Mass Mining,

García, A., Castro-Fresno, D., Polanco, J., & Thomas, C. (2012). Abrasive wear evolution in concrete pavements. Road Materials and Pavement Design, 13(3), 534-548.

Gercek, H. (2007). Poisson's ratio values for rocks. International Journal of Rock Mechanics and Mining Sciences, 44(1), 1-13.

Ghosh, D., & Vogt, A. (2012). Outliers: An evaluation of methodologies. Joint statistical meetings,

Gignac, G. (2019). How2statsbook (online edition 1). http://www.how2statsbook.com/

Gignac, G. E. (2019). How2statsbook - Online digital book, Chapter 2 "Descriptive Statistics" (1st ed.). http://www.how2statsbook.com/

Gill, D. E., Corthésy, R., & Leite, M. H. (2005). Determining the minimal number of specimens for laboratory testing of rock properties. Engineering Geology, 78(1-2), 29-51.

Goktan, R., & Ayday, C. (1993). A suggested improvement to the Schmidt rebound hardness ISRM suggested method with particular reference to rock machineability. International Journal of Rock Mechanics and Mining Sciences, 30(3).

Goktan, R., & Gunes, N. (2005). A comparative study of Schmidt hammer testing procedures with reference to rock cutting machine performance prediction. International Journal of Rock Mechanics and Mining Sciences, 42(3), 466-472.

Golder. (2012). Review of In-situ stress measurements at Niobec Mine: Project 002-11-1221-0087 MTA Rev0.

Gong, F., Dai, J., & Xu, L. (2023). A strength-stress coupling criterion for rockburst: Inspirations from 1114 rockburst cases in 197 underground rock projects. Tunnelling and Underground Space Technology, 142, 105396.

Grubbs, F. E. (1950). Sample Criteria for Testing Outlying Observations. The Annals of Mathematical Statistics, 21(1), 27-58, 32. https://doi.org/10.1214/aoms/1177729885

Gul, M., Kotak, Y., Muneer, T., & Ivanova, S. (2018). Enhancement of albedo for solar energy gain with particular emphasis on overcast skies. Energies, 11(11), 2881.

Gumbel, E. (1958). Statistics of Extremes. Columbia University Press.

Hadi, A. S., Imon, A. R., & Werner, M. (2009). Detection of outliers. Wiley Interdisciplinary Reviews: Computational Statistics, 1(1), 57-70.

Hammoum, S. (2017). Modélisation numérique du comportement mécanique d'une excavation à grande profondeur à l'aide d'une loi d'écrouissage tenant compte des effets du temps-application à la mine Westwood (In French). Ecole Polytechnique, Montreal (Canada).

Han, L., Wang, L., & Zhang, W. (2020). Quantification of statistical uncertainties of rock strength parameters using Bayesian-based Markov Chain Monte Carlo method. IOP Conference Series: Earth and Environmental Science,

Hassanpour, J., Rostami, J., Khamehchiyan, M., Bruland, A., & Tavakoli, H. (2010). TBM performance analysis in pyroclastic rocks: a case history of Karaj water conveyance tunnel. Rock Mech Rock Eng, 43(4), 427-445.

Hawkes, I. (1966). Significance of in-situ stress levels. Proc. 1st Intl. Cong. Intl. Soc. of Rock Mech, 3, 445-463.

He, M., Cheng, T., Qiao, Y., & Li, H. (2023). A review of rockburst: Experiments, theories, and simulations. Journal of Rock Mechanics and Geotechnical Engineering, 15(5), 1312-1353.

He, S., Song, D., He, X., Li, Z., Chen, T., Shen, F., Chen, J., & Mitri, H. (2023). Numerical modelling of rockburst mechanism in a steeply dipping coal seam. Bulletin of Engineering Geology and the Environment, 82(7), 261.

Hedley, D. G. (1992). Rockburst handbook for Ontario hardrock mines. (No Title).

Heidarzadeh, S., Saeidi, A., Lavoie, C., & Rouleau, A. (2021a). Geomechanical characterization of a heterogenous rock mass using geological and laboratory test results: a case study of the Niobec Mine, Quebec (Canada). SN Applied Sciences, 3, 1-20.

Heidarzadeh, S., Saeidi, A., Lavoie, C., & Rouleau, A. (2021b). Geomechanical characterization of a heterogenous rock mass using geological and laboratory test results: a case study of the Niobec Mine, Quebec (Canada). SN Applied Sciences, 3(6), 1-20.

Herget, G. (1973a). First experiences with the CSIR triaxial strain cell for stress determinations. International Journal of Rock Mechanics and Mining Sciences & Geomechanics Abstracts,

Herget, G. (1973b). First experiences with the CSIR triaxial strain cell for stress determinations. International Journal of Rock Mechanics and Mining Sciences & Geomechanics Abstracts, 10(6), 509-522.

Herget, G. (1973c). Variation of rock stresses with depth at a Canadian iron mine. International Journal of Rock Mechanics and Mining Sciences & Geomechanics Abstracts, 10(1), 37-51. https://doi.org/https://doi.org/10.1016/0148-9062(73)90058-2

Herget, G. (1980). Regional stresses in the Canadian Shield. 13th Canadian Rock Mechanics Symposium, The Canadian Institute of Mining and Metallurgy,

Herget, G. (1982). High Stress Occurrences In The Canadian Shield. The 23rd U.S Symposium on Rock Mechanics (USRMS),

Herget, G. (1987). Stress assumptions for underground excavations in the Canadian Shield. International Journal of Rock Mechanics and Mining Sciences & Geomechanics Abstracts,

Herget, G., & Arjang, B. (1990). Update on ground stresses in the Canadian Shield. Proc. Stresses in Underground Structures, Ottawa (Eds. Herget G, Arjang B, Bétournay M, Gyenge M, Vongpaisal S, Yu Y), 33-47.

Hoaglin, D. C., & Iglewicz, B. (1987). Fine-Tuning Some Resistant Rules for Outlier Labeling. Journal of the American Statistical Association, 82(400), 1147-1149. https://doi.org/10.2307/2289392

Hoek, E. (2007). Practical Rock Engineering. Rocscience. https://www.rocscience.com/assets/resources/learning/hoek/Practical-Rock-Engineering-Full-Text.pdf

Hoek, E., & Brown, E. (2019). The Hoek–Brown failure criterion and GSI–2018 edition. Journal of Rock Mechanics and Geotechnical Engineering, 11(3), 445-463.

Hopgood, A. M. (1987). Imbricate structure. In Structural Geology and Tectonics (pp. 334-336). Springer Berlin Heidelberg. https://doi.org/10.1007/3-540-31080-0_50

Hubert, M., & Vandervieren, E. (2008). An adjusted boxplot for skewed distributions. Computational statistics & data analysis, 52(12), 5186-5201. https://doi.org/https://doi.org/10.1016/j.csda.2007.11.008

Hunt, R. E. (2005). Geotechnical engineering investigation handbook. Crc Press.

Hussain, I., & Uddin, M. (2019). Functional and multivariate hydrological data visualization and outlier detection of Sukkur Barrage. International Journal of Computer Applications, 178(28), 20-29.

IAMGOLD. (2019a). IAMGOLD Corporation - Exploitations - The Westwood Gold Mine. http://www.iamgold.com/French/exploitations/mines-en-exploitation/projet-westwood-canada/default.aspx

IAMGOLD. (2019b). IAMGOLD Corporation- Exploitations- the Westwood Gold Mine. http://www.iamgold.com/French/exploitations/mines-en-exploitation/projet

westwood-canada/default.aspx

Iglewicz, B., & Hoaglin, D. C. (1993). How to detect and handle outliers (Vol. 16). Asq Press.

JMP-Pro. (2021). JMP Pro. V.17 Software. In SAS Institute Inc.

Kaiser, P. (2019). From common to best practices in underground rock engineering. ISRM Congress,

Kaiser, P., Maloney, S., & Yong, S. (2016). Role of large scale heterogeneities on in-situ stress and induced stress fields. ARMA US Rock Mechanics/Geomechanics Symposium,

Kaiser, P. K., & Cai, M. (2012). Design of rock support system under rockburst condition. Journal of Rock Mechanics and Geotechnical Engineering, 4(3), 215-227. https://doi.org/https://doi.org/10.3724/SP.J.1235.2012.00215

Kalenchuk, K., Mercer, R., & Williams, E. (2017). Large-magnitude seismicity at the Westwood mine, Quebec, Canada. Deep Mining 2017: Proceedings of the Eighth International Conference on Deep and High Stress Mining,

Kamari, A., Khaksar-Manshad, A., Gharagheizi, F., Mohammadi, A. H., & Ashoori, S. (2013). Robust model for the determination of wax deposition in oil systems. Industrial & Engineering Chemistry Research, 52(44), 15664-15672.

Kannan, K. S., Manoj, K., & Arumugam, S. (2015). Labeling methods for identifying outliers. International Journal of Statistics and Systems, 10(2), 231-238.

Khanlari, G.-R., Heidari, M., Sepahigero, A.-A., & Fereidooni, D. (2014). Quantification of strength anisotropy of metamorphic rocks of the Hamedan province, Iran, as determined from

cylindrical punch, point load and Brazilian tests. Engineering Geology, 169, 80-90. https://doi.org/https://doi.org/10.1016/j.enggeo.2013.11.014

Kim, H.-S., Kim, H.-K., Shin, S.-Y., & Chung, C.-K. (2012). Application of statistical geo-spatial information technology to soil stratification in the Seoul metropolitan area. Georisk: Assessment and Management of Risk for Engineered Systems and Geohazards, 6(4), 221-228.

Kim, H.-S., Sun, C.-G., Lee, M.-G., & Cho, H.-I. (2021). Multivariate geotechnical zonation of seismic site effects with clustering-blended model for a city area, South Korea. Engineering Geology, 294, 106365.

Kimber, A. (1990). Exploratory data analysis for possibly censored data from skewed distributions. Journal of the Royal Statistical Society Series C: Applied Statistics, 39(1), 21-30.

Koca, M. Y., & Kıncal, C. (2022). A new approach to the anisotropy classification based on curve length measurement method: a case study in Ürkmez dam site-İzmir, Türkiye. Arabian Journal of Geosciences, 15(17), 1-26.

Kor, K., Ertekin, S., Yamanlar, S., & Altun, G. (2021). Penetration rate prediction in heterogeneous formations: A geomechanical approach through machine learning. Journal of Petroleum Science and Engineering, 207, 109138.

Kottegoda, N. T., & Rosso, R. (2008). Applied statistics for civil and environmental engineers.

Kouame Arthur Joseph, K., Fuxing, J., Sitao, Z., & Yu, F. (2017). OVERVIEW OF ROCK BURST RESEARCH IN CHINA AND ITS APPLICATION IN IVORY COAST. GEOMATE Journal, 12(29), 204-211. https://geomatejournal.com/geomate/article/view/916

Kwak, S. K., & Kim, J. H. (2017). Statistical data preparation: management of missing values and outliers. Korean journal of anesthesiology, 70(4), 407-411.

Labat, G., Gervais, F., Kavanagh-Lepage, C., Jannin, S., & Crowley, J. L. (2020). Ductile nappe extrusion in constrictive strain at the origin of transverse segments of the Allochthon Boundary Thrust in the Manicouagan Imbricate Zone (Central Grenville Province, Québec). Journal of Structural Geology, 138, 104117.

Lach, S. (2018). The application of selected statistical tests in the detection and removal of outliers in water engineering data based on the example of piezometric measurements at the Dobczyce dam over the period 2012-2016. E3S Web of Conferences,

Lalancette, S. (2018). Dimensionnement des chantiers remblayés de la mine Niobec en utilisant la modélisation 3D Université du Québec à Chicoutimi].

Lehmann, R. (2015). Observation error model selection by information criteria vs. normality testing. Studia Geophysica et Geodaetica, 59(4), 489-504. https://doi.org/10.1007/s11200-015-0725-0

Li, D., Liu, Z., Armaghani, D. J., Xiao, P., & Zhou, J. (2022). Novel ensemble tree solution for rockburst prediction using deep forest. Mathematics, 10(5), 787.

Li, S., Wang, Y., & Xie, X. (2021). Prediction of Uniaxial Compression Strength of Limestone Based on the Point Load Strength and SVM Model. Minerals, 11(12), 1387.

Li, X. (2014). Rock dynamics fundamentals and applications. Science, Beijing.

Liang, W., Sari, A., Zhao, G., McKinnon, S. D., & Wu, H. (2020). Short-term rockburst risk prediction using ensemble learning methods. Natural Hazards, 104(2), 1923-1946.

Liang, W., Zhao, G., Wu, H., & Dai, B. (2019). Risk assessment of rockburst via an extended MABAC method under fuzzy environment. Tunnelling and Underground Space Technology, 83, 533-544.

Limb, B. J., Work, D. G., Hodson, J., & Smith, B. L. (2017). The Inefficacy of Chauvenet's Criterion for Elimination of Data Points. Journal of Fluids Engineering, 139(5).

Lin, S., Zheng, H., Han, C., Han, B., & Li, W. (2021). Evaluation and prediction of slope stability using machine learning approaches. Frontiers of Structural and Civil Engineering, 15(4), 821-833.

Liu, X., & Wang, E. (2018). Study on characteristics of EMR signals induced from fracture of rock samples and their application in rockburst prediction in copper mine. Journal of Geophysics and Engineering, 15(3), 909-920.

Lu, H., Li, H., & Meng, X. (2022). Spatial Variability of the Mechanical Parameters of High-Water-Content Soil Based on a Dual-Bridge CPT Test. Water, 14(3), 343. https://www.mdpi.com/2073-4441/14/3/343

Lucas, S. B., & St-Onge, M. (1998). Geology of the precambrian Superior and Grenville Provinces and precambian fossils in North America. Geological Society of America.

Ludden, J., Hubert, C., & Gariépy, C. (1986). The tectonic evolution of the Abitibi greenstone belt of Canada. Geological Magazine, 123(2), 153-166.

Ma, T.-H., Tang, C.-A., Tang, S.-B., Kuang, L., Yu, Q., Kong, D.-Q., & Zhu, X. (2018). Rockburst mechanism and prediction based on microseismic monitoring. International Journal of Rock Mechanics and Mining Sciences, 110, 177-188.

Madritsch, H., Schmid, S. M., & Fabbri, O. (2008). Interactions between thin- and thick-skinned tectonics at the northwestern front of the Jura fold-and-thrust belt (eastern France). Tectonics, 27(5). https://doi.org/https://doi.org/10.1029/2008TC002282

Maloney, S., Kaiser, P., & Vorauer, A. (2006). A re-assessment of in situ stresses in the Canadian Shield. ARMA US Rock Mechanics/Geomechanics Symposium,

Manouchehrian, A., & Cai, M. (2018). Numerical modeling of rockburst near fault zones in deep tunnels. Tunnelling and Underground Space Technology, 80, 164-180. https://doi.org/https://doi.org/10.1016/j.tust.2018.06.015

Manouchehrian, A., Gholamnejad, J., & Sharifzadeh, M. (2014). Development of a model for analysis of slope stability for circular mode failure using genetic algorithm. Environmental Earth Sciences, 71, 1267-1277.

Manouchehrian, A., Sharifzadeh, M., & Moghadam, R. H. (2012). Application of artificial neural networks and multivariate statistics to estimate UCS using textural characteristics. Int J Min Sci Technol, 22(2), 229-236. https://doi.org/https://doi.org/10.1016/j.ijmst.2011.08.013

Martin, C. (1990). Characterizing in situ stress domains at the AECL Underground Research Laboratory. Canadian Geotechnical Journal, 27(5), 631-646.

Martin, C. D., Kaiser, P. K., & Christiansson, R. (2003). Stress, instability and design of underground excavations. International Journal of Rock Mechanics and Mining Sciences, 40(7), 1027-1047. https://doi.org/https://doi.org/10.1016/S1365-1609(03)00110-2

MATLAB R2022a. In. (2022). MathWorks.

Mazaira, A., & Konicek, P. (2015). Intense rockburst impacts in deep underground construction and their prevention. Canadian Geotechnical Journal, 52(10), 1426-1439. https://doi.org/10.1139/cgj-2014-0359

Mazraehli, M., & Zare, S. (2020). An application of uncertainty analysis to rock mass properties characterization at porphyry copper mines. Bulletin of Engineering Geology and the Environment, 79(7), 3721-3739.

Meng, F., Wong, L. N. Y., & Zhou, H. (2021). Rock brittleness indices and their applications to different fields of rock engineering: A review. Journal of Rock Mechanics and Geotechnical Engineering, 13(1), 221-247.

Minitab. In. (2021). (Version 20.3) Minitab, LLC. . https://www.minitab.com/

Miranda, E. E. (1972). Deformation and fracture of concrete under uniaxial impact loading.

Misra, S., Chakravarty, A., Bhoumick, P., & Rai, C. S. (2019). Unsupervised clustering methods for noninvasive characterization of fracture-induced geomechanical alterations. Machine Learning for Subsurface Characterization, 39.

Mitchell, F. (2007). Structural analysis of brittle deformation features along Grenvillian shear zones in southeastern Ontario

Mohammadi, Y., & Kaushik, S. (2005). Flexural fatigue-life distributions of plain and fibrous concrete at various stress levels. Journal Of Materials in civil engineering, 17(6), 650-658.

Monteiro, D. D., Duque, M. M., Chaves, G. S., Ferreira Filho, V. M., & Baioco, J. S. (2020). Using data analytics to quantify the impact of production test uncertainty on oil flow rate forecast. Oil & Gas Science and Technology–Revue d'IFP Energies nouvelles, 75, 7.

Muscolino, G., Genovese, F., & Sofi, A. (2022). Reliability bounds for structural systems subjected to a set of recorded accelerograms leading to imprecise seismic power spectrum. ASCE-ASME Journal of Risk and Uncertainty in Engineering Systems, Part A: Civil Engineering, 8(2), 04022009.

Naji, A. M., Rehman, H., Emad, M. Z., & Yoo, H. (2018). Impact of shear zone on rockburst in the deep neelum-jehlum hydropower tunnel: A numerical modeling approach. Energies, 11(8), 1935.

Nazareth, A. F. D. V., & Lana, M. S. (2021). A methodology for the definition of geotechnical mine sectors based on multivariate cluster analysis. Geotechnical and Geological Engineering, 39, 4405-4426.

Olewuezi, N. (2011). Note on the comparison of some outlier labeling techniques. Journal of Mathematics and Statistics, 7(4), 353-355.

Owusu-Ansah, D., Tinoco, J., Lohrasb, F., Martins, F., & Matos, J. (2023). A decision tree for rockburst conditions prediction. Applied Sciences, 13(11), 6655.

Pan, J., Bai, Z., Cao, Y., Zhou, W., & Wang, J. (2017). Influence of soil physical properties and vegetation coverage at different slope aspects in a reclaimed dump. Environmental Science and Pollution Research, 24, 23953-23965.

Panabaker, H. (2006). Geological Provinces of the Canadian Shield. The Canadian Encyclopedia. https://www.thecanadianencyclopedia.ca/en/article/shield

Peirce, B. (1852). Criterion for the rejection of doubtful observations. The Astronomical Journal, 2, 161-163.

Peng, S., & Zhang, J. (2007). Rock properties and mechanical behaviors. In Engineering Geology for Underground Rocks (pp. 1-26). Springer Berlin Heidelberg. https://doi.org/10.1007/978-3-540-73295-2_1

Pepe, G., Cevasco, A., Gaggero, L., & Berardi, R. (2017). Variability of intact rock mechanical properties for some metamorphic rock types and its implications on the number of test specimens. Bulletin of Engineering Geology and the Environment, 76(2), 629-644.

Percival, J. A., & Easton, R. M. (2007). Geology of the Canadian Shield in Ontario: an update; Ontario Geological Survey, Open File Report 6196.

Percival, J. A., McNicoll, V., Brown, J. L., & Whalen, J. B. (2004). Convergent margin tectonics, central Wabigoon subprovince, Superior Province, Canada. Precambrian research, 132(3), 213-244. https://doi.org/https://doi.org/10.1016/j.precamres.2003.12.016

Percival, J. A., Sanborn-Barrie, M., Skulski, T., Stott, G., Helmstaedt, H., & White, D. (2006). Tectonic evolution of the western Superior Province from NATMAP and Lithoprobe studies. Canadian Journal of Earth Sciences, 43(7), 1085-1117.

Percival, J. A., Skulski, T., Sanborn-Barrie, M., Stott, G., Leclair, A., Corkery, T., & Boily, M. (2012). Geology and tectonic evolution of the Superior Province, Canada; Chapter 6 In Tectonic Styles in Canada: The Lithoprobe Perspective. Geological Association of Canada.

Pereira, M. L., F da Silva, P., Fernandes, I., & Chastre, C. (2021). Characterization and correlation of engineering properties of basalts. Bulletin of Engineering Geology and the Environment, 80(4), 2889-2910.

Pereira, M. L., F. da Silva, P., Fernandes, I., & Chastre, C. (2021). Characterization and correlation of engineering properties of basalts. Bulletin of Engineering Geology and the Environment, 80(4), 2889-2910. https://doi.org/10.1007/s10064-021-02107-7

Perras, M. A., & Diederichs, M. S. (2014). A review of the tensile strength of rock: concepts and testing. Geotechnical and Geological Engineering, 32, 525-546.

Petrone, P., Allocca, V., Fusco, F., Incontri, P., & De Vita, P. (2023). Engineering geological 3D modeling and geotechnical characterization in the framework of technical rules for geotechnical design: the case study of the Nola's logistic plant (southern Italy). Bulletin of Engineering Geology and the Environment, 82(1), 12.

Pfiffner, O. A. (2017). Thick-Skinned and Thin-Skinned Tectonics: A Global Perspective. Geosciences, 7(3), 71. https://www.mdpi.com/2076-3263/7/3/71

Poblet, J., & Lisle, R. J. (2011). Kinematic evolution and structural styles of fold-and-thrust belts. Geological Society, London, Special Publications, 349(1), 1-24. https://doi.org/doi:10.1144/SP349.1

Retamales, R., Davies, R., Mosqueda, G., & Filiatrault, A. (2013). Experimental seismic fragility of cold-formed steel framed gypsum partition walls. Journal of Structural Engineering, 139(8), 1285-1293.

@Risk. In. (2022). Palisade Corporation https://www.palisade.com/risk/.

Roberts, D. G., & Bally, A. W. (2012). Regional Geology and Tectonics: Principles of Geologic Analysis. Elsevier. https://doi.org/https://doi.org/10.1016/B978-0-444-53042-4.00070-4

Rochim, A. F. R. F. (2021). Chauvenet's Criterion, Peirce's Criterion, and Thompson's Criterion (Literatures Review). In.

Rocscience. (2022). RS2. In (Version 11)

Rojas Perez, C., Wei, W., Gilvesy, A., Borysenko, F.-J., & Mitri, H. S. (2024). Rockburst assessment and control: a case study of a deep sill pillar recovery. Deep Mining 2024: Proceedings of the 10th International Conference on Deep and High Stress Mining,

Romão, X., & Vasanelli, E. (2021). Identification and Processing of Outliers. In Non-Destructive In Situ Strength Assessment of Concrete: Practical Application of the RILEM TC 249-ISC Recommendations (pp. 161-180). Springer.

Ross, S. M. (2003). Peirce's criterion for the elimination of suspect experimental data. Journal of engineering technology, 20(2), 38-41.

Rousell, D. H., & Brown, G. H. E. (2009). A Field Guide to the Geology of Sudbury, Ontario.

Roy, J., Eberhardt, E., Bewick, R., & Campbell, R. (2023). Application of Data Analysis Techniques to Identify Rockburst Mechanisms, Triggers, and Contributing Factors in Cave Mining. Rock Mechanics and Rock Engineering, 1-36.

Russenes, B. (1974). Analysis of rock spalling for tunnels in steep valley sides. Norwegian Institute of Technology.

Saeidi, A., Heidarzadeh, S., Lalancette, S., & Rouleau, A. (2021). The effects of in situ stress uncertainties on the assessment of open stope stability: case study at the Niobec Mine, Quebec (Canada). Geomechanics for Energy and the Environment, 25, 100194.

Saeidi, M., Eftekhari, A., & Taromi, M. (2012). Evaluation of rock burst potential in Sabzkuh water conveyance tunnel, IRAN: a case study. ISRM International Symposium-Asian Rock Mechanics Symposium,

Saeidi, O., Vaneghi, R. G., Rasouli, V., & Gholami, R. (2013). A modified empirical criterion for strength of transversely anisotropic rocks with metamorphic origin. Bulletin of Engineering Geology and the Environment, 72(2), 257-269. https://doi.org/10.1007/s10064-013-0472-9

Sainoki, A., & Mitri, H. S. (2014a). Dynamic behaviour of mining-induced fault slip. International Journal of Rock Mechanics and Mining Sciences, 66, 19-29. https://doi.org/https://doi.org/10.1016/j.ijrmms.2013.12.003

Sainoki, A., & Mitri, H. S. (2014b). Dynamic modelling of fault-slip with Barton's shear strength model. International Journal of Rock Mechanics and Mining Sciences, 67, 155-163. https://doi.org/https://doi.org/10.1016/j.ijrmms.2013.12.023

Sainsbury, B.-A. (2020). Impact of intact rock properties on proneness to rockbursting. Bulletin of Engineering Geology and the Environment, 79(4), 1939-1946.

Salamon, M. (1964). Elastic analysis of displacements and stresses induced by the mining of seam or reef deposits: Part II: Practical methods of determining displacement, strain and stress components from a given mining geometry. Journal of the Southern African Institute of Mining and Metallurgy, 64(6), 197-218.

Saleem, S., Aslam, M., & Shaukat, M. R. (2021). A review and empirical comparison of univariate outlier detection methods. Pakistan Journal of Statistics, 37(4).

Sanou, A.-G., Saeidi, A., Heidarzadeh, S., Chavali, R. V. P., Samti, H. E., & Rouleau, A. (2022). Geotechnical Parameters of Landslide-Prone Laflamme Sea Deposits, Canada: Uncertainties and Correlations. Geosciences, 12(8), 297.

Schwertman, N. C., & de Silva, R. (2007). Identifying outliers with sequential fences. Computational statistics & data analysis, 51(8), 3800-3810.

Seo, S. (2006). A review and comparison of methods for detecting outliers in univariate data sets University of Pittsburgh].

Shao, Z., Armaghani, D. J., Bejarbaneh, B. Y., Mu'azu, M., & Mohamad, E. T. (2019). Estimating the friction angle of black shale core specimens with hybrid-ANN approaches. Measurement, 145, 744-755.

Shaygan, K., & Jamshidi, S. (2023). Prediction of rate of penetration in directional drilling using data mining techniques. Geoenergy Science and Engineering, 221, 111293.

Shirani Faradonbeh, R., Shaffiee Haghshenas, S., Taheri, A., & Mikaeil, R. (2020). Application of self-organizing map and fuzzy c-mean techniques for rockburst clustering in deep underground projects. Neural Computing and Applications, 32, 8545-8559.

Shirani Faradonbeh, R., Taheri, A., & Karakus, M. (2022). The propensity of the over-stressed rock masses to different failure mechanisms based on a hybrid probabilistic approach. Tunnelling and Underground Space Technology, 119, 104214. https://doi.org/https://doi.org/10.1016/j.tust.2021.104214

Shnorhokian, S., Mitri, H. S., & Moreau-Verlaan, L. (2015). Stability assessment of stope sequence scenarios in a diminishing ore pillar. International Journal of Rock Mechanics and Mining Sciences, 74, 103-118.

Solak, T. (2009). Ground behavior evaluation for tunnels in blocky rock masses. Tunnelling and Underground Space Technology, 24(3), 323-330.

Sonmez, H., Gokceoglu, C., & Ulusay, R. (2004). Indirect determination of the modulus of deformation of rock masses based on the GSI system. International Journal of Rock Mechanics and Mining Sciences, 41(5), 849-857. https://doi.org/https://doi.org/10.1016/j.ijrmms.2003.01.006

SOUFI, A., BAHI, L., & OUADIF, L. (2018). Adjusted Anisotropic Strength Model for Mea-Siltstones and Prediction of UCS from Indirect Tensile Test. International Journal of Civil Engineering and Technology.

Spiegel, M. R. (1966). Theory and problems of statistics.

SPSS. (2022). IBM Corp. IBM SPSS Statistics for Windows. In (Version 28)

Stone, D. (2010). Precambrian geology of the central Wabigoon Subprovince area, northwestern Ontario. Ontario Geological Survey.

Sun, J.-s., Zhu, Q.-h., & Lu, W.-b. (2007). Numerical Simulation of Rock Burst in Circular Tunnels Under Unloading Conditions. Journal of China University of Mining and Technology, 17(4), 552-556. https://doi.org/https://doi.org/10.1016/S1006-1266(07)60144-8

Taherynia, M. H., Fatemi Aghda, S. M., & Fahimifar, A. (2016). In-situ stress state and tectonic regime in different depths of earth crust. Geotechnical and Geological Engineering, 34, 679-687.

Tao, Z.-Y. (1988). Support design of tunnels subjected to rockbursting. ISRM International Symposium,

Tiryaki, B. (2008). Predicting intact rock strength for mechanical excavation using multivariate statistics, artificial neural networks, and regression trees. Engineering Geology, 99(1), 51-60. https://doi.org/https://doi.org/10.1016/j.enggeo.2008.02.003

Tomaszewski, D., Rapiński, J., Stolecki, L., & Śmieja, M. (2022). Switching Edge Detector as a tool for seismic events detection based on GNSS timeseries. Archives of Mining Sciences, 317-332-317-332.

Tóth, Z., McNicoll, V., Lafrance, B., & Dubé, B. (2022). Early depositional and magmatic history of the Beardmore-Geraldton Belt: Formation of a transitional accretionary belt along the Wabigoon-Quetico Subprovince boundary in the Archean Superior Craton, Canada. Precambrian research, 371, 106579. https://doi.org/https://doi.org/10.1016/j.precamres.2022.106579

Tremblay, K. (2020). Determination of geological and geomechanical parameters intensifying the risk of landslides near the Bousquet Fault at the Westwood mine, MSc. Thesis (in French) Université du Québec à Chicoutimi].

Tukey, J. W. (1977). Exploratory data analysis. Addison-Wesley. http://catalogue.bnf.fr/ark:/12148/cb37362350z

van Gool, J. A. M., Kriegsman, L. M., Marker, M., & Nichols, G. T. (1999). Thrust stacking in the inner Nordre Strømfjord area, West Greenland: Significance for the tectonic evolution of the Palaeoproterozoic Nagssugtoqidian orogen. Precambrian research, 93(1), 71-86. https://doi.org/https://doi.org/10.1016/S0301-9268(98)00098-9

Verma, S. P., Quiroz-Ruiz, A., & Díaz-González, L. (2008a). A1-A41: Critical values and standard errors of the mean for 33 test variants. A42-A60: Interpolation equations for outlier tests for 100≤ n≤ 1000. A61-A64: Application data compiled for the comparison of multiple-test method with box-and-whisker plot and 2s methods. Revista mexicana de ciencias geológicas, 25(1), 82-96.

Verma, S. P., Quiroz-Ruiz, A., & Díaz-González, L. (2008b). Critical values for 33 discordancy test variants for outliers in normal samples up to sizes 1000, and applications in quality control in Earth Sciences. Revista mexicana de ciencias geológicas, 25(1), 82-96.

Wah, W. S. L., Owen, J. S., Chen, Y.-T., Elamin, A., & Roberts, G. W. (2019). Removal of masking effect for damage detection of structures. Engineering Structures, 183, 646-661.

Walker, M. L., Dovoedo, Y. H., Chakraborti, S., & Hilton, C. W. (2018). An Improved Boxplot for Univariate Data. The American Statistician, 72(4), 348-353. https://doi.org/10.1080/00031305.2018.1448891

Wang, J.-A., & Park, H. (2001). Comprehensive prediction of rockburst based on analysis of strain energy in rocks. Tunnelling and Underground Space Technology, 16(1), 49-57.

Wang, J., Apel, D. B., Pu, Y., Hall, R., Wei, C., & Sepehri, M. (2021). Numerical modeling for rockbursts: A state-of-the-art review. Journal of Rock Mechanics and Geotechnical Engineering, 13(2), 457-478. https://doi.org/https://doi.org/10.1016/j.jrmge.2020.09.011

Wang, J., Apel, D. B., Xu, H., & Wei, C. (2022). Evaluation of the performance of yielding rockbolts during rockbursts using numerical modeling method. International Journal of Coal Science & Technology, 9(1), 87.

Wang, Z., Qi, C., Ban, L., Yu, H., Wang, H., & Fu, Z. (2022). Modified Hoek–Brown failure criterion for anisotropic intact rock under high confining pressures. Bulletin of Engineering Geology and the Environment, 81(8), 333. https://doi.org/10.1007/s10064-022-02831-8

Wei, F. (2013). Gross error elimination and index determination of shearing strength parameters in triaxial test. Applied Mechanics and Materials,

Xue, Y., Bai, C., Qiu, D., Kong, F., & Li, Z. (2020). Predicting rockburst with database using particle swarm optimization and extreme learning machine. Tunnelling and Underground Space Technology, 98, 103287.

Yan, T., Shen, S.-L., & Zhou, A. (2023). Identification of geological characteristics from construction parameters during shield tunnelling. Acta Geotechnica, 18(1), 535-551.

Yang, H., Song, K., & Zhou, J. (2022). Automated recognition model of geomechanical information based on operational data of tunneling boring machines. Rock Mechanics and Rock Engineering, 1-18.

Yang, M., Wang, R., Li, M., & Liao, M. (2022). A PSI targets characterization approach to interpreting surface displacement signals: A case study of the Shanghai metro tunnels. Remote Sensing of Environment, 280, 113150.

Yazdanpanah, M., Xu, C., & Sharifzadeh, M. (2022). A new statistical method to segment photogrammetry data in order to obtain geological information. International Journal of Rock Mechanics and Mining Sciences, 150, 105008.

Yergeau, D. (2015). Geology of the atypical Westwood synvolcanic gold deposit, Abitibi, Quebec., PhD thesis (in French) Université du Québec, Institut national de la recherche scientifique (INRS)].

Yong, S., & Maloney, S. (2015). An update to the Canadian Shield stress database. Number September.

Yu, S., Zhang, Z., Wang, S., Huang, X., & Lei, Q. (2023). A performance-based hybrid deep learning model for predicting TBM advance rate using attention-ResNet-LSTM. Journal of Rock Mechanics and Geotechnical Engineering.

Yu, Y., & Xu, J. (2021). Multi-stage perforation and hydraulic fracture stage selection based on machine learning methods. Journal of Physics: Conference Series,

Zhang, C., Feng, X.-T., & Zhou, H. (2012). Estimation of in situ stress along deep tunnels buried in complex geological conditions. International Journal of Rock Mechanics and Mining Sciences, 52, 139-162.

Zhang, J. (2008). Rockburst and its criteria and control. Chin. J. Rock Mech. Eng., 27, 2034.

Zhang, L. (2016). Engineering properties of rocks. Butterworth-Heinemann.

Zhang, Q., Liu, C., Guo, S., Wang, W., & Luo, H. (2022). Evaluation of rock burst intensity of cloud model based on CRITIC method and order relation analysis method.

Zhang, X.-P., Wong, L. N. Y., Wang, S.-J., & Han, G.-Y. (2011). Engineering properties of quartz mica schist. Engineering Geology, 121(3), 135-149. https://doi.org/https://doi.org/10.1016/j.enggeo.2011.04.020

Zhao, X., Wang, J., Cai, M., Ma, L., Zong, Z., Wang, X., Su, R., Chen, W., Zhao, H., & Chen, Q. (2013). In-situ stress measurements and regional stress field assessment of the Beishan area, China. Engineering Geology, 163, 26-40.

Zheng, S., Zhu, Y.-X., Li, D.-Q., Cao, Z.-J., Deng, Q.-X., & Phoon, K.-K. (2021). Probabilistic outlier detection for sparse multivariate geotechnical site investigation data using Bayesian learning. Geoscience Frontiers, 12(1), 425-439.

Zhou, J., Li, E., Yang, S., Wang, M., Shi, X., Yao, S., & Mitri, H. S. (2019). Slope stability prediction for circular mode failure using gradient boosting machine approach based on an updated database of case histories. Safety Science, 118, 505-518.

Zhou, J., Li, X., & Mitri Hani, S. (2016). Classification of Rockburst in Underground Projects: Comparison of Ten Supervised Learning Methods. Journal of Computing in Civil Engineering, 30(5), 04016003. https://doi.org/10.1061/(ASCE)CP.1943-5487.0000553

Zhou, J., Li, X., & Mitri, H. S. (2016). Classification of rockburst in underground projects: comparison of ten supervised learning methods. Journal of Computing in Civil Engineering, 30(5), 04016003.

Zhou, J., Li, X., & Mitri, H. S. (2018). Evaluation method of rockburst: State-of-the-art literature review. Tunnelling and Underground Space Technology, 81, 632-659. https://doi.org/https://doi.org/10.1016/j.tust.2018.08.029

Zhou, J., Li, X., & Shi, X. (2012). Long-term prediction model of rockburst in underground openings using heuristic algorithms and support vector machines. Safety science, 50(4), 629-644.

Zolnai, A., Price, R., & Helmstaedt, H. (1984). Regional cross section of the Southern Province adjacent to Lake Huron, Ontario: implications for the tectonic significance of the Murray Fault Zone. Canadian Journal of Earth Sciences, 21(4), 447-456.

Zubelewicz, A., & Mroz, Z. (1983). Numerical simulation of rock burst processes treated as problems of dynamic instability. Rock Mechanics and Rock Engineering, 16(4), 253-274.

APPENDIX

A Proper Methodology to Characterize the Associated Variability of UCS Data for the Metamorphic Rocks Based on Outlier Detection Methods

Behzad Dastjerdy[1], Ali Saeidi[2], Shahriyar Heidarzadeh[3]

[1]Department of applied sciences, University of Quebec at Chicoutimi (UQAC), G7H 2B1, Chicoutimi (QC), Canada, 555 Blvd. de l'Université, Behzad.dastjerdy2@uqac.ca

[2]Department of applied sciences, University of Quebec at Chicoutimi (UQAC), G7H 2B1, Chicoutimi (QC), Canada, 555 Blvd. de l'Université, Ali_saeidi@uqac.ca

[3]SNC-Lavalin Group Inc., Montreal, QC H2Z 1Z3, Canada Shahriyar.heidarzadeh@snclgroup.com

Abstract:

This paper presents a methodology for analyzing the uncertainties of Uniaxial Compressive Strength (UCS) test data for metamorphic rocks based on statistical and mineralogical analyses. The methodology consists of three steps: data treatment process, schistosity angle, and mineralogy. The treatment process involved different data treatment techniques to assess the variabilities of UCS data, and to determine appropriate outlier detection methods based on multiple decision-making criteria and engineering judgment. The results showed that adjusted boxplot and 2SD method provided more accurate outcomes in detecting outliers. The findings reveal that traditional boxplot may not be the best for treating UCS data. Moreover, the study examined the impact of schistosity angle and suggests removing samples within a specific angle range to decrease UCS variabilities. The mineralogical analysis examined the impact of various minerals on UCS variations, revealing a correlation between the dispersion and the variabilities of both hard and soft minerals.

Keywords: UCS variability, outlier detection method, statistical data treatment

1. Introduction

Rock mass characterization plays a crucial role in geomechanical engineering, as it provides essential information for the design and construction of rock engineering projects. However, a significant challenge in rock mass characterization is the inherent variability of intact rocks, which can introduce uncertainties in determining geomechanical parameters. Metamorphic rocks, in particular, exhibit

considerable variability in geomechanical properties due to the varying degrees of metamorphism they undergo during their formation process. Uniaxial Compressive Strength (UCS) is a fundamental geomechanical parameter used to characterize the strength and deformation behavior of rocks, and it is commonly determined through laboratory testing using uniaxial compressive tests (Pepe et al., 2017b). However, even with careful sample preparation and adherence to testing protocols, UCS test results for metamorphic rocks often show scattered and variable data (Pepe et al., 2017b). Indeed, the scattered outcomes of rock strength tests should be considered as raw data and treated with caution in geomechanical studies to minimize uncertainties and ensure accurate characterization of rock mass behavior (F Agliardi et al., 2016; Peirce, 1852). From the statistical perspective, these extreme abnormal values are called outliers, which considerably diverge from the mainstream of the other values (Kannan et al., 2015; Saleem et al., 2021). Outliers can significantly impact the analysis of UCS data and introduce further uncertainties if not appropriately identified and treated. Therefore, selecting an appropriate outlier detection method is essential to ensure reliable analysis of UCS data for metamorphic rocks. However, the selection of an appropriate outlier detection method is not straightforward, as it requires consideration of various factors such as sample size, data distribution, and engineering judgment.

In the field of engineering, the process of identifying outliers is often specific to the particular conditions and objectives of the analysis being conducted. It requires careful consideration of engineering judgment, as the identified outliers should also be reasonable in the context of geomechanics, which deals with the mechanical behavior of geological materials. Several well-known methods for outlier detection have been widely used in the literature. One commonly used method is the boxplot, which has gained popularity in analyzing geomechanical data due to its simplicity and visual appeal. Boxplots have been applied for assessing the variability of rock strength and deformability parameters (Heidarzadeh et al., 2021a; Tiryaki, 2008) and also to identify potential outliers in rockburst analyses or slope stability studies using machine learning (Roy et al., 2023; Xue et al., 2020). However, boxplots have some limitations, such as their inapplicability to greatly skewed data (Walker et al., 2018), which has led to modifications to address this limitation, which will be discussed in this study. Another commonly used method is Grubbs' test, which has been used to identify outliers in geotechnical data, such as soil properties, rock mechanics, and foundation performance (Dindarloo & Siami-Irdemoosa, 2015a; Shao et al., 2019). However, Grubbs' test assumes that the data are normally distributed, which may not be appropriate for datasets that do not follow a normal distribution. In addition to boxplots and Grubbs' test, Chauvenet's test has been used to identify irregular data points in the Schmidt hammer test (Goktan & Ayday, 1993). The application of these outlier detection methods is essential for engineers as it helps eliminate data points that may not be representative of the underlying population and could potentially skew the results of their analyses. By removing outliers, engineers can improve the accuracy and reliability of their results, leading to more robust geomechanical analyses.

In this study, we carefully analyze the raw UCS data to eliminate potential uncertainties and improve the accuracy of rock mass characterization, based on three steps: data treatment process, consideration of schistosity angle, and mineralogical analysis. A comprehensive statistical analysis is performed using different data treatment techniques to assess the variabilities of UCS data, and the most appropriate outlier detection methods are determined based on multiple decision-making criteria and engineering judgment. Additionally, the influence of schistosity angle, which is known to affect rock strength, is considered to reduce potential biases in the results. Furthermore, the correlation between

mineralogy and UCS variations is explored to gain insights into the role of different minerals in the variability of UCS data.

2. Methodology

As presented in Figure 1, a proper methodology for analyzing the Uniaxial Compressive Strength (UCS) variation in intact rocks was proposed which consists of five steps. In Step 1, a suitable site is selected for statistical data analysis based on geotechnical considerations and availability of adequate UCS data. In Step 2, applicable outlier detection methods are applied to the UCS data, including fence labeling methods and statistical tests, to identify potential outliers. Fence labeling methods involve the creation of lower and upper thresholds in the dataset, and observations outside this range are considered outliers. Statistical tests, on the other hand, identify outliers through statistical hypothesis tests that involve null hypothesis and alternative hypothesis. This step helps to identify and remove any data points that deviate significantly from the expected behavior, ensuring the robustness of the analysis. In Step 3, a comparative analysis is conducted to select the most appropriate outlier detection methods based on multiple decision-making criteria and engineering judgment. This step ensures that the most suitable outlier detection methods are chosen, tailored to the specific characteristics of the UCS data under investigation. The outliers identified by the selected methods are treated in step 4, and goodness-of-fit tests are then performed to determine the best fitted probability distribution function (PDF) for the UCS data. Finally, in Step 5, the impact of schistosity and existing minerals of rock samples on the UCS variation is evaluated through additional analyses to find a meaningful relationship. This methodology aims to systematically analyze the UCS variation in intact rocks, accounting for outliers, appropriate statistical techniques, decision-making criteria, and engineering judgment to ensure reliable results.

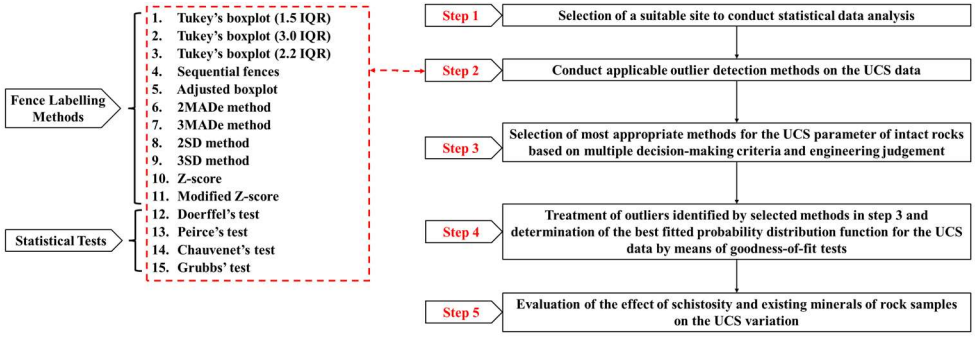

Figure 1. The methodology for evaluation of the variability of UCS data

3. Project description

Westwood Mine, located in the Abitibi greenstone belt in Quebec, is a major gold deposit discovery in Canada (Figure 2). Commercial production commenced in 2014, and the mine is approximately 420 km northwest of Montreal (IAMGOLD, 2019a). The rock mass at Westwood Mine has been influenced by regional metamorphism, resulting in changes in lithological units from greenschist facies to the lower amphibolite facies (Tremblay, 2020). Yergeau (2015b) developed a lithological classification system that identifies six rock units, with Units 3, 4, and 5 being recognized as the most susceptible to rockburst incidents (Bouzeran et al., 2019; Kalenchuk et al., 2017). This study analyzed a total of 288 UCS tests (conducted at the Université du Québec à Chicoutimi), with 61, 157 and 70

rock samples extracted from Units 3, 4, and 5, respectively. These units experienced recent rockburst occurrences, leading to the closure of the Westwood mine in previous years (Tremblay, 2020).

Figure 2. Westwood Mine location in Quebec Province, Canada (IAMGOLD, 2019a)

4. Statistical treatment of UCS database

In this section, we apply a total of 15 different treatment approaches to the UCS database, with the goal of minimizing uncertainties and selecting the most appropriate treatment technique which can provide reliable outcomes for engineering designs. The findings of this comprehensive statistical analysis will contribute to a better understanding of the geomechanical behavior of the rock units in Westwood Mine, and provide valuable insights for future mining operations. Table 1 briefly illustrate the mathematical relationships for each outlier detection method.

Table 1. The summary of outlier detection relationships

Treatment technique	Outlier detection rule	Constant
Tukey's boxplot	$if: \begin{cases} x_i < Q_1 - k \times IQR \\ x_i > Q_3 + k \times IQR \end{cases} \rightarrow x_i \text{ is outlier}$ $(Eq.1)$	$k = 1.5$
		$k = 3.0$
	$IQR = Q3 - Q1$ $(Eq.2)$	$k = 2.2$
Sequential fences[1] (Schwertman & de Silva, 2007)	$if: \begin{cases} x_i < Q_2 - \frac{t_{df,\alpha_{nm}}}{k_n}(IQR) \\ x_i > Q_2 + \frac{t_{df,\alpha_{nm}}}{k_n}(IQR) \end{cases} \rightarrow x_i \text{ is outlier}$ $(Eq.3)$	
Adjusted boxplot (Hubert & Vandervieren, 2008)	$MC > 0, if: \begin{cases} x_i < Q_1 - 1.5e^{-4MC}IQR \\ x_i > Q_3 + 1.5e^{+3MC}IQR \end{cases} \rightarrow x_i \text{ is outlier}$ $(Eq.4)$	
	$MC < 0, if: \begin{cases} x_i < Q_1 - 1.5e^{-3MC}IQR \\ x_i > Q_3 + 1.5e^{+4MC}IQR \end{cases} \rightarrow x_i \text{ is outlier}$ $(Eq.5)$	
	$MC = \underset{x_i \le Q_2 \le x_j}{median} h(x_i, x_j)$ $(Eq.6)$	

	$h\left(x_i, x_j\right) = \frac{\left(x_j - Q_2\right) - \left(Q_2 - x_i\right)}{x_j - x_i}$ $(Eq.7)$	
2MADe method	$if: \begin{cases} x_i < \ median - k \times MADe \\ x_i > \ median + k \times MADe \end{cases} \rightarrow x_i \ is \ outlier$ $(Eq.8)$	$k = 2$
3MADe method	$MAD_e = 1.483 \times [median\ (\lvert x_i - median \rvert)]$ $(Eq.9)$	$k = 3$
Z-score method	$Z_{score} = \frac{x_i - X_m}{S}$ $(Eq.10)$ $if: \begin{cases} Z_{score} < -3 \\ Z_{score} > +3 \end{cases} \rightarrow x_i \ is \ outlier$ $(Eq.11)$	
Modified Z-score method	$M_i = \frac{0.6745\ (x_i - median)}{MAD}$ $(Eq.12)$ $MAD = [median\ (\lvert x_i - median \rvert)]$ $(Eq.13)$ $if: \begin{cases} M_i < -3.5 \\ M_i > +3.5 \end{cases} \rightarrow x_i \ is \ outlier$ $(Eq.14)$	
2SD method	$if: \begin{cases} x_i < X_m - k \times S \\ x_i > X_m + k \times S \end{cases} \rightarrow x_i \ is \ outlier$ $(Eq.15)$	$k = 2$
3SD method		$k = 3$
Doerffel's Test (Doerffel, 1967)	$if: x_i > X_m + g.S \rightarrow x_i \ is \ outlier$ $(Eq.16)$	
Peirce's Test[2] (Ross, 2003)	$if: \frac{\lvert x_i - X_m \rvert}{S} > R$ $\rightarrow x_i \ is \ an \ outlier$ $(Eq.17)$	
Chauvenet's Test[3] (Gul et al., 2018)	$if: \frac{\lvert x_i - X_m \rvert}{S} > T$ $\rightarrow x_i \ is \ an \ outlier$ $(Eq.18)$	
Grubbs' Test[4] (Grubbs, 1950)	$if\ G_{statistic} = \frac{X_m - x_{min}}{S} > G_{critical}$ $\rightarrow x_{min} \ is \ outlier$ $(Eq.19)$ $if\ G_{statistic} = \frac{x_{max} - X_m}{S} > G_{critical}$ $\rightarrow x_{max} \ is \ outlier$ $(Eq.20)$ $G_{Critical} = \frac{(n-1)}{\sqrt{n}} \sqrt{\frac{t^2_{(\alpha/n, n-2)}}{n - 2 + t^2_{(\alpha/n, n-2)}}}$ $(Eq.21)$	

[1] "k_n" can be found at Schwertman and de Silva (2007).

[2] "R" values are available at Ross (2003).

[3] "T" values are referred to in Gul et al. (2018).

[4] "$G_{critical}$" can be found at Grubbs (1950).

4.1. Selection of most suitable treatment approaches

When selecting the most appropriate outlier detection method for the UCS data, it is crucial to consider both statistical and geomechanical principles. Two key criteria are the physical meaningfulness of the interval values estimated by different outlier methods, and the statistical acceptability of the number of detected outliers. Once the most suitable outlier detection method is identified, the next step is to remove the outliers from the remaining data.

4.2. Results and discussion

When selecting an outlier detection method for UCS data from metamorphic rocks, it is important to consider the expected mechanical behavior of the rock type, and having a deep understanding of the geology and behavior of these rocks is paramount. Also, the confidence interval should align with rock mechanics principles and highlight a reliable range of UCS values. Any values lying outside this range should be treated as outliers. For the statistical tests, the number of detected outliers was the sole criterion, which may vary among different tests. The findings revealed that several outlier detection methods were not suitable for UCS data. Peirce and Grubbs tests were deemed inapplicable due to their limitation in sample size. Doerffel's test failed to detect low extreme outliers, leading to a significant increase in UCS uncertainties. Chauvenet's test had a conservative approach in labeling the outliers. As a result, most of fence labeling methods resulted in incorrect values for the UCS data, rendering them unsuitable for creating acceptable intervals due to the lack of physical meaning for negative bound values. Based on the analysis, the adjusted boxplot and 2SD method were found to create statistically and physically suitable intervals for the UCS datasets. Table 2 summarized the results of outlier detection analysis on the UCS data. Therefore, these methods were selected as the most appropriate outlier detection methods for the UCS data, considering their reliability and accuracy in identifying outliers and creating meaningful intervals for the UCS values.

4.3. Limitations of the selected methods and future recommendations

While the selected methods demonstrated certain strengths in addressing the UCS data of metamorphic rocks, they also come with some inherent limitations. In this study, the 2SD method is sensitive to extreme values, given its reliance on mean and standard deviation. This may make it vulnerable when applied to datasets with significant outliers, especially in the context of metamorphic rocks which inherently possess notable heterogeneity. In general, metamorphic rocks, with their natural variability stemming from diverse geological processes, pose challenges. The current methods might not always capture this complicated situation, potentially leading to over-simplifications. Moreover, while both the 2SD method and adjusted boxplot can handle various data distributions, they might not thoroughly address the inherent scaling and applicability issues specific to metamorphic rocks.

To improve uncertainty quantification for metamorphic rocks, it would be useful to assemble a comprehensive dataset spanning various metamorphism grades and diverse geological settings. Identifying the metamorphism grade for each data sample allows for systematic categorization of UCS data, thereby integrating the metamorphic grade into the analytical process. Broadening the dataset will refine the evaluations, and utilizing advanced statistical or computational techniques might offer targeted outlier detection strategies tailored to the distinct characteristics of each metamorphic rock type.

Table 2. Summary of outlier detection methods applied on the UCS data in the three rock units (3, 4 and 5)

Outlier detection methods	Interval values (MPa)			Number of detected outliers					
	Unit 3	Unit 4	Unit 5	Unit 3		Unit 4		Unit 5	
				LB	UB	LB	UB	LB	UB
Tukey's boxplot (1.5IQR)	-10.9 < UCS < 321.1	26.1 < UCS < 266.1	-47.2 < UCS < 356.1	0	0	0	10	0	0
Tukey's boxplot (3IQR)	-135.4 < UCS < 445.6	-63.9 < UCS < 356.1	-198.5 < UCS < 507.3	0	0	0	1	0	0
Tukey's boxplot (2.2IQR)	-69.0 < UCS < 379.2	-15.9 < UCS < 308.1	-117.8 < UCS < 426.6	0	0	0	2	0	0
Sequential fences	-56.5 < UCS < 360.3	62.4 < UCS < 237.1	-112.5 < UCS < 408.1	0	0	4	15	0	0
adjusted boxplot	**6.9 < UCS < 336.7**	**32.2 < UCS < 271.0**	**16.5 < UCS < 432.8**	0	0	0	8	0	0
2MADe	23.3 < UCS < 280.4	49.8 < UCS < 249.7	-10.8 < UCS < 306.4	0	0	3	12	0	0
3MADe	-40.9 < UCS < 408.9	-0.1 < UCS < 349.7	-90.2 < UCS < 465.1	0	0	0	1	0	0
Modified Z-score	-3.5 < Mi < 3.5	-3.5 < Mi < 3.5	-3.5 < Mi < 3.5	0	0	0	2	0	0
Z-score	-3 < Z-score < 3	-3 < Z-score < 3	-3 < Z-score < 3	0	0	0	2	0	0
2SD	**42.2 < UCS < 264.5**	**40.8 < UCS < 270.3**	**30.6 < UCS < 280.4**	1	2	1	8	0	1
3SD	-13.3 < UCS < 320.1	-16.5 < UCS < 326.6	-31.7 < UCS < 342.8	0	0	0	2	0	0
Doerffel's test	Test-based methods identify the outliers based on critical values			N/A	0	N/A	1	N/A	0
Peirce' test				N/A	N/A	N/A	N/A	N/A	N/A
Chauvenet's test				0	0	0	1	0	0
Grubbs' test				0	0	N/A	N/A	0	0

*(the LB and UB are the lower bound and upper bound, respectively)

4.4. Determination of the best fitted PDF for the UCS data

To determine the best-fitted PDF for the UCS data in each rock unit, the Akaike information criterion (AIC) test, was applied. The AIC test is a goodness-of-fit test that assesses how well a sample data follows a specific distribution. Lower AIC statistics indicate a better fit to the distributions. The results of the AIC tests conducted on the UCS Unit 3 data using the adjusted boxplot and 2SD method

are shown in Figure 3, with the 2SD method demonstrating a better fit based on lower AIC values (Table 3). Thus, the 2SD method was selected as the preferred outlier detection method for the UCS dataset in all three rock units.

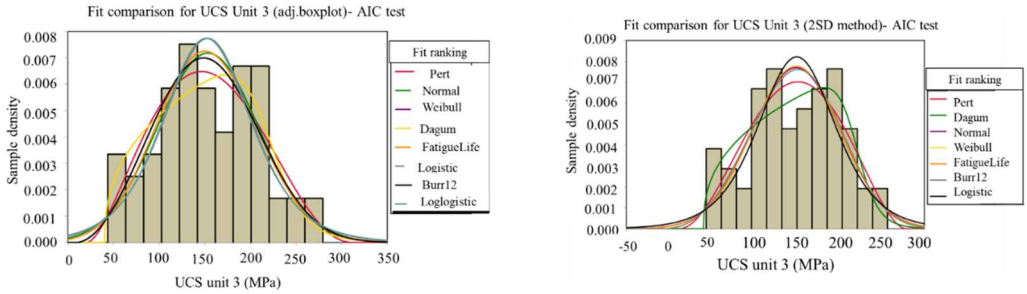

(a) (b)

Figure 3. Fit comparison using the AIC test in the UCS Unit 3 data treated by adjusted boxplot and 2SD method

Table 3. Comparison of UCS datasets treated by adjusted boxplot and 2SD method based on the AIC test in three rock units

Distribution	Unit 3		Unit 4		Unit 5	
	adj. boxplot	2SD	adj. boxplot	2SD	adj. boxplot	2SD
Burr12	669.55	639.66	1570.02	1552.44	779.94	765.88
Dagum	667.84	635.98	1569.72	1553.59	*	*
Fatigue Life	668.63	638.72	1567.79	1550.05	782.17	767.96
Loglogistic	*	*	1568.37	1551.74	788.59	774.44
Logistic	669.47	640.06	1568.76	1553.40	786.78	772.46
Normal	666.51	636.51	1568.59	1552.72	780.60	766.10
Pert	666.27	635.50	1576.41	1555.39	774.25	759.91
Weibull	667.26	637.35	1570.39	1551.51	777.69	763.62

Furthermore, the most fitted PDF was assigned based on the treated UCS data for each rock unit, and the calculated mean and standard deviation values were illustrated in Figure 4. The mean values of UCS data in Units 3, 4, and 5 were found to be 149.25 MPa, 148.37 MPa, and 152.47 MPa, respectively, despite some uncertainties. The distribution fit ranking of the UCS data treated by the 2SD method revealed that the Pert distribution was the most suitable for Unit 3 and Unit 5, while the Fatigue Life distribution was the best fit for Unit 4, as shown in Figure 4 (a-c).

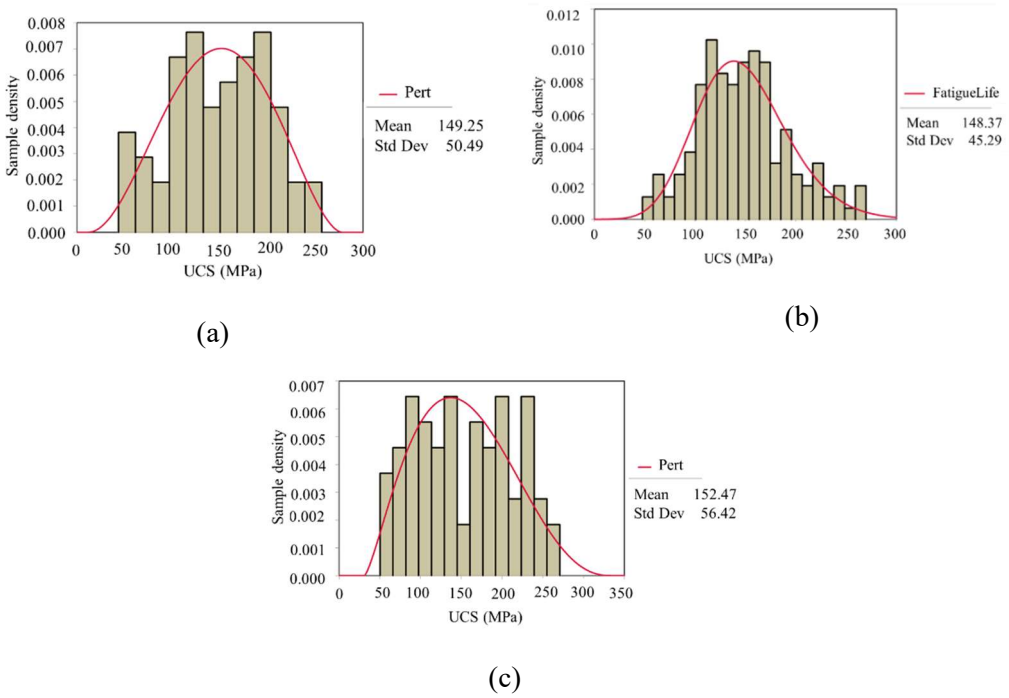

Figure 4. Best distribution assigned for the UCS data treated by 2SD method, unit 3 (a), unit 4 (b) and unit 5 (c)

5. The impact of schistosity on the UCS dispersion

Despite applying the most appropriate outlier detection methods and best fitted PDFs, the UCS data for different lithological units at the Westwood mine still exhibited significant dispersion. To mitigate this, the impact of schistosity angle (β) on uncertainties was evaluated. The angle of schistosity has a strong effect on rock strength and is an important factor in analyzing UCS data in rock units. Previous studies have shown that rock strength is closely correlated with the angle between the schistosity plane and the loading orientation. In this study, schistosity angles were measured for rock samples from Units 3 and 4, and it was found that UCS values are most variable when schistosity angles fall within the range of 30° to 60°, which is referred to as the variation range, as highlighted in Figure 5 (a & b). When schistosity angles are less than 30° or greater than 60°, they have less influence on UCS values. The orientation of schistosity planes is also important in the failure mechanism of rocks, especially when the schistosity angle is within the range of 30° to 60°, as it can dominate the failure behavior. Therefore, excluding UCS data within the variation range can improve the accuracy of the dataset and minimize the negative impact of schistosity on UCS variation. Analysis of the schistosity angles of rock samples from Unit 3 and Unit 4 showed that UCS data in Unit 3 was less influenced by schistosity angles compared to Unit 4, and excluding data within the variation range can effectively mitigate the impact of schistosity on UCS data variability in both units (presented in Figure 6).

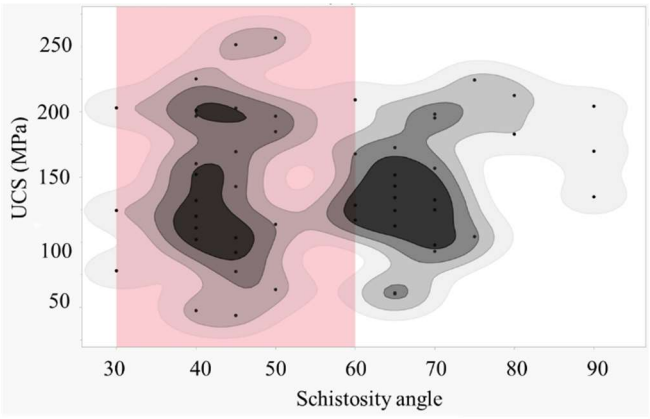

(a)

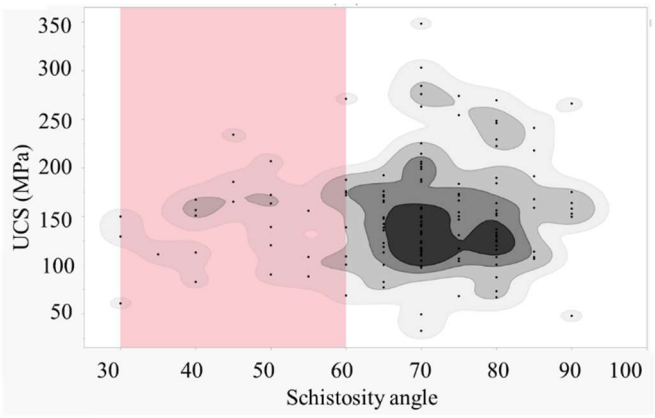

(b)

Figure 5. The dispersion of schistosity angle of rock samples in unit 3 (a) and unit 4 (b)

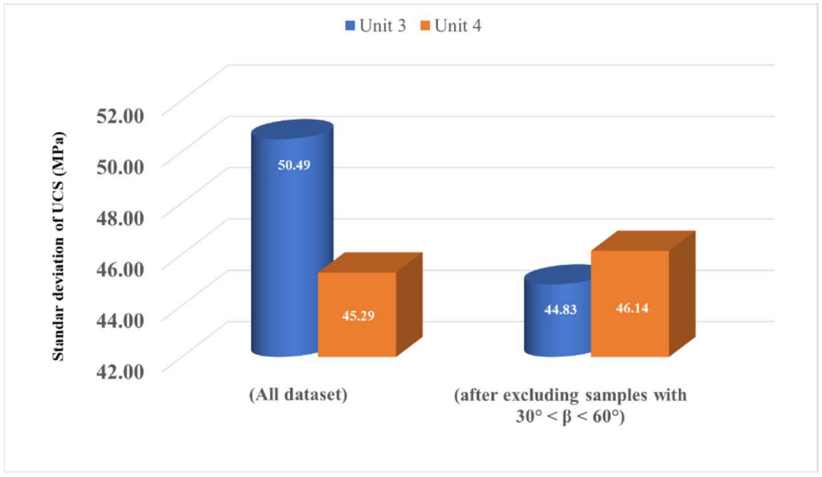

Figure 6. Standard deviations of the UCS dataset in units 3 and 4 before and after excluding the schistosity range

6. Impact of mineralogy on the variability of UCS data

In the third step of the methodology, we examined the impact of mineralogy on the uncertainties of UCS data. To investigate this, we conducted a comprehensive petrographic analysis of thin-section rock samples using the X-ray diffraction method. The analysis allowed us to identify the predominant minerals in each lithological unit, and we created a database of 62 thin-section samples. We divided the minerals into two main groups - hard minerals (e.g., Quartz, Epidote, Amphibole, Plagioclase, Pyrite, and Magnetite) and soft minerals (e.g., Feldspar, Chlorite, Sericite, Muscovite, Carbonate, and Biotite) - and conducted statistical analyses on each group. The results revealed that the main minerals in both lithological units were identical, but their proportions were considerably different. The higher variation of UCS data in unit 4 compared to unit 3 can be attributed to the dispersion of hard and soft mineral proportions, as the standard deviation of unit 4 (19.7MPa) was greater than that of unit 3 (18.4MPa) (Table 4). However, we could not establish a reasonable relationship between soft and hard minerals in both rock units, as the UCS values varied (Figure 7). Overall, our mineralogy results provide valuable information that can be used to evaluate UCS uncertainties in terms of mineral variations.

Table 4. Descriptive statistics of hard and soft minerals of rock samples referred to Units 3 and 4

Unit	Mineral type	Treated sample size	Number of detected outliers	St. Dev	Mean	Min	Max
				Values in percentage			
U3	Hard	24	1	**18,4**	51.8	13	79
	Soft				48.2	21	87
U4	Hard	37	0	**19,7**	47.9	15	91
	Soft				52.1	9	85

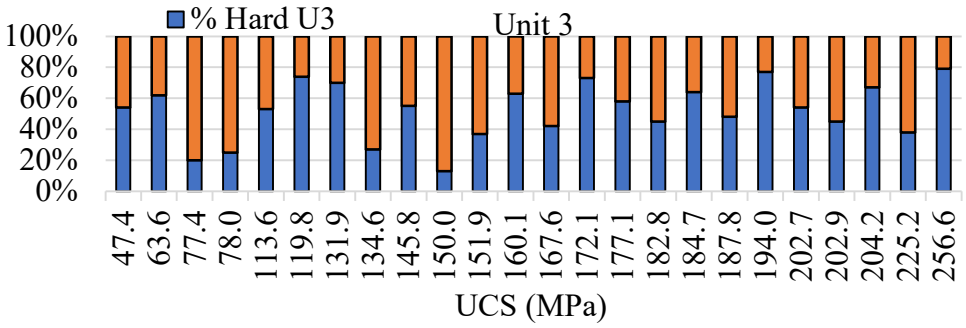

(a)

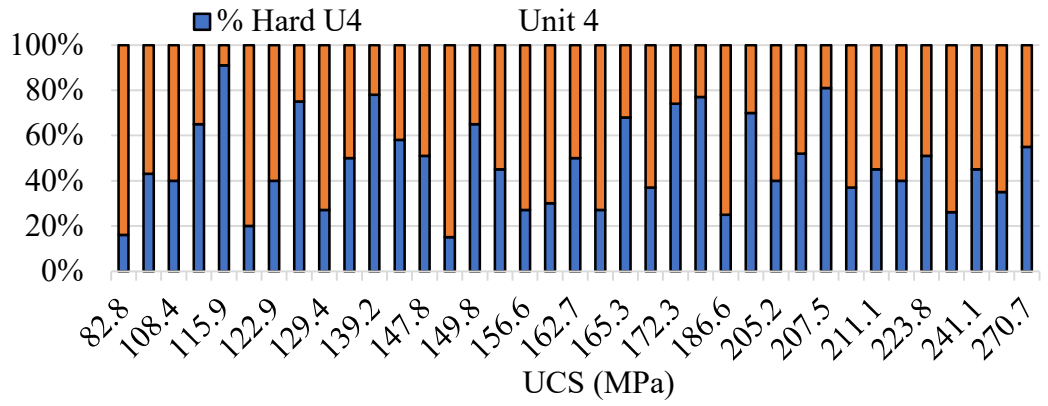

(b)

Figure 7. Proportion of hard and soft minerals based on the UCS value: a) Unit 3, b) Unit 4

7. Conclusion

This paper presents a methodology for analyzing the uncertainties of UCS intact rocks, which is a crucial factor for predicting and analyzing stability in underground openings. Treatment processes of intact rock samples can help estimate the mean and standard deviation of the sample population more accurately, considering that extracted intact rock samples represent a subset of the whole rock population. Metamorphic intact rocks may exhibit extreme variation in geomechanical parameters, particularly UCS values, due to varying degrees of metamorphism. The proposed statistical data treatment approach effectively addresses these uncertainties by identifying and addressing abnormal high or low values in the dataset, ensuring the reliability of the results. The study also identified the best outlier detection methods for UCS data, with the adjusted boxplot and 2SD methods being the most suitable. The traditional boxplot method was found to be inadequate for treating rock strength data, and the study recommends using the adjusted boxplot method instead. The statistical methods tested in this study were not effective in determining the uncertainties of metamorphic rocks. The results also revealed that the best-fitting probability distribution function for UCS data may not be normal, highlighting the importance of selecting appropriate probability distributions for geomechanical modeling. Schistosity planes were found to significantly influence the uncertainties of UCS data in metamorphic rocks, and the variation of mineral proportions had a crucial effect on UCS data uncertainties so that the reason for the greater variability of UCS data in unit 4, as compared to unit 3, can be explained by the distribution of hard and soft minerals. The findings of this study can aid in reducing uncertainties in geomechanical studies of metamorphic rocks, improving our understanding of their mechanical behavior, and informing probable mining hazards such as rockburst prediction models.

References

Agliardi, F., Sapigni, M., & Crosta, G. (2016). Rock mass characterization by high-resolution sonic and GSI borehole logging. *Rock Mech Rock Eng*, *49*(11), 4303-4318.

Bouzeran, L., Pierce, M., Andrieux, P., & Williams, E. (2019, 24-25 June 2019). *Accounting for rock mass heterogeneity and buckling mechanisms in the study of excavation performance in foliated ground at Westwood mine* Deep Mining 2019: Proceedings of the Ninth International Conference on Deep and High Stress Mining, Muldersdrift.

Dindarloo, S. R., & Siami-Irdemoosa, E. (2015). Maximum surface settlement based classification of shallow tunnels in soft ground. *Tunnelling Underground Space Technology*, *49*, 320-327.

Doerffel, K. (1967). *Die statistische Auswertung von Analysenergebnissen* (Vol. 2). Springer.

Goktan, R., & Ayday, C. (1993). A suggested improvement to the Schmidt rebound hardness ISRM suggested method with particular reference to rock machineability. *Int. J. Rock Mech. Min.*, *30*(3).

Grubbs, F. E. (1950). Sample Criteria for Testing Outlying Observations. *The Annals of Mathematical Statistics*, *21*(1), 27-58, 32. https://doi.org/10.1214/aoms/1177729885

Gul, M., Kotak, Y., Muneer, T., & Ivanova, S. (2018). Enhancement of albedo for solar energy gain with particular emphasis on overcast skies. *Energies*, *11*(11), 2881.

Heidarzadeh, S., Saeidi, A., Lavoie, C., & Rouleau, A. (2021). Geomechanical characterization of a heterogenous rock mass using geological and laboratory test results: a case study of the Niobec Mine, Quebec (Canada). *SN Applied Sciences*, *3*, 1-20.

Hubert, M., & Vandervieren, E. (2008). An adjusted boxplot for skewed distributions. *Computational statistics & data analysis*, *52*(12), 5186-5201.

IAMGOLD. (2019). *IAMGOLD Corporation - Exploitations - The Westwood Gold Mine*.

Kalenchuk, K., Mercer, R., & Williams, E. (2017). Large-magnitude seismicity at the Westwood mine, Quebec, Canada. Deep Mining 2017: Proceedings of the Eighth International Conference on Deep and High Stress Mining,

Kannan, K. S., Manoj, K., & Arumugam, S. (2015). Labeling methods for identifying outliers. *IJSS*, *10*(2), 231-238.

Peirce, B. (1852). Criterion for the rejection of doubtful observations. *The Astronomical Journal*, *2*, 161-163.

Pepe, G., Cevasco, A., Gaggero, L., & Berardi, R. (2017). Variability of intact rock mechanical properties for some metamorphic rock types and its implications on the number of test specimens. *Bull. Eng. Geol. Environ.*, *76*(2), 629-644.

Ross, S. M. (2003). Peirce's criterion for the elimination of suspect experimental data. *Journal of engineering technology*, *20*(2), 38-41.

Roy, J., Eberhardt, E., Bewick, R., & Campbell, R. (2023). Application of Data Analysis Techniques to Identify Rockburst Mechanisms, Triggers, and Contributing Factors in Cave Mining. *Rock Mechanics and Rock Engineering*, 1-36.

Saleem, S., Aslam, M., & Shaukat, M. R. (2021). A review and empirical comparison of univariate outlier detection methods. *PJS*, *37*(4).

Schwertman, N. C., & de Silva, R. (2007). Identifying outliers with sequential fences. *Computational statistics & data analysis*, *51*(8), 3800-3810.

Shao, Z., Armaghani, D. J., Bejarbaneh, B. Y., Mu'azu, M., & Mohamad, E. T. (2019). Estimating the friction angle of black shale core specimens with hybrid-ANN approaches. *Measurement*, *145*, 744-755.

Tiryaki, B. (2008). Predicting intact rock strength for mechanical excavation using multivariate statistics, artificial neural networks, and regression trees. *Eng. Geol.*, *99*(1), 51-60.

Tremblay, K. (2020). *Determination of geological and geomechanical parameters intensifying the risk of landslides near the Bousquet Fault at the Westwood mine (in French)* Université du Québec à Chicoutimi].

Walker, M. L., Dovoedo, Y. H., Chakraborti, S., & Hilton, C. W. (2018). An Improved Boxplot for Univariate Data. *The American Statistician*, *72*(4), 348-353.

Xue, Y., Bai, C., Qiu, D., Kong, F., & Li, Z. (2020). Predicting rockburst with database using particle swarm optimization and extreme learning machine. *Tunn. Undergr. Space Technol.*, *98*, 103287.

Yergeau, D. (2015). *Geology of the atypical Westwood synvolcanic gold deposit, Abitibi, Quebec., PhD thesis (in French)* Université du Québec, Institut national de la recherche scientifique].

Evaluation of the applicability of statistical tools for developing stress-depth relationships for the Canadian Shield

B. Dastjerdy & A. Saeidi
University of Quebec at Chicoutimi (UQAC), Chicoutimi, Quebec, Canada

Sh. Heidarzadeh
AtkinsRéalis, Montreal, Quebec, Canada

ABSTRACT: Understanding stress-depth relationships is crucial for designing optimal underground structures in geologically diverse regions like the Canadian Shield. This study evaluates the applicability of statistical tools in developing stress-depth relationships, emphasizing the limitations of relying solely on these methods. Past relationships categorized in-situ stress data into depth domains primarily using statistical techniques, often overlooking the complex geology of the Canadian Shield. Assessing the efficacy of these models revealed their inadequacy, especially in classifying zones deeper than 600m as undisturbed. Our methodology intentionally disregards geological influences to focus on statistical tools in an expanded dataset of 330 stress measurements. Utilizing multiple outlier detection and clustering (K-means, Hierarchical, Normal Mixture) methods, we defined new depth domains, but the results showed weak fitness in the developed models. This study highlights the need for a balanced integration of statistical tools with robust geological insights to comprehensively understand in-situ stress state in the Canadian Shield.

1. INTRODUCTION

In the design of underground structures, a critical consideration is the assessment of the in-situ stress state, representing the inherent and undisturbed stress conditions within the Earth's crust prior to any engineering activities. This evaluation is particularly crucial for projects in deep underground settings, where in-situ stress becomes a dominant factor influencing the stability of the rock mass. The Canadian Shield, with its complex Precambrian geology in eastern and central Canada, holds significant geological and economic importance (Figure 1). With a complex history evolved by geotectonic and metamorphic histories over billions of years, the Canadian Shield faces certain engineering challenges for mineral extraction and infrastructure planning due to uncertainties in stress measurements arising from varied geological history, rock heterogeneity, and tectonic activities (Amadei & Stephansson, 1997). A thorough assessment of in-situ stress is vital for ensuring the safety and efficiency of mining and other underground projects in this diverse region.

Figure 1. Geographic extent of the Canadian Shield in Canada

Since the 1970s, research on in-situ stresses in the Canadian Shield began with Herget's experiments at G.W. Macleod Iron mine, Ontario (Herget, 1973a). Subsequent studies by Herget (1982); Maloney et al. (2006); Yong and Maloney (2015) proposed models capturing the complexities of the Canadian Shield's in-situ stress state. Herget (1982) categorized stress-depth data into two ranges (0-900m, 900-2200m), while recent contributions suggested a three-zone categorization: stress-released (0-300m), transition (300-600m), and undisturbed stress zone (600-1500m). However, uncertainties persist, emphasizing ongoing challenges in understanding stress-depth relationships in the Canadian Shield. In this paper, we critically assess the use of statistical tools for predicting stress-depth models in the Canadian Shield. We evaluate previous stress-depth relationships, conduct detailed data treatment analysis to identify outliers, and apply clustering techniques to establish new depth ranges. This comprehensive approach aims to enhance our understanding of the applicability and limitations of statistical tools in predicting stress-depth relationships within the geologically complex Canadian Shield.

2. STATISTICAL ASSESSMENT OF PREVIOUS STRESS-DEPTH RELATIONSHIPS

In this study, all available stress data were collected from various sources, establishing a dataset of 330 stress values along with associated orientations. To focus on statistical aspects, our methodology intentionally disregarded geological influences to solely evaluate the effectiveness of statistical tools in establishing stress-depth relationships within the Canadian Shield, which potentially provide insights into the predictive capabilities and limitations of statistical tools.

To assess the efficacy of previous stress-depth relationships, we systematically applied depth domains, as proposed by Herget (1982) and Maloney et al. (2006), to our dataset, Figures 2 & 3 present the stress-depth equations for each depth domain across all three stress components ($\sigma_H, \sigma_h, \sigma_v$). Comparison of the coefficient of determination (R^2) values within these domains and the entire dataset revealed consistently lower accuracy within the depth-specific categories, emphasizing the limited predictive accuracy of such relationships in the Canadian Shield. Results indicated that prior relationships were often driven by statistical inferences from specific datasets, neglecting the complex geology of the Canadian Shield. The classification of zones as undisturbed beyond 600m zones demonstrated limited applicability across the Canadian Shield, leading to less robust and more uncertain predictions for all stress components. Subsequent sections focus on a data treatment process and cluster analysis aimed at defining new and more accurate depth domains within the stress database.

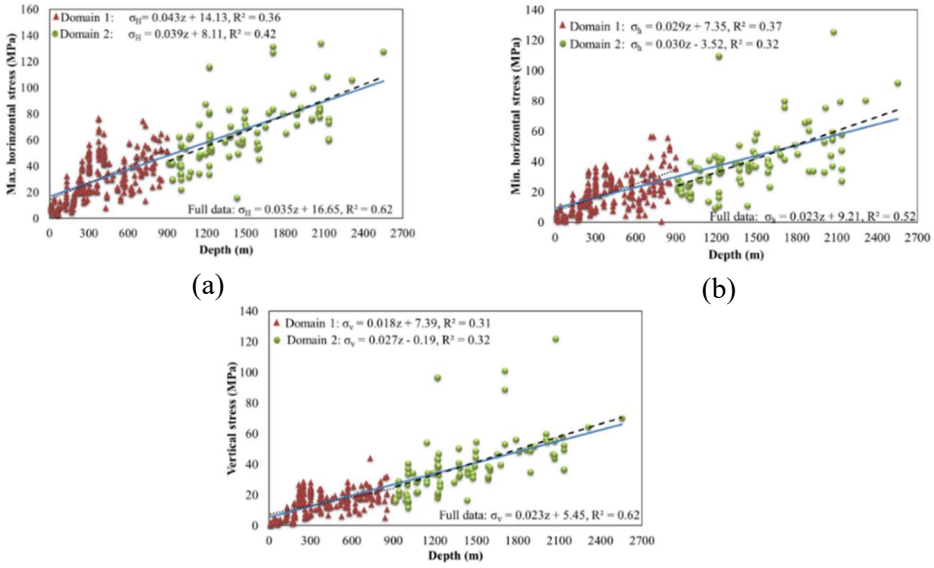

Figure 2. Applying depth domains of Herget (1982) on the stress database: a) max horizontal stress, b) min horizontal stress and c) vertical stress

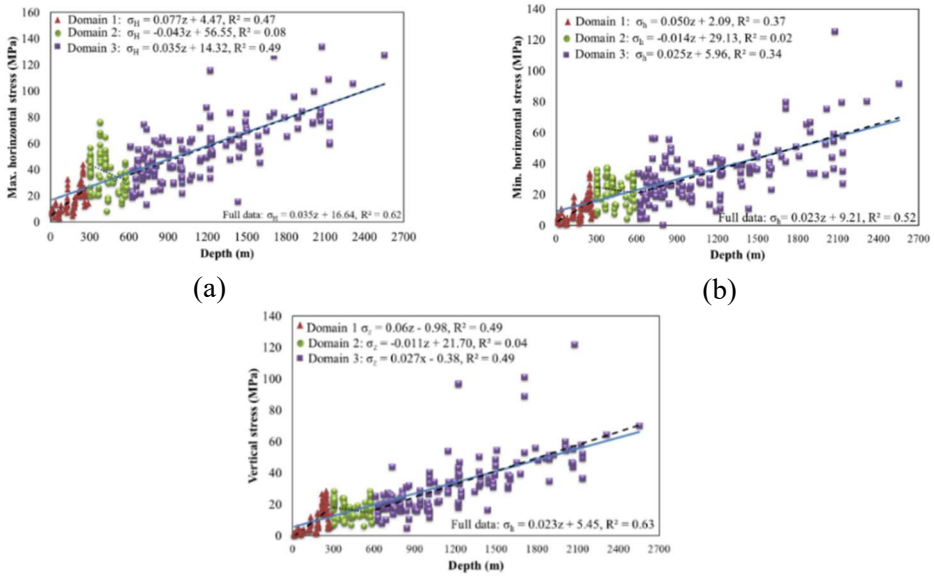

Figure 3. Applying depth domains of Maloney et al. (2006) on the stress database: a) max horizontal stress, b) min horizontal stress and c) vertical stress

3. TREATMENT OF STRESS-DEPTH DATA USING MULTIVARIABLE OUTLIER DETECTION METHODS

In this phase, we conducted data treatment analysis using JMP v.16 to identify potential outliers in stress-depth data—data points significantly deviating from the majority (Dastjerdy et al., 2023, 2024a; JMP-Pro., 2021). Focusing on key parameters, stress and depth, we employed four multivariable outlier detection methods: Mahalanobis, Jackknife, T2, and KNN (Table 1). These methods assess deviations of data points from the expected distribution center in a multivariate dataset, with the most deviated data labelled as outliers (Zheng et al., 2021). Following a detailed analysis of the identified outliers and extreme data, the Mahalanobis method appeared to yield more reliable results, as visually depicted in Figure 4.

Table 1. Results of multivariable outlier detection methods on the stress-depth data

Multivariable outlier detection method	Number of detected outliers
Mahalanobis	25
Jackknife	26
T2	26
K-Nearest Neighbor (KNN)	20

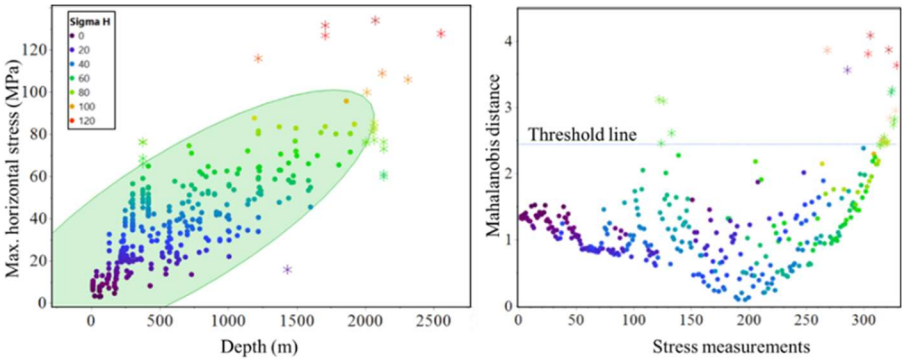

Figure 4. Treatment of stress-depth data of the Canadian Shield using Mahalanobis method

4. DEVELOPING NEW DEPTH DOMAINS BY MEANS OF CLUSTERING TECHNIQUES

After eliminating outliers, a cluster analysis was conducted on the refined stress data to define new depth domains in the Canadian Shield. Initially, we utilized the Elbow method to determine the optimal number of clusters (Figure 5a). Then, K-means, Hierarchical and Normal Mixture clustering methods were employed to establish four meaningful depth domains. K-means partitions the dataset, updating cluster centers based on mean points, while Normal Mixture method classify data as a mixture of normal distributions, accommodating complex patterns and subpopulations. Also, Hierarchical method forms a tree-like structure (JMP-Pro., 2021). The hierarchical approach proved more suitable, providing clusters with clearer distinctions compared to the relatively overlapped clusters of other methods (Figure 5b, c, d). Resulting depth domains are: 0-750m, 751-1250m, 1251-1750m, and 1751-2500m (Figure 5e). To analyze the suitability of new depth domains on stress determinations, the statistical robustness of the estimated equations for each domain was examined (Table 2). Despite the structured statistical approach, the R^2 and R^2 adjusted values for all domains remain considerably lower than that of the entire database.

5. OPTIMIZING STRESS-DEPTH RELATIONSHIPS THROUGH GEOLOGICAL INTEGRATION

Integrating geological conditions with statistical tools is essential for understanding the complexities of the Canadian Shield and optimizing stress-depth relationships. Our region-specific methodology categorized stress data based on structural, metamorphic and lithological factors, resulting in six distinct regional groups: Wabigoon & Quetico, Abitibi & Wawa, Uchi & Berens River, Pikwitonei, Grenville and Southern. In this paper, we focus on equations suggested for the Wabigoon & Quetico group.

In the Wabigoon&Quetico group, vertical stress notably diverges from lithostatic pressure line, potentially hinting additional tectonic forces. Our regression analysis proposed a nonlinear model ($R^2 = 0.51, \sigma_z = 1.08z^{0.49}$), capturing the influence of additional tectonic forces on vertical stress beyond the weight of overburden rock layers (Figure 6a). While our model may not estimate with high accuracy due to scattered data, this variability might be influenced by regional tectonism, such as thin- and thick-skinned tectonism observed in this region, likely contributing to the huge variability in stress environments within this geological group. Horizontal stresses align with a trend similar to vertical stress, showing higher R^2 values (Figure 6b), possibly indicating an influence from regional tectonism. However, these justifications should be approached cautiously due to the inherent uncertainties associated with statistical estimations. We also applied the Anderson faulting approach

to identify the dominant stress regime in the Wabigoon & Quetico group. According to this theory, the dominant stress regime in this region is Revere Faulting (*RF*), aligning with the Canadian Shield's overall tectonic regime. While *RF* regime predominantly governs the stress regime, an interesting shift to the Strike-Slip (*SS*) regime occurs in certain depth ranges, suggesting the presence of shear stress layers or zones (Figure 6c).

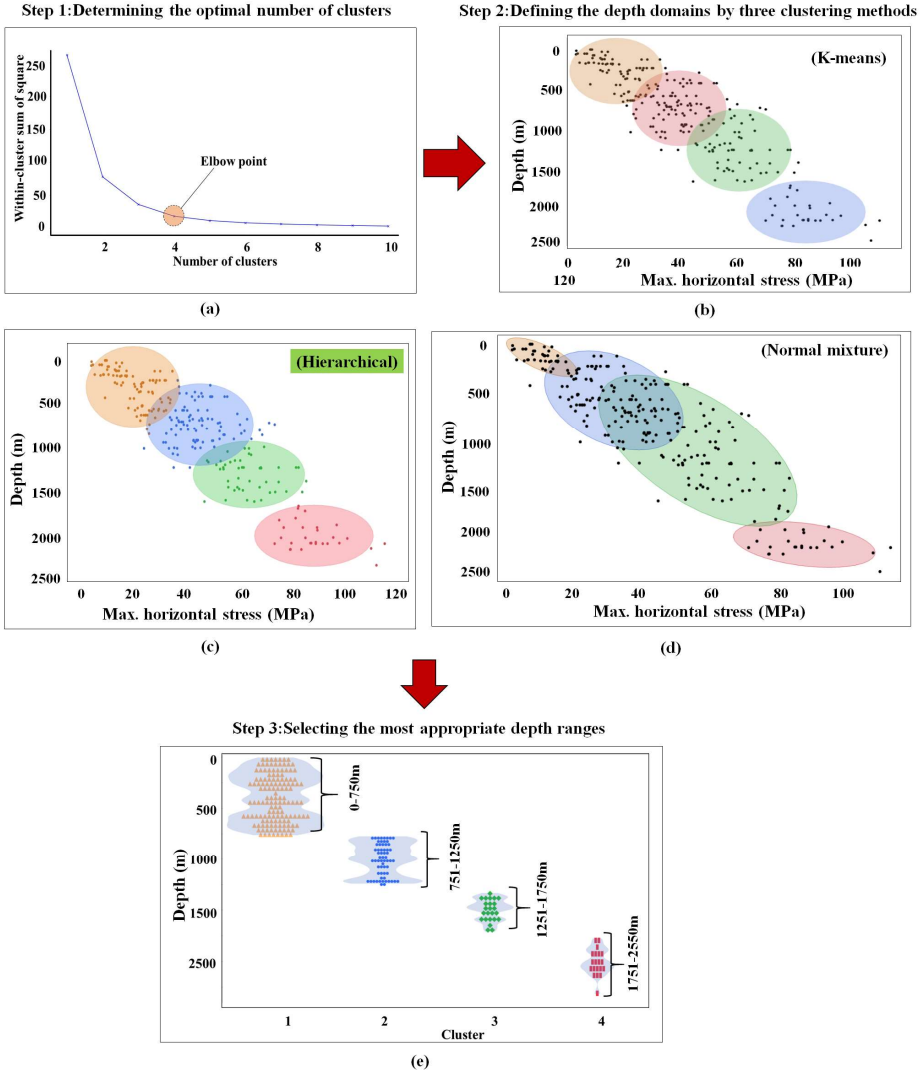

Figure 5. Cluster analysis to define new depth domains for the stress database

Table 2. Statistical assessment of stress-depth relationships across clusters in the Canadian Shield

Dataset	Depth domains (m)	R2	Adjusted R2
Cluster 1	0-750	0.51	0.50
Cluster 2	751-1250	0.19	0.18
Cluster 3	1251-1750	0.05	0.01
Cluster 4	1751-2550	0.23	0.19
Entire database	0-2550	0.78	0.78

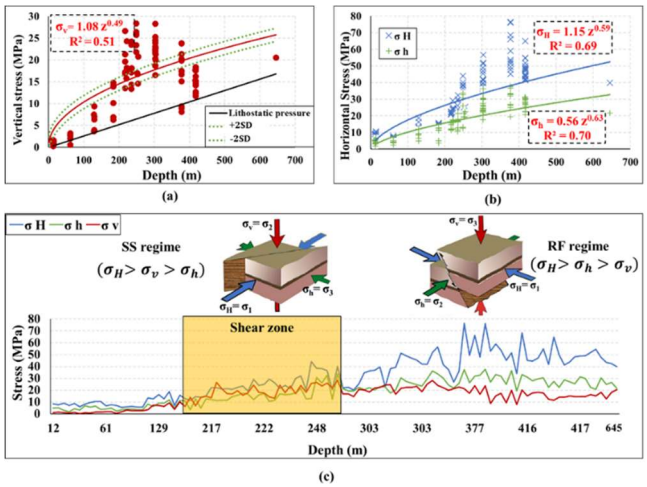

Figure 6. Suggested relationships in the Wabigoon&Quetico group (σ_H and σ_h are the maximum, minimum horizontal stresses, respectively, and σ_v is vertical stress)

6. CONCLUSIONS

This study critically assessed the applicability of statistical tools in characterizing the in-situ stress within the Canadian Shield. Categorizing stress data into depth zones exhibited weaker statistical fitness compared to an ungrouped dataset, indicating limitations in this approach. Oversimplifying areas as 'undisturbed' and assuming linear trends in previous stress-depth overlook the impacts of past tectonic events or ongoing regional geological features. Outlier detection methods and clustering techniques were used to refine the dataset, but their effectiveness was limited. Therefore, solely relying on statistical methods for stress-depth relationships presents challenges, highlighting the importance of integrating geological understanding for accurate modeling. We recommend adopting a region-specific approach considering lithological and tectonic similarities to improve stress estimation and predictive models in the Canadian Shield.

References

Amadei, B. & Stephansson, O. 1997. *Rock stress and its measurement*, Springer Science & Business Media.

Dastjerdy, B., Saeidi, A. & Heidarzadeh, S. 2023. Review of Applicable Outlier Detection Methods to Treat Geomechanical Data. *Geotechnics,* 3**,** 375-396.

Dastjerdy, B., Saeidi, A. & Heidarzadeh, S. 2024. Determination of uncertainties of geomechanical parameters of metamorphic rocks using petrographic analyses. *Journal of Rock Mechanics and Geotechnical Engineering,* 16**,** 345-364.

Herget, G. 1973. First experiences with the CSIR triaxial strain cell for stress determinations. *International Journal of Rock Mechanics and Mining Sciences & Geomechanics Abstracts,* 10**,** 509-522.

Herget, G. High Stress Occurrences In The Canadian Shield. The 23rd U.S Symposium on Rock Mechanics (USRMS), 1982. ARMA-82-203.

JMP-Pro. 2021. SAS Institute Inc. . 16 ed.: SAS Institute Inc. .

Maloney, S., Kaiser, P. & Vorauer, A. A re-assessment of in situ stresses in the Canadian Shield. ARMA US Rock Mechanics/Geomechanics Symposium, 2006. ARMA, ARMA-06-1096.

Yong, S. & Maloney, S. 2015. An update to the Canadian Shield stress database. *Number September*.

Zheng, S., Zhu, Y.-X., Li, D.-Q., Cao, Z.-J., Deng, Q.-X. & Phoon, K.-K. 2021. Probabilistic outlier detection for sparse multivariate geotechnical site investigation data using Bayesian learning. *Geoscience Frontiers,* 12**,** 425-439.

A novel region-specific methodology to characterize in-situ stress-depth relationships in the Canadian Shield

Behzad Dastjerdy, Ali Saeidi

Department of applied sciences, University of Quebec at Chicoutimi, Saguenay, Quebec, Canada

Shahriyar Heidarzadeh

AtkinsRéalis, Montreal, Quebec, Canada

ABSTRACT

The reliable determination of in-situ stress is crucial for ensuring the stability of rock masses in deep underground projects, especially within a geologically complicated area of the Canadian Shield. Despite extensive research, uncertainties persist in stress-depth relationships, necessitating a critical reassessment. This study introduces a novel region-specific methodology, categorizing distinct regions based on lithological and tectonic similarities. By integrating statistical analysis with geological insights, this paper aims to establish robust stress-depth equations aligned with rock engineering principles. We analyzed the profound influence of tectonic activities on stress redistribution across diverse regions and identified key geotectonic events. This region-specific methodology provides practical guidance for future geotechnical projects and contributes to a broader understanding of in-situ stress in the Canadian Shield, addressing uncertainties and enhancing the reliability of stress determinations in underground engineering endeavors. With a comprehensive approach, this study bridges gaps in current knowledge, facilitating safer and more efficient engineering practices.

RÉSUMÉ

La détermination fiable de la contrainte in-situ est cruciale pour garantir la stabilité des massif rocheux dans les projets souterrains, surtout dans la région géologiquement complexe du Bouclier canadien. Malgré des recherches approfondies, des incertitudes persistent dans les relations entre la contrainte et la profondeur, nécessitant une réévaluation critique. Cette étude introduit une nouvelle méthodologie spécifique à la région, catégorisant les régions en fonction de similarités lithologiques et tectoniques. En intégrant l'analyse statistique avec des connaissances géologiques, cette étude vise à établir des équations robustes de contrainte en fonction de la profondeur, améliorant la fiabilité des déterminations de stress dans les projets d'ingénierie souterraine. Cette méthodologie offre un guide pratique pour les futurs projets géotechniques et contribue à une meilleure compréhension du stress in-situ dans le Bouclier canadien, facilitant des pratiques d'ingénierie plus sûres et plus efficaces.

1. INTRODUCTION

The design of underground structures mainly relies on two fundamental considerations: understanding geomechanical parameters and characterizing in-situ stress. Uncertainties in these factors can lead to significant deviations in design outcomes, necessitating a careful mitigation approach (Dastjerdy et al., 2024a). Accurate assessments of in-situ stress are crucial for ensuring the stability of rock masses in deep underground projects, particularly within the complex geological domain of the Canadian Shield. The geological complexity and economic significance of the Canadian Shield may require precise estimations of in-situ stress for mining and geotechnical projects. However, uncertainties persist due to factors like diverse geological history, rock heterogeneity, and measurement limitations (Amadei & Stephansson, 1997; Saeidi et al., 2021). Any significant misinterpretation or inaccuracy in depicting this stress profile, can lead to structural vulnerabilities, elevated safety risks, and potential environmental challenges. Thus, a comprehensive analysis of the Canadian Shield's in-situ stress state is essential, to ensure the safety and efficiency of mining operations in this region. Two main approaches are employed to measure in-situ stresses: direct and indirect methods. Direct methods involve measuring stress within the rock mass using techniques like hydraulic fracturing or overcoring, providing precise measurements. Indirect methods estimate stresses based on observed rock behavior with slight disturbance of rock, such as borehole breakout, and the acoustic method (Kaiser effect).

Despite continuous refinement since the 1970s, challenges persist in understanding stress-depth relationships in the Canadian Shield (Herget, 1973a). Several studies including those by Herget (1982); Maloney et al. (2006); Yong and Maloney (2015), have suggested stress-depth relationships aiming to capture the complexities of the Canadian Shield’s in-situ stress state. Herget (1982) categorized stress-depth data into two ranges (0-900m, 900-2200m), while recent contributions introduced a three-zone categorization: stress-released (0-300m), transition (300-600m), and undisturbed stress zone (600-1500m). However, grouping stress data into depth zones has introduced uncertainty. While this approach offers insights into varying stress trends, the geological justifications for these divisions remain unclear. Arbitrary boundaries between depth domains may skew the stress profile, and labeling vast areas beyond 600m depth as "undisturbed" might oversimplify complexities. Also, most of previous relationships have been linear, suggesting uniform stress changes from near-surface to greater depths, while linear models may not fully capture the complex impacts of past tectonic events and regional geological conditions. In this study, we aim to reassess the adequacy of linear stress-depth relationships and evaluate the potential for more realistic nonlinear models. To address these challenges, this study proposes a novel region-specific methodology for categorizing regions within the Canadian Shield based on lithological and tectonic similarities. By integrating statistical analysis with geological insights, this research aims to develop robust stress-depth relationships aligned with the geological realities of each region, providing practical guidance for future geotechnical projects and contributing to a broader understanding of the in-situ stress state in the Canadian Shield.

2. METHODOLOGY

We introduce a robust methodology to develop stress-depth relationships within the Canadian Shield, as depicted in Figure 1. Step 1 involves collecting and processing stress data from previous campaigns and technical reports, ensuring data accuracy. Next, we critically assess the limitations of relying solely on statistical methods in for developing stress-depth relationships. Step 3 categorizes the stress database based on the Shield's diverse geological regions, considering specific structural and lithological similarities. In Step 4, we analyze the influence of major geotectonic events within each

group, assessing their effects on stress patterns. Finally, Step 5 integrates these insights to establish reliable, region-specific stress-depth relationships tailored to the Shield's unique geotectonic characteristics.

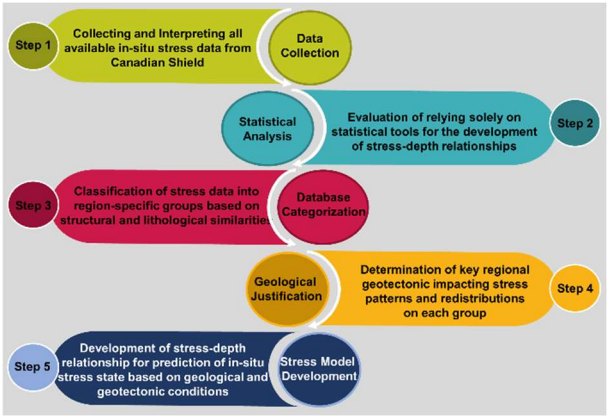

Figure 1. Suggested methodology to develop the in-situ stress-depth relationships in the Canadian Shield

3. STRESS DATA COLLECTION AND INTERPRETATION

In this study, we compiled a substantial dataset of 324 stress values with corresponding orientations, a significantly higher number compared to previous studies. To establish the database, we meticulously compiled all available stress data from various measurement campaigns, including Corthésy et al. (1997); Corthésy and Leite (2013); Golder (2012); Hammoum (2017); Herget (1973a); Lalancette (2018); Maloney et al. (2006); Martin (1990); Yong and Maloney (2015). This dataset covers depths ranging from 11 to 2550 meters. Figure 2 illustrates the geographical distribution of stress data across the Canadian Shield, sourced from three key geological provinces: Grenville (10 datapoints), Southern (59 datapoints), and Superior provinces (255 datapoints). Specifically, within the Superior province, data were obtained from distinct subprovinces—Abitibi, Wawa, Uchi, Berens River, Quetico, Wabigoon, and Pikwitonei—allowed us to conduct a region-specific analysis that considers the unique geological characteristics and stress patterns within each subdivision (Lucas & St-Onge, 1998; Percival et al., 2012).

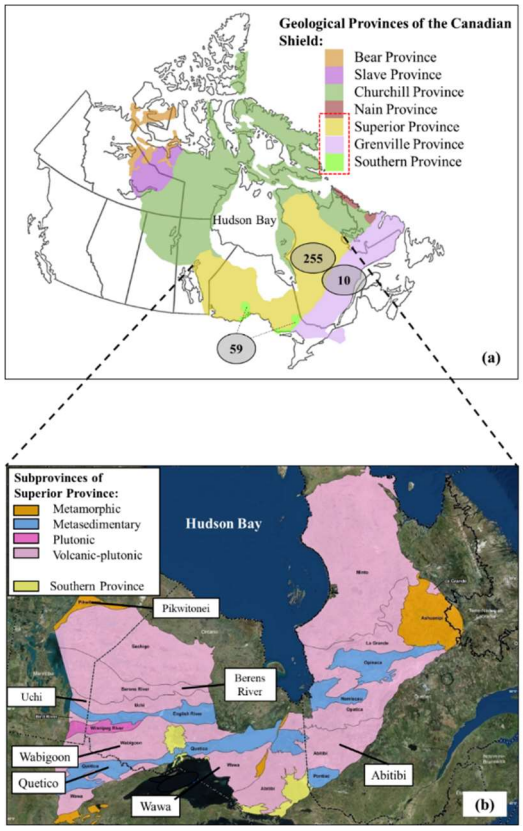

Figure 2. Geographical distribution of collected stress data - (a) Across the Canadian Shield, (b) Within subprovinces of the Superior Province (modified from Lucas and St-Onge (1998)

4. LIMITATION OF STATISTICAL ANALYZING TOOLS TO CHARACTERIZE IN-SITU STRESS

In this section, we evaluate the applicability of using pure statistical analysis to establish stress-depth relationships within the Canadian Shield. We address two key aspects:

4.1. Statistical Assessment of Domain-based Approaches

We systematically apply depth domains, suggested by Maloney et al. (2006), to our dataset of 324 stress values. By grouping data into depth domains, we aim to enhance the applicability of stress-depth equations. However, our analysis reveals lower coefficient of determination values (R^2) within each domain compared to the full data (Figure 3). This suggests that categorizing the Canadian Shield into depth domains leads to less robust predictions, possibly influenced by statistical inferences.

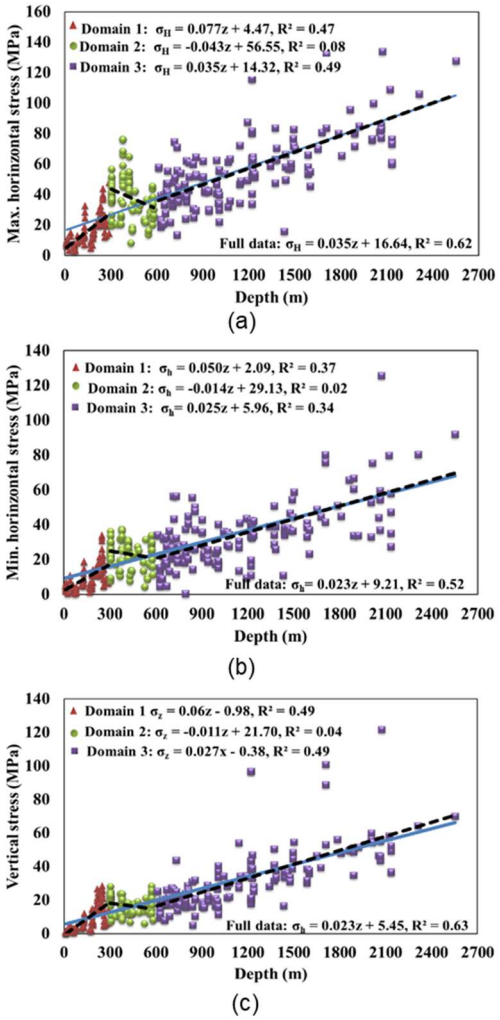

Figure 3. Stress-depth equations using the depth domains, suggested by Maloney et al. (2006)

4.2. Adjusting New Depth Domains by A Clustering Technique

In this section, our aim is to refine the depth domains using statistical tools to categorize the entire stress database effectively. Initially, we employed the Mahalanobis method to detect and eliminate outliers, identifying 25 outliers in the stress-depth data. The Mahalanobis method evaluates the multivariate distance of a data point from the center of the distribution, identifying points with Mahalanobis distances that significantly deviate from the expected range within the distribution (See figure 4 step 1). Subsequently, we conducted cluster analysis to establish meaningful depth domains. In the clustering analysis, we initially quantified the most suitable number of clusters through the Elbow method. This technique involves plotting the variance explained as a function of the number of clusters and identifying the "elbow point," where adding more clusters no longer significantly enhances the model's ability to capture data patterns (Figure 4 step 2).

Using the Mahalanobis method for outlier detection and the Elbow method to determine the optimal number of clusters, we applied hierarchical clustering to define four depth domains: 0-750m, 751-1250m, 1251-1750m, and 1751-2500m (illustrated in Figure 4). However, regression analysis for these clusters yielded lower R^2 compared to the uncategorized dataset, indicating unsatisfactory results in the developed models (as shown in Figure 5).

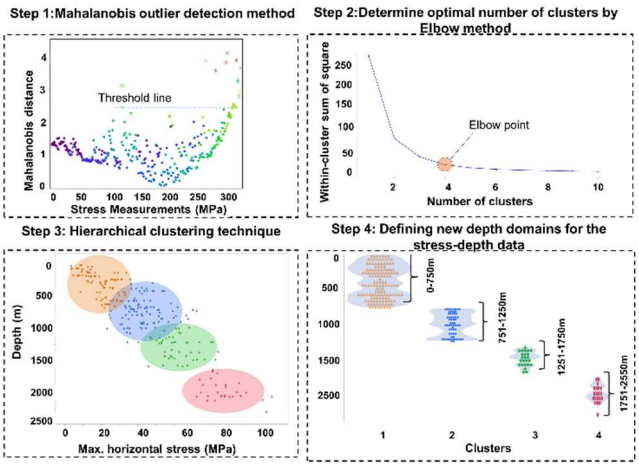

Figure 4. Categorization of Stress database of the Canadian Shield by application of clustering methods

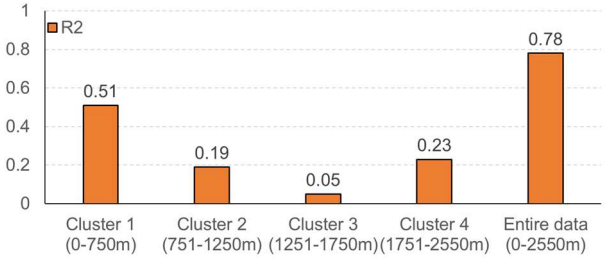

Figure 5. Comparison of statistical robustness for new depth domains with the ungrouped data

Notably, extreme data points, identified and removed as outliers, could carry geological or tectonic significance. Instead of excluding them outright, thorough geological analysis is essential as these outliers may signal unique geological or tectonic conditions. This aspect will be explored further in the subsequent section. In conclusion, relying solely on statistical methods for establishing stress-depth relationships in the Canadian Shield may lead to misleading interpretations. While statistical methods offer insights, their results may prove insufficient, highlighting the importance of integrating geological and geotectonic factors into stress assessments. This integration ensures a more accurate comprehension of geological influences on stress distribution, facilitating the development of dependable predictive models.

5. GEOLOGICAL AND GEOTECTONIC ANALYSIS OF THE CANADIAN SHIELD

The geological and tectonic analysis of the Canadian Shield plays a crucial role in understanding in-situ stress patterns and the uncertainties. We analyzed the Shield's complex geological and history, focusing on three geological provinces— Superior, Southern, and Grenville provinces—where stress data were collected. Notably, the Superior province, comprising 78% of our dataset, holds particular significance. To address uncertainties in regional stress trends, we propose a novel geological classification based on structural characteristics, metamorphism, and lithological composition. These factors profoundly influence the in-situ stress of rocks within the Canadian Shield. Structural characteristics and tectonic history provide insights into the present and past state of geological structures, affecting stress redistributions. Moreover, metamorphism and lithological composition have great impacts on the mechanical behavior of rocks. This classification divides the Canadian Shield into six groups, including Abitibi & Wawa, Wabigoon & Quetico, Uchi & Berens River, Pikwitonei, Grenville, and Southern. In this paper, we focus on stress characterization within the Abitibi & Wawa and Wabigoon & Quetico groups.

The Abitibi & Wawa group features east-west trending structures with significant shear zones and multiple deformation phases, including various folds and volcanic activities such as Timiskaming-

type volcanism. Metamorphism is mainly low-grade, with Abitibi showing regional metamorphism and hydrothermal metasomatism, and Wawa ranging from greenschist to upper amphibolite facies. Both subprovinces have similar lithology, dominated by mafic to intermediate volcanic rocks and common plutonic rocks such as gabbro, diorite, and granite.

The Wabigoon & Quetico group experienced complex tectonics with shear and compressional forces, leading to north-south shortening and significant shear zones. Both subprovinces underwent regional metamorphism, ranging from greenschist to amphibolite facies. Lithologically, they share low- to medium-grade metasedimentary rocks, including mafic gneiss, wacke, siltstone, and iron formations, indicating parallel geological evolution.

5.1. Determination of Key Regional Geotectonic Events

In the Abitibi & Wawa group, two prominent regional tectonic events seem dominant: synvolcanic extension in the Abitibi subprovince and transpressional tectonics in the Wawa subprovince. Synvolcanic extension, depicted in Figure 6(a), involves crustal stretching during volcanic activity, leading to significant faulting and the creation of domal antiforms and volcanic sequences in the Abitibi greenstone belt. Meanwhile, transpressional tectonics, illustrated in Figure 6(b), entail simultaneous compression and displacement in the Wawa subprovince, creating a complex stress environment. Unlike simpler compression or extension-dominated settings, transpression introduces additional stress components that may alter principal stresses. This process in Wawa could trigger structural changes, such as fault reactivation, complex folding, and stress variations with depth, potentially leading to stress redistribution on local and regional scales. These events collectively create intricate stress fields, influencing the in-situ stress state.

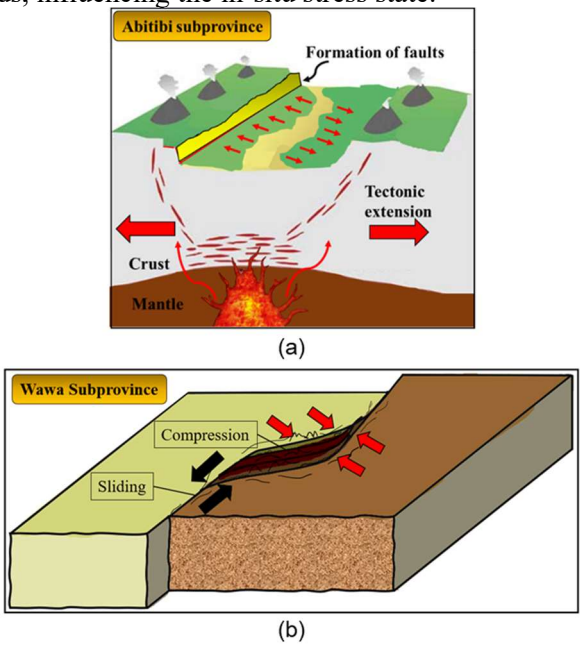

Figure 6. Key regional tectonic event: a) synvolcanic extension in Abitibi, b) transpressional tectonic in the Wawa

In the Wabigoon & Quetico group, the regional geology is significantly shaped by two distinct tectonic processes: thin-skinned and thick-skinned tectonism (Figure 7). Thin-skinned tectonism primarily affects upper crustal layers, initiating with the formation of a décollement layer that facilitates horizontal movement along faults and folds, resulting in compression, folding, or thrusting of overlying sedimentary layers. This process induces structural complexities, leading to localized stress variations near faults or folds. On the other hand, thick-skinned tectonism penetrates deeper into both sedimentary layers and rigid crystalline rocks, driven by intense compressional forces. This

deeper involvement often causes reverse faulting and deep-rooted deformation, potentially uplifting deeper crustal sections to the surface. The combination of these tectonic mechanisms in the Wabigoon & Quetico group creates a complex geological setting with diverse stress variations influenced by both shallow and deep-seated structural processes.

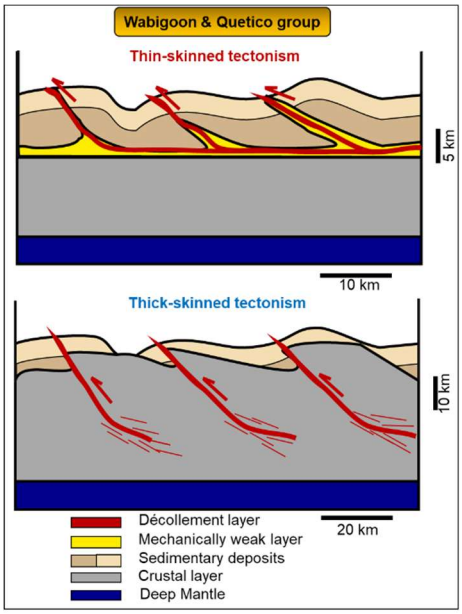

Figure 7. Thin- and thick-skinned tectonism in the Wabigoon & Quetico group

6. DEVELOPMENT OF STRESS-DEPTH RELATIONSHIPS

Through precise regression analyses, we developed reliable stress-depth equations for key parameters including vertical stress (σ_v), maximum and minimum horizontal stresses (σ_H, σ_h), and maximum and minimum stress ratios (K_{max} *and* K_{min}). This approach potentially enhances our understanding of how these key stress parameters change with depth and how they impact the design phase of underground structures in different regions within the Canadian Shield.

Within the Wabigoon & Quetico group, vertical stresses demonstrate a distinctive pattern, deviating significantly from the expected lithostatic pressure line, which can be calculated by $P=\gamma h$ (γ and h are rock density and depth, respectively). Most data points fall beyond a confidence interval of two standard deviations ($\pm 2SD$), indicating considerable variability (Figure 8a). Our regression analysis suggests a nonlinear model for vertical stress in this group ($R^2 = 0.51, \sigma_z = 1.08z^{0.49}$), potentially capturing additional tectonic forces influencing vertical stress beyond the weight of overlying rock layers. It should be noted that while the model's predictability may not be high, this can be accepted due to the high variability in existing scattered data, largely influenced by regional tectonic events such as thin- and thick-skinned tectonism.

Similar trends are observed in horizontal stresses, with higher R^2 values indicating potential influence from regional tectonism (Figure 8b). However, these findings should be approached with caution due to inherent uncertainties in statistical estimations.

Once the vertical and horizontal stress elements were identified, we applied the Anderson faulting method to ascertain the primary stress conditions within the Wabigoon & Quetico group (Anderson, 1951b). According to this principle, the prevailing stress pattern in this area is predominantly characterized by thrust or Revere Faulting (*RF*), where σ_H represents the maximum principal stress, σ_v indicates the minimum principal stress, and σ_h denotes the intermediate stress. This overall tectonic setting is consistent with the Canadian Shield. Figure 8c depicts these trends via a line graph. Despite the dominance of *RF* in governing the stress regime, an intriguing transition to the Strike-Slip (SS) regime occurs within specific depth intervals, notably between 180m and 250m. This finding suggests

that, alongside the prevailing compressive forces, there may exist layers or zones experiencing shear stress, as depicted in Figure 8c.

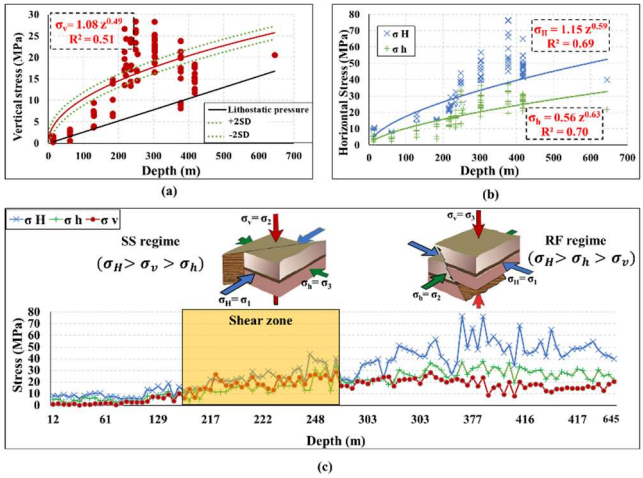

Figure 8. In-situ stress status in the Wabigoon&Quetico: a) Vertical stress (σ_v), b) Maximum horizontal stress (σ_H), and c) Minimum horizontal stress (σ_h)

Furthermore, establishing reliable stress ratio relationships minimizes risks and optimizes construction processes, aiding engineers in anticipating and addressing ground behavior challenges. In the Wabigoon & Quetico group, relationships for two stress ratios, K_{max} and K_{min}, were developed (Figure 9). These equations show a hyperbolic trend similar to well-known models, suggesting alignment with global trends, particularly beyond 500m depth. Moreover, high K values in shallow zones may align reasonably with geotectonic and rock mechanics principles. In contrast, relationships presented by Yong & Maloney (2015) show a constant linear function with a low gradient (-0.0006 for K_{max} and -0.0003 for K_{min}), indicating a less reliable relationship. Despite the coefficient of determination (R2) around 0.50, reflecting substantial data variation, our correlation values stand as the highest among the comparisons. It is worth mentioning that the equations proposed by Herget (1987) and Yong & Maloney (2015) did not provide the associated R2 values, which pose a limitation to their assessment. Table 1 presents the comparison of previous relationships within the Canadian Shield and proposed equations for the Wabigoon&Quetico group.

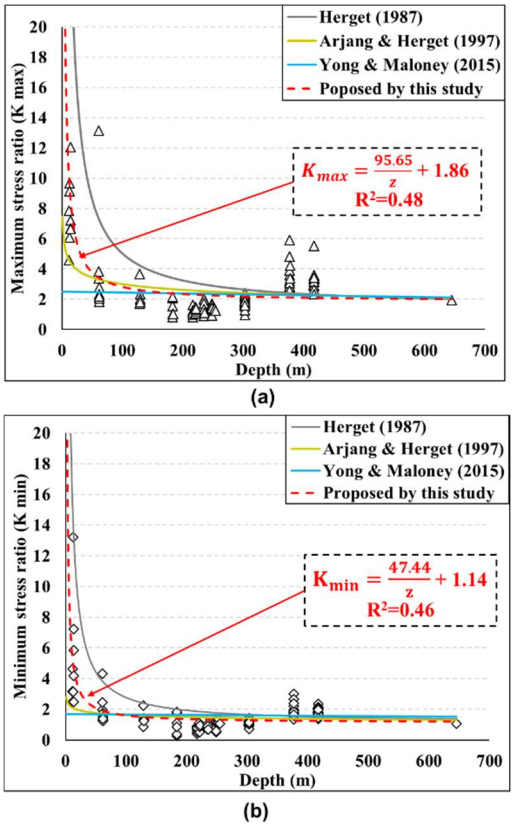

Figure 9. Comparative illustration of regression equations for the Wabigoon&Quetico group with previous models: a) Maximum stress ratio, b) Minimum stress ratio

In the Abitibi&Wawa group, vertical stress closely corresponds to lithostatic pressure ($\sigma_z=0.027z$), while horizontal stresses exhibit a non-linear pattern. This group maintains a minor disparity between the maximum and minimum horizontal stresses. Both equations ($\sigma_H=0.47z^{0.68}$ and $\sigma_h=0.47z^{0.61}$) depict a relatively uniform stress regime, likely influenced by significant regional tectonic activities, such as synvolcanic extension in the Abitibi subprovince and transpressional tectonics in the Wawa subprovince. Figure 10 illustrated the proposed regression lines for these groups within the Canadian Shield.

Table 1. Comparison of stress-depth relationships of the defined groups with past equations for stress ratios (K)

Groups		In-situ stress parameters				
		σ_v	σ_H	σ_h	K_{max}	K_{min}
Wabigoon& Quetico	Eq.	1.08 z^0.49	1.15 z^0.59	0.56 z^0.63	$95.6/z + 1.8$	$47.4/z + 1.1$
	R^2	0.51	0.69	0.70	0.48	0.46
Abitibi& Wawa	Eq.	$0.027z$	0.47 z^0.68	0.47 z^0.61	7.3 z^(−0.19)	3.4 z^(−0.15)
	R^2	0.65	0.66	0.49	0.29	0.18
Entire Shield (Herget (1987))	Eq.	Not applicable			$357/z + 1.46$	$167/z + 1.10$
	R^2				Not provided	
Entire Shield (Arjang & Herget (1997))	Eq.				7.44 z^(−0.198)	2.81 $z^{-0.120}$
	R^2				0.36	0.16
Entire Shield (Yong & Maloney (2015))	Eq.				$-0.0006z + 2.489$	$-0.0003z + 1.705$
	R^2				Not provided	

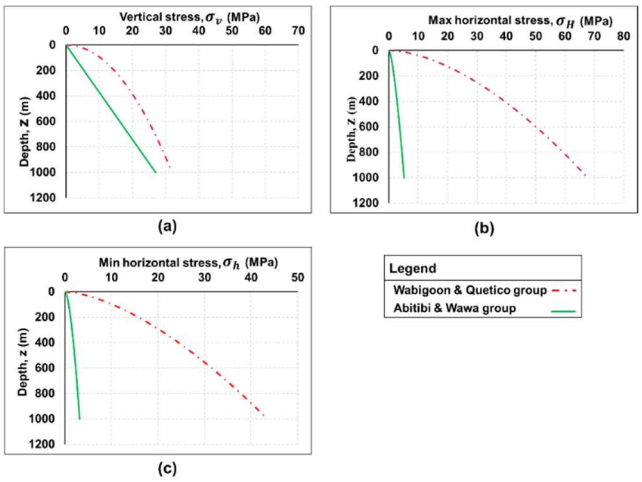

Figure 10. Comparing developed equations of the Abitibi& Wawa group with the Wabigoon & Quetico group

7. CONCLUSIONS

This study aimed to deepen our understanding of in-situ stress in the Canadian Shield, linking geological conditions to stress-depth relationships. Key findings include:

- The proposed methodology categorized the Canadian Shield into six distinct groups based on regional lithological and structural similarities. This innovative approach would enhance the accuracy of stress-depth relationships by capturing the complexities unique to each defined group.
- This study evaluated the use of statistical tools in characterizing in-situ stress in the Canadian Shield. The findings indicated that the previous relationships were significantly influenced by statistical inferences. By highlighting the need for a more geologically justified classification for the in-situ stress data, we argued that arbitrary depth boundaries for stress-depth relationships could oversimplify the complex geological conditions in the Canadian Shield, and also the designated depth-domains for the stress data may not be universally applicable throughout the entire Canadian Shield, lacking a strong reason aligned with rock engineering principles.
- This research identified key regional tectonic events in each geological group, providing potential justifications for deviations in vertical and horizontal stresses. The unique stress-depth relationships within the six defined groups consider regional tectonic events as possible influential factors.

- Regression analyses provided equations for crucial stress parameters, offering valuable engineering insights. Developed stress ratio relationships exhibit better robustness compared to previous models. It is important to note that the proposed relationships may not exhibit very high R^2 values due to the considerable variability in the stress-depth data within the specified groups. This variability can largely be attributed to regional tectonic events, which are a primary factor in this scattering. Nonetheless, our suggested stress ratios demonstrate improved fitness compared to previous estimates. This indicates the robustness of our region-specific methodology in developing stress-depth relationships within the Canadian Shield.

8. REFERENCE

Abdaqadir, Z. K., & Alshkane, Y. M. (2018). Physical and mechanical properties of metamorphic rocks. *Journal of Garmian University*, *5*(2), 160-173.

Adel, S., Mansour, Z., & Ardeshir, H. (2021). Geochemical behavior investigation based on k-means and artificial neural network prediction for titanium and zinc, Kivi region, Iran. *Известия Томского политехнического университета. Инжиниринг георесурсов*, *332*(3), 113-125.

Afraei, S., Shahriar, K., & Madani, S. H. (2018). Statistical analysis of rock-burst events in underground mines and excavations to present reasonable data-driven predictors. *Journal of Statistical Computation and Simulation*, *87*(17), 3336-3376.

Agliardi, F., Sapigni, M., & Crosta, G. (2016). Rock mass characterization by high-resolution sonic and GSI borehole logging. *Rock Mechanics and Rock Engineering*, *49*(11), 4303-4318.

Agliardi, F., Sapigni, M., & Crosta, G. B. (2016). Rock Mass Characterization by High-Resolution Sonic and GSI Borehole Logging. *Rock Mechanics and Rock Engineering*, *49*(11), 4303-4318. https://doi.org/10.1007/s00603-016-1025-x

Akaike, H. (1974). A new look at the statistical model identification. *IEEE transactions on automatic control*, *19*(6), 716-723.

Ali, E., Guang, W., zhiming, Z., & Weixue, J. (2014). Assessments of Strength Anisotropy and Deformation Behavior of Banded Amphibolite Rocks. *Geotechnical and Geological Engineering*, *32*(2), 429-438. https://doi.org/10.1007/s10706-013-9724-5

Almeida, A. P., & Liu, J. (2018). Statistical evaluation of design methods for micropiles in Ontario soils. *DFI Journal-The Journal of the Deep Foundations Institute*, *12*(3), 133-146.

Amadei, B., & Stephansson, O. (1997). *Rock stress and its measurement*. Springer Science & Business Media.

Anderson, E. M. (1951a). *The dynamics of faulting and dike formation with applications to Britain*. Oliver and Boyd, Edinburgh, [1951].

Anderson, E. M. (1951b). The dynamics of faulting and dyke formation with applications to Britain. *(No Title)*.

Anderson, T. W., & Darling, D. A. (1952). Asymptotic theory of certain" goodness of fit" criteria based on stochastic processes. *The annals of mathematical statistics*, 193-212.

Arjang, B. (1989). Pre-mining stresses at some hard rock mines in the Canadian Shield. The 30th US Symposium on Rock Mechanics (USRMS),

Arjang, B. (1998). Canadian crustal stresses and their application in mine design. Mine Planning and Equipment Selection 1998,

Askaripour, M., Saeidi, A., Mercier-Langevin, P., & Rouleau, A. (2022). A Review of Relationship between Texture Characteristic and Mechanical Properties of Rock. *Geotechnics*, *2*(1), 262-296.

Azad, S. T., Moghaddassi, N., & Sayehbani, M. (2022). Digital Shoreline Analysis System improvement for uncertain data detection in measurements. *Environmental Monitoring and Assessment*, *194*(9), 646.

Bao, Y., Song, C., Wang, W., Ye, T., Wang, L., & Yu, L. (2013). Damage Detection of Bridge Structure Based on SVM. *Mathematical Problems in Engineering*, *2013*, 490372. https://doi.org/10.1155/2013/490372

Barbato, G., Barini, E., Genta, G., & Levi, R. (2011). Features and performance of some outlier detection methods. *Journal of Applied Statistics*, *38*(10), 2133-2149.

Barnett, O., & Cohen, A. (2000). The histogram and boxplot for the display of lifetime data. *Journal of Computational and Graphical Statistics*, *9*(4), 759-778.

Barnett, V., & Lewis, T. (1994). *Outliers in statistical data* (Vol. 3). Wiley New York.

Bawa, S., & Singh, S. P. (2020). Analysis of fatigue life of hybrid fibre reinforced self-compacting concrete. *Proceedings of the Institution of Civil Engineers-Construction Materials*, *173*(5), 251-260.

Bennett, T. J., & Marshall, M. E. (2001). Identification of rockbursts and other mining events using regional signals at international monitoring system stations. *Science Applications International Corp Mclean VA*.

Bidgoli, M. N., & Jing, L. (2014). Anisotropy of strength and deformability of fractured rocks. *Journal of Rock Mechanics and Geotechnical Engineering*, *6*(2), 156-164.

Blake, W. (1972). Rock burst mechanics. *1970-1979-Mines Theses & Dissertations*.

Blake, W., & Hedley, D. G. (2003). *Rockbursts: case studies from North American hard-rock mines*. SME.

Board, M., & Voegele, M. (1981). EXAMINATION AND DEMONSTRATION OF UNDERCUT AND FILL STOPPING FOR GROUND CONTROL IN DEEP VEIN MINING.

Bolla, A., & Paronuzzi, P. (2021). *UCS field estimation of intact rock using the Schmidt hammer: A new empirical approach* IOP Conference Series: Earth and Environmental Science,

Borosnyói, A. (2014). Variability case study based on in-situ rebound hardness testing of concrete: Part 1. Statistical analysis of inherent variability parameters. *Építöanyag (Online)*(3), 85.

Bouzeran, L., Pierce, M., Andrieux, P., & Williams, E. (2019, 24-25 June 2019). *Accounting for rock mass heterogeneity and buckling mechanisms in the study of excavation performance in foliated ground at Westwood mine* Deep Mining 2019: Proceedings of the Ninth International Conference on Deep and High Stress Mining, Muldersdrift. https://papers.acg.uwa.edu.au/p/1952_03_Bouzeran/

Bozorgzadeh, N., Dolowy-Busch, M., & Harrison, J. P. (2015). *Obtaining Robust Estimates of Rock Strength for Rock Engineering Design* 13th ISRM International Congress of Rock Mechanics,

Brady, B. H. G. (1979). *Boundary element methods for mine design* University of London].

Brown, E., & Hoek, E. (1978). Technical note trends in relationships between measured in-situ stress and depth. *Int. J. Rock Mech. Min. Sci. and Geomech. Abstr*, *15*(4), 211-215.

Cai, M. (2013). Principles of rock support in burst-prone ground. *Tunnelling and Underground Space Technology*, *36*, 46-56. https://doi.org/https://doi.org/10.1016/j.tust.2013.02.003

Cai, M. (2016). Prediction and prevention of rockburst in metal mines – A case study of Sanshandao gold mine. *Journal of Rock Mechanics and Geotechnical Engineering*, *8*(2), 204-211. https://doi.org/https://doi.org/10.1016/j.jrmge.2015.11.002

Cai, M., Kaiser, P. K., Morioka, H., Minami, M., Maejima, T., Tasaka, Y., & Kurose, H. (2007). FLAC/PFC coupled numerical simulation of AE in large-scale underground excavations. *International Journal of Rock Mechanics and Mining Sciences*, *44*(4), 550-564. https://doi.org/https://doi.org/10.1016/j.ijrmms.2006.09.013

Cai, M., Kaiser, P. K., Uno, H., Tasaka, Y., & Minami, M. (2004). Estimation of rock mass deformation modulus and strength of jointed hard rock masses using the GSI system. *International Journal of Rock Mechanics and Mining Sciences*, *41*(1), 3-19. https://doi.org/https://doi.org/10.1016/S1365-1609(03)00025-X

Card, K. (1990). A review of the Superior Province of the Canadian Shield, a product of Archean accretion. *Precambrian research*, *48*(1-2), 99-156.

Card, K., & Ciesielski, A. (1986). Subdivisions of the Superior Province of the Canadian shield. *Geoscience Canada*.

Carling, K. (2000). Resistant outlier rules and the non-Gaussian case. *Computational statistics & data analysis*, *33*(3), 249-258. https://doi.org/https://doi.org/10.1016/S0167-9473(99)00057-2

Carmona, S., Molins, C., Aguado, A., & Mora, F. (2016). Distribution of fibers in SFRC segments for tunnel linings. *Tunnelling and Underground Space Technology*, *51*, 238-249.

Carter, T. (2021). Towards improved definition of numerical modelling the Hoek-Brown constant m i for. *The Evolution of Geotech-25 Years of Innovation*, 93.

Castro, L., Bewick, R., & Carter, T. (2012). An overview of numerical modelling applied to deep mining. *Innovative numerical modelling in geomechanics*, 393-414.

Chambers, J. M., Cleveland, W. S., Kleiner, B., & Tukey, P. A. (2018). *Graphical methods for data analysis*. Chapman and Hall/CRC.

Chauvenet, W. (1960). *A manual of spherical and practical astronomy, (Spherical astronomy)* (5th ed., Vol. 1). Dover Publication.

Chen, X., Cao, W., Gan, C., Ohyama, Y., She, J., & Wu, M. (2021). Semi-supervised support vector regression based on data similarity and its application to rock-mechanics parameters estimation. *Engineering Applications of Artificial Intelligence*, *104*, 104317. https://doi.org/https://doi.org/10.1016/j.engappai.2021.104317

Choi, S.-I., Shim, S., Kong, S.-M., Kim, Y. B., & Lee, S.-W. (2022). Efficiency Analysis of Filter-Based Calibration Technique to Improve Tunnel Measurement Reliability. *KSCE Journal of Civil Engineering*, *26*(6), 2926-2938.

Chown, E., Daigneault, R., Mueller, W., & Mortensen, J. (1992). Tectonic evolution of the northern volcanic zone, Abitibi belt, Quebec. *Canadian Journal of Earth Sciences*, *29*(10), 2211-2225.

Connor Langford, J., & Diederichs, M. S. (2015). Quantifying uncertainty in Hoek–Brown intact strength envelopes. *International Journal of Rock Mechanics and Mining Sciences*, *74*, 91-102. https://doi.org/https://doi.org/10.1016/j.ijrmms.2014.12.008

Corfu, F., & Stone, D. (1998). Age structure and orogenic significance of the Berens River composite batholiths, western Superior Province. *Canadian Journal of Earth Sciences*, *35*(10), 1089-1109.

Corkum, A., Damjanac, B., & Lam, T. (2018). Variation of horizontal in situ stress with depth for long-term performance evaluation of the Deep Geological Repository project access shaft. *International Journal of Rock Mechanics and Mining Sciences*, *107*, 75-85.

Corthésy, R., Gill, D. E., & Leite, M. H. (1997). Élaboration d'un modèle de prédiction des contraintes in-situ dans le nord-ouest Québécois.

Corthésy, R., & Leite, M. (2000). *Mesure de contraintes in situ, Mine Niobec (In French)* (Centre de développement technologique de l'École Polytechnique, Issue 1).

Corthésy, R., & Leite, M. (2013). *Mesure de contraintes in situ, Mine Niobec - Niveau 2400 (In French)*.

Corthésy, R., Leite, M. H., & Gill, D. E. (1996). Mesures des contraintes in-situ à la mine Kiena: projet IRSST.

Couëslan, C. (2019). *Field Trip Guidebook: Stratigraphy and ore deposits in the Thompson nickel belt, Manitoba*. M. G. Survey.

Cui, Z. S. Q. L. Q. Z. G. I. t. A. o. M. P. o. S. R. w. P. N. M. (2021). *Sustainability*, *13*(2).

Dai, J., Gong, F., & Xu, L. (2024). Rockburst criterion and evaluation method for potential rockburst pit depth considering excavation damage effect. *Journal of Rock Mechanics and Geotechnical Engineering*, *16*(5), 1649-1666.

Dastjerdy, B., Saeidi, A., & Heidarzadeh, S. (2023). Review of Applicable Outlier Detection Methods to Treat Geomechanical Data. *Geotechnics*, *3*(2), 375-396. https://www.mdpi.com/2673-7094/3/2/22

Dastjerdy, B., Saeidi, A., & Heidarzadeh, S. (2024a). Determination of uncertainties of geomechanical parameters of metamorphic rocks using petrographic analyses. *Journal of Rock Mechanics and Geotechnical Engineering*, *16*(2), 345-364. https://doi.org/https://doi.org/10.1016/j.jrmge.2023.09.011

Dastjerdy, B., Saeidi, A., & Heidarzadeh, S. (2024b). *A novel region-specific methodology to characterize in-situ stress-depth relationships in the Canadian Shield* GeoMontreal 2024, Montreal.

Dastjerdy, B., Saeidi, A., & Heidarzadeh, S. (2024c). *A Proper Methodology to Characterize the Associated Variability of UCS Data for the Metamorphic Rocks Based on Outlier Detection Methods* Geo-Congress 2024, https://ascelibrary.org/doi/abs/10.1061/9780784485309.002

Davis, D. W. (2002). U–Pb geochronology of Archean metasedimentary rocks in the Pontiac and Abitibi subprovinces, Quebec, constraints on timing, provenance and regional tectonics. *Precambrian research*, *115*(1), 97-117. https://doi.org/https://doi.org/10.1016/S0301-9268(02)00007-4

Dawson, R. (2011). How significant is a boxplot outlier? *Journal of Statistics Education*, *19*(2).

Dight, P., & Hsieh, A. (2016). The study of stress determination and back calculation in the canadian shield. ISRM International Symposium on In-Situ Rock Stress,

Dindarloo, S. R., & Siami-Irdemoosa, E. (2015a). Maximum surface settlement based classification of shallow tunnels in soft ground. *Tunnelling Underground Space Technology*, *49*, 320-327.

Dindarloo, S. R., & Siami-Irdemoosa, E. (2015b). Maximum surface settlement based classification of shallow tunnels in soft ground. *Tunn. Undergr. Space Technol.*, *49*, 320-327.

Dixon, W. J. (1950). Analysis of extreme values. *The Annals of Mathematical Statistics*, *21*(4), 488-506.

Doerffel, K. (1967). *Die statistische Auswertung von Analysenergebnissen* (Vol. 2). Springer.

Dovoedo, Y., & Chakraborti, S. (2015). Boxplot-based outlier detection for the location-scale family. *Communications in statistics-simulation and computation*, *44*(6), 1492-1513.

Duchnowski, R. (2010). Median-based estimates and their application in controlling reference mark stability. *Journal of surveying engineering*, *136*(2), 47-52.

Fanjie, Y., Hui, Z., Haibin, X., Azhar, M. U., Yong, Z., & Fudong, C. (2022). Numerical simulation method for the process of rockburst. *Engineering Geology*, *306*, 106760.

Feng, X.-T. (2017). *Rockburst: mechanisms, monitoring, warning, and mitigation*. Butterworth-Heinemann.

Fossen, H. (2016). *Structural geology*. Cambridge university press.

Garces, D., Rebolledo, H., & Miranda, P. (2020). Incorporating vulnerability of hang-ups and secondary breaking to drawpoints availability for short-term cave plans, El Teniente mine. MassMin 2020: Proceedings of the Eighth International Conference & Exhibition on Mass Mining,

García, A., Castro-Fresno, D., Polanco, J., & Thomas, C. (2012). Abrasive wear evolution in concrete pavements. *Road Materials and Pavement Design*, *13*(3), 534-548.

Gercek, H. (2007). Poisson's ratio values for rocks. *International Journal of Rock Mechanics and Mining Sciences*, *44*(1), 1-13.

Ghosh, D., & Vogt, A. (2012). Outliers: An evaluation of methodologies. Joint statistical meetings,

Gignac, G. (2019). *How2statsbook (online edition 1)*. http://www.how2statsbook.com/

Gignac, G. E. (2019). *How2statsbook - Online digital book, Chapter 2 "Descriptive Statistics"* (1st ed.). http://www.how2statsbook.com/

Gill, D. E., Corthésy, R., & Leite, M. H. (2005). Determining the minimal number of specimens for laboratory testing of rock properties. *Engineering Geology*, *78*(1-2), 29-51.

Goktan, R., & Ayday, C. (1993). A suggested improvement to the Schmidt rebound hardness ISRM suggested method with particular reference to rock machineability. *International Journal of Rock Mechanics and Mining Sciences*, *30*(3).

Goktan, R., & Gunes, N. (2005). A comparative study of Schmidt hammer testing procedures with reference to rock cutting machine performance prediction. *International Journal of Rock Mechanics and Mining Sciences*, *42*(3), 466-472.

Golder. (2012). *Review of In-situ stress measurements at Niobec Mine: Project 002-11-1221-0087 MTA Rev0*.

Gong, F., Dai, J., & Xu, L. (2023). A strength-stress coupling criterion for rockburst: Inspirations from 1114 rockburst cases in 197 underground rock projects. *Tunnelling and Underground Space Technology*, *142*, 105396.

Grubbs, F. E. (1950). Sample Criteria for Testing Outlying Observations. *The Annals of Mathematical Statistics*, *21*(1), 27-58, 32. https://doi.org/10.1214/aoms/1177729885

Gul, M., Kotak, Y., Muneer, T., & Ivanova, S. (2018). Enhancement of albedo for solar energy gain with particular emphasis on overcast skies. *Energies*, *11*(11), 2881.

Gumbel, E. (1958). *Statistics of Extremes*. Columbia University Press.

Hadi, A. S., Imon, A. R., & Werner, M. (2009). Detection of outliers. *Wiley Interdisciplinary Reviews: Computational Statistics*, *1*(1), 57-70.

Hammoum, S. (2017). *Modélisation numérique du comportement mécanique d'une excavation à grande profondeur à l'aide d'une loi d'écrouissage tenant compte des effets du temps-application à la mine Westwood (In French)*. Ecole Polytechnique, Montreal (Canada).

Han, L., Wang, L., & Zhang, W. (2020). Quantification of statistical uncertainties of rock strength parameters using Bayesian-based Markov Chain Monte Carlo method. IOP Conference Series: Earth and Environmental Science,

Hassanpour, J., Rostami, J., Khamehchiyan, M., Bruland, A., & Tavakoli, H. (2010). TBM performance analysis in pyroclastic rocks: a case history of Karaj water conveyance tunnel. *Rock Mech Rock Eng*, *43*(4), 427-445.

Hawkes, I. (1966). Significance of in-situ stress levels. *Proc. 1st Intl. Cong. Intl. Soc. of Rock Mech*, *3*, 445-463.

He, M., Cheng, T., Qiao, Y., & Li, H. (2023). A review of rockburst: Experiments, theories, and simulations. *Journal of Rock Mechanics and Geotechnical Engineering*, *15*(5), 1312-1353.

He, S., Song, D., He, X., Li, Z., Chen, T., Shen, F., Chen, J., & Mitri, H. (2023). Numerical modelling of rockburst mechanism in a steeply dipping coal seam. *Bulletin of Engineering Geology and the Environment*, *82*(7), 261.

Hedley, D. G. (1992). Rockburst handbook for Ontario hardrock mines. *(No Title)*.

Heidarzadeh, S., Saeidi, A., Lavoie, C., & Rouleau, A. (2021a). Geomechanical characterization of a heterogenous rock mass using geological and laboratory test results: a case study of the Niobec Mine, Quebec (Canada). *SN Applied Sciences*, *3*, 1-20.

Heidarzadeh, S., Saeidi, A., Lavoie, C., & Rouleau, A. (2021b). Geomechanical characterization of a heterogenous rock mass using geological and laboratory test results: a case study of the Niobec Mine, Quebec (Canada). *SN Applied Sciences*, *3*(6), 1-20.

Herget, G. (1973a). First experiences with the CSIR triaxial strain cell for stress determinations. *International Journal of Rock Mechanics and Mining Sciences & Geomechanics Abstracts*, *10*(6), 509-522.

Herget, G. (1973b). First experiences with the CSIR triaxial strain cell for stress determinations. International Journal of Rock Mechanics and Mining Sciences & Geomechanics Abstracts,

Herget, G. (1973c). Variation of rock stresses with depth at a Canadian iron mine. *International Journal of Rock Mechanics and Mining Sciences & Geomechanics Abstracts*, *10*(1), 37-51. https://doi.org/https://doi.org/10.1016/0148-9062(73)90058-2

Herget, G. (1980). Regional stresses in the Canadian Shield. 13th Canadian Rock Mechanics Symposium, The Canadian Institute of Mining and Metallurgy,

Herget, G. (1982). High Stress Occurrences In The Canadian Shield. The 23rd U.S Symposium on Rock Mechanics (USRMS),

Herget, G. (1987). Stress assumptions for underground excavations in the Canadian Shield. International Journal of Rock Mechanics and Mining Sciences & Geomechanics Abstracts,

Herget, G., & Arjang, B. (1990). Update on ground stresses in the Canadian Shield. *Proc. Stresses in Underground Structures, Ottawa (Eds. Herget G, Arjang B, Bétournay M, Gyenge M, Vongpaisal S, Yu Y)*, 33-47.

Hoaglin, D. C., & Iglewicz, B. (1987). Fine-Tuning Some Resistant Rules for Outlier Labeling. *Journal of the American Statistical Association*, *82*(400), 1147-1149. https://doi.org/10.2307/2289392

Hoek, E., & Brown, E. (2019). The Hoek–Brown failure criterion and GSI–2018 edition. *Journal of Rock Mechanics and Geotechnical Engineering*, *11*(3), 445-463.

Hopgood, A. M. (1987). Imbricate structure. In *Structural Geology and Tectonics* (pp. 334-336). Springer Berlin Heidelberg. https://doi.org/10.1007/3-540-31080-0_50

Hubert, M., & Vandervieren, E. (2008). An adjusted boxplot for skewed distributions. *Computational statistics & data analysis*, *52*(12), 5186-5201.

Hunt, R. E. (2005). *Geotechnical engineering investigation handbook*. Crc Press.

Hussain, I., & Uddin, M. (2019). Functional and multivariate hydrological data visualization and outlier detection of Sukkur Barrage. *International Journal of Computer Applications*, *178*(28), 20-29.

IAMGOLD. (2019a). *IAMGOLD Corporation - Exploitations - The Westwood Gold Mine*. http://www.iamgold.com/French/exploitations/mines-en-exploitation/projet-westwood-canada/default.aspx

IAMGOLD. (2019b). *IAMGOLD Corporation- Exploitations- the Westwood Gold Mine.* http://www.iamgold.com/French/exploitations/mines-en-exploitation/projet

westwood-canada/default.aspx

Iglewicz, B., & Hoaglin, D. C. (1993). *How to detect and handle outliers* (Vol. 16). Asq Press.

JMP-Pro. (2021). *JMP Pro. V.17 Software*. In SAS Institute Inc.

JMP-Pro. (2021). *SAS Institute Inc.* . In (Version 16) SAS Institute Inc. .

Kaiser, P. (2019). From common to best practices in underground rock engineering. ISRM Congress,

Kaiser, P., Maloney, S., & Yong, S. (2016). Role of large scale heterogeneities on in-situ stress and induced stress fields. ARMA US Rock Mechanics/Geomechanics Symposium,

Kaiser, P. K., & Cai, M. (2012). Design of rock support system under rockburst condition. *Journal of Rock Mechanics and Geotechnical Engineering*, *4*(3), 215-227. https://doi.org/https://doi.org/10.3724/SP.J.1235.2012.00215

Kalenchuk, K., Mercer, R., & Williams, E. (2017). Large-magnitude seismicity at the Westwood mine, Quebec, Canada. Deep Mining 2017: Proceedings of the Eighth International Conference on Deep and High Stress Mining,

Kamari, A., Khaksar-Manshad, A., Gharagheizi, F., Mohammadi, A. H., & Ashoori, S. (2013). Robust model for the determination of wax deposition in oil systems. *Industrial & Engineering Chemistry Research*, *52*(44), 15664-15672.

Kannan, K. S., Manoj, K., & Arumugam, S. (2015). Labeling methods for identifying outliers. *International Journal of Statistics and Systems*, *10*(2), 231-238.

Khanlari, G.-R., Heidari, M., Sepahigero, A.-A., & Fereidooni, D. (2014). Quantification of strength anisotropy of metamorphic rocks of the Hamedan province, Iran, as determined from

cylindrical punch, point load and Brazilian tests. *Engineering Geology*, *169*, 80-90. https://doi.org/https://doi.org/10.1016/j.enggeo.2013.11.014

Kim, H.-S., Kim, H.-K., Shin, S.-Y., & Chung, C.-K. (2012). Application of statistical geo-spatial information technology to soil stratification in the Seoul metropolitan area. *Georisk: Assessment and Management of Risk for Engineered Systems and Geohazards*, *6*(4), 221-228.

Kim, H.-S., Sun, C.-G., Lee, M.-G., & Cho, H.-I. (2021). Multivariate geotechnical zonation of seismic site effects with clustering-blended model for a city area, South Korea. *Engineering Geology*, *294*, 106365.

Kimber, A. (1990). Exploratory data analysis for possibly censored data from skewed distributions. *Journal of the Royal Statistical Society Series C: Applied Statistics*, *39*(1), 21-30.

Koca, M. Y., & Kıncal, C. (2022). A new approach to the anisotropy classification based on curve length measurement method: a case study in Ürkmez dam site-İzmir, Türkiye. *Arabian Journal of Geosciences*, *15*(17), 1-26.

Kor, K., Ertekin, S., Yamanlar, S., & Altun, G. (2021). Penetration rate prediction in heterogeneous formations: A geomechanical approach through machine learning. *Journal of Petroleum Science and Engineering*, *207*, 109138.

Kottegoda, N. T., & Rosso, R. (2008). Applied statistics for civil and environmental engineers.

Kouame Arthur Joseph, K., Fuxing, J., Sitao, Z., & Yu, F. (2017). OVERVIEW OF ROCK BURST RESEARCH IN CHINA AND ITS APPLICATION IN IVORY COAST. *GEOMATE Journal*, *12*(29), 204-211. https://geomatejournal.com/geomate/article/view/916

Kwak, S. K., & Kim, J. H. (2017). Statistical data preparation: management of missing values and outliers. *Korean journal of anesthesiology*, *70*(4), 407-411.

Labat, G., Gervais, F., Kavanagh-Lepage, C., Jannin, S., & Crowley, J. L. (2020). Ductile nappe extrusion in constrictive strain at the origin of transverse segments of the Allochthon Boundary Thrust in the Manicouagan Imbricate Zone (Central Grenville Province, Québec). *Journal of Structural Geology*, *138*, 104117.

Lach, S. (2018). The application of selected statistical tests in the detection and removal of outliers in water engineering data based on the example of piezometric measurements at the Dobczyce dam over the period 2012-2016. E3S Web of Conferences,

Lalancette, S. (2018). *Dimensionnement des chantiers remblayés de la mine Niobec en utilisant la modélisation 3D* Université du Québec à Chicoutimi].

Langford, J. C. (2013). *Application of reliability methods to the design of underground structures*. Queen's University (Canada).

Lehmann, R. (2015). Observation error model selection by information criteria vs. normality testing. *Studia Geophysica et Geodaetica*, *59*(4), 489-504. https://doi.org/10.1007/s11200-015-0725-0

Li, D., Liu, Z., Armaghani, D. J., Xiao, P., & Zhou, J. (2022). Novel ensemble tree solution for rockburst prediction using deep forest. *Mathematics*, *10*(5), 787.

Li, S., Wang, Y., & Xie, X. (2021). Prediction of Uniaxial Compression Strength of Limestone Based on the Point Load Strength and SVM Model. *Minerals*, *11*(12), 1387.

Li, X. (2014). Rock dynamics fundamentals and applications. *Science, Beijing*.

Liang, W., Sari, A., Zhao, G., McKinnon, S. D., & Wu, H. (2020). Short-term rockburst risk prediction using ensemble learning methods. *Natural Hazards*, *104*(2), 1923-1946.

Liang, W., Zhao, G., Wu, H., & Dai, B. (2019). Risk assessment of rockburst via an extended MABAC method under fuzzy environment. *Tunnelling and Underground Space Technology*, *83*, 533-544.

Limb, B. J., Work, D. G., Hodson, J., & Smith, B. L. (2017). The Inefficacy of Chauvenet's Criterion for Elimination of Data Points. *Journal of Fluids Engineering*, *139*(5).

Lin, S., Zheng, H., Han, C., Han, B., & Li, W. (2021). Evaluation and prediction of slope stability using machine learning approaches. *Frontiers of Structural and Civil Engineering*, *15*(4), 821-833.

Liu, X., & Wang, E. (2018). Study on characteristics of EMR signals induced from fracture of rock samples and their application in rockburst prediction in copper mine. *Journal of Geophysics and Engineering*, *15*(3), 909-920.

Lu, H., Li, H., & Meng, X. (2022). Spatial Variability of the Mechanical Parameters of High-Water-Content Soil Based on a Dual-Bridge CPT Test. *Water*, *14*(3), 343. https://www.mdpi.com/2073-4441/14/3/343

Lucas, S. B., & St-Onge, M. (1998). *Geology of the precambrian Superior and Grenville Provinces and precambian fossils in North America*. Geological Society of America.

Ludden, J., Hubert, C., & Gariépy, C. (1986). The tectonic evolution of the Abitibi greenstone belt of Canada. *Geological Magazine*, *123*(2), 153-166.

Ma, T.-H., Tang, C.-A., Tang, S.-B., Kuang, L., Yu, Q., Kong, D.-Q., & Zhu, X. (2018). Rockburst mechanism and prediction based on microseismic monitoring. *International Journal of Rock Mechanics and Mining Sciences*, *110*, 177-188.

Madritsch, H., Schmid, S. M., & Fabbri, O. (2008). Interactions between thin- and thick-skinned tectonics at the northwestern front of the Jura fold-and-thrust belt (eastern France). *Tectonics*, *27*(5). https://doi.org/https://doi.org/10.1029/2008TC002282

Maloney, S., Kaiser, P., & Vorauer, A. (2006). A re-assessment of in situ stresses in the Canadian Shield. ARMA US Rock Mechanics/Geomechanics Symposium,

Manouchehrian, A., & Cai, M. (2018). Numerical modeling of rockburst near fault zones in deep tunnels. *Tunnelling and Underground Space Technology*, *80*, 164-180. https://doi.org/https://doi.org/10.1016/j.tust.2018.06.015

Manouchehrian, A., Gholamnejad, J., & Sharifzadeh, M. (2014). Development of a model for analysis of slope stability for circular mode failure using genetic algorithm. *Environmental Earth Sciences*, *71*, 1267-1277.

Manouchehrian, A., Sharifzadeh, M., & Moghadam, R. H. (2012). Application of artificial neural networks and multivariate statistics to estimate UCS using textural characteristics. *Int J Min Sci Technol*, *22*(2), 229-236. https://doi.org/https://doi.org/10.1016/j.ijmst.2011.08.013

Martin, C. (1990). Characterizing in situ stress domains at the AECL Underground Research Laboratory. *Canadian Geotechnical Journal*, *27*(5), 631-646.

Martin, C., Kaiser, P., & Christiansson, R. (2003). Stress, instability and design of underground excavations. *International Journal of Rock Mechanics and Mining Sciences*, *40*(7-8), 1027-1047.

Martin, C. D., Kaiser, P. K., & Christiansson, R. (2003). Stress, instability and design of underground excavations. *International Journal of Rock Mechanics and Mining Sciences*, *40*(7), 1027-1047. https://doi.org/https://doi.org/10.1016/S1365-1609(03)00110-2

MATLAB R2022a. In. (2022). MathWorks.

Mazaira, A., & Konicek, P. (2015). Intense rockburst impacts in deep underground construction and their prevention. *Canadian Geotechnical Journal*, *52*(10), 1426-1439. https://doi.org/10.1139/cgj-2014-0359

Mazraehli, M., & Zare, S. (2020). An application of uncertainty analysis to rock mass properties characterization at porphyry copper mines. *Bulletin of Engineering Geology and the Environment*, *79*(7), 3721-3739.

Meng, F., Wong, L. N. Y., & Zhou, H. (2021). Rock brittleness indices and their applications to different fields of rock engineering: A review. *Journal of Rock Mechanics and Geotechnical Engineering*, *13*(1), 221-247.

Minitab. In. (2021). (Version 20.3) Minitab, LLC. . https://www.minitab.com/

Miranda, E. E. (1972). Deformation and fracture of concrete under uniaxial impact loading.

Misra, S., Chakravarty, A., Bhoumick, P., & Rai, C. S. (2019). Unsupervised clustering methods for noninvasive characterization of fracture-induced geomechanical alterations. *Machine Learning for Subsurface Characterization*, *39*.

Mitchell, F. (2007). Structural analysis of brittle deformation features along Grenvillian shear zones in southeastern Ontario

Mohammadi, Y., & Kaushik, S. (2005). Flexural fatigue-life distributions of plain and fibrous concrete at various stress levels. *Journal Of Materials in civil engineering*, *17*(6), 650-658.

Monteiro, D. D., Duque, M. M., Chaves, G. S., Ferreira Filho, V. M., & Baioco, J. S. (2020). Using data analytics to quantify the impact of production test uncertainty on oil flow rate forecast. *Oil & Gas Science and Technology–Revue d'IFP Energies nouvelles*, *75*, 7.

Muscolino, G., Genovese, F., & Sofi, A. (2022). Reliability bounds for structural systems subjected to a set of recorded accelerograms leading to imprecise seismic power spectrum. *ASCE-ASME Journal of Risk and Uncertainty in Engineering Systems, Part A: Civil Engineering*, *8*(2), 04022009.

Naji, A. M., Rehman, H., Emad, M. Z., & Yoo, H. (2018). Impact of shear zone on rockburst in the deep neelum-jehlum hydropower tunnel: A numerical modeling approach. *Energies*, *11*(8), 1935.

Nazareth, A. F. D. V., & Lana, M. S. (2021). A methodology for the definition of geotechnical mine sectors based on multivariate cluster analysis. *Geotechnical and Geological Engineering*, *39*, 4405-4426.

Olewuezi, N. (2011). Note on the comparison of some outlier labeling techniques. *Journal of Mathematics and Statistics*, *7*(4), 353-355.

Owusu-Ansah, D., Tinoco, J., Lohrasb, F., Martins, F., & Matos, J. (2023). A decision tree for rockburst conditions prediction. *Applied Sciences*, *13*(11), 6655.

Pan, J., Bai, Z., Cao, Y., Zhou, W., & Wang, J. (2017). Influence of soil physical properties and vegetation coverage at different slope aspects in a reclaimed dump. *Environmental Science and Pollution Research*, *24*, 23953-23965.

Peirce, B. (1852). Criterion for the rejection of doubtful observations. *The Astronomical Journal*, *2*, 161-163.

Peng, S., & Zhang, J. (2007). Rock properties and mechanical behaviors. In *Engineering Geology for Underground Rocks* (pp. 1-26). Springer Berlin Heidelberg. https://doi.org/10.1007/978-3-540-73295-2_1

Pepe, G., Cevasco, A., Gaggero, L., & Berardi, R. (2017a). Variability of intact rock mechanical properties for some metamorphic rock types and its implications on the number of test specimens. *Bulletin of Engineering Geology and the Environment*, *76*(2), 629-644.

Pepe, G., Cevasco, A., Gaggero, L., & Berardi, R. (2017b). Variability of intact rock mechanical properties for some metamorphic rock types and its implications on the number of test specimens. *Bull. Eng. Geol. Environ.*, *76*(2), 629-644.

Percival, J. A., & Easton, R. M. (2007). *Geology of the Canadian Shield in Ontario: an update; Ontario Geological Survey, Open File Report 6196*.

Percival, J. A., McNicoll, V., Brown, J. L., & Whalen, J. B. (2004). Convergent margin tectonics, central Wabigoon subprovince, Superior Province, Canada. *Precambrian research*, *132*(3), 213-244. https://doi.org/https://doi.org/10.1016/j.precamres.2003.12.016

Percival, J. A., Sanborn-Barrie, M., Skulski, T., Stott, G., Helmstaedt, H., & White, D. (2006). Tectonic evolution of the western Superior Province from NATMAP and Lithoprobe studies. *Canadian Journal of Earth Sciences*, *43*(7), 1085-1117.

Percival, J. A., Skulski, T., Sanborn-Barrie, M., Stott, G., Leclair, A., Corkery, T., & Boily, M. (2012). *Geology and tectonic evolution of the Superior Province, Canada; Chapter 6 In Tectonic Styles in Canada: The Lithoprobe Perspective*. Geological Association of Canada.

Pereira, M. L., F da Silva, P., Fernandes, I., & Chastre, C. (2021). Characterization and correlation of engineering properties of basalts. *Bulletin of Engineering Geology and the Environment*, *80*(4), 2889-2910.

Pereira, M. L., F. da Silva, P., Fernandes, I., & Chastre, C. (2021). Characterization and correlation of engineering properties of basalts. *Bulletin of Engineering Geology and the Environment*, *80*(4), 2889-2910. https://doi.org/10.1007/s10064-021-02107-7

Perras, M. A., & Diederichs, M. S. (2014). A review of the tensile strength of rock: concepts and testing. *Geotechnical and Geological Engineering*, *32*, 525-546.

Petrone, P., Allocca, V., Fusco, F., Incontri, P., & De Vita, P. (2023). Engineering geological 3D modeling and geotechnical characterization in the framework of technical rules for geotechnical design: the case study of the Nola's logistic plant (southern Italy). *Bulletin of Engineering Geology and the Environment*, *82*(1), 12.

Pfiffner, O. A. (2017). Thick-Skinned and Thin-Skinned Tectonics: A Global Perspective. *Geosciences*, *7*(3), 71. https://www.mdpi.com/2076-3263/7/3/71

Retamales, R., Davies, R., Mosqueda, G., & Filiatrault, A. (2013). Experimental seismic fragility of cold-formed steel framed gypsum partition walls. *Journal of Structural Engineering*, *139*(8), 1285-1293.

@Risk. In. (2022). Palisade Corporation https://www.palisade.com/risk/.

Roberts, D. G., & Bally, A. W. (2012). *Regional Geology and Tectonics: Principles of Geologic Analysis*. Elsevier. https://doi.org/https://doi.org/10.1016/B978-0-444-53042-4.00070-4

Rochim, A. F. R. F. (2021). Chauvenet's Criterion, Peirce's Criterion, and Thompson's Criterion (Literatures Review). In.

Rocscience. (2022). *RS2*. In (Version 11)

Rojas Perez, C., Wei, W., Gilvesy, A., Borysenko, F.-J., & Mitri, H. S. (2024). Rockburst assessment and control: a case study of a deep sill pillar recovery. Deep Mining 2024: Proceedings of the 10th International Conference on Deep and High Stress Mining,

Romão, X., & Vasanelli, E. (2021). Identification and Processing of Outliers. In *Non-Destructive In Situ Strength Assessment of Concrete: Practical Application of the RILEM TC 249-ISC Recommendations* (pp. 161-180). Springer.

Ross, S. M. (2003). Peirce's criterion for the elimination of suspect experimental data. *Journal of engineering technology*, *20*(2), 38-41.

Rousell, D. H., & Brown, G. H. E. (2009). *A Field Guide to the Geology of Sudbury, Ontario*.

Roy, J., Eberhardt, E., Bewick, R., & Campbell, R. (2023). Application of Data Analysis Techniques to Identify Rockburst Mechanisms, Triggers, and Contributing Factors in Cave Mining. *Rock Mechanics and Rock Engineering*, 1-36.

Russenes, B. (1974). Analysis of rock spalling for tunnels in steep valley sides. *Norwegian Institute of Technology*.

Saeidi, A., Heidarzadeh, S., Lalancette, S., & Rouleau, A. (2021). The effects of in situ stress uncertainties on the assessment of open stope stability: Case study at the Niobec Mine, Quebec (Canada). *Geomechanics for Energy and the Environment*, *25*, 100194.

Saeidi, M., Eftekhari, A., & Taromi, M. (2012). Evaluation of rock burst potential in Sabzkuh water conveyance tunnel, IRAN: a case study. ISRM International Symposium-Asian Rock Mechanics Symposium,

Saeidi, O., Vaneghi, R. G., Rasouli, V., & Gholami, R. (2013). A modified empirical criterion for strength of transversely anisotropic rocks with metamorphic origin. *Bulletin of Engineering Geology and the Environment*, *72*(2), 257-269. https://doi.org/10.1007/s10064-013-0472-9

Sainoki, A., & Mitri, H. S. (2014a). Dynamic behaviour of mining-induced fault slip. *International Journal of Rock Mechanics and Mining Sciences*, *66*, 19-29. https://doi.org/https://doi.org/10.1016/j.ijrmms.2013.12.003

Sainoki, A., & Mitri, H. S. (2014b). Dynamic modelling of fault-slip with Barton′s shear strength model. *International Journal of Rock Mechanics and Mining Sciences*, *67*, 155-163. https://doi.org/https://doi.org/10.1016/j.ijrmms.2013.12.023

Sainsbury, B.-A. (2020). Impact of intact rock properties on proneness to rockbursting. *Bulletin of Engineering Geology and the Environment*, *79*(4), 1939-1946.

Salamon, M. (1964). Elastic analysis of displacements and stresses induced by the mining of seam or reef deposits: Part II: Practical methods of determining displacement, strain and stress components from a given mining geometry. *Journal of the Southern African Institute of Mining and Metallurgy*, *64*(6), 197-218.

Saleem, S., Aslam, M., & Shaukat, M. R. (2021). A review and empirical comparison of univariate outlier detection methods. *Pakistan Journal of Statistics*, *37*(4).

Sanou, A.-G., Saeidi, A., Heidarzadeh, S., Chavali, R. V. P., Samti, H. E., & Rouleau, A. (2022). Geotechnical Parameters of Landslide-Prone Laflamme Sea Deposits, Canada: Uncertainties and Correlations. *Geosciences*, *12*(8), 297.

Schwertman, N. C., & de Silva, R. (2007). Identifying outliers with sequential fences. *Computational statistics & data analysis*, *51*(8), 3800-3810.

Seo, S. (2006). *A review and comparison of methods for detecting outliers in univariate data sets* University of Pittsburgh].

Shao, Z., Armaghani, D. J., Bejarbaneh, B. Y., Mu'azu, M., & Mohamad, E. T. (2019). Estimating the friction angle of black shale core specimens with hybrid-ANN approaches. *Measurement*, *145*, 744-755.

Shaygan, K., & Jamshidi, S. (2023). Prediction of rate of penetration in directional drilling using data mining techniques. *Geoenergy Science and Engineering*, *221*, 111293.

Shirani Faradonbeh, R., Shaffiee Haghshenas, S., Taheri, A., & Mikaeil, R. (2020). Application of self-organizing map and fuzzy c-mean techniques for rockburst clustering in deep underground projects. *Neural Computing and Applications*, *32*, 8545-8559.

Shirani Faradonbeh, R., Taheri, A., & Karakus, M. (2022). The propensity of the over-stressed rock masses to different failure mechanisms based on a hybrid probabilistic approach. *Tunnelling and Underground Space Technology*, *119*, 104214. https://doi.org/https://doi.org/10.1016/j.tust.2021.104214

Shnorhokian, S., Mitri, H. S., & Moreau-Verlaan, L. (2015). Stability assessment of stope sequence scenarios in a diminishing ore pillar. *International Journal of Rock Mechanics and Mining Sciences*, *74*, 103-118.

Solak, T. (2009). Ground behavior evaluation for tunnels in blocky rock masses. *Tunnelling and Underground Space Technology*, *24*(3), 323-330.

Sonmez, H., Gokceoglu, C., & Ulusay, R. (2004). Indirect determination of the modulus of deformation of rock masses based on the GSI system. *International Journal of Rock Mechanics and Mining Sciences*, *41*(5), 849-857. https://doi.org/https://doi.org/10.1016/j.ijrmms.2003.01.006

SOUFI, A., BAHI, L., & OUADIF, L. (2018). Adjusted Anisotropic Strength Model for Mea-Siltstones and Prediction of UCS from Indirect Tensile Test. *International Journal of Civil Engineering and Technology*.

Spiegel, M. R. (1966). *Theory and problems of statistics*.

SPSS. (2022). *IBM Corp. IBM SPSS Statistics for Windows*. In (Version 28)

Stone, D. (2010). *Precambrian geology of the central Wabigoon Subprovince area, northwestern Ontario*. Ontario Geological Survey.

Sun, J.-s., Zhu, Q.-h., & Lu, W.-b. (2007). Numerical Simulation of Rock Burst in Circular Tunnels Under Unloading Conditions. *Journal of China University of Mining and Technology*, *17*(4), 552-556. https://doi.org/https://doi.org/10.1016/S1006-1266(07)60144-8

Suorineni, F., Hebblewhite, B., & Saydam, S. (2014). Geomechanics challenges of contemporary deep mining: a suggested model for increasing future mining safety and productivity. *Journal of the Southern African Institute of Mining and Metallurgy*, *114*(12), 1023-1032.

Taherynia, M. H., Fatemi Aghda, S. M., & Fahimifar, A. (2016). In-situ stress state and tectonic regime in different depths of earth crust. *Geotechnical and Geological Engineering*, *34*, 679-687.

Tao, Z.-Y. (1988). Support design of tunnels subjected to rockbursting. ISRM International Symposium,

Tiryaki, B. (2008). Predicting intact rock strength for mechanical excavation using multivariate statistics, artificial neural networks, and regression trees. *Engineering Geology*, *99*(1), 51-60. https://doi.org/https://doi.org/10.1016/j.enggeo.2008.02.003

Tomaszewski, D., Rapiński, J., Stolecki, L., & Śmieja, M. (2022). Switching Edge Detector as a tool for seismic events detection based on GNSS timeseries. *Archives of Mining Sciences*, 317-332-317-332.

Tóth, Z., McNicoll, V., Lafrance, B., & Dubé, B. (2022). Early depositional and magmatic history of the Beardmore-Geraldton Belt: Formation of a transitional accretionary belt along the Wabigoon-Quetico Subprovince boundary in the Archean Superior Craton, Canada. *Precambrian research*, *371*, 106579. https://doi.org/https://doi.org/10.1016/j.precamres.2022.106579

Tremblay, K. (2020). *Determination of geological and geomechanical parameters intensifying the risk of rockburst near the Bousquet Fault at the Westwood mine, MSc. Thesis (in French)* Université du Québec à Chicoutimi].

Tukey, J. W. (1977). *Exploratory data analysis*. Addison-Wesley. http://catalogue.bnf.fr/ark:/12148/cb37362350z

van Gool, J. A. M., Kriegsman, L. M., Marker, M., & Nichols, G. T. (1999). Thrust stacking in the inner Nordre Strømfjord area, West Greenland: Significance for the tectonic evolution of the Palaeoproterozoic Nagssugtoqidian orogen. *Precambrian research*, *93*(1), 71-86. https://doi.org/https://doi.org/10.1016/S0301-9268(98)00098-9

Verma, S. P., Quiroz-Ruiz, A., & Díaz-González, L. (2008a). A1-A41: Critical values and standard errors of the mean for 33 test variants. A42-A60: Interpolation equations for outlier tests for 100≤ n≤ 1000. A61-A64: Application data compiled for the comparison of multiple-test method with box-and-whisker plot and 2s methods. *Revista mexicana de ciencias geológicas*, *25*(1), 82-96.

Verma, S. P., Quiroz-Ruiz, A., & Díaz-González, L. (2008b). Critical values for 33 discordancy test variants for outliers in normal samples up to sizes 1000, and applications in quality control in Earth Sciences. *Revista mexicana de ciencias geológicas*, *25*(1), 82-96.

Wah, W. S. L., Owen, J. S., Chen, Y.-T., Elamin, A., & Roberts, G. W. (2019). Removal of masking effect for damage detection of structures. *Engineering Structures*, *183*, 646-661.

Walker, M. L., Dovoedo, Y. H., Chakraborti, S., & Hilton, C. W. (2018). An Improved Boxplot for Univariate Data. *The American Statistician*, *72*(4), 348-353. https://doi.org/10.1080/00031305.2018.1448891

Wang, J.-A., & Park, H. (2001). Comprehensive prediction of rockburst based on analysis of strain energy in rocks. *Tunnelling and Underground Space Technology*, *16*(1), 49-57.

Wang, J., Apel, D. B., Pu, Y., Hall, R., Wei, C., & Sepehri, M. (2021). Numerical modeling for rockbursts: A state-of-the-art review. *Journal of Rock Mechanics and Geotechnical Engineering*, *13*(2), 457-478.

Wang, J., Apel, D. B., Xu, H., & Wei, C. (2022). Evaluation of the performance of yielding rockbolts during rockbursts using numerical modeling method. *International Journal of Coal Science & Technology*, *9*(1), 87.

Wang, Z., Qi, C., Ban, L., Yu, H., Wang, H., & Fu, Z. (2022). Modified Hoek–Brown failure criterion for anisotropic intact rock under high confining pressures. *Bulletin of Engineering Geology and the Environment*, *81*(8), 333. https://doi.org/10.1007/s10064-022-02831-8

Wei, F. (2013). Gross error elimination and index determination of shearing strength parameters in triaxial test. Applied Mechanics and Materials,

Xue, Y., Bai, C., Qiu, D., Kong, F., & Li, Z. (2020). Predicting rockburst with database using particle swarm optimization and extreme learning machine. *Tunnelling and Underground Space Technology*, *98*, 103287.

Yan, T., Shen, S.-L., & Zhou, A. (2023). Identification of geological characteristics from construction parameters during shield tunnelling. *Acta Geotechnica*, *18*(1), 535-551.

Yang, H., Song, K., & Zhou, J. (2022). Automated recognition model of geomechanical information based on operational data of tunneling boring machines. *Rock Mechanics and Rock Engineering*, 1-18.

Yang, M., Wang, R., Li, M., & Liao, M. (2022). A PSI targets characterization approach to interpreting surface displacement signals: A case study of the Shanghai metro tunnels. *Remote Sensing of Environment*, *280*, 113150.

Yazdanpanah, M., Xu, C., & Sharifzadeh, M. (2022). A new statistical method to segment photogrammetry data in order to obtain geological information. *International Journal of Rock Mechanics and Mining Sciences*, *150*, 105008.

Yergeau, D. (2015a). *Geology of the atypical Westwood synvolcanic gold deposit, Abitibi, Quebec., PhD thesis (in French)* Université du Québec, Institut national de la recherche scientifique (INRS)].

Yergeau, D. (2015b). *Geology of the atypical Westwood synvolcanic gold deposit, Abitibi, Quebec., PhD thesis (in French)* Université du Québec, Institut national de la recherche scientifique].

Yong, S., & Maloney, S. (2015). An update to the Canadian Shield stress database. *Number September*.

Yu, S., Zhang, Z., Wang, S., Huang, X., & Lei, Q. (2023). A performance-based hybrid deep learning model for predicting TBM advance rate using attention-ResNet-LSTM. *Journal of Rock Mechanics and Geotechnical Engineering*.

Yu, Y., & Xu, J. (2021). Multi-stage perforation and hydraulic fracture stage selection based on machine learning methods. Journal of Physics: Conference Series,

Zhang, C., Feng, X.-T., & Zhou, H. (2012). Estimation of in situ stress along deep tunnels buried in complex geological conditions. *International Journal of Rock Mechanics and Mining Sciences*, *52*, 139-162.

Zhang, J. (2008). Rockburst and its criteria and control. *Chin. J. Rock Mech. Eng.*, *27*, 2034.

Zhang, L. (2016). *Engineering properties of rocks*. Butterworth-Heinemann.

Zhang, Q., Liu, C., Guo, S., Wang, W., & Luo, H. (2022). Evaluation of rock burst intensity of cloud model based on CRITIC method and order relation analysis method.

Zhang, X.-P., Wong, L. N. Y., Wang, S.-J., & Han, G.-Y. (2011). Engineering properties of quartz mica schist. *Engineering Geology*, *121*(3), 135-149. https://doi.org/https://doi.org/10.1016/j.enggeo.2011.04.020

Zhao, X., Wang, J., Cai, M., Ma, L., Zong, Z., Wang, X., Su, R., Chen, W., Zhao, H., & Chen, Q. (2013). In-situ stress measurements and regional stress field assessment of the Beishan area, China. *Engineering Geology*, *163*, 26-40.

Zheng, S., Zhu, Y.-X., Li, D.-Q., Cao, Z.-J., Deng, Q.-X., & Phoon, K.-K. (2021). Probabilistic outlier detection for sparse multivariate geotechnical site investigation data using Bayesian learning. *Geoscience Frontiers*, *12*(1), 425-439.

Zhou, J., Li, E., Yang, S., Wang, M., Shi, X., Yao, S., & Mitri, H. S. (2019). Slope stability prediction for circular mode failure using gradient boosting machine approach based on an updated database of case histories. *Safety Science*, *118*, 505-518.

Zhou, J., Li, X., & Mitri Hani, S. (2016). Classification of Rockburst in Underground Projects: Comparison of Ten Supervised Learning Methods. *Journal of Computing in Civil Engineering*, *30*(5), 04016003. https://doi.org/10.1061/(ASCE)CP.1943-5487.0000553

Zhou, J., Li, X., & Mitri, H. S. (2016). Classification of rockburst in underground projects: comparison of ten supervised learning methods. *Journal of Computing in Civil Engineering*, *30*(5), 04016003.

Zhou, J., Li, X., & Mitri, H. S. (2018). Evaluation method of rockburst: state-of-the-art literature review. *Tunnelling and Underground Space Technology*, *81*, 632-659.

Zhou, J., Li, X., & Shi, X. (2012). Long-term prediction model of rockburst in underground openings using heuristic algorithms and support vector machines. *Safety science*, *50*(4), 629-644.

Zolnai, A., Price, R., & Helmstaedt, H. (1984). Regional cross section of the Southern Province adjacent to Lake Huron, Ontario: implications for the tectonic significance of the Murray Fault Zone. *Canadian Journal of Earth Sciences*, *21*(4), 447-456.

Zubelewicz, A., & Mroz, Z. (1983). Numerical simulation of rock burst processes treated as problems of dynamic instability. *Rock Mechanics and Rock Engineering*, *16*(4), 253-274.